Vaccinia virus protein C6 modulates innate immunity and contributes to virulence

Rebecca Pamela Sumner

Imperial College London, Section of Virology

A THESIS SUBMITTED FOR THE DEGREE OF DOCTOR OF PHILOSOPHY

2011

Declaration

The work detailed herein is the work of the candidate except where clearly indicated. In particular, the inoculation and handling of animals, and the collection of tissue samples for the *in vivo* experiments was performed by Hongwei Ren. Chromium release cytotoxicity assays were also performed in conjunction with Hongwei Ren. Work with regards to the TANK truncation mutants was performed in conjunction with Daniela Muhl. The pulse field gel electrophoresis experiment to analyse viral genomic DNA was performed with Laura McCoy. Part of this work was published in collaboration with Prof. Andrew Bowie's laboratory, Trinity College Dublin in the following publication:

Unterholzner L, Sumner RP, Baran M, Ren H, Mansur DS, Bourke NM, Randow F, Smith GL, Bowie AG (2011) Vaccinia Virus Protein C6 Is a Virulence Factor that Binds TBK-1 Adaptor Proteins and Inhibits Activation of IRF3 and IRF7. *PLoS Pathog* **7:** e1002247

Acknowledgements

Firstly, and most importantly, I would like to thank Professor Geoffrey L Smith for allowing me to undertake a PhD in his laboratory and for his support, guidance and excellent advice during this time, all of which I am incredibly grateful for. I would also like to thank Dr Daniel Mansur for being an excellent laboratory supervisor and friend during the first year of my PhD, and for his continued advice and interest in my research. I would further like to acknowledge the Wellcome Trust for providing the funding for this project.

I have thoroughly enjoyed the last three years, in the most part due to the friends I have made in the Smith lab – both past and present. I wish to thank them all for their support and entertainment both inside and outside of work. I have also made many friends within the Section of Virology, of which I would particularly like to acknowledge Kim Roberts, a fellow Guide leader and a true friend who am I very grateful to for her advice, encouragement and for being there when I needed someone to talk to.

Although I have made many friends in the Smith lab I would particularly like to thank Brian Ferguson, Carlos Maluquer de Motes, Virginie Doceul and fellow PhD students Nick Peters, Nuno Saraiva and Guia Carrara for being incredibly helpful inside the lab and providing company at tea breaks and in the pub. I would also like to thank Ben Johnson for being an excellent Masters project supervisor and a trusty tea break buddy for the last three years. Outside the lab I would particularly like to thank Raj Singh, Sonja Tattermusch, Eoin Leen and Stephen Holland (all of whom have been crazy enough to do a PhD!) for providing much entertainment on a Monday night at the pub quiz and on many other occasions.

Finally I would like to thank my parents and brother Matthew for their love, support and encouragement during this time, without which I would have found completing my PhD a much more difficult task.

Abstract

To establish a productive infection pathogens must counteract the innate immune response. VACV is a large DNA virus that was used as the vaccine to eradicate smallpox and expresses many proteins that modulate the host response to the benefit of the virus. Protein C6, encoded by ORF *022* of VACV strain WR, is one such example.

C6 is a small intracellular protein that is expressed early during infection and localises to both the nucleus and cytoplasm, and can form homo-dimers. This protein is a predicted member of the VACV Bcl-2 protein family and like other members of this family C6 possesses immunomodulatory properties. C6 is an inhibitor of IFNβ production, targeting the IRF3, but not the NF-κB, innate signalling pathway. C6 exerts its inhibitory effect at the level of the non-canonical IKK complex and TANK, SINTBAD and NAP1, important adaptor molecules for IFNβ activation, were identified as C6 interaction partners. C6 interacts with TANK via the N-terminal coiled-coil region of this adaptor, a domain that is shared amongst all three adaptor molecules. In addition C6 is an inhibitor of ISRE activation downstream of IFNα.

Tandem affinity purification followed by mass spectrometry was used as a non-biased method to find interaction partners and identified UBR1, UBR2, Hsp70, SMARCC1, TROVE2 and VACV protein I1 as C6 binding partners. Of these, the interaction of C6 with UBR1 and SMARCC1 was confirmed by co-immunoprecipitation assays.

Deletion of C6 from VACV strain WR had no effect on replication and spread *in vitro*, but significantly attenuated the virus in both the intranasal and intradermal models of murine infection. In addition, a virus lacking C6 had enhanced immunogenicity in a VACV challenge model, identifying this gene as a target for removal to improve VACV as a vaccine vector.

Contents

List of abbreviations

2’-5’-OAS	2’-5’-Oligoadenylate synthetases
Ab	Antibody
AEC	Aminoethylcarbazole
AIDS	Acquired immune deficiency syndrome
AIM2	Absent in melanoma 2
AMP	Adenosine monophosphate
AP-1	Activating protein-1
APAF	Apoptosis protease-activating factor
APC	Antigen presenting cell
AraC	Cytosine arabinoside
ASC	Apoptosis-associated speck-like protein containing a CARD
ATF2	Activating transcription factor 2
ATP	Adenosine triphosphate
BAFF	B cell-activating factor belonging to the TNF family
BAL	Bronchoalveolar lavage
Bcl	B cell lymphoma
BCR	B cell receptor
BIR	Baculovirus inhibitor repeat
BME	β-mercaptoethanol
bp	Base pairs
CARD	Caspase activation and recruitment domain
CBP	CREB-binding protein
CD	Cluster of differentiation
cDC	Conventional dendritic cell
cDNA	Complementary DNA
CEV	Cell-associated enveloped virus
CHO	Chinese hamster ovary
CMC	Carboxy methyl cellulose
CMLV	Camelpox virus
CPXV	Cowpox virus
CREB	cAMP response element-binding protein
Crm	Cytokine response modifier
CTL	Cytotoxic T lymphocyte
CV	Column volume
DAI	DNA-dependent activator of IFN
DAPI	4',6-diamidino-2-phenylindole
DAMP	Damage-associated molecular pattern
DC	Dendritic cell
DDX3	DEAD box protein 3
DMEM	Dulbecco’s modified Eagle’s medium
DNA	Deoxyribonucleic acid
DNA-PK	DNA-protein kinase
DNA-PKcs	DNA-protein kinase catalytic subunit
ds	Double stranded
doxy	Doxycycline
Ecogpt	Escherichia coli guanylphosphoribosyl transferase
ECTV	Ectromelia virus
EEV	Extracellular enveloped viruses

EGFP	Enhanced green fluorescent protein
eIF2α	Translation initiation factor 2α
ELISA	Enzyme-linked immunosorbent assay
ELISPOT	Enzyme-linked immunosorbent spot
EMCV	Encephalomyocarditis virus
ER	Endoplasmic reticulum
EV	Empty vector
FACS	Fluorescence-activated cell sorting
FADD	Fas-associated protein with death domain
FBS	Foetal bovine serum
GAF	Gamma-activated factor
GAGs	Glucosoaminoglycans
GAS	Gamma-activated site
GFP	Green fluorescent protein
HA	Haemaglutinin
HIS	Histidine
HIV	Human immunodeficiency virus
HRP	Horse radish peroxidase
Hsp	Heat shock protein
HSPV	Horsepox virus
HSV	Herpes simplex virus
hTANK	Human TANK
HX	Hypoxanthine
i.d.	Intradermal
IEV	Intracellular enveloped virus
IFN	Interferon
IFNAR	IFNα/β receptor
IFNGR	IFNγ receptor
Ig	Immunoglobulin
IκB	Inhibitor of κB
IKK	Inhibitor of κB kinase
IL	Interleukin
IL-1R	IL-1 receptor
IMV	Intracellular mature virus
i.n.	Intransal
IP	Immunoprecipitation
IRAK	IL-1R-associated kinase
IRF	IFN regulatory factor
ISG	IFN-stimulated gene
ISGF3	IFN-stimulated gene factor 3
ISRE	Interferon-stimulated response element
ITRs	Inverted terminal repeats
JAK	Janus tyrosine kinase
JNK	c-Jun NH_2-terminal kinase
kb	Kilo base pairs
kDa	Kilo Dalton
KRT4	Keratin 4
KSHV	Kaposi's sarcoma herpesvirus
LB	Luria Broth
LC-MS/MS	Liquid chromatography-mass spectrometry

LMB	Leptomycin B
LPG2	Laboratory of genetics and physiology 2
LPS	Lipopolysaccharide
LRR	Leucine rich repeat
LRRFIP1	Leucine rich repeat flightless interacting protein 1
LUC	Renilla luciferase
LUMIER	Luminescence-based mammalian interactome
MAPK	Mitogen-activated protein kinase
MAP2K	MAPK kinase
MAP3K	MAPK kinase kinase
MAVS	Mitochondrial antiviral signalling adaptor
MCMV	Murine cytomegalovirus
MDA-5	Melanoma differentiation-associated protein 5
MDP	Muramyldipeptide
MEF	Murine embryonic fibroblast
MEM	Minimum essential medium
MHC	Major histocompatibility complex
MMTV	Mouse mammary tumour virus
MPA	Mycophenolic acid
MPXV	Monkeypox virus
mRNA	Messenger ribonucleic acids
mTANK	Murine TANK
MVA	Modified virus Ankara
NACHT	Nucleotide-binding and oligomerisation
NAP1	NF-κB-activating kinase-associated protein 1
NCS	Newborn calf serum
NDP52	Nuclear dot protein 52 kDa
NDV	Newcastle disease virus
NEAA	Non-essential amino acids
NEMO	NF-κB essential moldulator
NES	Nuclear export signal
NET	Neutrophil extracellular traps
NF-κB	Nuclear factor kappa-light-chain-enhancer of activated B cells
NFAT	Nuclear factor of activated T cells
NIK	NF-κB-inducing kinase
NK	Natural killer
NLR	NOD-like receptor
NLS	Nuclear localisation sequence
NMR	Nuclear magnetic resonance
NOD	Nucleotide-binding oligomerisation domain-containing protein
OPV	Orthopoxvirus
ORF	Open reading frame
PAMP	Pathogen-associated molecular pattern
PBS	Phosphate-buffered saline
PBST	Phosphate-buffered saline + 0.01 % (v/v) Tween 20
PDCD6IP	Programmed cell death 6 interacting protein
PCR	Polymerase chain reaction
pDC	Plasmacytoid dendritic cell
p.f.u.	Plaque forming unit
p.i.	Post-infection

PI3K	Phosphatidylinositol-3 kinase
PKR	dsRNA-activated protein kinase
PRRs	Pattern recognition receptors
P/S	Penicillin/streptomycin
PYD	Pyrin domain
qRT-PCR	Quantitative reverse transcriptase-PCR
RIG-I	Retinoic acid inducible gene
RIP	Receptor interacting protein
RLR	RIG-I-like receptor
RLT	RNeasy lysis buffer
RNA	Ribonucleic acid
RNAi	RNA interference
RNP	Ribonucleoprotein
RPXV	Rabbitpox virus
RSV	Respiratory syncytial virus
SARS	Severe acute respiratory syndrome
SDD	Scaffold/dimerisation domain
SDS	Sodium dodecyl sulphate
SDS-PAGE	Sodium dodecyl sulphate – polyacrylamide gel electrophoresis
Serpin	Serine protease inhibitor
SeV	Sendai virus
SINTBAD	Similar to NAP1 TBK1 adaptor
SMARCC1	SWI/SNF related, matrix associated, actin dependent regulator of chromatin, subfamily c, member 1
SOC	Super optimal broth with catabolite repression
ss	Single stranded
STAT	Signal transducer and activator of transcription
STING	Stimulator of IFN genes
Strep	Streptavidin
TAK1	TGF-β-activating kinase 1
TANK	TRAF family member-associated NF-κB activator
TAP	Tandem affinity purification
TATV	Taterapox virus
TBD	TBK1-binding domain
TBK1	TANK-binding kinase 1
TBS	Tris-buffered saline
TBS	Tris-buffered saline + 0.1 % (w/v) Tween-20
TCR	T cell receptor
TGF-β	Transforming growth factor-β
T_H	T helper cell
TIR	Toll/interleukin-1 receptor
TIRAP	TIR domain-containing adaptor protein
TK	Thymidine kinase
TLR	Toll-like receptor
TNFα	Tumour necrosis factor α
TNFR	TNFα receptor
TNNI2	Troponin I
TRADD	TNF receptor type 1-associated DEATH domain protein
TRAIL	TNF-related apoptosis-inducing ligand
TRAF	TNF receptor-associated factor

TRAM	TRIF-related adaptor molecule
TRIF	TIR domain-containing adaptor-inducing IFNβ
TRIM	Tripartite motif
TROVE2	TROVE domain family member 2.
Ub	Ubiquitin
UBR	Ubiquitin protein ligase E3 component n-recognin
ULD	Ubiquitin-like domain
VACV	Vaccinia virus
VARV	Variola virus
vCCI	Viral CC chemokine inhibitor
VCP	VACV complement control protein
vGAAP	Viral golgi anti-apoptotic protein
VIPER	Viral inhibitor peptide of TLR4
VSV	Vesicular stomatitis virus
WHO	World Health Organisation
WR	Western Reserve
X	Xanthine

Chapter 1: Introduction

1.1Viruses, the poxvirus family and vaccinia virus

1.1.1 Viruses and their classification

Viruses are small infectious particles that are obligate parasites, requiring cells of a living organism in order to replicate. The virus family is large and diverse, containing microorganisms with the ability to infect animals, plants, bacteria and archaea. Viruses vary greatly in their size, shape, complexity, genetic material and replication cycle. As such, viruses can be classified in a number of ways. The Baltimore classification, defined in 1971 by David Baltimore, classifies viruses into seven groups depending on the genome type of the virus, how the genome is coverted into mRNAs, and mode of replication (see Table 1.1) (Baltimore, 1971).

Groups I and II of the Baltimore classification contain viruses with a DNA genome. Viruses with a double-stranded (ds) deoxyribonucleic acid (DNA) genome are classified as group I. These viruses replicate their genetic material using a DNA-dependent DNA polymerase. For members of the adenovirus and herpesvirus families this occurs within the nucleus of infected cells. For poxviruses, however, replication occurs in the cytoplasm, requiring viruses in this family to encode their own machinery for replication and transcription. Group II viruses have a single-stranded (ss)DNA genome, from which a dsDNA intermediate is produced before replication of the genome can occur.

Viruses in groups III, IV and V have ribonucleic acid (RNA) genomes. Group III viruses have a dsRNA genome. In order to produce positive-sense (+)ssRNA that can be used as a template for host ribosomes in the production of proteins, an RNA-dependent RNA polymerase, an enzyme which is not encoded by the host, is packaged in the virion core. Viruses in group IV have a (+)ssRNA genome meaning their genetic material can be directly utilised for the production of proteins, akin to messenger RNA (mRNA). A virus-encoded RNA-dependent RNA polymerase copies the viral RNA to a dsRNA form, which can be replicated to form new virions. Group V viruses on the other hand have a negative-sense (-)ssRNA genome and therefore, like group III viruses, their virions are packaged with an

RNA-dependent RNA polymerase which uses the (-)ssRNA as a template to produce (+)ssRNA.

Groups VI and VII of the Baltimore classification contain reverse transcribing (RT) viruses. Group VI viruses have a ssRNA genome that is replicated via a DNA intermediate. This group includes the retroviruses, which encode a reverse transcriptase enzyme that converts the (+)ssRNA genome into DNA, which is then integrated into the host genome by a virus-encoded integrase enzyme. Replication of the proviral genome thus occurs during cell division. Retroviruses also make use of the host RNA polymerase II enzyme to make new genomes. Group VII is a small group of viruses including the hepadnavirus hepatitis B virus. This virus has a partially dsDNA genome and utilises a virus-encoded reverse transcriptase to replicate via an RNA intermediate.

Table 1.1 The Baltimore classification of viruses

Baltimore classification	**Genome**	**Examples**
I	dsDNA	adenoviruses (e.g. adenovirus 5), poxviruses (e.g. vaccinia virus), herpesviruses (e.g. herpes simplex virus 1)
II	ssDNA	parvoviruses (e.g. parvovirus B19), anelloviruses (e.g. torque teno virus)
III	dsRNA	reoviruses (e.g. bluetongue virus), birnaviruses (e.g. infectious bursal disease virus)
IV	(+)ssRNA	picornaviruses (e.g. hepatitis A virus), togaviruses (e.g. Sindbis virus)
V	(-)ssRNA	rhabdoviruses (e.g. rabies virus), orthomyxoviruses (e.g. influenza A virus)
VI	ssRNA-RT	retroviruses (e.g. human immunodeficiency virus 1)
VII	dsDNA-RT	hepadnaviruses (e.g. hepatitis B virus)

1.1.2 Vaccinia virus classification

Vaccinia virus (VACV) is a large dsDNA virus that replicates in the cytoplasm of infected cells. It is the prototype member of the *Poxviridae*, a large family of cytoplasmic viruses that infect a wide range of eukaryotic hosts including mammals, reptiles, birds and insects. Poxviruses are classified into two subfamilies; the *Chordopoxvirinae* that infect vertebrates and the *Entomopoxvirinae* that infect insects. These subfamilies are further subdivided into genera. The *Chordopoxvirinae* consist of 8 genera; *Orthopoxvirus* (OPV), *Parapoxvirus, Avipoxvirus, Capripoxvirus, Leporipoxvirus, Suipoxvirus, Molluscipoxvirus and Yatapoxvirus*, whilst the *Entomopoxvirinae* consist of 3 genera termed A, B and C. VACV, a member of the OPV genus, is the best studied poxvirus and is well known as the agent used for the vaccination against and eradication of smallpox (Fenner, 1988), a devastating human disease caused by *Variola virus* (VARV), another member of the OPV genus.

1.1.3 Phylogenetic analysis

The viral DNA polymerase gene is one of several conserved genes used to determine the phylogenetic relationship for the poxvirus family, since this gene is essential for replication and it is likely to have been inherited vertically from a common ancestral virus. Phylogenetic analysis of poxvirus genomes, of which there are over 100 complete genomic sequences, have indicated poxviral proteins to be more similar to eukaryotic proteins than bacterial or archaebacterial proteins (Lefkowitz et al, 2006). Phylogenetic analysis of chordopoxvirus genomes using multiple gene alignments shows that they separate into four main sub-groups (Gubser et al, 2004). The *Molluscipox* and *Avipox* genera group separately and are more divergent, with the largest number of unique genes. The largest cluster of chordopoxviruses includes the *Yatapoxvirus*, *Capripoxvirus*, *Suipoxvirus* and *Leporipoxvirus* genera. Finally the OPVs form a fourth group and cluster together. Many poxviral proteins appear to have a common evolutionary origin with proteins of their eukaryotic hosts indicating that gene acquisition by horizontal transfer may have occurred during viral evolution. There is also evidence of duplication of viral genes and subsequent divergence, thus creating paralogues (Smith et al, 1991b). This may be the case for VACV protein C16, which is diploid in the genome (Fahy et al, 2008) and C4, which shares 43 % amino acid identity with C16. A further interesting example is the VACV B cell lymphoma (Bcl)-2-like family of proteins

which may have arisen from a single gene acquisition from a eukaryotic host and subsequent duplication and diversification of genes (see 1.4.5.1). Importantly, the virion structure is able to accommodate variable amounts of genetic material allowing such gene acquisitions and duplications to occur (Ball, 1995; Smith & Moss, 1983).

1.1.4 Poxviruses that cause disease in humans

In addition to VARV, the poxvirus family contains several other viruses capable of causing disease in humans. Of these, molluscum contagiosum virus is the only human-specific pathogen, with no known animal reservoir, that causes benign wart-like lesions (Hanson & Diven, 2003). More serious cases of human disease have resulted after zoonotic transmission events with monkeypox virus (MPXV), which can produce a smallpox-like disease (Reynolds et al, 2004) and cowpoxvirus (CPXV), where fatalities in immune-compromised individuals have been reported (Czerny et al, 1991). In addition, other zoonotic transmissions have been reported with VACV, orf virus, bovine papular stomatitis, tanapox virus, pseudocowpox virus and parapoxvirus of seals and reindeer, which normally result in uncomplicated localised lesions (reviewed in (Essbauer et al, 2010)).

1.1.5 VACV as a vaccine

The history of vaccination began with poxviruses. In the late eighteenth century Jenner discovered that inoculation with CPXV protected individuals from smallpox, and this was later explained by the significant antigenic similarity between CPXV and VARV (Macdonald & Downie, 1950). High antigenic similarity was also observed with VACV, which was used as the live vaccine during the smallpox eradication campaign organised by the World Health Organisation (WHO) in the 1960s (Fenner et al, 1988). This campaign was successful, in part, due to the lack of an animal reservoir for the virus and the fact that VACV provides effective and long-lasting immunity. Despite VARV being the first human infectious disease to be eradicated through the use of VACV as a vaccine, arguably one of the greatest achievements of mankind, VACV remains an enigma because its origin and natural host are unknown (Baxby, 1981).

Other than its use as a smallpox vaccine, VACV is still studied intensely as a vaccine vector to protect against other human and animal pathogens. In particular, the highly attenuated VACV strain modified virus Ankara (MVA) is being tested as a vaccine for several diseases including acquired immune deficiency syndrome (AIDS), malaria and tuberculosis (Gomez et al, 2008). This virus has proven useful as a vaccine vector due to its safety record, efficient expression of foreign antigens and ability to induce a robust immune response. MVA cannot replicate fully in most mammalian cell lines and therefore is a safe vaccine even in immune-compromised individuals (Moss et al, 1996).

1.1.6 Other research on VACV

Despite smallpox being eradicated more than 30 years ago VACV remains a very useful tool in many fields of biological research. As VACV is easy to manipulate and has a wide cell tropism it has been used as a model to study many aspects of virus replication, morphogenesis and interactions between the virus and the host cell. A significant topic of interest in poxvirus research involves understanding viral immune evasion strategies, which includes modulation of both the innate and adaptive immune responses (Haga & Bowie, 2005; Smith et al, 1997b). Studying the roles of these proteins leads not only to a better understanding of how viruses evade elimination by the host, but also enhances our knowledge of the host immune system and the signalling pathways involved. Ultimately this can lead to the design of enhanced and/or novel therapeutics not only for viral infection, but also for disorders caused by inflammation and autoimmunity (Unterholzner & Bowie, 2008). Growing interest in VACV and poxvirus research has also arisen from the potential threat of an intentional release of VARV as a bio-terrorism weapon (Mahy, 2003). Further, VACV is being studied as an oncolytic therapy for the treatment of cancer (Breitbach et al, 2011; Worschech et al, 2009).

1.1.7 Life cycle

The life cycle of VACV is complicated by the existence of 4 virion types. There are 2 intracellular forms; the intracellular mature virus (IMV) and the intracellular enveloped virus (IEV), a cell-associated form; the cell-associated enveloped virus (CEV) and an extracellular form; the extracellular enveloped virus (EEV). These forms differ in their structure and their

relative contributions to the spread of infection within the host. Importantly the IMV, IEV, CEV and EEV are surrounded by different numbers of membranes which are associated with different viral proteins making these forms of virion structurally, antigenically and functionally different (Boulter & Appleyard, 1973).

1.1.7.1 Morphogenesis

During entry into the cell the membrane(s) surrounding the virion are removed and the core is transported further into the cytoplasm on microtubules (Figure 1.1) (Carter et al, 2003). The cores accumulate in the perinuclear region and partial uncoating occurs, allowing the transcription of early mRNAs by the virus-associated DNA-dependent RNA polymerase to occur. Here, viral factories are formed and within these the viral genome is replicated, viral structural proteins are synthesised and new virions are produced. Viral cytoplasmic factories are largely devoid of cellular organelles. The first visible structure is crescent-shaped and composed of protein and lipid. The structure grows to form a spherical or oval structure that encloses the virion core, forming an immature virion. The genome is packaged in this structure and the proteolytic cleavage of core proteins yields the characteristic brick-shaped IMV (Figure 1.1) (Moss & Rosenblum, 1973).

The majority of virions remain as IMV, however a significant minority are transported away from the viral factory on microtubules. The IMVs move to an area of the cytoplasm where they become wrapped by a double layer of membrane, forming an IEV particle (Figure 1.1) (Hiller & Weber, 1985). The wrapping membranes have been reported to derive from both endosomal (Tooze et al, 1993) and trans-Golgi cisterna (Hiller & Weber, 1985). At least 9 proteins are associated with this membrane, including B5, F13, A33, A34, A36, A56, F12, K2 and E2 (Roberts & Smith, 2008). The IEVs then move to the periphery on microtubules, a process involving both F12 (Zhang et al, 2000), a protein containing a motor binding motif, and with structural similarity to kinesin light chain (Morgan et al, 2010), and protein A36 (Ward & Moss, 2001).

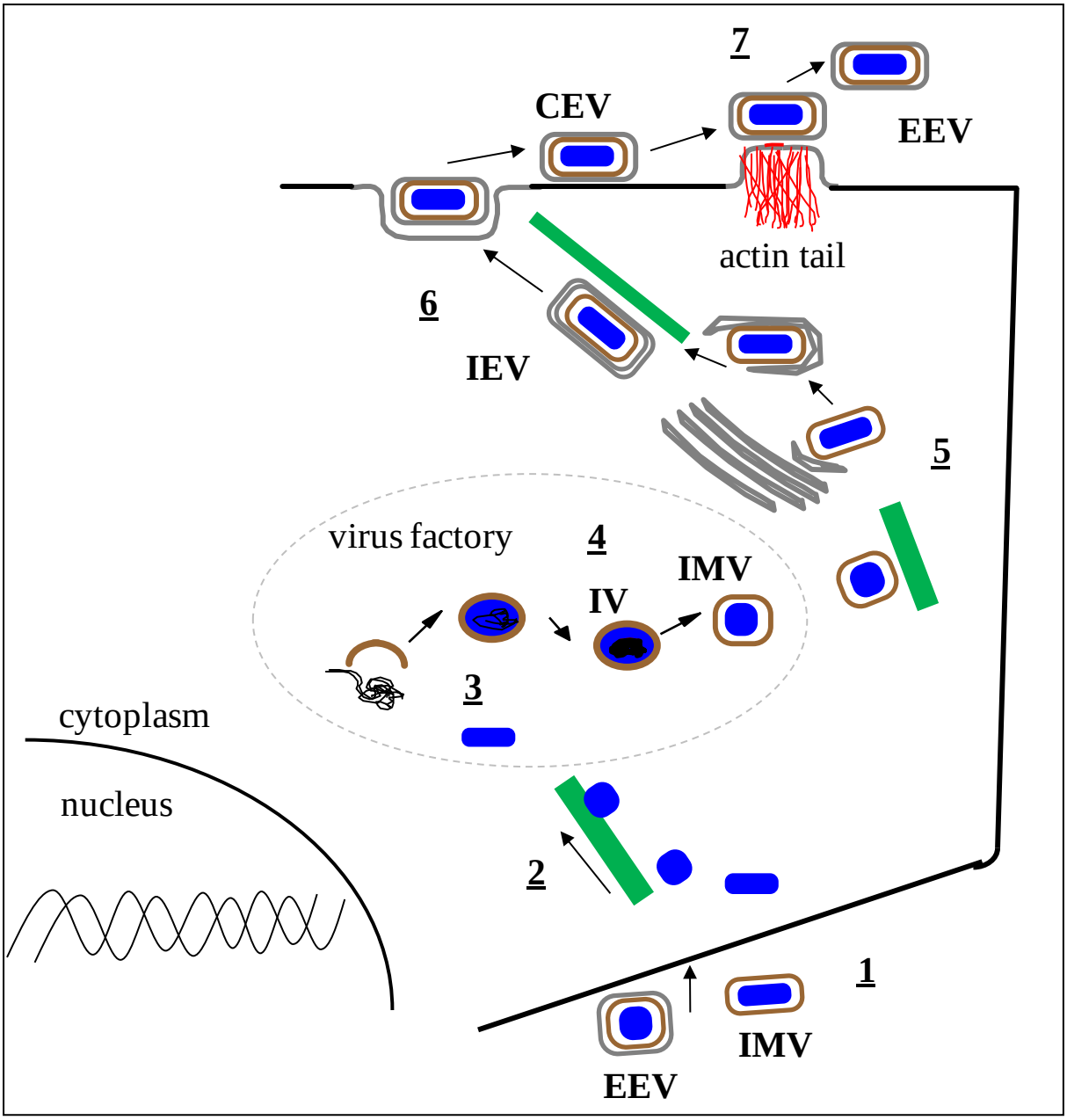

Figure 1.1: The VACV life cycle. Upon entry the membranes of the EEV and IMV are removed (1) and the viral cores are transported on microtubules to a perinuclear region (2). Here, within virus factories the genome is replicated and viral proteins are synthesised. A spherical structure composed of protein and lipid is formed and encapsidates the DNA (3) forming an immature virion (IV). Proteolytic cleavage of core proteins and core condensation forms the brick-shaped IMV particle (4). A proportion of IMV are transported away from the factory on microtubules where they become wrapped in a double layer of intracellular membrane forming an IEV particle (5). The IEVs move to the cell surface on microtubules where the outer membrane fuses with the plasma membrane exposing a CEV particle on the cell surface (6). The formation of actin tails under the CEV push it away from the cell surface. If a CEV particle is released from the cell it is called an EEV particle (7). (Adapted from Roberts & Smith, 2008).

At the cell surface the IEV membrane and plasma membrane fuse, exposing a CEV particle on the cell surface. Protein A36 is then observed to localise underneath the CEV where it becomes phosphorylated by Src kinase, triggering a signalling cascade that leads to actin polymerisation (Frischknecht et al, 1999). The formation of actin filaments pushes the CEV outward away from the infected cell, releasing it as an EEV (Figure 1.1). Viral re-entry (or super-infection) is prevented by proteins A56 and K2, which form a complex on the cell surface and bind to the fusion machinery on the IMV surface and so block entry (Brum et al, 2003).

1.1.7.2 Spread

The IMV represent the majority of infectious progeny and are retained in the cell until their release during cell lysis at late stages of infection. The IMV particle is physically robust and resistant to freezing and thawing, allowing it to survive outside of the host for prolonged periods. These virions are therefore important for transmission from one host to another (Boulter & Appleyard, 1973). These particles, however, are poorly adapted for spread within the host because several IMV proteins including L1, A27 and H3 are targets of host neutralising antibodies (Abs) (Putz et al, 2006). The IMV are also destroyed by complement, even in the absence of specific Ab (Vanderplasschen et al, 1998).

The CEV particle is important for intercellular viral spread, particularly between neighbouring cells. Although EEV are less abundant than IMV or CEV, they play a crucial role in the long-range dissemination of the virus within the host, and also in tissue culture (Payne, 1980; Smith et al, 2002). This is demonstrated by the small plaque phenotype observed with mutant viruses that are unable to make actin tails (Smith et al, 2002). Both CEV and EEV are suited to viral spread as they are wrapped in a host-derived membrane, so reducing exposure to host Ab and complement. Nevertheless, EEV protein B5 is a target of neutralising Abs (Chen et al, 2006b; Putz et al, 2006).

Recently VACV was demonstrated to employ a novel mechanism to enhance viral spread, where the expression of 2 early proteins, A33 and A36, on the surface of an infected cell led to the induction of actin tail formation upon contact with an incoming EEV (Doceul et al,

2010). This actin tail was shown to repel the superinfecting virion away from the infected cell towards uninfected cells.

1.1.7.3 Entry

To date, the cell receptors for the IMV or EEV particle are unknown. A number of proteins have been reported to interact with cell surface glucosoaminoglycans (GAGs) including H3 (Lin et al, 2000), A27 (Chung et al, 1998) and D8 (Hsiao et al, 1999), however GAGs were later shown to be non-essential for infection (Carter et al, 2005). A number of pathways have been suggested for IMV entry and are both cell type- and VACV strain-specific. One suggestion is that the IMV membrane fuses with the plasma membrane in a pH-independent manner (Carter et al, 2005). Another suggestion is that IMV are endocytosed, followed by the fusion of the virus and vesicular membranes, releasing the virion into the cytoplasm (Townsley et al, 2006). The process of membrane fusion, either at the plasma membrane or in endocytic vesicles is complex and requires at least 9 proteins (Senkevich et al, 2005). It has also been suggested that IMV can induce cell-surface blebbing and macropinocytosis to gain entry into cells (Mercer & Helenius, 2008). For EEV entry, it has been demonstrated that the EEV membrane is ruptured upon contact with the cell surface, revealing an IMV particle that can presumably enter by one of the mechanisms described above (Law et al, 2006). More recently it has been demonstrated that EEV particles can enter via a macropinocytic mechanism of endocytosis, actively triggered by the particle itself. Acid exposure in endocytic vacuoles was then needed to disrupt the outer EEV membrane exposing the IMV particle which presumably fused its membrane with the vacuolar membrane thus releasing the core into the cytoplasm (Ichihashi, 1996; Schmidt et al, 2011).

1.1.8 Genome structure and replication

Poxvirus genomes are large linear dsDNA molecules, differing in size from 130 to 360 kb. The ends of the genome contain inverted terminal repeats (ITRs) of variable size (<0.1 – 12.4 kb), and the two strands of DNA are covalently linked to produce hairpin termini (Baroudy et al, 1982). The length of the ITRs varies considerably and is influenced by recombination between blocks of repeated sequences within the ITRs and also by terminal transpositions from one end of the genome to the other. Poxviral genes tend to be arranged in blocks that are

transcribed in the same direction, possibly reducing collisions between transcription complexes and reducing the formation of dsRNA from overlapping transcripts. A common feature of poxvirus genomes is that they contain little non-coding DNA and the open reading frames (ORFs) lack introns.

Approximately 50 core genes, found in the central region of the genome are common to all sequenced poxviruses. There are a further 40 genes that are also common to all chordopoxviruses (Gubser et al, 2004; Upton et al, 2003). These genes fulfil important functions such as replication, transcription and virion assembly. An array of additional genes that can vary greatly between species are found towards the ends of the genome. These variable peripheral genes are generally non-essential for virus replication but have allowed the poxvirus family to include viruses that infect a large range of eukaryotic hosts (reviewed in (Lefkowitz et al, 2006)). Many of the VACV terminal genes encode proteins that modulate the host's anti-viral response and many of these contribute to virulence.

Replication requires the viral transcription complex within the core. DNA replication is initiated after 1-2 h post-infection (p.i.) and progeny virions are produced after 8 h (Salzman, 1960). In order to replicate in the cytoplasm VACV encodes its own DNA polymerase, as well as other enzymes such as thymidine kinase, thymidylate kinase, ribonucleotide reductase, DNA topoisomerase and a DNA ligase (Moss, 2007). The mechanism by which poxviruses replicate their DNA is not fully understood, although the rolling hairpin strand displacement mechanism, as suggested for parvoviruses, is generally the accepted model (Tattersall & Ward, 1976). In this model a nick is introduced within the terminal 200 base pairs (bp) of the genome providing a 3' end for priming of the replication complex (Moyer & Graves, 1981). The resulting newly synthesised DNA strand, which includes the hairpin loop, folds back on itself allowing the rest of the genome to then be copied.

1.1.9 Gene transcription

Like other viruses, the transcription of VACV genes is regulated temporally. Three major classes of genes exist; early, intermediate and late, and their transcription is mediated by the timed synthesis of class-specific transcription initiation factors (Broyles, 2003). All classes of genes are transcribed by the virus-encoded RNA polymerase, a large complex consisting of

more than nine subunits and totalling more than 500 kilo Dalton (kDa) (Moss, 1994). Despite significant differences in genome composition, poxviruses use similar transcriptional mechanisms (Broyles, 2003). The genes involved in mRNA synthesis are among the most conserved genes in poxviruses, as are the promoter structures themselves (reviewed in (Lefkowitz et al, 2006)). Accordingly, promoters from one poxvirus species are functional in cells, or extracts from cells, infected with another poxvirus species (Prideaux et al, 1990; Vos et al, 1992).

After entry the virion undergoes a preliminary uncoating allowing a large set of early genes to be transcribed. Amongst the early mRNAs are those encoding for proteins involved in blocking host anti-viral defences, transcription, DNA replication and transcription factors for intermediate class genes (reviewed in Broyles, 2003). Approximately half of VACV genes are transcribed early and have been suggested to be subdivided into immediate (within 30 min p.i.) and delayed (within 2 h p.i.) early classes (Assarsson et al, 2008), although a more recent study found no evidence for these early subgroups (Yang et al, 2010). Viral mRNA is synthesised within the virus core where all the enzymes and proteins required for this are packaged together with the genome. Viral mRNA then leaves through pores on the virion surface (Kates & McAuslan, 1967).

Intermediate transcription occurs after the viral DNA has replicated. It is thought that replication provides a suitable naked DNA template for intermediate and late transcription (Keck et al, 1990). Intermediate mRNAs include those that encode the RNA polymerase, capping enzyme and late transcription factors (Baldick & Moss, 1993). The late genes encode virion proteins, envelope proteins and factors required for early transcription to be packaged into the progeny virion particles (Broyles, 2003).

1.2 The immune response to infection

1.2.1 Detection of pathogens

The mammalian immune system, consisting of both innate and adaptive components, provides the host with a defence mechanism against invading pathogens. The innate immune system is the primary, early barrier to infection and leads to the initiation of an adaptive

response, the activation of which is crucial for long-lasting immunity and importantly, the induction of immune memory.

The innate immune system (discussed in detail in 1.3) recognises conserved molecular structures on pathogens, also known as pathogen-associated molecular patterns (PAMPs). PAMPs include proteins, lipids, carbohydrates and nucleic acids, and distinguish pathogens from self molecules, and their detection initiates the host innate immune response to infection. PAMPs are recognised by germline encoded pattern recognition receptors (PRRs) (Janeway, 1989; Medzhitov, 2009). PRRs include the Toll-like receptors (TLRs), retinoic acid inducible gene (RIG-I)-like receptors (RLRs), nucleotide-binding oligomerisation domain-containing protein (NOD)-like receptors (NLRs) and cytoplasmic DNA sensors. The detection of pathogens by PRRs initiates complex signalling cascades that ultimately activate key transcription factors including nuclear factor kappa-light-chain-enhancer of activated B cells (NF-κB), the interferon (IFN) regulatory factors (IRFs), in particular IRF3 and activating protein-1 (AP-1). Together these transcription factors co-ordinate the transcription of pro-inflammatory cytokines and type I IFNs.

Inflammatory cytokines such as tumour necrosis factor α (TNFα) and interleukin-6 (IL-6), and inflammatory chemokines such as CCL-5 and CXCL-10 initiate and coordinate innate immune responses through the recruitment of professional immune cells including macrophages and dendritic cells (DCs). These cells play a critical role in pathogen clearance and the priming of an adaptive response. Type I IFN is particularly important for the defence against invading viral pathogens. IFN was discovered in 1957 by Isaacs and Lindeman as a secreted molecule produced by cells after treatment with heat-inactivated influenza virus. It was named IFN due to its ability to "interfere" with live virus replication (Isaacs & Lindenmann, 1957). Work over the last 50 years has indicated the existence of a whole family of IFNs. These molecules can bind to cells in a paracrine or autocrine manner and induce the transcription of IFN-stimulated genes (ISGs). These induce an antiviral state in the cell and enhance viral clearance by inhibiting viral replication, inducing apoptosis, increasing the lytic capacity of natural killer (NK) cells, upregulating major histocompatibility complex (MHC) class I molecules and activating various components of the adaptive immune response (Hoebe & Beutler, 2004).

1.2.2 Cells of the innate immune system

The cells of the innate immune system provide the first defence against pathogens. They play an important role in detecting pathogens, promoting pathogen clearance and activating the adaptive immune response.

1.2.2.1 Macrophages

Macrophages are myeloid cells that mature from monocyte precursors. These cells play a major role in pathogen clearance by phagocytosing whole pathogens or pathogen-infected cells. Once phagocytosed, the pathogen is encapsulated in an intracellular compartment called the phagosome, which then fuses with the lysosome causing digestion of the microorganism or infected cell. Macrophages are professional antigen presenting cells (APCs) and play a major role in activating the adaptive immune system. These cells present antigen to T cells on MHC molecules. Macrophages are also contributors to inflammation because they secrete a range of pro-inflammatory cytokines and chemokines. A subset of macrophages known as alternatively activated, or M2 macrophages are thought to play a role in immune regulation and tissue repair following infection (Martinez et al, 2008). During VACV infection both DCs and macrophages have been demonstrated to present antigen to T cells within 2 h p.i. (Ramirez & Sigal, 2002).

1.2.2.2 Dendritic cells

Like macrophages, DCs are professional APCs and contribute to the presentation of antigen on MHC molecules to T cells. DCs sample the environment and are therefore found in tissues such as the skin, the respiratory tract, the lungs and the digestive system which are continuously in contact with the external environment. Once activated, for example by encountering a pathogen, DCs then migrate to the lymph nodes where they present antigen to cells of the adaptive immune system. Importantly these activated DCs express co-stimulatory molecules on their surfaces that are essential for T cell activation. Two subsets of DCs exist; the conventional DCs (cDCs) and the plasmacytoid DCs (pDCs). TLRs are highly expressed on both type of DCs, but the pDCs express particularly high levels and these cells produce very large amounts of type I IFN in antiviral immunity (Shortman & Naik, 2007).

1.2.2.3 Neutrophils

Neutrophils are some of the first cells recruited to the site of infection, migrating towards sites of IL-8 and IFNγ release. Neutrophils are an important source of cytokines and contribute to the recruitment of other immune cells during inflammation. Neutrophils contribute to pathogen clearance via three main processes. Firstly, like macrophages, neutrophils are professional phagocytes. Secondly, they can degranulate, releasing anti-microbial compounds, such as cathepsins, bactericidal/permeability-increasing protein and defensins, into the extracellular environment (Segal, 2005). More recently neutrophils have also been shown to release web-like structures of chromatin and serine proteases called neutrophil extracellular traps (NETs), which can trap and kill pathogens (Brinkmann et al, 2004).

1.2.2.4 NK cells

NK cells play an important role in the immune response, particularly to viral infection. These cells provide an immediate method for containing viral infection whilst the antigen-specific adaptive immune response is being generated. NK cells are of lymphoid origin and contribute to antiviral immunity in two ways. Firstly, they are major producers of IFNγ, contributing to the antiviral state of neighbouring cells and the activation of other immune cells such as macrophages. Secondly, NK cells act by lysing pathogen-infected cells, often by recognising their lack, or low level of MHC class I molecule expression. NK cells can release cytoplasmic granules that contain perforin, a molecule that inserts into lipid membranes leading to cell lysis and granzyme which causes cells to undergo apoptosis (Vivier et al, 2008).

1.2.3 Adaptive immunity

Adaptive immunity is mediated via the generation of antigen-specific B and T lymphocytes. The adaptive immune response provides a mechanism for clearing pathogens in a specific manner and allows for the formation of immunological memory.

1.2.3.1 T lymphocytes

T cells are part of the cell-mediated immune response and have a unique cell surface receptor known as the T cell receptor (TCR), arising from recombination of various germline encoded segments (V(D)J recombination). There are many subsets of T cells with unique functions and roles in contributing to the host defence against invading microorganisms. Cytotoxic T lymphocytes (CTLs) are crucial for the defence against viruses as they are able to specifically kill virus-infected cells, as well as tumour cells. CTLs can be identified by the expression of the glycoprotein cluster of differentiation 8 (CD8) on their surface. CTLs recognise antigen (peptide) presented by MHC class I. T helper (T_H) cells on the other hand express CD4 on their surface and recognise antigen presented by MHC class II. These cells assist other leukocytes in immunological processes such as the maturation of B cells, and the activation of CTLs and macrophages by the secretion of cytokines. A number of T_H cell subsets exist including T_{H1} cells that secrete IFNγ and TNFβ and aid the killing capacity of macrophages and CTLs, T_{H2} cells that secrete IL-4, -5, -6, -10 and -13 and stimulate B cell proliferation and Ab class switching and T_{H17} cells that secrete IL-17 and play a role in the defence against extracellular pathogens (McGeachy & Cua, 2008). Memory T cells, along with Ab contribute to immunological memory and persist long after the infection has been cleared. Upon encountering antigen they divide rapidly, providing immediate protection against the invading pathogen. Regulatory T cells are crucial for the maintenance of immune tolerance and the resolution of immune responses (Rudensky, 2011).

1.2.3.2 B lymphocytes

B lymphocytes are part of the humoral response and their principal functions include Ab production in response to specific antigens, acting as APCs and eventually developing into memory B cells. Each B lymphoctye has a unique B cell receptor (BCR) on its surface, which is a membrane-bound immunoglobulin (Ig) and recognises a single antigen. Once the BCR encounters antigen and a second signal is received from a T_H cell the B cell differentiates into a plasma B cell, which secretes Ab, or into a memory B cell. The BCR Ig is composed of two light chains and two heavy chains, with a variable region that is determined in the process of VDJ recombination, similar to the TCR, thus producing a unique Ig. Plasma B lymphocytes secrete soluble Ig, also known as Ab, of which there are five isotypes; IgG, IgD, IgM, IgA

and IgE, each of which has a distinct function. The function of Ab is to bind to antigens exposed by pathogens leading to direct neutralisation of pathogen infectivity, or opsonisation and subsequent phagocytosis, or activation of the complement cascade leading to pathogen destruction (Murphy, 2008).

1.2.4 Complement

The complement system is composed of a cascade of zymogens that once activated contribute to the opsonisation and destruction of invading pathogens (Ricklin et al, 2010). Complement can be activated via three main pathways. The classical pathway is initiated when C1q of the C1 complement complex binds to Ab complexed with antigen. This leads to a cascade of cleavages of various complement proteins including C4, C2 and C3. The alternative pathway is activated by the spontaneous proteolytic activation of C3 on microbial surfaces. Finally the lectin pathway is initiated following the recognition of lectins on the pathogen surface by mannose-binding-lectin and ficolins. All three pathways ultimately lead to the formation of the membrane attack complex that can insert into the membranes of pathogens, or pathogen-infected cells, and initiate lysis. In addition some complement components can act as opsonins and others can trigger mast cell degranulation.

1.2.5 Apoptosis

Apoptosis, or programmed cell death is a mechanism by which cells can undergo death without causing local inflammation and potential damage. During apoptosis cells undergo changes such as cell shrinkage, nuclear fragmentation, chromatin condensation and chromosomal DNA fragmentation. Unlike necrosis, apoptosis produces small cell fragments that can be phagocytosed by neighbouring macrophages and other phagocytic cells, without the release of the cytoplasmic contents of the dying cell. Apoptosis is an important part of the innate immune response because it provides a means for infected cells to undergo death thus preventing the completion of virus replication and potential spread of infection. As such, many pathogens have evolved ways of preventing apoptosis (see 1.4.2) (Taylor & Barry, 2006).

Apoptosis can be triggered by two main pathways; the extrinsic pathway and the intrinsic (or mitochondrial) pathway. The extrinsic pathway can be induced by the binding of TNFα (Carswell et al, 1975), Fas ligand (Trauth et al, 1989; Yonehara et al, 1989) or TNF-related apoptosis-inducing ligand (TRAIL) (Wiley et al, 1995) to their respective receptors. This induces receptor oligomerisation and the subsequent assembly of the death-inducing signalling complex (Kischkel et al, 1995). This activates a caspase cascade starting from caspase-8 and ending with the effector caspases and nucleases; caspase-3, -6, -7 and caspase-activated DNase (Kroemer et al, 2007). The intrinsic pathway is controlled by mitochondria. Several intracellular signals including DNA damage, reactive oxygen species and endoplasmic reticulum (ER) stress can induce mitochondrial outer membrane permeabilisation, causing the release of pro-apoptotic factors from the intermembrane space. These include cytochrome *c*, which induces the apoptosis protease-activating factor 1 (APAF-1) and ATP/dATP to assemble the apoptosome, a molecular platform that promotes the activation and proteolytic cleavage of pro-caspase-9 (Zou et al, 1999). Caspase-9 then cleaves and activates the effector caspases, which finally lead to the apoptotic phenotype (Kroemer et al, 2007). A family of proteins with a Bcl-2 fold play an important role in controlling the permeability of the mitochondrial membrane and includes pro-apoptotic members such as Bid, Bad and Bax, and anti-apoptotic members such as Bcl-2, Bcl-xl and Bcl-w (Youle & Strasser, 2008).

1.3 The innate immune response

1.3.1 PRRs in detail

1.3.1.1 TLRs

The TLRs are a family of type I membrane glycoproteins consisting of extracellular leucine rich repeats (LRRs) that recognise PAMP ligands and a cytoplasmic Toll/interleukin-1 receptor (TIR) domain which is required for interactions with adaptor molecules and downstream signalling. The first TLR was discovered in flies (Lemaitre et al, 1996). In humans there are 10 TLRs and in mice there are 12. Of these, TLRs 1-9 are conserved in both species. TLRs 1, 2, 4, 5 and 6 are expressed primarily at the cell surface and recognise PAMPs derived from bacteria, fungi and protozoa. TLRs 3, 7, 8 and 9 are expressed exclusively in endocytic compartments and primarily recognise nucleic acid PAMPs derived

from various viruses and bacteria (Kumar et al, 2011). These receptors are delivered to endosomes through their association with ER membrane protein UNC93B1 (Kim et al, 2008). Crystal structures have been solved for the TLR3 homodimer (Bell et al, 2005; Choe et al, 2005), the TLR1-TLR2 heterodimer (Jin et al, 2007) and the TLR4-MD2 complex (Kim et al, 2007). From these structures it appears that ligand binding induces receptor dimerisation and a conformational change. The TIR domains are thus brought into close proximity and the formation of dimers or oligomers provides a platform for the recruitment of TIR domain-containing adaptor proteins to bind to. These adaptor molecules then recruit kinases that via signalling cascades activate NF-κB, IRFs and AP-1.

1.3.1.1.1 Bacterial recognition

Various bacterial PAMPs are recognised by multiple TLRs including 1, 2, 4, 5, 6, 7 and 9. Much research has focussed on TLR4, which along with the accessory protein MD2 (Shimazu et al, 1999) senses lipopolysaccharide (LPS), a major bacterial cell wall component (Poltorak et al, 1998). Bacterial peptidoglycan on the other hand is sensed by TLR2 (Schwandner et al, 1999), as is mycobacterial lipoarabinomannan (Underhill et al, 1999). TLR2 in conjunction with TLR1 or TLR6 also senses diacyl or triacyl lipopeptides. TLR5 senses bacterial flagellin. Bacterial nucleic acids are sensed by TLRs 7 and 9 (Kumar et al, 2011). TLR9 senses DNA rich in unmethylated CpG, whereas TLR7 recognises ssRNA and is important for detection of Group B streptococci in the phagosome (Mancuso et al, 2009). The recognition of PAMPs by TLRs 1, 2, 4, 5 and 6 induces the production of pro-inflammatory cytokines, whereas engagement of TLRs 7 and 9 induces type I IFN.

1.3.1.1.2 Viral recognition

As with bacterial pathogens, nucleic acid from viruses is sensed by both TLRs 7 and 9. DNA from herpes simplex virus (HSV) and murine cytomegalovirus (MCMV) is sensed by TLR9, whereas viral RNA is sensed by TLRs 3, 7 and 8. TLR7 is activated by ssRNA from viruses such as influenza virus and vesicular stomatitis virus (VSV) (Diebold et al, 2004). TLR8 is a close paralogue of TLR7 and there seems to be some functional redundancy. For example, both TLR7 and 8 recognise human immunodeficiency virus (HIV)-1-derived uridine-rich RNAs (Meier et al, 2007). TLR3 recognises dsRNA (Alexopoulou et al, 2001) and in the

case of influenza virus it has been shown to actually promote disease due to excessive downstream inflammation (Le Goffic et al, 2006). This is an example of how an inappropriate or uncontrolled immune response can be detrimental to the host. In addition MCMV and VACV are also sensed by TLR3 because convergent transcription of DNA viruses produces dsRNA. Beside viral nucleic acids the coat protein of respiratory syncytial virus (RSV) and mouse mammary tumour virus (MMTV) are recognised by TLR4 and the measles virus heamagglutinin protein is sensed by TLR2 (Bowie & Unterholzner, 2008).

1.3.1.1.3 Fungal recognition

TLRs play a role in the recognition of several fungi including *Candida albicans* and *Aspergillus fumigatus*, however to induce an inflammatory response additional receptors are required. These include dectins, CD14, mannose receptors or DC-SIGN. Beta-glucans for example are recognised by TLR2 in association with dectin-1 and glucuronoxylomannans are sensed by TLR4 and CD14 (Kumar et al, 2011).

1.3.1.1.4 Protozoal recognition

TLRs 2 and 4 are also important in the detection of protozoa. Unsaturated alkylacylglycerol from *Trypanosoma species* and lipophosphoglycan from *Leishmania species* are both recognised by TLR2. Glycoinositolphospholipids and glycosylphosphatidylinositol anchors from *Trypanosoma species*, *Plasmodium falciparum* and *Toxoplasma gondii* are recognised by both TLR2 and 4. In addition TLR9 plays a role in sensing the genomic DNA of *Trypanosoma species* and hematin crystals of *Plasmodium species* (Kumar et al, 2011).

1.3.1.2 RLRs

The RLR family of cytoplasmic RNA sensors comprises three members; RIG-I (Yoneyama et al, 2004), melanoma differentiation-associated protein 5 (MDA5) (Andrejeva et al, 2004) and laboratory of genetics and physiology 2 (LGP2) (Rothenfusser et al, 2005). All three members contain a DExD/H-box RNA helicase domain that is required for ligand recognition. In addition, RIG-I and MDA5 contain N-terminal caspase activation and recruitment domains (CARDs) that are essential for downstream signalling. Engagement of

RIG-I and MDA5 with their ligands leads to a conformational change within the sensor exposing the CARD domains which can then interact with the CARD-containing adaptor protein mitochondrial antiviral signalling adaptor (MAVS) (Seth et al, 2005) (also known as IPS-1 (Kumar et al, 2006), Cardif (Meylan et al, 2005) and VISA (Xu et al, 2005). MAVS localises to the mitochondrion and peroxisomes and both localisations are required for robust antiviral responses. A recent study indicated that peroxisomal MAVS signals via IRF1, contributing to the early response to infection, whereas mitochondrial MAVS induces a delayed response via IRF3 (Dixit et al, 2010). MAVS is regulated negatively by NLRX1, a NLR family member that also localises to the mitochondrion (Moore et al, 2008). It is also regulated negatively by autophagosome components Atg5 and Atg12 (Jounai et al, 2007).

Endogenous host RNAs do not activate the RLRs because they are generally ssRNA and have 5' ends that are protected with a methylguanosine cap or are monophosphates, or are modified with unusual bases such as pseudouridine, preventing recognition by RIG-I and MDA-5.

1.3.1.2.1 RIG-I

RIG-I recognises members of the *Paramyxoviridae* family including *Newcastle disease virus* (NDV) and VSV and also members of the *Flaviviridae* family including *Japanese encephalitis virus* and *hepatitis C virus*. In addition, RIG-I recognises enzymatically synthesised RNA *in vitro*. Originally it was believed that ssRNAs bearing a 5' triphosphate were the only essential component for this recognition (Hornung et al, 2006; Pichlmair et al, 2006), however recent studies have indicated that during enzymatic synthesis a secondary structure of dsRNA is generated and this 'pan handle' acts as the ligand (Schlee et al, 2009; Schmidt et al, 2009). As with other innate immune signalling pathways, Ub plays a key role in RIG-I-mediated cascades. For signalling to occur the CARDs within RIG-I require K63-linked ubiquitination in the presence of RNA and ATP, and recently it was shown that free K63-linked Ub chains activate RIG-I-dependent signalling (Zeng et al, 2010). Further, the initial recognition of ligands by RIG-I is regulated positively by the two E3 Ub ligases tripartite motif (TRIM) 25 (Gack et al, 2007) and RNF135 via K63-linked ubiquitination (Oshiumi et al, 2009), whereas K48-linked ubiquitination by RNF125 leads to down-regulation of RIG-I-mediated signalling (Arimoto et al, 2007).

1.3.1.2.2 MDA5

Viruses that produce large amounts of dsRNA during their life cycle, such as picornaviruses are sensed my MDA5 (Gitlin et al, 2006). Some DNA viruses can produce considerable amounts of dsRNA owing to convergent transcription from opposite DNA strands, where two adjacent reading frames are transcribed in opposite directions and the transcripts can overlap. Positive-sense RNA viruses that use a dsRNA intermediate during their replication cycle are also subject to recognition by MDA5 (Weber et al, 2006). In addition MDA5 recognises the synthetic dsRNA analogue poly I:C, whereas only enzymatically shortened poly I:C was recognised by RIG-I. These data suggested that these two RLRs recognise RNAs of different lengths, with MDA5 showing a preference for longer molecules (Kato et al, 2008). Studies with RIG-I- and/or MDA5-deficient cells have indicated that some viruses, such as dengue virus and West Nile Virus, are recognised by both RIG-I and MDA5 and this dual recognition is required to generate a robust innate response (Takeuchi & Akira, 2008).

1.3.1.2.3 LGP2

Unlike RIG-I and MDA5, LGP2 lacks a CARD and therefore does not interact with the CARD-containing protein MAVS and does not initiate downstream signalling. Instead this molecule was described as a negative regulator of RIG-I- and MDA5-mediated signalling (Rothenfusser et al, 2005). However, more recent studies have suggested LGP2 to have a positive regulatory role on these pathways (Satoh et al, 2010).

1.3.1.3 NLRs

The NLRs are a group of cytoplasmic molecules that sense a wide range of ligands including PAMPs and host-derived damage-associated molecular patterns (DAMPs). In humans there are 23 members, comprising three domains; the C-terminal domain consisting of several LRRs thought to be involved in ligand recognition, the N-terminal domain consisting of a death effector domain, a pyrin domain (PYD), a CARD, baculovirus inhibitor repeats (BIRs) and an acidic domain, and the intermediate domain consisting of nucleotide-binding and oligomerisation (NACHT) domains. The NACHT domains are required for ligand-induced, ATP-dependent oligomerisation of the sensors and subsequent formation of active receptor

complexes. These sensors either activate NF-κB or mitogen-activated protein kinases (MAPKs) leading to the production of inflammatory cytokines, or they activate multiprotein complexes called inflammasomes. The inflammasomes then facilitate the maturation of inflammatory cytokines such as IL-1β and IL-18 from their zymogen forms, or they induce cell death (Kanneganti, 2010).

1.3.1.3.1 NOD1 and NOD2

The NOD1 and NOD2 receptors recognise peptidoglycans, a major component of bacterial cell walls (McDonald et al, 2005). NOD2 is also important for the immune defence against pathogenic protozoal parasites such as *Toxoplasma gondii* (Shaw et al, 2009). Ligand recognition by NOD1 and NOD2 induces the oligomerisation of these sensors and the subsequent recruitment of the adaptor molecule receptor interacting protein (RIP)2 via CARD-CARD interactions (Park et al, 2007). This leads to the activation of NF-κB and MAPKs. Evidence for the direct recognition of these PAMPs by NOD1 and NOD2 is lacking, a common theme in the field of NLRs.

1.3.1.3.2 NLRP3

The NLRP3 inflammasome is the best studied inflammasome complex and plays an important role in macrophages and DCs. It is composed of NLRP3, apoptosis-associated speck-like protein containing a CARD (ASC) and pro-caspase 1 (Martinon et al, 2002). Upon stimulation NLRP3 oligomerises and clusters ASC via PYD-PYD interactions. The CARD of ASC then interacts with the CARD of procaspase-1, inducing its proteolysis. Active caspase-1 further promotes the proteolysis of the zymogen form of the IL-1 cytokine family members IL-1β and IL-18. This inflammasome responds to all classes of pathogens including viruses, for example adenovirus (Barlan et al, 2011), bacteria (Muruve et al, 2008), fungi, for example via β-glucans (Hise et al, 2009) and DAMPs such as β-amyloid (Halle et al, 2008), uric acid crystals (Martinon et al, 2002), silica crystals and aluminium salts, an adjuvant used frequently in vaccines (Hornung et al, 2008). The mechanism by which this inflammasome senses so many ligands is not well understood and again the question is raised as to whether NLRP3 senses ligands directly or indirectly.

1.3.1.3.3 NLRC4

NLRC4 (also known as IPAF) is also part of an inflammasome containing procaspase-1 (Poyet et al, 2001). The requirement for the adaptor protein ASC in this complex is unclear. NLRC4 senses bacteria such as *Legionella pneumophilia*, *Salmonella typhimurium*, *Pseudomonas aeruginosa* and *Shigella flexneri* indicating a type III or IV secretion system might be involved in NLRC4 inflammasome activation.

1.3.1.3.4 NLRP1

The NLRP1 infammasome comprises NLRP1, ASC and procaspase-1 and it senses the bacterial cell wall constituent muramyldipeptide (MDP) (Faustin et al, 2007). ASC does not seem to be essential but facilitates the activation of caspase-1. In mice the NLRP1 paralogue NLRP1b senses lethal toxins from *Bacillus anthracis* and plays a role in pathogenesis (Boyden & Dietrich, 2006).

1.3.1.3.5 NLRC5

NLRC5 is the most recently characterised NLR and conflicting data exists as to the role it plays in innate immunity. NLRC5 mRNA and protein expression are induced by stimulation of myeloid and lymphoid cells with IFNγ, LPS, poly I:C and viral infection (Benko et al, 2010). Several studies have demonstrated that NLRC5 over-expression dampens inflammatory cytokine and type I IFN production (Benko et al, 2010; Cui et al, 2010). Mechanistically, Cui et al found NLRC5 to interact with the inhibitor of κB (IκB) kinase (IKK) complex and inhibit its activation, as well as interacting with RIG-I and MDA-5 and suppressing downstream signalling (Cui et al, 2010). However, other studies have suggested that NLRC5 over-expression induces IFNβ promoter activation and enhances RIG-I and MDA5-mediated antiviral responses (Kuenzel et al, 2010; Neerincx et al, 2010) as well as inducing caspase-1-dependent maturation of IL-1 family cytokines (Kumar et al, 2010). A further study demonstrated that this molecule enhances the transcription of MHC class I molecules (Meissner et al, 2010). However, work performed *in vivo* with NLRC5-deficient mice found comparable levels of inflammatory cytokines and type I IFNs in response to a

challenge with poly I:C compared to wild-type mice and thus the role of this molecule is still unclear (Kumar et al, 2010).

1.3.1.4 Cytoplasmic DNA sensors

The existence of cytoplasmic DNA sensors was first questioned when work by Ishii et al and Stetson and Medzhitov demonstrated that type I IFN could be induced in cells by delivery of B-form dsDNA to the cytoplasm (Ishii et al, 2006) or by infection with invasive *Listeria monocytogenes* (Stetson & Medzhitov, 2006). Both groups described this induction to be dependent on IRF3, but independent of TLR9, the only characterised sensor of foreign DNA at the time. Much work was then focussed on identifying the sensor(s) for DNA delivered to the cytoplasm.

1.3.1.4.1 DAI

The first identified putative sensor of foreign DNA was DNA-dependent activator of IFN (DAI, also known as DLM1 and ZBP1) (Takaoka et al, 2007). These initial *in vitro* studies indicated DAI to be essential for type I IFN induction, and this was via the non-canonical IKK kinases TRAF family member-associated NF-κB activator (TANK)-binding kinase (TBK)1 and IKKε. However further *in vitro* and *in vivo* studies questioned this finding and demonstrated DAI to be dispensable for DNA-mediated innate immune responses (Ishii et al, 2008; Wang et al, 2008).

1.3.1.4.2 AIM2

A second putative DNA sensor to be identified was absent in melanoma 2 (AIM2). This cytoplasmic molecule and member of the HIN-200 family has a PYD domain, allowing it to interact with ASC to form an AIM2 inflammasome along with procaspase-1. Infection with DNA viruses or introduction of DNA into the cytoplasm was demonstrated to induce the production of IL-1β through this AIM2 inflammasome (Burckstummer et al, 2009; Fernandes-Alnemri et al, 2009; Hornung et al, 2009; Roberts et al, 2009). The use of AIM2-deficient mice has demonstrated that this molecule is critical for caspase-1 activation and subsequent production of IL-1β and IL-18 after infection with *Francisella tularensis*

(Fernandes-Alnemri et al, 2010), VACV and MCMV (Rathinam et al, 2010). Nonetheless AIM2 was shown not to act via IRF3 and thus other DNA sensors were believed to exist.

1.3.1.4.3 RNA polymerase III

RNA polymerase III has also been identified as a DNA sensor. This molecule transcribes DNA into RNA with a 5' tri-phosphate, which is then sensed by RIG-I (Ablasser et al, 2009; Chiu et al, 2009). RNA polymerase III recognises AT-rich DNA, such as the synthetic ligand poly dA:dT, and interruption of the AT rich sequence leads to abrogation of type I IFN induction (Chiu et al., 2009). This sensor has only been shown to be important in HEK293 cells and studies *in vivo* are currently lacking.

1.3.1.4.4 Ku 70

Recently Ku70 was described as a novel cytosolic DNA sensor that induces type III rather than type I IFN in HEK293 cells (Zhang et al, 2011). Also our group has described the DNA-protein kinase (DNA-PK) complex, comprising Ku 70, Ku 80 and DNA-PK catalytic subunit (DNA-PKcs) as a DNA sensor important in murine embryonic fibroblasts (MEFs) and adult skin fibroblasts that induces type I IFN, CXCL-10 and IL-6 expression via a pathway dependent on stimulator of IFN genes (STING), TBK1 and IRF3 (Brian Ferguson et al, submitted).

1.3.1.4.5 IFI16

Recently, a molecule with similarity to AIM2, IFI16, was shown to activate IRF-3 in response to DNA in macrophages (Unterholzner et al, 2010). A subsequent study further highlighted the role for this molecule in the activation of the inflammasome in response to Kaposi's sarcoma herpesvirus (KSHV) (Kerur et al., 2011), although this virus, like other herpes viruses, replicates in the nucleus and is not thought to expose genomic DNA in the cytoplasm.

1.3.1.4.6 LRRFIP1

Further, the leucine rich repeat flightless interacting protein 1 (LRRFIP1) has been characterised as a DNA sensor functioning within macrophages to upregulate type I IFN (Yang et al., 2010). This pathway involved β-catenin and IRF3. Interestingly DNA from *Listeria monocytogenes* and RNA from VSV both appeared to stimulate LRRFIP1 indicating it to be a nucleic acid sensor rather than a DNA-specific receptor.

1.3.1.4.7 STING

STING was identified by functional screening for IFNβ promoter activators and appears to be essential for the induction of cytokines and IFNs in response to cytoplasmic DNA. This molecule is localised in the ER, interacts with TBK1 and signals via IRF3. As this molecule does not interact directly with DNA it has been suggested as an adaptor molecule rather than a DNA sensor (Ishikawa & Barber, 2008; Zhong et al, 2008). Furthermore STING-deficient mice are more susceptible to infection with both a DNA virus (HSV) and an RNA virus (VSV) suggesting a wider role for this adaptor protein than initially thought (Ishikawa et al, 2009).

1.3.2. The NF-κB signalling pathway

NF-κB is a key mediator of the immune inflammatory response and is activated downstream of the TLRs, RLRs, some NLRs and DNA sensors, as well as the TNFα receptor (TNFR) and IL-1 receptor (IL-1R). NF-κB refers to a family of transcription factors consisting of p65 (also known as RelA), c-Rel, RelB, p50 and p52. These molecules all have a C-terminal Rel-homology domain in common, which mediates their homo- and hetero-dimerisation. p65 and c-Rel typically hetero-dimerise with p50, whereas RelB hetero-dimerises with p52 (Vallabhapurapu & Karin, 2009).

All TLRs activate NF-κB and all TLRs, except TLR3, recruit myeloid differentiation factor 99 (MyD88) to do this (Medzhitov et al, 1998). On the other hand, TLR3 recuits TIR domain-containing adaptor-inducing IFNβ (TRIF) to activate downstream signalling events (see Figure 1.2). NF-κB-activating signalling converges on the IKK complex, consisting of

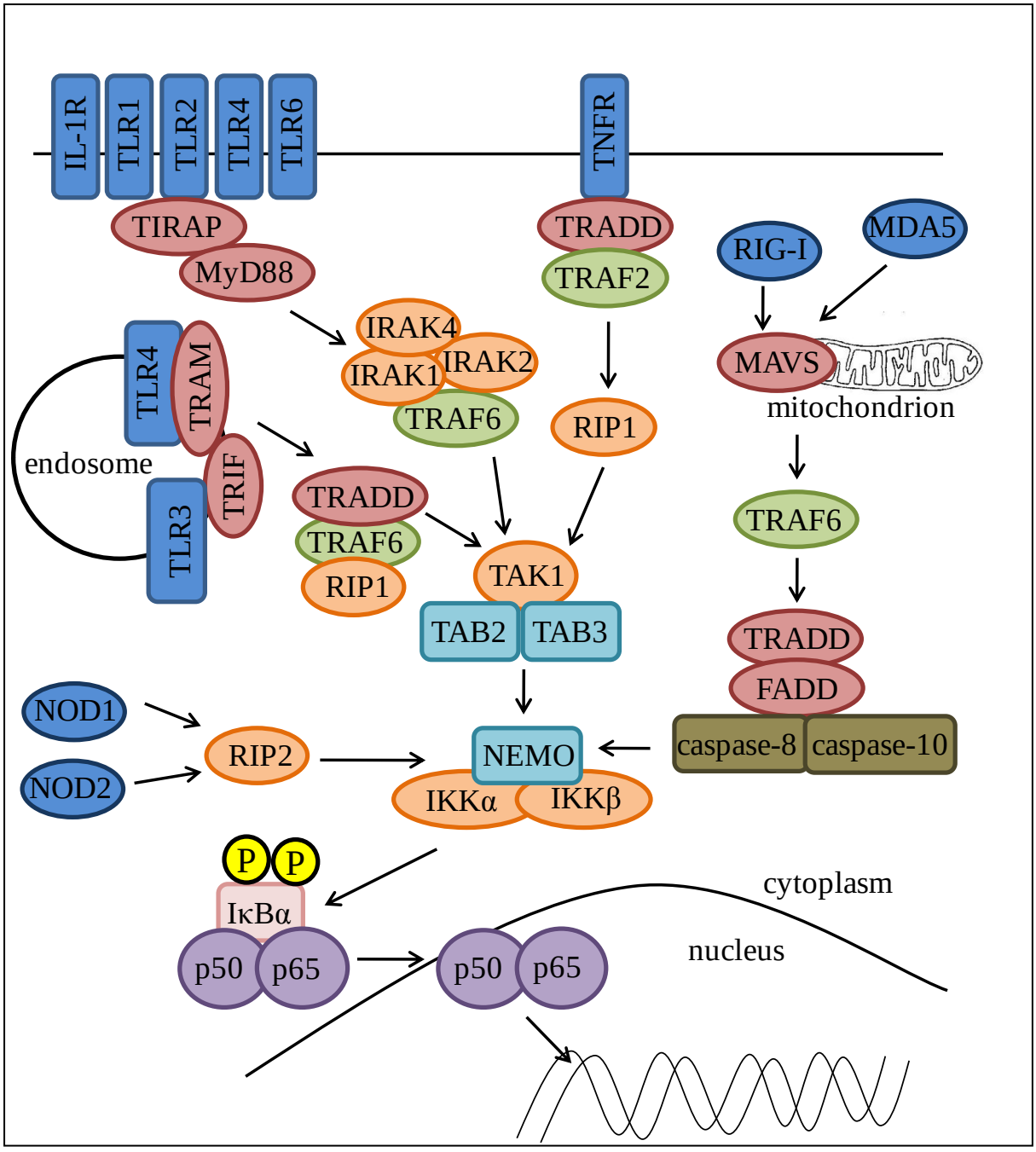

Figure 1.2: Overview of immune signalling pathways leading to NF-κB activation. Signalling pathways leading to the activation of NF-κB converge on the canonical IKK complex (IKKα, IKKβ, NEMO). This complex phosphorylates IκBα, targeting it for degradation by the proteasome, and thus allowing NF-κB components p50 and p65 to translocate to the nucleus and bind to the promoter of NF-κB-responsive genes. Signalling downstream of thr TLRs, the IL-1R and the TNFR at the cell surface, and downstream of TLR3 and TLR4 in endosomes occurs via the TAK1 complex. Signalling downstream of the RLRs activates the canonical IKKs via a complex consisting of caspase-8 and -10, whereas signalling downstream of NOD1 and NOD2 requires RIP2.

the canonical IKKs; IKKα and IKKβ (Zandi et al, 1997) and NF-κB essential modulator (NEMO) or IKKγ, a non-enzymatic regulatory component (Rothwarf et al, 1998). Recently the crystal structure of xenopus IKKβ was solved and comprises of a kinase domain, a Ub-like domain (ULD) and an elongated, α-helical scaffold/dimerisation domain (SDD) (Xu et al, 2011). The IKKs phosphorylate members of the inhibitor of κB (IκB) family directly, which normally sequester NF-κB in an inactive form in the cytosol. The phosphorylation of the IκB proteins induces their polyubiquitination, followed by their degradation by the 26 S proteasome (Scherer et al, 1995). NF-κB is then free to translocate to the nucleus to induce transcription of pro-inflammatory cytokines and IFNβ.

For TLRs 1, 2, 4 and 6 TIR domain-containing adaptor protein (TIRAP) is required to link ligand recognition to MyD88 (Horng et al, 2001). On the other hand, TLR4 is able to activate NF-κB via both MyD88-dependent and –independent pathways. At the cell surface TLR4 first recruits TIRAP and signals in a MyD88-dependent manner for the first round of activation. Following dynamin-dependent endocytosis TLR4 then engages the TIR domain-containing TRIF-related adaptor molecule (TRAM), which can recruit TRIF for a second wave of NF-κB, and also IRF3 signalling (Oshiumi et al, 2003b).

1.3.2.1 MyD88-dependent signalling

MyD88-dependent signalling occurs via the recruitment of IL-1R-associated kinase (IRAK) family of signalling proteins. IRAK4 is first recruited to MyD88, followed by the activation and recruitment of IRAK1 and IRAK2. Recently the crystal structure of the MyD88-IRAK4-IRAK2 complex was solved and was shown to consist of six molecules of MyD88 and four molecules of both IRAK4 and the IRAK2 death domain (Lin et al, 2010). This active signalling complex then interacts with TNF receptor-associated factor 6 (TRAF6), an E3 ubiquitin (Ub) ligase. TRAF6, along with the E2 Ub-conjugating enzymes Ubc13 and Uev1A, ubiquitinates itself and IRAK1, forming K63-linked polyUb chains (Deng et al, 2000). This leads to the recruitment and activation of the transforming growth factor-β (TGF-β)-activating kinase 1 (TAK1) complex, consisting of the kinase TAK1 and adaptor proteins TAB2 and TAB3. The adaptor proteins are essential for this recruitment as they bind Ub chains (Kanayama et al, 2004). Active TAK1 then promotes the downstream activation of the IKK complex.

1.3.2.2 TRIF-dependent signalling

In the case of TLR3-induced signalling, TRIF interacts directly with the TIR domain of this receptor (Oshiumi et al, 2003a). However, downstream of other PRRs an adaptor molecule is required to link to TRIF, such as TRAM in the case of TLR4 (Oshiumi et al, 2003b). Downstream of TRIF, TRAF6, RIP1 and TNF receptor type 1-associated death domain protein (TRADD) are recruited (Meylan et al, 2004). TRIF undergoes K63-linked polyubiquitination, activating the TAK1 complex, and further activating NF-κB via the IKK complex (see Figure 1.2).

1.3.2.3 RLR activation of NF-κB

Signalling downstream of the RLRs is achieved via MAVS, which has a TRAF-interaction motif allowing it to interact with TRAF6. A complex containing MAVS, TRADD, Fas-associated protein with death domain (FADD), caspase-8 and caspase-10 is recruited and this activates the IKK complex (Kumar et al, 2006; Takahashi et al, 2006) (see Figure 1.2).

1.3.2.4 Other pathways activating NF-κB

Other than recognition of pathogens by the TLRs and RLRs, engagement of the TNFR and IL-1R by their respective ligands initiates a signalling cascade leading to the activation of NF-κB. Signalling downstream of the TNFR involves the adaptor proteins TRADD and TRAF2. This leads to the activation of RIP, a kinase that can activate the TAK complex, subsequently activating the canonical IKK complex. Downstream of the IL-1R a different pathway is stimulated. This involves the adaptor MyD88, IRAK1 and IRAK4 and TRAF6, which ultimately activates the TAK complex as with TNF signalling (Verstrepen et al, 2008) (see Figure 1.2).

Other stimuli such as lymphotoxin-β (Dejardin et al, 2002), B cell-activating factor belonging to the TNF family (BAFF) (Claudio et al, 2002) and CD40L (Coope et al, 2002) trigger NF-κB activation through an alternative pathway which is dependent on IKKα, but independent of IKKβ and NEMO. This signalling cascade uses NF-κB-inducing kinase (NIK) rather than TAK1 (Xiao et al, 2004). NF-κB can also be activated downstream of NOD1 and NOD2 via

RIP2 and the subsequent activation of the canonical IKK complex (Park et al, 2007) (see Figure 1.2).

1.3.3 The IRF3 signalling pathway

In response to viral infection IRF3 and IRF7 are the most important transcription factors regulating type I IFN expression. IRF3 is expressed at high constitutive levels in most cells and is believed to be responsible for the early wave of IFNβ production (reviewed in (Taniguchi et al, 2001)). IRF3 shuttles to the nucleus via its nuclear localisation sequence (NLS), but due to the existence of a nuclear export signal (NES) it remains mainly cytoplasmic at steady state. IRF3 can be activated and induced to translocate to the nucleus downstream of a number of PRRs including TLRs 3 and 4, RLRs and cytoplasmic DNA sensors.

IRF3 is activated following phosphorylation by the non-canonical IKKs; TBK1, also known as NF-κB-activating kinase and TRAF2-interacting kinase, and IKKε, also known as inducible IKK (Fitzgerald et al, 2003; Sharma et al, 2003). Phosphorylation of a serine/threonine cluster in the C-terminal region of IRF3 induces a conformational change, revealing an IRF-association domain and DNA-binding domain, and allowing IRF3 to dimerise and bind to the promoters of IRF3-dependent genes. Phosphorylation also facilitates the association of IRF3 with cAMP response element-binding protein (CREB)-binding protein (CBP) and p300, further preventing the export of IRF3 to the cytoplasm (Lin et al, 1999b). A consensus motif in both IRF3 and IRF7 has been identified as a target for phosphorylation; SxSxxxS that is targeted by the non-canonical IKKs (Paz et al, 2006). Residues in IRF3 whose phosphorylation is critical for activation are Ser386 (Mori et al, 2004) and also Ser396 in response to stimulation by dsRNA (Servant et al, 2003).

Downstream of TLRs 3 and 4 the adaptor molecule TRIF recruits the non-canonical IKKs via another adaptor molecule TRAF3 (Oganesyan et al, 2006). In addition, TRAF3 links signalling downstream of the RLRs to the non-canonical IKKs by interacting with MAVS (Saha et al, 2006). The detection of cytosolic DNA downstream of DNA sensors leads to the activation of IRF3 in a pathway dependent on STING (Ishikawa et al, 2009) and TBK1 activation (Ishii et al, 2008). Finally, IRF3 can further be phosphorylated by the kinase Akt,

which is activated downstream of phosphatidylinositol-3 kinase (PI3K). TLR3 can be phosphorylated on two key tyrosine residues in response to its engagement with dsRNA and this recruits PI3K (Sarkar et al, 2004) (see Figure 1.3).

1.3.3.1 The non-canonical IKKs

The structure of the non-canonical IKKs, TBK1 and IKKε, are predicted to be highly similar to the canonical IKKs, IKKα and IKKβ. Despite a predicted structural similarity the enzymatic properties of these kinases are distinct and these proteins have different substrate preferences. In addition, the non-canonical IKKs require phosphorylation at serine 172 in the kinase activation loop for the induction of enzymatic activity (Kishore et al, 2002).

The involvement of the non-canonical IKKs in the phosphorylation of IRF3 took a number of years to uncover. Initially TBK1 was described as an NF-κB-activating kinase, based on the construction of TBK1-null mice, which died from massive liver apoptosis *in utero* (Bonnard et al, 2000), similar to mice with abrogated NF-κB signalling such as those deficient in p65 (Beg et al, 1995), IKKβ (Li et al, 1999a; Li et al, 1999b) or NEMO (Rudolph et al, 2000). TBK1 was also shown to target IKKβ *in vitro* (Tojima et al, 2000). Despite this earlier work, both non-canonical IKKs were later shown to target IRF3 *in vitro* (McWhirter et al, 2004). IRF3-dependent gene expression and type I IFN production in response to infection with Sendai virus (SeV) or NDV, or treatment of cells with dsRNA or LPS was reduced severely in TBK1-null MEFs, indicating a crucial role for this protein in IRF3 activation (Hemmi et al, 2004; McWhirter et al, 2004). On the other hand, MEFs deficient for IKKε showed no defect in IRF3 gene induction in these cells, but double knockout MEFs were completely devoid of IFN production (Hemmi et al, 2004). The authors concluded that IKKε might account for the residual gene expression remaining in TBK1-null MEFs. Supporting this proposal was the fact that IKKε partially compensates for the lack of TBK1, suggesting some functional redundancy between these two molecules (Hemmi et al, 2004).

The differential requirement for the non-canonical IKKs in deficient MEFs may be explained by the existence of cell-specific roles for these two proteins. Indeed the expression of the non-canonical IKKs differs, with TBK1 being constitutively expressed and IKKε expression being restricted to immune cells (Perry et al, 2004; Shimada et al, 1999). IKKε expression

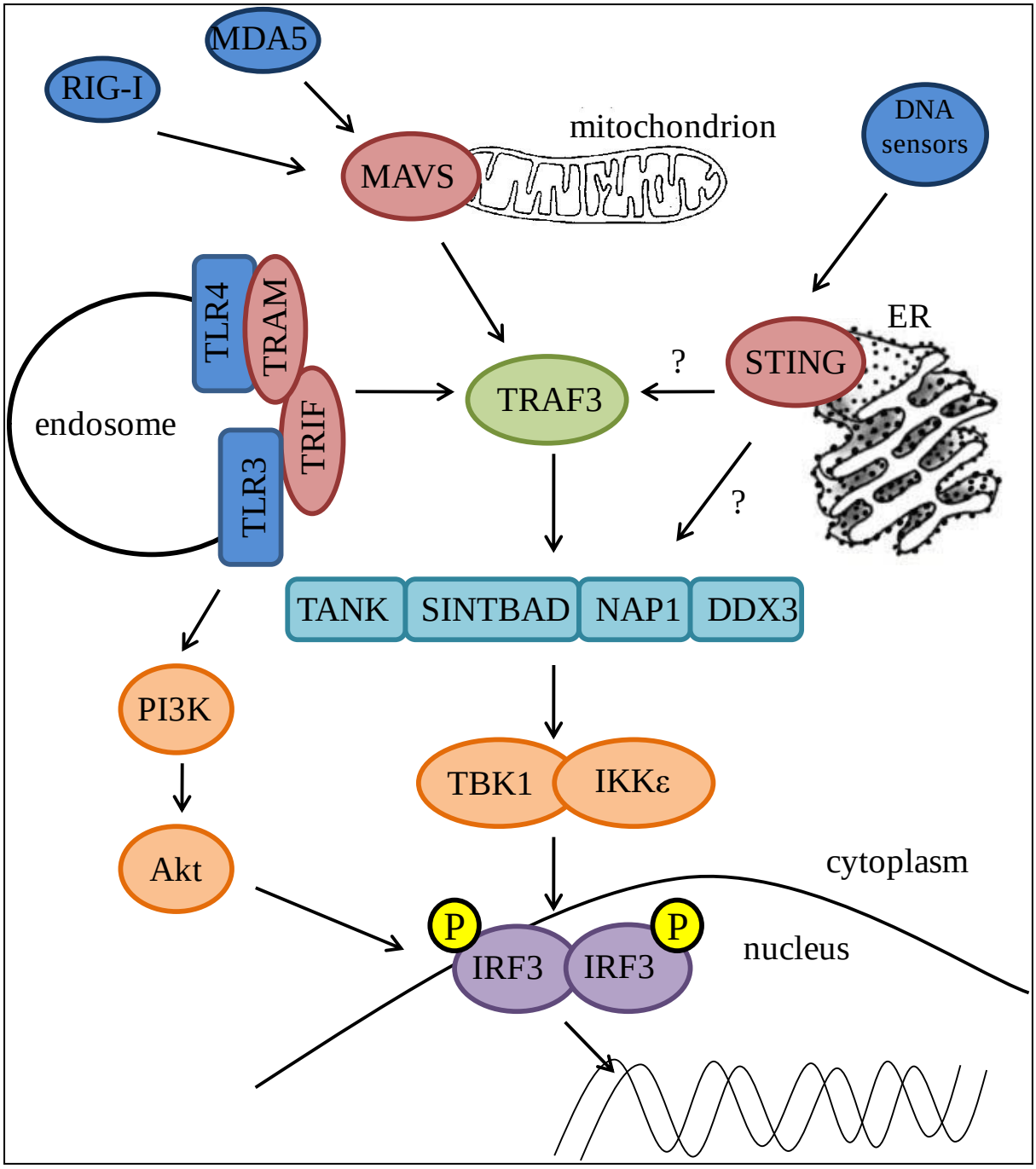

Figure 1.3: Overview of immune signalling pathways leading to IRF3 activation. Signalling downstream of TLRs, RLRs and cytoplasmic DNA sensors converges on the non-canonical IKKs; TBK1 and IKKε. These PRRs utilise various adaptors but generally require TRAF3 to co-ordinate upstream signalling events and the activation of TBK1 and IKKε, which in turn phosphorylate IRF3 causing it to dimerise and translocate to the nucleus. The adaptors TANK, SINTBAD, NAP1 and DDX3 have all been shown to play a role in activating IRF3 and are able to interact with the non-canonical kinases. TLR3 can activate IRF3 via an alternative pathway involving the kinases PI3K and Akt.

can also be induced in non-haematopoietic cells after pro-inflammatory stimulation and this was shown to be NF-κB dependent (Kravchenko et al, 2003). More recently, it has been demonstrated that IKKε is required for the transcription of a subset of ISGs because the IFN-stimulated gene factor 3 (ISGF3) complex, activated downstream of type I IFNs, failed to bind to the promoters of the affected genes including *Adar1*, *Ifit3* and *Ifi203* in IKKε-deficient cells. IKKε was found to phophorylate the signal transducer and activator of transcription 1 (STAT1) component of ISGF3 and this was required to induce binding to the promoters of these ISGs (Tenoever et al, 2007).

Whilst the composition of the heterodimeric canonical IKK complex has been well described and documented, it is currently unclear whether the non-canonical IKKs function in a similar manner or whether they function as separate homodimeric complexes. Given their different expression patterns and the differential requirement for these kinases in IRF3 activation the formation of homodimeric complexes seems more probable. Like the canonical IKKs, the non-canonical IKKs also seem to make use of non-enzymatic adaptor proteins. Rather than a single regulatory subunit, as is the case for the canonical IKKs, a number of potential adaptor proteins have been described to bind TBK1 and IKKε and contribute to IRF3 activation, including NF-κB-activating kinase-associated protein 1 (NAP1) (Fujita et al, 2003), similar to NAP1 TBK1 adaptor (SINTBAD) (Ryzhakov & Randow, 2007), TANK (Pomerantz & Baltimore, 1999) and DEAD box protein 3 (DDX3) (Soulat et al, 2008). This field is still in its infancy and although data would suggest that there is a differential requirement for the adaptor proteins downstream of distinct ligands, it remains unclear what these exact requirements are, which other signalling molecules are involved and whether functional redundancy exists. In addition, mechanistic data of how these adaptors might contribute to the activation of the kinases and subsequent downstream signalling is lacking. Recently, two splice variants of IKKε have been identified that are unable to activate IRF3. Both of these splice variants are able to form dimers with full-length IKKε and act in a dominant-negative manner (Koop et al, 2011). The lack of IRF3 activation by these molecules is likely due to their failure to interact with the adapter proteins TANK, NAP1, and/or SINTBAD, highlighting an important role for IKKε adaptor proteins in IRF3 activation.

1.3.3.2 TANK

Like the non-canonical IKKs, TANK, also known as I-TRAF, was thought originally to have a role in the NF-κB pathway as a TNFα-induced NF-κB activator (Rothe et al, 1996). TANK associated with TRAF2, but when phosphorylated by either of the non-canonical IKKs this interaction was lost allowing TRAF2 to activate NF-κB via the canonical IKK complex (Nomura et al, 2000; Pomerantz & Baltimore, 1999). Further support for a role for this molecule in the NF-κB pathway came from the demonstration that TANK also interacts with NEMO (Chariot et al, 2002), an interaction that is regulated negatively by the phosphorylation of TANK by IKKβ following TNFα stimulation (Bonif et al, 2006). Furthermore the knockdown of TANK by RNA interference (RNAi) reduced the induction of a subset of NF-κB target genes in response to TNFα treatment (Bonif et al, 2006; Gatot et al, 2007). This reduction was only observed for a subset of genes and this may be explained by later work from a number of groups indicating that the non-canonical IKKs, in addition to the canonical IKKs, contribute to NF-κB activation by directly phosphorylating numerous NF-κB family members (Adli & Baldwin, 2006; Harris et al, 2006; Mattioli et al, 2006; Wietek et al, 2006). TANK may therefore act to connect upstream signals, for example via TRAF2 and/or NEMO to the activation of the non-canonical kinases, thus promoting canonical IKK-independent phosphorylation of NF-κB inhibitory proteins.

TANK also has an important role in IRF3 activation and interacts constitutively with both TBK1 (Pomerantz & Baltimore, 1999) and IKKε (Nomura et al, 2000). TANK knockdown in cells infected with SeV exhibited defective IFNβ production (Guo & Cheng, 2007) and TANK was important for IRF3 phosphorylation through the TLR4 pathway in LPS-responsive cells such as macrophages (Gatot et al, 2007). TANK is subject to phosphorylation and non-degradative polyubiquitination in a stimulus-dependent manner (Gatot et al, 2007). The phosphorylation of TANK is mediated by the non-canonical IKKs and these molecules are also required for LPS-mediated TANK polyubiquitination, although their kinase activity is dispensable. The E3 ligase involved in this polyubiquitination is yet to be identified. Both the non-canonical IKKs have a ULD that is crucial for substrate recognition and kinase activity, but this has not been shown to bind to known Ub-binding domains so far (Ikeda et al, 2007).

In addition to the non-canonical IKKs, TRAF2 and NEMO, TANK interacts with a number of other signalling proteins. TANK is known to be part of a trimeric complex including TRAF3 and TBK1, which is predicted to link upstream signalling via TRAF3 to the activation of the non-canonical IKKs (Gatot et al, 2007). Following viral infection, TANK is part of complexes containing MAVS or TRIF, and TRAF3 and TBK1 (Guo & Cheng, 2007). Furthermore TANK interacts with the IRFs themselves. Gatot and colleagues found an interaction of TANK with IRF3 and also identified IRF7 as a TANK-interacting protein through yeast two-hybrid analyses (Gatot et al, 2007). Furthermore they showed that IRF7 was phosphorylated by a TANK-containing immune complex in macrophages treated with a TLR9 ligand. Finally TANK has also been shown to homo-dimerise (Chin et al, 1999; Ryzhakov & Randow, 2007).

Although the structure of TANK is yet to be solved it is predicted to consist of a single coiled-coil domain at the N terminus, which may be involved in TANK oligomerisation (Chin et al, 1999). A domain in the centre of the molecule is critical for binding to TBK1, termed the TBK1-binding domain (TBD). This region is predicted to be α-helical and is shared amongst TANK, SINTBAD and NAP1 (Ryzhakov & Randow, 2007). The binding of TANK to TRAF2 and TRAF3 involves residues 170 to 191 of TANK (Gatot et al, 2007). At the C terminus of TANK there is a Zinc finger domain, which in addition to the N terminus of the molecule (residues 31 to 70), is important for binding to NEMO (Gatot et al, 2007) (see Figure 1.4).

1.3.3.3 NAP1

NAP1 was identified as a TBK1-interacting protein with structural similarity to TANK (Fujita et al, 2003). In this study NAP1 over-expression enhanced induction of an NF-κB-dependent reporter gene, and *in vivo* depletion reduced this expression. With regards to the IRF3 pathway, the knockdown of NAP1 by RNAi revealed a role for this protein in IFNβ promoter activation downstream of poly I:C or infection with RSV or VSV (Sasai et al, 2005; Sasai et al, 2006). These studies revealed NAP1 to be important downstream of RIG-I, and in the TLR3 and TLR4 pathways it acted downstream of TRIF. Furthermore an interaction between NAP1 and TRIF has been suggested (Funami et al, 2007; Tatematsu et al, 2010). Supporting these findings, RNAi knockdown of NAP1 also caused defects in SeV-induced

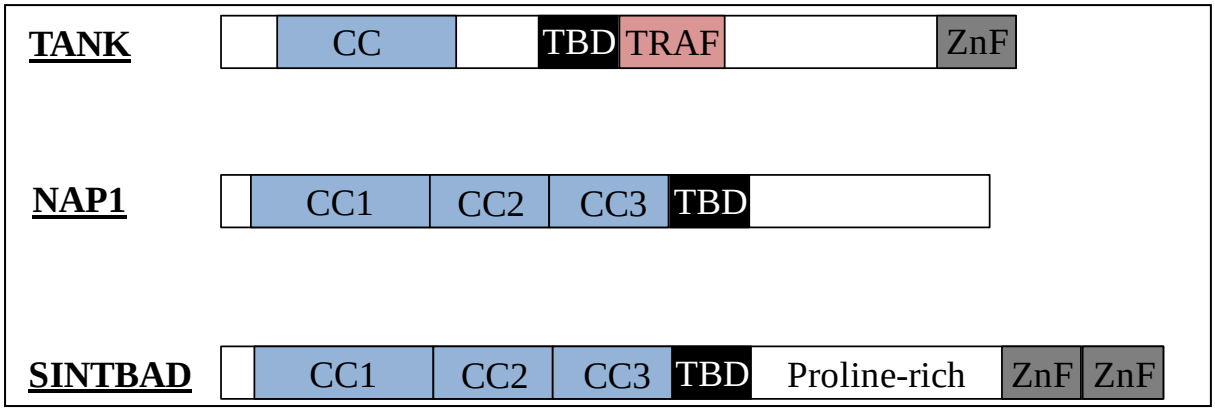

Figure 1.4: Domain composition of TANK, SINTBAD and NAP1. Schematic representation of the domain composition of the three related non-canonical IKK complex adaptor proteins. CC: coiled-coil, TBD: TBK1-binding domain, TRAF: region where the interaction with TRAF2 and TRAF3 has been mapped, ZnF: Zinc finger domain.

activation of an interferon-stimulated response element (ISRE) reporter plasmid (Ryzhakov & Randow, 2007). NAP1 also binds to nuclear dot protein 52 kDa (NDP52), an autophagy receptor that binds to Ub-coated *Salmonella typhirium* (Thurston et al, 2009). The binding of NAP1 to NDP52 links the detection of *S. typhirium* to TBK1. NAP1 consists of three N-terminal coiled-coil regions and a TDB, but lacks a C-terminal Zinc finger domain (see Figure 1.4). Like TANK it is able to oligomerise, and also showed some weak interaction with SINTBAD, but not TANK (Ryzhakov & Randow, 2007).

1.3.3.4 SINTBAD

SINTBAD is the most recently identified of the three related adaptors. Like NAP1 and TANK, SINTBAD binds constitutively to both IKKε and TBK1 via its TBD and is believed to have a role in IRF3 activation because RNAi knockdown of this protein led to a reduction in ISRE reporter activity following infection of cells with SeV (Ryzhakov & Randow, 2007). Like NAP1, SINTBAD binds to NDP52, thus contributing to the immune response to infection by *Salmonella spp*. (Thurston et al, 2009). SINTBAD consists of three N-terminal coiled-coil regions, a TBD, a proline-rich region and two C-terminal Zinc finger domains (see Figure 1.4). Like the other related adaptors it is able to oligomerise, and also showed some weak interaction with NAP1, but not TANK (Ryzhakov & Randow, 2007).

1.3.3.5 DDX3

DDX3 is a member of the DEAD-box helicase family whose members have roles in a wide variety of RNA-related cellular processes, including RNA splicing, mRNA export, transcriptional and translational regulation, RNA decay and ribosome biogenesis (Rocak & Linder, 2004). This protein was also implicated in innate immune signalling by its identification as a host binding partner for VACV protein K7, an inhibitor of IFNβ induction downstream of multiple PRRs (see 1.4.5.1.5) (Schroder et al, 2008). DDX3 was shown to associate transiently with IKKε after virus stimulation and knockdown of this protein by RNAi led to a decreased induction of the IFNβ promoter and IRF3/7-mediated transactivation. Furthermore, DDX3 was identified as a TBK1 phosphorylation target and associated with the IFNβ promoter after PRR stimulation, suggesting an additional role for this protein as a transcriptional cofactor. (Soulat et al, 2008). Recently, DDX3 was identified in a yeast two-hybrid screen as a protein that interacts with the CARD domain of MAVS, implicating it in the signalling pathway downstream of the RLRs (Oshiumi et al, 2010). Like all DEAD-box helicases, DDX3 binds to RNA and potentially also to DNA (Franca et al, 2007). Oshiumi et al thus suggest that DDX3 acts as a sensor of viral RNAs and interacts with the RLRs, RIG-I and MDA5 (Oshiumi et al, 2010). Unlike RIG-I, the constitutive levels of DDX3 are relatively high and therefore the authors suggest that DDX3 senses viral RNA and facilitates signalling through MAVS at the very early stages of infection when RIG-I levels are low. Data implicating the role of this protein to the activation of type I IFN *in vivo* is currently lacking.

1.3.4 Crosstalk of the IKKs and immune regulation

It has become apparent over recent years that although the canonical IKKs and the non-canonical IKKs have unique physiological substrates, such as IκBα, p105 and RelA for the canonical IKKs, and IRF3 for the non-canonical IKKs, they also share some common substrates such as NEMO and TANK (Clark et al, 2011). In addition, a number of molecules now known to have an important role in IRF3 activation were first identified as having roles in NF-κB signalling. For example, TBK-1 was characterised as an IKK homologue involved in TNFα-mediated NF-κB activation (Bonnard et al, 2000; Pomerantz & Baltimore, 1999), acting upstream of IKKβ (Tojima et al, 2000). Both TANK (Rothe et al, 1996) and NAP1

(Fujita et al, 2003) were also shown to play a role in NF-κB dependent gene transcription. Indeed, the canonical IKKs can directly phosphorylate and activate the non-canonical IKKs (Clark et al, 2011; Tenoever et al, 2007), whereas the non-canonical IKKs phosphorylate both the canonical IKKs and the regulatory subunit NEMO, which is associated with reduced IKK activity and NF-κB-dependent gene transcription (Clark et al, 2011). This is an example of how the activation of one pathway can impact negatively on the activation of another pathway, which is an important mechanism contributing to immune regulation. A direct link between the two pathways was also provided when the interaction between TANK and NEMO was discovered (Chariot et al, 2002; Zhao et al, 2007).

In addition to crosstalk between the IKK complexes, the NF-κB and IRF3 signalling pathways also share some common molecules. A20 regulates negatively both signalling pathways by promoting the K48-linked degradative polyubiquitination of RIP1 (Wertz et al, 2004) and preventing IRF3 dimerisation through direct binding to the non-canonical IKKs (Saitoh et al, 2005). TRAF3 on the other hand positively regulates TLR- and RLR-dependent IRF3 activation, but negatively regulates the alternative NF-κB pathway involving NIK and IKKα (Hauer et al, 2005).

1.3.5 Other IRFs in innate immunity

Another transcription factor important for the induction of the type I IFNs is IRF7. Unlike IRF3, IRF7 is present at much lower levels in uninfected or unstimulated cells, but its expression can be induced following infection or stimulation with poly I:C. Several pathways contribute to the activation of IRF7. TBK1 and IKKε are able to phosphorylate and activate IRF7 in a manner very similar to IRF3 and therefore ligands that activate these non-canonical IKKs activate IRF7 subsequently (Sharma et al, 2003). In pDCs an alternative pathway of IRF7 activation exists and IRF3 is dispensable for the induction of type I IFNs (Honda et al, 2005). These cells express much higher levels of IRF7 than monocyte-derived DCs (Izaguirre et al, 2003) and when stimulated with TLR7 and TLR9 PAMPs, IKKα is induced to phosphorylate and activate IRF7. This pathway involves the signalling proteins MyD88, IRAK1, IRAK4 and TRAF6 (Kawai et al, 2004). Other proteins such as osteopontin (a protein induced after stimulation with TLR9), PI3K, mTOR and p70S6K also play critical roles in IRF7 activation.

IRF5 may also play an important role in the production of pro-inflammatory cytokines. Induction of TNF, IL-6 and IL-12 by various TLR ligands was impaired severely in a number of cell types from IRF5-deficient mice (Takaoka et al, 2005).

1.3.6 MAPK signalling pathways

A further pathway that can be activated downstream of PRRs is the MAPK pathway, which leads to the activation of key transcription factors such as activating transcription factor 2 (ATF-2) and c-JUN, which together form AP-1 and contribute to the transcription of IFNβ. MAPKs are a family of serine/threonine kinases that require phosphorylation on both threonine and tyrosine residues to be activated. Phosphorylation of MAPKs occurs via an ordered signalling cascade where MAPK kinases (MAP2Ks) phosphorylate and activate MAPKs, and MAPK kinase kinases (MAP3Ks) phosphorylate MAP2Ks (Kyriakis & Avruch, 2001).

MAPKs are activated by signalling downstream of TLRs via TAK1. In addition to activating the canonical IKK complex, TAK1 (a MAP3K) can phosphorylate and activate the MAP2Ks, MKK3 and MKK6. These kinases act upstream of p38 MAPKs and c-Jun NH_2-terminal kinase (JNK), which then activate AP-1 (Holtmann et al, 2001). MAPKs are also activated downstream of the RLRs, a pathway that requires MAVS, TRAF6 and the MAP3K MEKK1 (Yoshida et al, 2008). Other transcription factors activated by the MAPK signalling pathway are c-Fos, Elk-1 and c-Myc (Kyriakis & Avruch, 2001).

1.3.7 IFNs

IFNs are cytokines that induce an antiviral state and can inhibit viral growth. IFN genes have been cloned from mammals, birds and fish, and some IFN-like activity has also been detected in amphibians (Schultz et al, 2004). In mammals the IFNs are divided into three types.

1.3.7.1 Type I IFNs

Type I IFNs include numerous IFNα proteins and a single IFNβ protein. The expression of these IFNs can be induced in most cell types. In addition IFNω, IFNε, IFNκ, IFNτ and IFNξ

are also type I IFNs but are expressed in a cell-type and species-specific manner. pDCs are the major producers of IFNα, and expression requires the activation of IRF7 (Honda et al, 2005). Transcription of IFNβ requires the formation of a large multi-protein complex called the enhanceosome, comprising several transcription factors, structural components such as the architectural protein HMG I(Y), which binds to the nucleosome-free positive regulatory domains of the promoter (Merika & Thanos, 2001), and basal transcription machinery (Agalioti et al, 2000; Thanos & Maniatis, 1995). The transcription factors required for IFNβ transcription are NF-κB, IRFs, in particular IRF3 and AP-1.

All type I IFNs bind the heterodimeric IFNα/β receptor (IFNAR) consisting of IFNAR1 and IFNAR2c. Upon engagement of the IFNAR a Janus tyrosine kinase (JAK)-STAT signalling pathway is initiated. The JAKs TYK2 and JAK1 are first recruited, phosphorylating each other and then the transcription factors STAT1 and STAT2. The STATs forms a heterodimer and associate with IRF9, forming the ISGF3 complex. This then translocates to the nucleus and binds to the promoter of ISGs with an ISRE (see Figure 1.5). Importantly, type I IFNs contribute to DC and macrophage activation and the up-regulation of MHC class I molecules (Fensterl & Sen, 2009).

1.3.7.2 Type II IFN

IFNγ is the only type II IFN and is mainly produced by activated T cells and NK cells. It is unrelated to the type I IFNs and is not produced in direct response to PAMPs. Instead IFNγ production is stimulated by IL-12 and IL-18 (which was called IFNγ-inducing factor originally), two cytokines produced by activated macrophages. IFNγ induction requires the transcription factors NF-κB, AP-1 and nuclear factor of activated T cells (NFAT). This IFN uses the heterodimeric IFNγ receptor (IFNGR) to initiate a signalling cascade. Dimeric IFNγ binds to IFNGR1, resulting in a complex that is stabilised by IFNGR2. In this instance the JAK-STAT pathway involves JAK1 and JAK2, which phosphorylate STAT1 inducing it to homodimerise and form the gamma-activated factor (GAF). This complex then translocates to the nucleus and binds to ISGs with a gamma-activated site (GAS) (Fensterl & Sen, 2009) (see Figure 1.5). The expression of type II IFN contributes to the transition from innate to adaptive responses by inducing the transcription factors IRF1 and CIITA, which govern MHC class II expression. In addition IFNγ regulates NK and B cell functions and

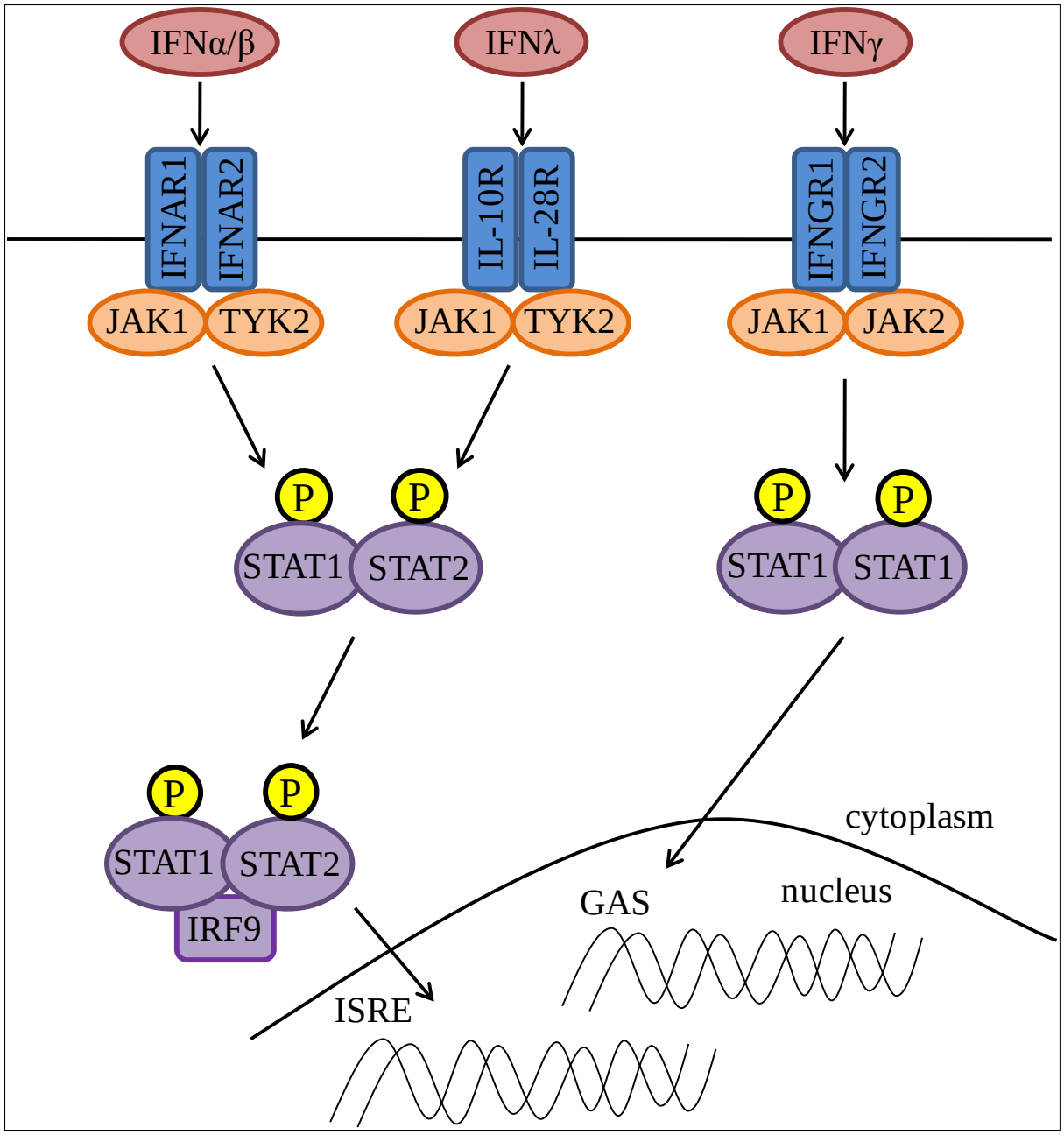

Figure 1.5: Overview of the intracellular signalling cascades induced by the IFNs. The binding of IFNα or IFNβ to the IRNAR (consisting of IFNAR1 and IFNAR2), and the binding of IFNλ to the heterodimeric IL-10R/IL28R initiates JAK-STAT signalling cascades involving JAK1 and TYK2. Once activated, these kinases phosphorylate STAT1 and STAT2, which can then interact with IRF9 to form the ISGF3 complex. This translocates to the nucleus to induce the expression of ISRE-dependent genes. The binding of IFNγ to the IFNGR (consisting of IFNGR1 and IFNGR2) on the other hand initiates a cascade involving JAK1 and JAK2, which phosphorylate STAT1, causing it to homo-dimerise and form the GAF complex. This then translocates to the nucleus, inducing the expression of GAS-dependent genes.

macrophage activation (reviewed in (Schroder et al, 2004)). IFNγ is an important cytokine promoting the T_{H1} cell-mediated adaptive immune response.

1.3.7.3 Type III IFNs

The type III IFNs comprise IFNλ1, 2 and 3, also known as IL-29, IL-28A and IL-28B respectively. These IFNs, like the type I IFNs are produced by most cell types in response to infection, and particularly by epithelial cells. Upon binding of a type III IFN to the heterodimeric IFNλ receptor, also known as IL10R2, a JAK-STAT signalling cascade is initiated, identical to that induced by the type I IFNs, leading to the activation of ISGF3 and its subsequent binding to the ISRE of ISGs (Fensterl & Sen, 2009) (see Figure 1.5).

1.3.8 Actions of ISGs

ISGs encode proteins that can directly impact on viral clearance, bring about an antiviral state in the cell and regulate the induction of an adaptive immune response. In addition ISGs include innate immune molecules such as RIG-I, TLR3, DAI, IRF7 and STAT1, whose up-regulation leads to an increased sensitivity of cells to PAMPs. Numerous ISRE-driven genes can be induced by virus-activated IRF3 directly due to sequence similarity in IRF elements and ISREs, providing an immediate ISG induction in infected cells (Andersen et al, 2008; Elco et al, 2005).

1.3.8.1 PKR

dsRNA-activated protein kinase (PKR) is constitutively expressed at low levels in many cell types and its expression is up-regulated rapidly by IFN. PKR becomes activated upon binding to dsRNA, causing dimerisation and autophosphorylation. Active PKR then phosphorylates translation initiation factor 2α (eIF2α), thus inhibiting all protein synthesis (Balachandran et al, 2000). PKR also inhibits the replication of RNA viruses such as VSV, encephalomyocarditis virus (EMCV) and hepatitis C virus, as well as the DNA virus HSV-1. Further PKR has been identified as a regulator of cytokine expression following viral infection or treatment of cells with poly I:C (Gilfoy & Mason, 2007; Silva et al, 2004).

1.3.8.2 2’-5’-OAS

2’-5’-Oligoadenylate synthetases (2’-5’-OAS) also require binding to dsRNA for activation. These enzymes synthesise 2’-5’-linked adenosine monophosphate (AMP)-oligomers from adenosine triphosphate (ATP), and these activate the latent ribonuclease, RNAseL. Upon activation, this enzyme dimerises and cleaves both cellular and viral ssRNA, thus inhibiting protein expression (Silverman, 2007). This has been demonstrated to be particularly effective against EMCV and influenza A virus infections. The cleavage products of RNAse L also act as ligands for RIG-I, further activating the innate immune response (Malathi et al, 2007).

1.3.8.3 MxA

Human MxA accumulates at cellular membranes around the nucleus, binds to viral nucleocapsids and inhibits viral intracellular trafficking. It is a particularly important defence mechanism against infection with influenza virus, measles virus, VSV and Semliki Forest virus. MxA forms a ring-like structure that surrounds the influenza virus nucleocapsid and inhibits viral trafficking, transcription and genome replication (Haller & Kochs, 2011).

1.3.8.4 APOBEC3 proteins

APOBEC3F and APOBEC3G are deoxycytidine deaminases and thus nucleic acid-editing enzymes. These proteins play an important role in inhibiting retroviruses by introducing C to U mutations in viral reverse transcribed DNA, or by directly interfering with reverse transcription (Aguiar & Peterlin, 2008; Bishop et al, 2004).

1.3.8.5 ISG15

ISG15 is a Ub-like protein that can be attached to a number of molecules involved in the innate immune response including JAK1, STAT1, RIG-I, PKR and RNase L (Zhao et al, 2005). ISG15 plays an important role in modulating signalling cascades much like K63-linked ubiquitination. The addition of ISG15 to IRF3 prevents its degradation and therefore enhances the IFN response (Lu et al, 2006). VACV Western Reserve (WR) infection is

enhanced in ISG15-null MEFs suggesting an important role for this protein in controlling poxviral infection (Guerra et al, 2008).

1.4 VACV and modulation of the immune response

1.4.1 VACV-specific immunity and detection

An extensive study in both human and mouse macrophages demonstrated that MDA-5, TLR2-TLR6 and the NALP3 inflammasome play an important role in the response to infection by VACV strain MVA. Deletion or knockdown of any of these components by RNAi led to a large defect in the production of IFNβ and pro-inflammatory cytokines and chemokines. MAVS was also demonstrated to contribute to MVA detection in these cells, but RIG-I was found to be dispensable (Delaloye et al, 2009). In addition, the cytoplasmic DNA sensors IFI16 (Unterholzner et al, 2010) and DNA-PK (B. Ferguson et al, submitted) contribute to IFNβ induction in response to infection with VACV strain MVA.

Both type I (Rodriguez et al, 1991) and type II (Huang et al, 1993) IFNs are crucial for the restriction of poxviral infections and mice deficient in IFN receptors are highly susceptible to VACV infection (van den Broek et al, 1995). In addition, type III IFN plays an important role against VACV *in vivo* because recombinant VACVs strain WR expressing either IFN-λ2 or IFN-λ3 were attenuated in a mouse intranasal (i.n.) infection model (Bartlett et al, 2005).

In addition, cells of the innate immune system play a critical role in poxvirus infection. Mice depleted of macrophages are unable to control ectromelia virus (ECTV) infection due to impaired virus clearance and antigen presentation (Karupiah et al, 1996). Furthermore, NK cells have a direct cytotoxic activity against VACV-infected cells *in vitro* (Brutkiewicz et al, 1992) and depletion of these cells *in vivo* increased disease caused by VACV (Bukowski et al, 1983). During VACV infection, complement is activated via the alternative pathway (Leddy et al, 1977) and IMV is sensitive to complement in the absence of Ab.

To establish a productive infection VACV must therefore counteract the innate immune response. The activation of NF-κB, IRFs and MAPKs leading to the induction of IFNs and inflammation clearly contributes to controlling infection because VACV has evolved a

multitude of mechanisms to counteract this. Not only does VACV inhibit the induction of these inflammatory mediators, their actions and the recruitment of immune cells, it also has measures to inhibit apoptosis and complement.

1.4.2 Inhibition of apoptosis

Several poxviral proteins have anti-apoptotic functions. The serine protease inhibitor (serpins) are a group of enzymes that regulate the function of several proteolytic enzymes involved in a range of cellular processes such as complement activation, inflammation and apoptosis. VACV encodes three serpins; SPI-1 (protein B22) and SPI-2 (protein B13) and SPI-3 (protein K2). SPI-2 has been described to inhibit apoptosis triggered by TNFα or Fas ligand, and inhibits caspase-1 function (Kettle et al, 1997). The CPXV orthologue of SPI-2, cytokine response modifier (Crm)A, in addition to inhibiting caspase-1 (Ray et al, 1992) is also a potent inhibitor of caspase-8 (Zhou et al, 1997). Furthermore, CrmA binds granzyme B, thus inhibiting apoptosis induced by lytic granules released by CTLs (Quan et al, 1995). Deletion of the rabbitpox virus (RPXV) counterpart of SPI-1 caused A459 cells to undergo apoptosis, suggesting that this viral serpin may also contribute to apoptosis inhibition (Brooks et al, 1995).

Deletion of the CPXV gene encoding the protein CP77 caused Chinese hamster ovary (CHO) cells infected by the CPXV deletion mutant to undergo apoptosis whereas CHO cell infected by WT CPXV did not, indicating a role for this protein in the inhibition of apoptosis (Ramsey-Ewing & Moss, 1998). Furthermore the deletion of E3, a host range factor, led to accelerated apoptosis in restricted cells (Kibler et al, 1997). Protein F1, which adopts a Bcl-2 fold, exerts its anti-apoptotic function by binding to a subset of BH3-containing death ligands and subsequently interfering with cytochrome *c* release (Kvansakul et al, 2008; Stewart et al, 2005). This protein also inhibits caspase-9 (Zhai et al, 2010). A second VACV protein that adopts a Bcl-2 fold and inhibits apoptosis is N1, which binds a subset of cellular pro-apoptotic Bcl-2 proteins (Cooray et al, 2007). In addition, myxoma virus expresses a protein with a Bcl-2 fold, M11 (Douglas et al, 2007), which also has a role in apoptosis inhibition (Everett et al, 2000). Viral Golgi anti-apoptotic protein (vGAAP) is able to protect cells from apoptosis induced by both intrinsic and extrinsic pathways (Gubser et al, 2007).

1.4.3 Inhibition of soluble immune factors

1.4.3.1 Inhibition of cytokine activity

The first viral cytokine receptor or binding protein to be identified was from a poxvirus. The Shope fibroma counterpart of VACV protein A53 is a soluble TNF receptor that binds TNFα and inhibits its actions (Smith et al, 1991a). In the same year, two proteins from VACV strain WR were shown to be related to the IL-1 receptor (Smith & Chan, 1991) and, subsequently, one of these (B15) was shown to be a secreted protein that bound IL-1β (Alcami & Smith, 1992; Spriggs et al, 1992). This protein is specific for IL-1β, and did not bind IL-1α or the IL-1 receptor antagonist protein, a selectively which later led to the characterisation of IL-1β as the major endogenous pyrogen activated during a poxvirus infection (Alcami & Smith, 1996). Further, the myxoma virus counterpart of VACV protein B8 is a soluble IFNγ receptor (Upton et al, 1992) (see Figure 1.6). All of these proteins have sequence similarity to the extracellular binding domains of the host cytokine receptors, but lack the transmembrane and signalling domains. VACV B18, which can be secreted or surface bound encodes a type I IFN binding protein (Colamonici et al, 1995; Symons et al, 1995) (see Figure 1.6), whereas as protein C12 binds to IL-18 and blocks its activity (Smith et al, 2000). C12 is related to both the human and mouse IL-18 binding proteins, which regulate IL-18 activity negatively by preventing IL-18 from binding to its receptor and inducing IFNγ induction (Novick et al, 1999). VACV protein A39 is a viral semaphorin that is secreted and binds to a virus encoded semaphorin receptor in macrophages, inducing the expression of cytokines (Comeau et al, 1998). This protein therefore has a pro-inflammatory effect in these cells. A39 binds to the semaphorin receptor plexin C1 found on DCs and inhibits integrin-mediated adhesion and spread, including phagocytosis (Walzer et al, 2005).

1.4.3.2 Chemokine inhibition

A number of poxviruses express a viral CC chemokine inhibitor (vCCI), which is unrelated to any known cellular proteins but binds CC chemokines with a high affinity (Lalani & McFadden, 1997; Smith et al, 1997a). vCCI is secreted from infected cells, binds to multiple CC chemokines including CCL2, CCL3, CCL5 and CCL11 and inhibits their functions (Alcami et al, 1998). The expression of vCCI inhibits eosinophil recruitment (Alcami et al, 1998) and leukocyte recruitment *in vivo* leading to decreased morbidity of mice and reduced

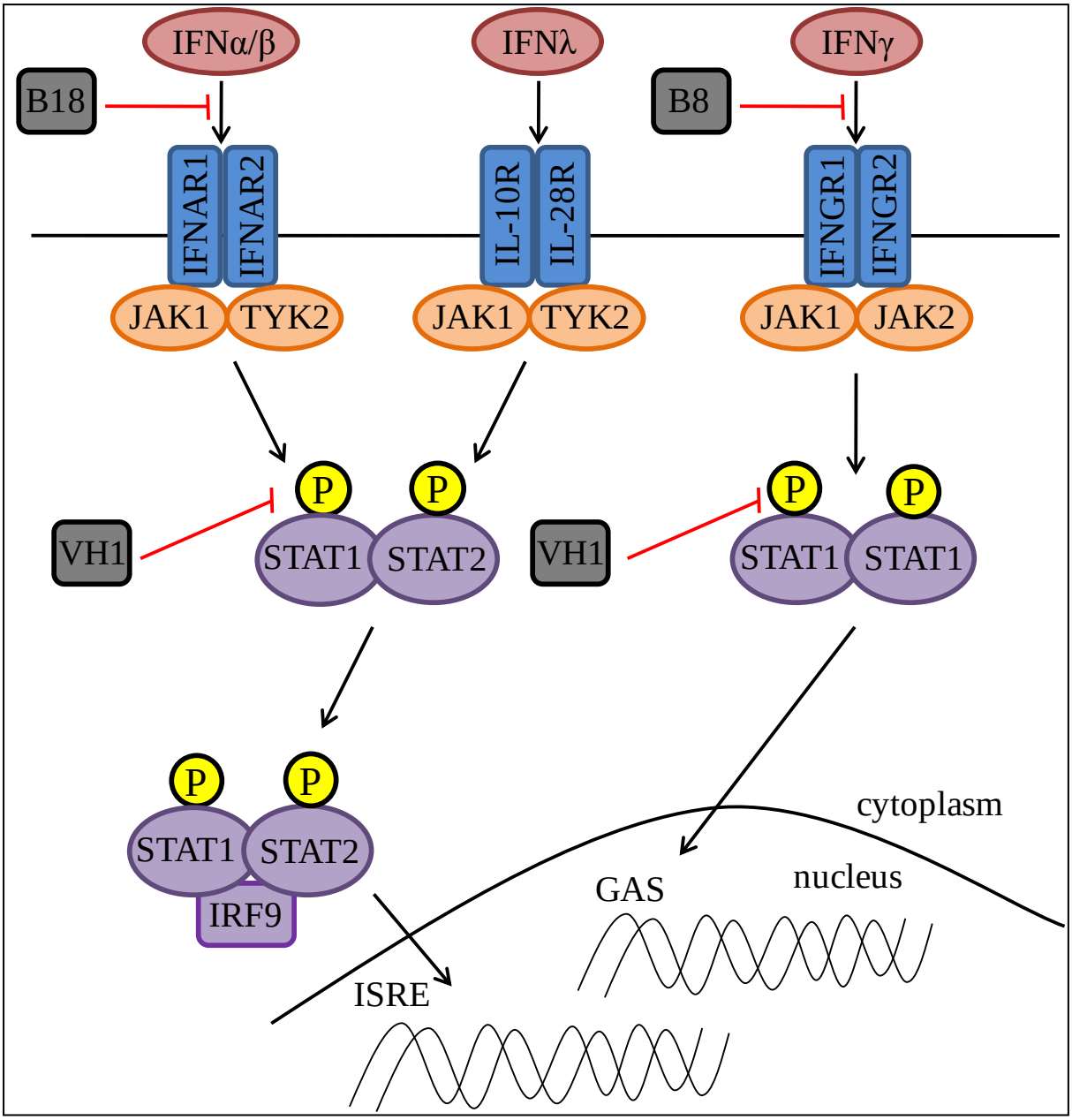

Figure 1.6: VACV inhibition of IFN signalling. VACV inhibits the actions of IFNs both intracellularly and extracellularly. B18 is secreted from cells and encodes a type I IFN binding protein, which binds IFNα and IFNβ, thus preventing them from engaging the IFNAR. B8 encodes a soluble IFNGR, which also functions extracellularly, binding IFNγ and preventing it from engaging its receptor. VH1 phosphatase on the other hand acts within cells, de-phosphorylating both STAT1 and STAT2 and thus preventing their translocation to the nucleus.

weight loss from VACV infection (Reading et al, 2003). VACV protein A41 shares some sequence similarity with vCCI and also binds to CC chemokines including CCL21, CCL25, CCL26 and CCL28 (Bahar et al, 2008). This glycoprotein is non-essential for replication but is a virulence factor *in vivo* (Ng et al, 2001).

1.4.3.3 Inhibition of complement

Protein C21, or VACV complement control protein (VCP) provides an effective countermeasure against the effects of complement during a VACV infection. C21 binds to both C3b and C4b, accelerating their decay and thus inhibiting both the classical and alternative complement pathways (Kotwal et al, 1990; Sahu et al, 1998). This protein shows amino acid similarity to human complement regulators such as factor H and C4b-binding protein. Functional studies demonstrated that VCP protects virions from Ab-dependent complement-mediated neutralization, and mutant viruses lacking this gene are attenuated *in vivo* (Isaacs et al, 1992). VACV incorporates the host complement proteins CD46, CD55 and CD59 into the EEV outer membrane, thus rendering it resistant to complement attack (Vanderplasschen et al, 1998).

1.4.4 Inhibition of inflammasomes

VACV WR protein B13/SPI-2 blocks caspase-1 activity and therefore inhibits inflammasome-mediated cleavage of proIL-1β or pro-IL18 (Dobbelstein & Shenk, 1996; Kettle et al, 1997). Myxoma protein M13, a PYD-containing protein, is also able to inhibit inflammasome activity by binding to ASC via a PYD-PYD interaction. This then inhibits caspase-1 activation with a similar downstream effect to SPI-2 (Johnston et al, 2005). A homologue of this protein is found in Shope fibroma virus (S013), but not in other poxviruses (Dorfleutner et al, 2007).

1.4.5 Evasion of intracellular innate immune signalling cascades

1.4.5.1 The VACV Bcl-2 family

Originally, VACV strain WR protein N1 was described as a secreted protein that contributes to virulence (Kotwal et al, 1989) but was shown subsequently to be an intracellular homo-dimer (Bartlett et al, 2002). Later N1 was described as an inhibitor of intracellular signalling pathways leading to the activation of IRF3 and NF-κB (DiPerna et al, 2004). In 2007 the crystal structure of N1 was determined and revealed a Bcl-2 fold (Aoyagi et al, 2007; Cooray et al, 2007). Cooray et al also demonstrated that the N1 protein had anti-apoptotic activity (Cooray et al, 2007). The following year structural studies revealed VACV proteins B14, A52 (Graham et al, 2008), K7 (Kalverda et al, 2008) and F1 (Kvansakul et al, 2008) also had Bcl-2 structures. Although F1 was found to have anti-apoptotic properties (Kvansakul et al, 2008), B14 and A52 lacked this function (Graham et al, 2008). Structural analyses identified a surface groove in cellular anti-apoptotic Bcl-2 proteins that binds BH3 peptides (Youle & Strasser, 2008) and a similar groove is conserved in proteins N1 and F1 (Cooray et al, 2007, Kvansakul et al., 2008). This groove is lacking in B14 and A52 and hence they are not anti-apoptotic (Graham et al., 2008). Instead these proteins (Bowie et al, 2000; Chen et al, 2008), in addition to K7 (Schroder et al, 2008) interfere with intracellular immune signalling cascades (see Figures 1.7 and 1.8).

Phylogenetic analysis indicates that these genes may have arisen from the acquisition of an ancestral mammalian gene encoding an anti-apoptotic Bcl-2 protein, followed by gene duplication and diversification, allowing these Bcl-2 proteins to inhibit innate immune signalling cascades rather than apoptosis (Graham et al, 2008). Interestingly phylogenetic analysis places N1, which is both anti-signalling and anti-apoptotic, as an evolutionary intermediate between F1, which is anti-apoptotic and does not have anti-signalling capacity, and B14 and A52 which are only anti-signalling. Subsequently, structural-based predictions indicated that VACV encodes additional Bcl-2-like proteins including A46, C6, C1, C16/B22 and N2 (Gonzalez & Esteban, 2010; Graham et al, 2008), of which A46 had also already been described to inhibit NF-κB activation (Bowie et al, 2000).

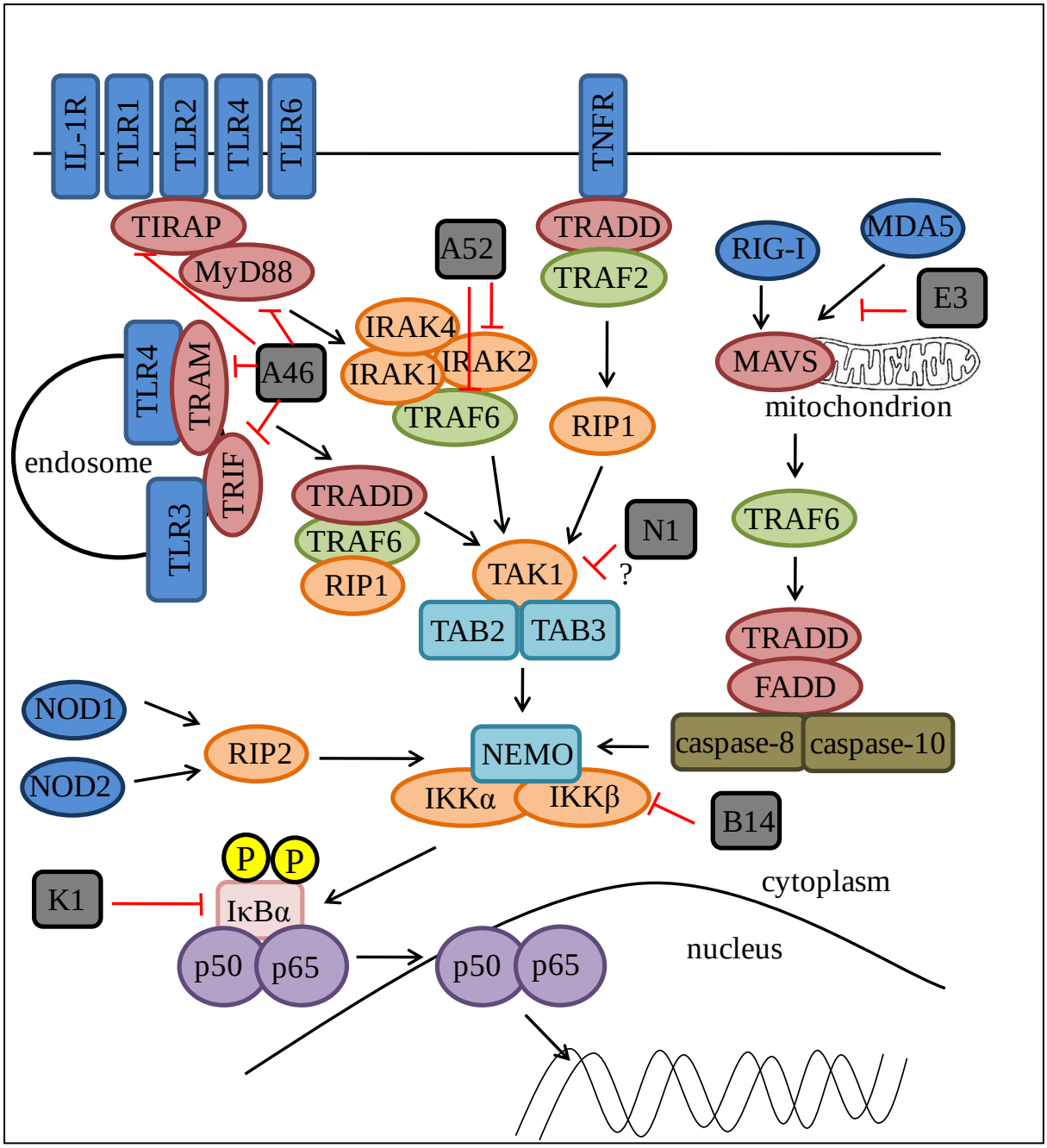

Figure 1.7: VACV inhibition of NF-κB activation. NF-κB activation is inhibited by VACV at multiple steps. E3 can bind RNA and sequester it from detection by the RLRs. A46 interacts with the TIR-containing adaptors TRAM, TRIF, TIRAP and MyD88 inhibiting downstream signalling cascades. A52 on the other hand interacts with IRAK2 and TRAF6. N1 is thought to inhibit NF-κB activation by targeting the TAK1 complex (C. Maluquer de Motes, unpublished results). B14 binds IKKβ, preventing the subsequent phosphorylation of IκBα, whereas K1 acts to inhibit IκBα degradation by the proteasome.

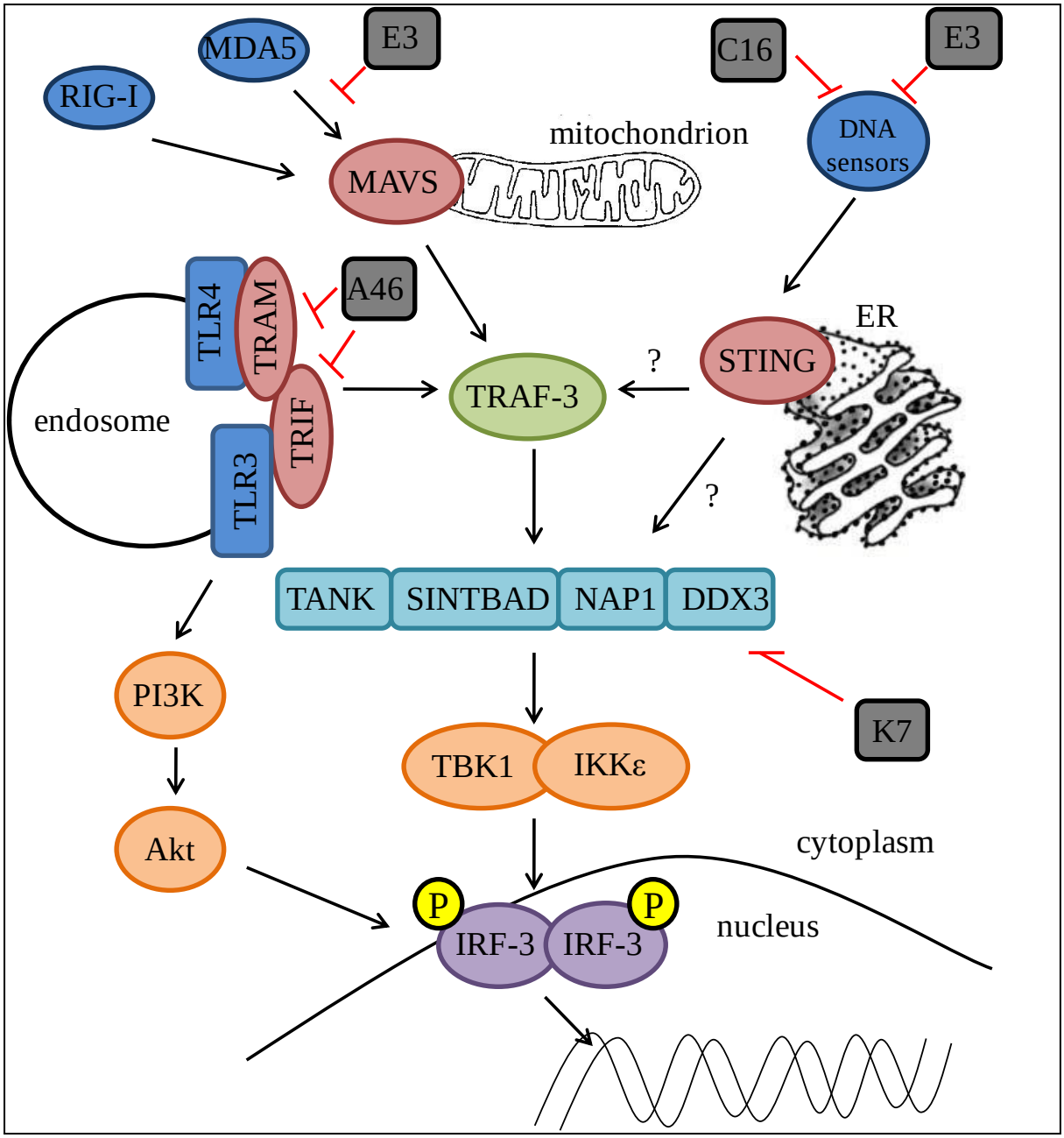

Figure 1.8: VACV inhibition of IRF3 activation. VACV targets IRF3 activation at multiple steps. Proteins C16 and E3 inhibit the cytoplasmic DNA sensors DNA-PK and DAI, respectively. In addition E3 can bind RNA and sequester it from detection by the RLRs. A46 interacts with the TIR-containing adaptors TRAM and TRIF, inhibiting downstream signalling cascades. K7 acts further downstream by binding DDX3, a protein that interacts with the non-canonical kinases and plays a role in IRF3 activation downstream of certain stimuli.

1.4.5.1.1 N1

N1L is an early gene (Assarsson et al, 2008; Bartlett et al, 2002). It is expressed as an intracellular homo-dimer that is non-essential for replication *in vitro*, but is a virulence factor as a virus lacking this gene is attenuated in both the i.n. and intradermal (i.d.) models of murine infection (Bartlett et al, 2002). Subsequently N1 was described to bind to both the canonical and non-canonical IKK complexes, thus inhibiting IRF3 and NF-κB activation (DiPerna et al, 2004). Although binding to these kinase complexes and inhibition of IRF3 has not been reproduced in our laboratory, N1 inhibits NF-κB activation downstream of both TNFα and IL-1β, although this action is upstream of the IKK complex (C. Maluquer de Motes, unpublished results, see Figure 1.7). N1 clearly has immunomodulatory functions *in vivo* because a stronger NK cell response was observed following infection with a virus lacking N1 expression (Jacobs et al, 2008) and the ECTV counterpart of N1 has been described to contribute to spread *in vivo* and may modulate T cell function (Gratz et al, 2011).

1.4.5.1.2 B14

Like N1, B14 is also expressed early during infection (Assarsson et al, 2008; Chen et al, 2006a) and is a potent inhibitor of NF-kB activation downstream of multiple pathways (Chen et al, 2008). This is achieved by the binding of B14 to IKKβ, which inhibits the phosphorylation of IKKβ in its activation loop (Chen et al, 2008) (see Figure 1.7). Like N1, B14 is also a virulence factor because a virus lacking this gene was attenuated in the i.d. model of murine infection, characterised with an increased infiltration of cells into the infected lesion (Chen et al, 2006a). This protein forms homo-dimers in the crystal (Graham et al, 2008), but this dimerisation was not required for functionality or binding to IKKβ and in fact the dimerisation and IKKβ-binding interfaces were found to overlap (Benfield et al, 2011). The MVA version of VACV WR B14, called 183, lacks an internal 6 amino acids that cause the protein to be unstable and to be unable to inhibit NF-κB activation (McCoy et al, 2010).

1.4.5.1.3 A52

A52 blocks both IL-1- and TLR4-mediated NF-κB activation (Bowie et al, 2000) and also contributes to virulence (Harte et al, 2003). Later work showed A52 inhibited NF-κB activation by TLR2, -3, -4, -5, -7, and -9 ligands via its interaction with IRAK2, but it did not inhibit IRF activation (Keating et al, 2007). In addition to IRAK2, A52 also interacts with TRAF6 (Harte et al, 2003) (see Figure 1.7), which leads to the activation of MAPK p38 and subsequently the IL-10 promoter (Maloney et al, 2005). IL-10 is an important cytokine for determining viral persistence *in vivo* (Brooks et al, 2006). Like B14, A52 is expressed very early after infection (Assarsson et al, 2008; Harte et al, 2003) and is a dimer in the crystal (Graham et al, 2008).

1.4.5.1.4 A46

A46 is expressed early during VACV infection (Assarsson et al, 2008; Stack et al, 2005) and inhibits NF-κB activation (Bowie et al, 2000). It interacts with several TIR domain-containing cellular proteins including MyD88, TIRAP, TRIF and TRAM allowing it to inhibit NF-κB downstream of multiple TLRs (Stack et al, 2005) (see Figure 1.7). Because it interacts with TRIF, A46 was also described to inhibit IRF3 activation downstream of TLR3 and TLR4 (see Figure 1.8). Further, A46 contributes to virulence in the i.n. model of murine infection (Stack et al, 2005). A small peptide from A46, termed viral inhibitor peptide of TLR4 (VIPER) inhibits TLR4 activation and thus has potential therapeutic use (Lysakova-Devine et al, 2010).

1.4.5.1.5 K7

K7 was identified as an inhibitor of TLR- and RLR-mediated IRF3 and IRF7 activation, and hence IFNβ induction. This function is presumed to be exerted by the binding of K7 to the cellular protein DDX3 (Schroder et al, 2008) (see Figure 1.8). This is a direct interaction and the binding site for K7 on DDX3 was narrowed down to the N-terminal region (Schroder et al, 2008). A crystal structure of K7 in complex with this DDX3 was solved and gave insight into the role of DDX3 in TBK1-mediated activation of IRF3 and IRF7 (Oda et al, 2009). Like the other Bcl-2 family members described above, K7 is expressed early after infection

(Assarsson et al, 2008), but nuclear magnetic resonance (NMR) (Kalverda et al, 2008) and crystallographic (Oda et al, 2009) structural analysis found it to be a monomer rather than a dimer.

1.4.5.2 Inhibitors of PKR

Two VACV proteins have been described that affect PKR activation. K3 prevents eIF2α phosphorylation and autophosphorlyation of PKR (Davies et al, 1992). E3 on the other hand binds and sequesters dsRNA, thus preventing it from activating PKR and any other RNA sensors that bind dsRNA such as MDA5 (Chang et al, 1992) (see Figures 1.7 and 1.8). In addition E3 inhibits the expression of cytokines, including IFNβ and TNFα in both a PKR-dependent and -independent manner, involving the inhibition of both NF-κB and IRF3 pathways (Myskiw et al, 2009).

1.4.5.3 Other inhibitors of NF-κB

A number of other proteins in addition to Bcl-2 family members N1, B14, A52 and A46 have also been characterised to have roles in NF-κB inhibition. K1 is a host range factor that inhibits the activation of NF-κB by preventing IκBα degradation (Shisler & Jin, 2004) (See Figure 1.7). On the other hand, M2 inhibits the phosphorylation of ERK2, thus preventing the activation of NF-κB via the MAPK pathway (Gedey et al, 2006). M2 was found to localise with cellular ER proteins, and this localisation was essential for its ability to inhibit NF-κB (Hinthong et al, 2008). E3 has also been shown to inhibit NF-κB activation in a PKR-dependent and –independent manner (Myskiw et al, 2009), as well as by inhibiting the RNA polymerase III-mediated dsDNA-sensing pathway (Myskiw et al, 2009; Valentine & Smith, 2010).

1.4.5.3 Inhibitors of IFN signalling

VACV protein VH1 is a phosphatase with the ability to dephosphorylate STAT proteins. This protein dephosphorylates both STAT1 and STAT2, but not other STATs, following the stimulation of cells with type I and type II IFNs (Mann et al, 2008; Najarro et al, 2001) (see Figure 1.6). VH1 is packaged within virions (Liu et al, 1995) suggesting that the immediate

inhibition of IFN signalling prior to gene expression may be beneficial to the virus. Some ISGs are transcribed in a STAT1-independent manner, although the factors that are required for this are currently not well understood. Nevertheless, VACV also has the ability to block the transcription of some STAT1-independent genes and the viral protein(s) responsible for this inhibition remain to be characterised (Mann et al., 2008).

1.4.5.4 Inhibitors of DNA sensing

VACV protein E3 can be split into distinct N- and C-terminal halves. The C terminus of E3 contains a dsRNA-binding domain that serves to sequester dsRNA produced during viral replication and prevent the activation of PKR and other RNA sensors (see 1.4.5.2). The N terminus, on the other hand, contains a region with amino acid similarity to the Z-DNA-binding domain of DAI. Subsequently E3 can inhibit IFNβ induction in response to DNA by preventing the activation of DAI (Wang et al, 2008) (see Figure 1.8). In this study the presence of E3 was found to reduce the binding of DAI to DNA. E3 has also been described to inhibit the RNA polymerase III-mediated dsDNA-sensing pathway, although this appears to be by sequestering the RNA polymerase III-transcribed RNA from RIG-I, as E3 was not found to interact with dsDNA (Marq et al, 2009; Valentine & Smith, 2010). Furthermore E3 acts as an immunomodulatory protein by directly targeting and disabling the function of ISG15 (Guerra et al, 2008). A second VACV protein that has been characterised to interfere with DNA sensing is C16, an early-expressed protein with immunomodulatory functions and a role as a virulence factor *in vivo* (Fahy et al, 2008). C16 was found to bind the recently identified DNA sensor Ku70/80 and inhibit the activation of IFNβ in response to dsDNA (N. Peters, manuscript in preparation, see Figure 1.8).

1.5 Project aims

Given the role of the characterised members of the VACV Bcl-2 family in innate immune evasion, the other members of this family are predicted to have similar roles. In addition to being a member of this family, *C6L* was identified from a screen of VACV ORFs whose expression in HEK cells was able to inhibit IFNβ induction (Unterholzner et al, 2011). The *C6L* gene is located near the left end of the VACV strain WR genome (ORF 022), a region rich in immunomodulatory proteins, and has been described to be expressed early during

infection, like many other proteins with roles in immune evasion (Assarsson et al, 2008). Taken together protein C6 was a strong candidate for further investigation and was the focus of this study. The aims of this project were to:

- Characterise C6 expression during viral infection
- Confirm the ability of C6 to inhibit IFNβ induction and characterise the mechanism
- Identify cellular interaction partners for C6
- Characterise the contribution of C6 to VACV virulence *in vivo*

Chapter 2: Materials and Methods

2.1 DNA preparation and manipulation

2.1.1 Polymerase chain reaction

Plasmids were constructed by amplifying the ORF of interest from a suitable template by polymerase chain reaction (PCR). Each PCR contained 100 ng template, 10 x HiFi buffer (Invitrogen), 2 mM $MgSO_4$, dNTPs (0.2 mM each), 0.2 μM of each oligonucleotide primer (see Table 2.1) and 1 U Taq HiFi polymerase (Invitrogen), made up to a total volume of 50 μl with water. PCRs were carried out in a thermo cycler using the following programme:

5 min	95 ^{o}C	
30 s	95 ^{o}C	
30 s	50 ^{o}C	5 cycles
90 s	68 ^{o}C	
30 s	95 ^{o}C	
30 s	55 ^{o}C	25 cycles
90 s	68 ^{o}C	
10 min	68 ^{o}C	

2.1.2 Agarose gel electrophoresis

PCR products were separated by agarose gel electrophoresis on a 1 % (w/v) agarose gel at 100 V in TAE buffer (40 mM Tris, 20 mM acetic acid, and 1 mM EDTA). DNA was visualised by staining with Syber Safe (Invitrogen) and illumination with long wave ultraviolet light.

2.1.3 Purification of DNA from agarose gel slices

DNA bands of interest were excised from agarose gels with a scalpel and the DNA was purified using the QIAgen gel extraction kit according to the manufacturer's protocol.

Table 2.1 Oligonucleotide primer sequences used for the plasmids constructed in this study

Plasmid	**Primers**
Z11ΔC6	5′ CTGAGGATCCGGTATTACGATGGCTAGAAAATAAAAG 3′ 5′ CTAGGCGGCCGCTCTAGACGTGCTGTATACCCATCATGAATGGATG 3′
Z11C6Rev	5′ CTGAGGATCCGGTATTACGATGGCTAGAAAATAAAAG 3′ 5′ CTAGGCGGCCGCTCTAGACGTGCTGTATACCCATCATGAATGGATG 3′
Z11C6FS	5′ TATTATACGCATTCTATGATAAACTTAATGAAAAATGTT 3′ 5′ TTCATTAAGTTTATCATAGAATGCGTATAATAAAGCCGA 3′
Z11C6HA	5′ TACCCATACGATGTTCCAGATTACGCTTGATTTTTTTCTTCCTAAACT 3′ 5′ TCAAGCGTAATCTGGAACATCGTATGGGTATCTATCTACATCATCACGTCTCTG 3′
pcDNA4/TO C6-TAP	5′ CTGAGGTACCATGAATGCGTATAATAAAGCCG 3′ 5′ CAGTGCGGCCGCTCTATCTACATCATCACGTC 3′
pcDNA4/TO C6FS-TAP	5′ CAGTGCGGCCGCTCTATCTACATCATCACGTC 3′ 5′ CTGAGGTACCATAGAATGCGTATAATAAAGCCG 3′
pcDNA4/TO FLAG-C6	5′ CGCGAATTCGCCACCATGGACTACAAGGATGACGATGACAAGAATGCGTATAATAAAGCCGATTCG 3′ 5′ GCCTCTAGATTATCTATCTACATCATCACGTCTC 3′
pcDNA4/TO C6-FLAG	5′ CGCGAATTCGCCACCATGAATGCGTATAATAAA GCCGAT TCG 3′ 5′ GCCTCTAGACTTGTCATCGTCATCCTTGTAGTCTCT ATCTACATCATCACGTCTC 3′
pcDNA4/TO TAP-C6	5′ GCCTCTAGATTATCTATCTACATCATCACGTCTC 3′ 5′ GAATGCGGCCGCGAATGCGTATAATAAAGCCGATTCG 3′
M5P LUC-C6	5′ CATGTCATGAATGCGTATAATAAAGCCGAT TCG 3′ 5′ ATTTGCGGCCGCTTATCTATCTACATCATCACGTCTC 3′
M5P FLAG-hTANK	5′ CATGCCATGGATAAAAACATTGGCGAGCAACTCA 3′ 5′ ATTTGCGGCCGCTTAAGTCTCTCCATTGAAGTGTG 3′
M5P LUC- hTANK	5′ CATGCCATGGATAAAAACATTGGCGAGCAACTCA 3′ 5′ ATTTGCGGCCGCTTAAGTCTCTCCATTGAAGTGTG 3′
M5P LUC- hTANK 1-69	5′ CATGCCATGGATAAAAACATTGGCGAGCAACTCA 3′ 5′ ATTTGCGGCCGCTTATTGAGTGGAATTCACAAG 3
M5P LUC- hTANK 1-135	5′ CATGCCATGGATAAAAACATTGGCGAGCAACTCA 3′

	5′ ATTTGCGGCCGCTTACCTTTCATGGAGCAAAG 3′
M5P LUC- hTANK 1-173	5′ CATGCCATGGATAAAAACATTGGCGAGCAACTCA 3′ 5′ ATTTGCGGCCGCTTAAGTTGCAGTGTCTGGTATATT 3′
M5P LUC- hTANK 1-391	5′ CATGCCATGGATAAAAACATTGGCGAGCAACTCA 3′ 5′ ATTTGCGGCCGCTTAATGCAGTTCTGAGTCTGTGC 3′
M5P LUC- hTANK 174-425	5′ CATGCCATGGAAACACAGTGCTCTGTGCCTATAC 3′ 5′ ATTTGCGGCCGCTTAAGTCTCTCCATTGAAGTGTG 3′
M5P LUC- hTANK 135-425	5′ ATGTCATGAGGGGTAATATAGAGAAGACTTTCTGGG 3′ 5′ ATTTGCGGCCGCTTAAGTCTCTCCATTGAAGTGTG 3′
M5P LUC- hTANK 70-425	5′ CATGCCATGGATAACAATTATGGCTGTGTTCCTC 3′ 5′ ATTTGCGGCCGCTTAAGTCTCTCCATTGAAGTGTG 3′
M5P LUC- mTANK 1-120	5′ CATGACATGTCTTTAAAGAGACATAGTCTGCGAAG 3′ 5′ ATTTGCGGCCGCTTACCTTCTGTCACTGTCTTC 3′
M5P LUC- mTANK 1-165	5′ CATGACATGTCTTTAAAGAGACATAGTCTGCGAAG 3′ 5′ ATTTGCGGCCGCTTAATGCAGAGGGATGTTGAG 3′
M5P LUC- mTANK 120-448	5′ CATGTCATGAGGAAGAATAATTTGACCCTTGATG 3′ 5′ ATTTGCGGCCGCTTAAGTCTCCCCATTAAAGTG 3′
M5P LUC- mTANK 162-448	5′ CATGTCATGATCCCTCTGCATCACGAAAGGG 3′ 5′ ATTTGCGGCCGCTTAAGTCTCCCCATTAAAGTG 3′
M5P C6-LUC	5′ CCCAAGCTTGCCGCCACCATGAATGCGTATAATAAAGCCG 3′ 5′ CCCAAGCTTTCTATCTACATCATCACGTCTC 3'
pcDNA4/TO TAP-019	5′ GAATGCGGCCGCGAATGCGTATAATAAAGCCGATTCG 3′ 5′ GCCTCTAGATCAGTTTAGGAAAAAAAAATATC 3′
pcDNA3.1 HA	5′ AATTCGCCACCATGTACCCATACGATGTTCCAGATTACGCTGC 3′ 5′ GGCCGCAGCGTAATCTGGAACATCGTATGGGTACATGGTGGCG 3′
pcDNA3.1 V5	5′ AATTCGCCACCATGGGAAAGCCGATCCCAAACCCTCTATTAGGTCTGGACTCCACCGC 3′ 5′ GGCCGCGGTGGAGTCCAGACCTAATAGAGGGTTTGGGATCGGCTTTCCCATGGTGGCG 3′
pcDNA3.1 HA-NAP1	5′ GAATGCGGCCGCGGACACGCTAGTAGAAGATGAC 3′ 5′ GCCTCTAGATTAACTTTTGTAAAGGCAG 3′
pcDNA3.1 HA-SINTBAD	5′ GAATGCGGCCGCGGAGTCCATGTTTGAAGATGAC 3′ 5′ GCCTCTAGACTAGATCTTGCTGTTCTCAAG 3′
pcDNA3.1 HA-TANK	5′ GAATGCGGCCGCGTCTTTAAAGAGACATAGTCTG 3′

	5′ GCCTCTAGATTAAGTCTCCCCATTAAAGTGTG 3′
pcDNA3.1 HA-C6	5′ GAATGCGGCCGCGAATGCGTATAATAAAGCCGATTCG 3′ 5′ GCCTCTAGATTATCTATCTACATCATCACGTCTC 3′
pcDNA3.1 V5-TBK1	5′ GAATGCGGCCGCGCAGAGCACCTCCAACCATCTG 3′ 5′ GCCGGGCCCCTAAAGACAGTCCACATTGCG 3′
pcDNA3.1 V5-TANK	5′ GAATGCGGCCGCGTCTTTAAAGAGACATAGTCTG 3′ 5′ GCCTCTAGATTAAGTCTCCCCATTAAAGTGTG 3′
pcDNA3.1 FLAG-TRAF3	5′ CGCGAATTCGCCACCATGGACTACAAGGATGACGATGACAAGGAGTCAAGCAAAAAGATGGATG 3′ 5′ ATTTGCGGCCGCTCAGGGGTCAGGCAGATCCGAG 3′
pcDNA3.1 HA-IRF3	5′ GAATGCGGCCGCGGAAACCCCGAAACCGCGGATTTTG 3′ 5′ GCCTCTAGATCAGATATTTCCAGTGGCCTG 3′

2.1.4 Restriction enzyme digestion

Each digestion contained 1.5 μg DNA, 1 μl appropriate 10 x restriction enzyme buffer (Roche), 0.5 μl of each restriction enzyme (Roche) and made up to 10 μl with water. Restriction digests were incubated at 37 ^{o}C for 2 h. Digestion products were analysed by agarose gel electrophoresis (see 2.1.2) and the DNA was purified from the gel (see 2.1.3).

2.1.5 DNA ligation

Each ligation reaction contained 100 ng digested plasmid vector, an appropriate quantity of digested insert to achieve a 2:1 molar ratio of insert:vector, 10 x T4 DNA ligase buffer (Promega) and 1 U T4 DNA ligase (Promega), made up to 10 μl with water. Ligation reactions were incubated at 16 ^{o}C for at least 2 h.

2.1.6 Transformation of *E. coli*

Ten μl of ligation reaction was used to transform 50 μl of transformation competent XL-10 *E. coli*. The ligation reaction and bacteria were mixed and incubated on ice for 30 min. The bacteria were then incubated at 42 ^{o}C for 1 min and returned to ice for a further 5 min. The bacteria were spread on Luria Broth (LB) agar plates containing the appropriate antibiotic; carbenicillin for ampicillin resistance (100 μg/ml) or kanamycin (50 μg/ml). When using plasmids with the kanamycin resistance gene, 200 μl super optimal broth with catabolite repression (SOC) medium (Invitrogen) was added and the bacteria were incubated with shaking at 37 ^{o}C for 1 h before plating.

2.1.7 Screening of colonies by PCR

To confirm the presence of the correct plasmid, bacterial colonies were subjected to screening by colony PCR. Colonies were picked in 2 ml LB containing the appropriate antibiotic (see 2.1.6) and incubated shaking at 37 ^{o}C for 1 h. Each PCR contained 1 μl bacterial culture, 10x GoTaq buffer (Promega), 2 mM $MgCl_2$, dNTPs (0.2 mM each), 0.2 μM of the primers that had been used to amplify the ORF of interest (see 2.1.1) and 1 U GoTaq polymerase

(Promega), made up to a total volume of 20 µl with water. PCRs were carried out in a thermo cycler using the following programme:

5 min	95 °C	
30 s	95 °C	
30 s	50 °C	5 cycles
90 s	68 °C	
30 s	95 °C	
30 s	55 °C	25 cycles
90 s	72 °C	
10 min	72 °C	

PCR products were analysed by agarose gel electrophoresis (see 2.1.2).

2.1.8 TA cloning of DNA fragments

Where direct restriction enzyme digestion of the PCR product for insertion into a digested vector was not successful, the PCR product was first inserted into the pCR2.1 TA cloning vector (Invitrogen) according to the manufacturer's instructions. The ORF of interest was then excised from this vector using restriction enzyme digestion as described in 2.1.4.

2.1.9 Small scale preparation of plasmid DNA

Bacterial clones containing the plasmid of interest were grown in 2-5 ml LB containing the appropriate antibiotic and incubated with shaking at 37 °C for 8 h during the day, or overnight. Plasmid DNA was purified using a rapid alkaline extraction method. The bacterial pellets were resuspended in resuspension buffer (50 mM Tris-HCl pH 7.5, 10 mM EDTA, 100 µg/ml RNase A), the cells were lysed in lysis buffer (10% (w/v) SDS, 0.2 M NaOH) and the proteins were precipitated by addition of a neutralisation buffer (1.32 M potassium acetate pH 4.8). The precipitate was collected by centrifugation at 14,000 x *g* for 5 min and the supernatant was transferred to a clean eppendorf tube. The DNA in the cleared lysate was precipitated with isopropanol, the DNA was then collected by centrifugation at 14,000 x *g* for 5 min and was washed in 70 % (v/v) ethanol followed by centrifugation at 14,000 x *g* for a further 5 min. The purified DNA was finally dissolved in 30 µl water.

2.1.10 Large scale preparation of plasmid DNA

For the large scale preparation of plasmid DNA, transformed bacteria were grown overnight shaking at 37 ^{o}C, in 200 ml LB containing the appropriate antibiotic. The DNA was then purified using the QIAgen midi or maxi preparation of plasmid DNA kit, depending on how much plasmid DNA was required, according to the manufacturer's protocol.

2.1.11 DNA sequencing

Plasmid DNA was sequenced using the service at Hammersmith Hospital, Imperial College London. Each reaction was prepared with 150 - 300 ng DNA per 3 kilo base pairs (kb) and 0.2 μM of sequencing primer (see below), made up to 10 μl with water.

Plasmid	**Primer**	**Sequence**
pcDNA3.1	CMV FWD BGH REV	5′ TAATACGACTCACTATAGGG 3′ 5′ CTAGAAGGCACAGTCGAGGC 3′
pcDNA4/TO	CMV FWD BGH REV	5′ TAATACGACTCACTATAGGG 3′ 5′ CTAGAAGGCACAGTCGAGGC 3′
Z11	P17 P64	5′ TTTTACGGTTCCTGGC 3′ 5′ TTAATGCGCCGCTAC 3′
pUC13	M13 FWD M13 REV	5′ GTAAAACGACGGCCAG 3′ 5′ CAGGAAACAGCTATGAC 3′
M5P FLAG	RS-56 CM-02	5′ CCACGTGAAGGCTGCCGACC 3′ 5′ TGACTCAACAATATCACCAG 3′
M5P LUC	CM-01 CM-02	5′ TCGCAAGAAGATGCACCTG 3′ 5′ TGACTCAACAATATCACCAG 3′

2.2 Cell culture

2.2.1 Maintenance of cells

BSC-1 (African green monkey epithelial cell line of kidney origin), HEK293 and HEK293ET (human embryonic kidney cell lines), CV-1 (African green monkey kidney fibroblast cell line) and HCT116 (human colon carcinoma cell line) cells were maintained in Dulbecco's modified Eagle's medium (DMEM) supplemented with 10 % (v/v) foetal bovine serum (FBS) that had been treated for 1 h at 56 °C to inactivate complement and penicillin/streptomycin (P/S) (50 μg/ml). NIH3T3 (murine fibroblast cell line) cells were maintained in DMEM supplemented with 10 % (v/v) newborn calf serum (NCS) and P/S.

HeLa (human cervical cancer cell line) cells were maintained in minimum essential medium (MEM) supplemented with 10 % (v/v) FBS, 1:100 non-essential amino acids (NEAA) (Sigma) and P/S (50 μg/ml). RK-13 (rabbit kidney cell line) and TK143 (human thymidine kinase-null osteosarcoma) cells were maintained in MEM supplemented with 10 % (v/v) FBS and P/S (50 μg/ml). HEK293 T-REx cells (Invitrogen) were maintained in DMEM supplemented with 10 % (v/v) FBS, P/S (50 μg/ml) and blasticidin (50 μg/ml). HEK293 T-REx C6 TAP cell lines were maintained in DMEM supplemented with 10 % (v/v) FBS, P/S (50 μg/ml), blasticidin (50 μg/ml) and zeocin (100 μg/ml).

2.2.2 Calcium phosphate transfection

Cells were seeded the day before transfection to achieve 50 % confluency at the time of transfection. Prior to preparing the transfection mixes the cell medium was aspirated and replaced with fresh medium (containing 10 % (v/v) FBS). For a 10-cm dish, 5 μg DNA, 445 μl H_20 and 50 μl 2.5 M $CaCl_2$ were mixed and incubated at room temperature for 20 min. For a well of a 6-well plate 1.5 μg DNA, 66 μl H_20 and 7.5 μl 2.5 M $CaCl_2$ were mixed and incubated as above. An equal volume of HBS pH 7.05 (280 mM NaCl, 10 mM KCl, 1.5 mM Na_2HPO_4, 12 mM glucose, 50 mM HEPES) was then added and incubated for a further 12-15 min. This solution was added dropwise directly into the cell medium. The following day the cells were either processed directly or washed twice with pre-warmed (37 ^oC) phosphate-buffered saline (PBS), fresh medium was added and the cells were allowed to grow for a further 24 h. See table 2.2 for a list of plasmids used in this study.

2.2.3 Fugene-6 and PEI transfection

Cells were seeded the day before transfection to achieve 70 % confluency at the time of transfection. Transfection mixes were prepared by mixing the appropriate quantity of DNA with OPTIMEM (50 μl per 1 μg of DNA). The appropriate volume of Fugene-6 reagent (Roche) or PEI (1 mg/ml) was then added (2 μl transfection reagent per 1 μg DNA) and mixed by vortexing briefly. After incubation at room temperature for 30 min, an appropriate volume of medium (containing 2 % (v/v) FBS) was added, the growth medium was aspirated from the cells and the medium containing the transfection mix was added. The cells were harvested after 24-48 h. See table 2.2 for a list of plasmids used in this study.

Table 2.2 Plasmids used in this study

Plasmid	Description
Z11ΔC6	pCI-based, 300-350 bp flanks of C6 ORF, Ecogpt.EGFP selection marker, AmpR, constructed by R. Sumner
Z11C6Rev	pCI-based, 300-350 bp flanks + C6 ORF, Ecogpt.EGFP selection marker, AmpR, constructed by R. Sumner
Z11C6FS	pCI-based, 300-350 bp flanks + C6FS ORF, Ecogpt.EGFP selection marker, AmpR, constructed by R. Sumner
Z11C6HA	pCI-based, 300-350 bp flanks + C6HA ORF, Ecogpt.EGFP selection marker, AmpR, constructed by R. Sumner
pcDNA3.1 HA	empty vector encoding HA epitope tag, AmpR, constructed by R. Sumner
pcDNA3.1 HA-C6	C6 with N-terminal HA tag, AmpR, constructed by R. Sumner
pcDNA3.1 HA-NAP1	NAP1 with N-terminal HA tag, AmpR, constructed by R. Sumner
pcDNA3.1 HA-SINTBAD	SINTBAD with N-terminal HA tag, AmpR, constructed by R. Sumner
pcDNA3.1 HA-TANK	TANK (murine sequence) with N-terminal HA tag, AmpR, constructed by R. Sumner
pcDNA3.1 HA-IRF3	IRF3 with N-terminal HA tag, AmpR, constructed by R. Sumner
pcDNA3.1 V5	empty vector encoding V5 epitope tag, AmpR, constructed by R. Sumner
pcDNA3.1 V5-TBK1	TBK1 with N-terminal V5 tag, AmpR, constructed by R. Sumner
pcDNA3.1 V5-TANK	TANK (murine sequence) with N-terminal V5 tag, AmpR, constructed by R. Sumner
pcDNA3.1 FLAG-TRAF3	TRAF-3 with N-terminal FLAG tag, AmpR, constructed by R. Sumner
pcDNA4/TO	empty vector control, doxy-inducible, zeocin selection marker, AmpR
pcDNA4/TO TAP	empty vector with TAP tag, doxy-inducible, zeocin selection marker, AmpR, constructed by B. Ferguson
pcDNA4/TO C6-TAP	C6 with C-terminal TAP tag, doxy-inducible, zeocin selection marker, AmpR, constructed by R. Sumner
pcDNA4/TO C6FS-TAP	C6FS with C-terminal TAP tag, doxy-inducible, zeocin selection marker, AmpR, constructed by R. Sumner
pcDNA4/TO FLAG-C6	C6 with N-terminal FLAG tag, doxy-inducible, zeocin selection marker, AmpR, constructed by R. Sumner
pcDNA4/TO C6-FLAG	C6 with C-terminal FLAG tag, doxy-inducible, zeocin selection marker, AmpR, constructed by R. Sumner
pcDNA4/TO TAP-C6	C6 with N-terminal TAP tag, doxy-inducible, zeocin selection marker, AmpR, constructed by R. Sumner
pcDNA4/TO TAP-019	MVA 019 with N-terminal TAP tag, doxy-inducible, zeocin selection marker, AmpR, constructed by R. Sumner
M5P FLAG-hTANK	human TANK with N-terminal FLAG tag, AmpR, constructed by R. Sumner
M5P FLAG-GFP	GFP with N-terminal FLAG tag, AmpR, obtained from F. Randow (MRC laboratory of Molecular Biology, Cambridge)
M5P FLAG-TRIFΔRIP	TRIFΔRIP with N-terminal FLAG tag, AmpR, obtained from F. Randow
M5P FLAG-TBK1	TBK1 with N-terminal FLAG tag, AmpR, obtained from F. Randow
M5P FLAG-IKKε	IKKε with N-terminal FLAG tag, AmpR, obtained from F. Randow

M5P FLAG-mTANK	murine TANK with N-terminal FLAG tag, AmpR, obtained from F. Randow
M5P LUC-hTANK	hTANK with N-terminal renilla luciferase tag, AmpR, constructed by D. Muhl
M5P LUC-hTANK 1-69	hTANK residues 1-69 with N-terminal renilla luciferase tag, AmpR, constructed by D. Muhl
M5P LUC-hTANK 1-135	hTANK residues 1-135 with N-terminal renilla luciferase tag, AmpR, constructed by D. Muhl
M5P LUC-hTANK 1-173	hTANK residues 1-173 with N-terminal renilla luciferase tag, AmpR, constructed by D. Muhl
M5P LUC-hTANK 1-391	hTANK residues 1-391 with N-terminal renilla luciferase tag, AmpR, constructed by D. Muhl
M5P LUC-hTANK 174-425	hTANK residues 174-425 with N-terminal renilla luciferase tag, AmpR, constructed by D. Muhl
M5P LUC-hTANK 135-425	hTANK residues 135-425 with N-terminal renilla luciferase tag, AmpR, constructed by D. Muhl
M5P LUC-hTANK 70-425	hTANK residues 70-425 with N-terminal renilla luciferase tag, AmpR, constructed by D. Muhl
M5P LUC-mTANK 1-120	mTANK residues 1-120 with N-terminal renilla luciferase tag, AmpR, constructed by R. Sumner
M5P LUC-mTANK 1-165	mTANK residues 1-165 with N-terminal renilla luciferase tag, AmpR, constructed by R. Sumner
M5P LUC-mTANK 120-448	mTANK residues 120-448 with N-terminal renilla luciferase tag, AmpR, constructed by R. Sumner
M5P LUC-mTANK 162-448	mTANK residues 162-448 with N-terminal renilla luciferase tag, AmpR, constructed by R. Sumner
M5P LUC-NAP1	NAP1 with N-terminal renilla luciferase tag, AmpR, obtained from F. Randow
M5P LUC-SINTBAD	SINTBAD with N-terminal renilla luciferase tag, AmpR, obtained from F. Randow
M5P LUC-IKKε	IKKε with N-terminal renilla luciferase tag, AmpR, obtained from F. Randow
M5P LUC-TBK1	TBK1 with N-terminal renilla luciferase tag, AmpR, obtained from F. Randow
M5P LUC-NEMO	NEMO with N-terminal renilla luciferase tag, AmpR, obtained from F. Randow
M5P LUC-IKKα	IKKα with N-terminal renilla luciferase tag, AmpR, obtained from F. Randow
M5P LUC-IKKβ	IKKβ with N-terminal renilla luciferase tag, AmpR, obtained from F. Randow
M5P LUC-C6	C6 with N-terminal renilla luciferase tag, AmpR, constructed by R. Sumner
M5P C6-LUC	C6 with C-terminal renilla luciferase tag, AmpR, constructed by R. Sumner
pEF.puro	pEF-based, empty vector control, puromycin selection marker, AmpR
pEF IRF3	Un-tagged IRF3, AmpR, obtained from A. Bowie (Trinity College Dublin)
pEF FLAG-MAVS	MAVS with N-terminal FLAG tag, AmpR, obtained from K. Shimotohno (Kyoto University, Japan)
pOPINE C6	C6 with C-terminal His tag, KanR, obtained from D. Stuart (Oxford University)
pOPINF C6	C6 with N-terminal His tag, KanR, obtained from D. Stuart
pCI B14-FLAG	B14 with N-terminal FLAG tag, AmpR, (Chen et al, 2008)
pCI C6	Un-tagged C6, AmpR, constructed by A. Postigo
pCS2 FLAG-Ub	Ubiquitin with N-terminal FLAG tag, AmpR, obtained from C. Brou (Pasteur Institute, France)
IFNβ-LUC	IFNβ promoter fused with firefly luciferase, AmpR, obtained from A. Bowie

ISG56.1-LUC	ISG56.1 promoter fused with firefly luciferase, AmpR, obtained from G. Sen (Lerner Research Institute, Ohio)
NF-κB-LUC	NF-κB promoter fused with firefly luciferase, AmpR, obtained from A. Bowie
ISRE-LUC	ISRE promoter fused with firefly luciferase, AmpR, obtained from A. Bowie
GAS-LUC	GAS promoter fused with firefly luciferase, AmpR, obtained from A. Bowie
TK-Ren LUC	TK promoter fused with renilla luciferase, AmpR, obtained from A. Bowie

2.2.4 JetPrime transfection

Cells were seeded the day before transfection to achieve 70 % confluency at the time of transfection. Prior to preparing the transfection mixes the cell medium was aspirated and replaced with fresh medium (containing 2 % (v/v) FBS). Transfection mixes were prepared by mixing the appropriate quantity of DNA with JetPrime buffer (100 µl per 1 µg of DNA). The appropriate volume of JetPrime transfection reagent (Polyplus) was then added (2 µl transfection reagent per 1 µg DNA) and mixed by vortexing briefly. After incubation at room temperature for 20-30 min the transfection mix was added drop-wise to the cells. The cells were harvested after 24-48 h. See table 2.2 for a list of plasmids used in this study.

2.3 Protein analysis

2.3.1 Preparation of cell lysates

Cell lysates were prepared by washing cells twice on ice with ice-cold PBS followed by scraping in an appropriate volume of cell lysis buffer (50 mM Tris pH 8, 150 mM NaCl, 1 mM EDTA, 10% (v/v) glycerol, 1 % (v/v) Triton X100, 0.05 % (v/v) NP40 supplemented with protease inhibitors (Roche), and phosphatase inhibitors (Roche) for immunoblotting with phospho-specific antibodies). The cells were collected in eppendorf tubes and the cell debris was collected by centrifugation at 14,000 x *g* for 20 min, 4 ^{o}C. The cleared lysate was transferred to a clean eppendorf and stored at -20 ^{o}C.

2.3.2 Protein quantification

To quantify the protein content of cell lysates a BCA protein assay kit (Pierce) was used according to the manufacturer's protocol.

2.3.3 SDS-PAGE

For sodium dodecyl sulphate (SDS) – polyacrylamide gel electrophoresis (SDS-PAGE) analysis cell lysates were heated at 100 ^{o}C for 5 min in 6x protein loading buffer, containing β-mercaptoethanol (BME) (50 mM Tris-HCl (pH 6.8), 2 % (w/v) SDS, 10% (v/v) glycerol,

0.1% (w/v) bromophenol blue, 100 mM BME) prior to loading on a 10 % or 12 % polyacrylamide gel. The proteins were separated by electrophoresis at 120 V in SDS running buffer (25 mM Tris-HCl, 250 mM glycine, 0.1 % (w/v) SDS).

2.3.4 Nu-PAGE

For the analysis of proteins using the Invitrogen Nu-PAGE system, proteins were heated at 100 ^{o}C for 5 min in 4x Nu-PAGE protein loading buffer (Invitrogen). The proteins were then separated on a 4-12 % Bis-Tris polyacrylamide gradient gel (Invitrogen) at 120 V in MES buffer (Invitrogen).

2.3.5 Immunoblotting

After PAGE, proteins were transferred to a Hybond ECL membrane (Amersham biosciences) in transfer buffer (25 mM Tris-HCl, 250 mM glycine, 20 % (v/v) methanol) using a semi-dry transfer system (Biorad) and blocked by incubation for 1 h at room temperature in 5 % (w/v) milk proteins + 0.01 % (v/v) Tween-20 in PBS (PBST). The membranes were then incubated overnight at 4 ^{o}C with primary antibody (Ab, see below) diluted in 5 % (w/v) milk proteins in PBST. Membranes were washed three times for 5 min in PBST and then were incubated with secondary Ab (see below) diluted in 5% (w/v) milk proteins in PBST for 1 h at room temperature. The membranes were again washed three times for 5 min in PBST, once in PBS and were developed with a chemiluminescent horse radish peroxidase (HRP) substrate (1.25 mM luminol, 0.4 mM p-coumaric acid, 0.1 M Tris pH 8.8, 0.0075 % (v/v) hydrogen peroxide) for approximately 10-20 s and exposed to X-ray film.

Antibody	Source	Dilution
Rabbit-anti-actin	Sigma (A2066)	1:1000
Rabbit-anti-C6 purified Ab	Polyclonal serum (eurogentec)	1:500-1:1000
Mouse-anti-D8	MAb 1.1 (Parkinson & Smith, 1994)	1:1000
Mouse-anti-DNA-PKcs	Thermo Fisher (LVMS423P1)	1:1000
Mouse-anti-FLAG	Sigma (F1804)	1:1000
Rabbit-anti-HA	Sigma (H6908)	1:1000
Rabbit-anti-IκBα	Cell signalling (9242L)	1:1000
Mouse-anti-phospho IκBα	Cell signalling (9246S)	1:500
Mouse-anti-Ku70	Abcam (ab3114)	1:1000
Mouse-anti-Lamins A+C	Abcam (ab8984)	1:1000

Mouse-anti-renilla luciferase	Millipore (MAB4400)	1:2000
Rabbit-anti-SMARCC1	Abcam (ab72503)	1:1000
Goat-anti-TANK	Santa Cruz (sc1997)	1:500
Mouse-anti-tubulin	Millipore (05-829)	1:5000
Rabbit-anti-UBR1	Abcam (ab42420)	1:500
Mouse-anti-V5	AbD Serotec Ltd. (MCA1360GA)	1:5000
Goat-anti-mouse HRP conjugated	Stratech Scientific (715-005-151)	1:20,000
Goat-anti-rabbit HRP conjugated	Stratech Scientific (111-035-003)	1:20,000
Rabbit-anti-goat HRP conjugated	DakoCytomation (P 0449)	1:20,000

2.3.6 Purification of immunoglobulins from anti-C6 serum

A C6 polyclonal antiserum was raised against C6 protein purified from *E. coli* (prepared by A. Postigo) and injected into rabbits (Eurogentec). For the purification of Igs from the serum, the particulate matter was first removed from 2 ml of serum by centrifugation at 3,000 x *g* for 30 min at 4 ^{o}C. The supernatant was incubated overnight with 1 ml saturated $(NH_4)_2SO_4$ (4.1 M at 25 ^{o}C), rotating at 4 ^{o}C. The serum was then centrifuged as above and the Igs in the serum were purified by high performance liquid chromatography using a 1 ml HiTrap protein A column (GE healthcare). The column was first equilibrated with 10 column volumes (CV) of binding buffer (12 mM Na_2HPO_4, 8.5 mM NaH_2PO_4) and the serum was then loaded onto the column diluted in binding buffer. The column was washed with 20 CV binding buffer and the Igs were eluted with 10 CV of elution buffer (100 mM citric acid monohydrate pH 3) into a 96-well collection plate containing 1.5 M Tris pH 8.8 to achieve a final pH of 7. The fractions containing Igs were pooled and dialysed overnight at 4 ^{o}C in dialysis buffer (20 mM NaHEPES pH 7.5, 300 mM NaCl) using a Slide-A-Lyzer 10,000 MWCO cassette (Thermo Fisher).

2.3.7 Silver staining of proteins

Proteins separated by PAGE were silver stained using the Invitrogen SilverQuest silver staining kit according to the manufacturer's protocol.

2.3.8 Immunofluorescence

For immunofluorescence assays cells were seeded in wells of a six-well plate containing glass coverslips and transfected (see 2.2.3) or infected (see 2.7.1) where appropriate. The cells were washed three times with cold PBS and fixed in 4 % (v/v) paraformaldehyde in PBS containing 250 mM HEPES (pH 7.4) by incubation on ice for 5 min and then at room temperature for 15 min. The cells were washed three times with PBS and then incubated in 50 mM ammonium chloride in PBS for 5 min to quench free aldehydes. The cells were washed three times in PBS and permeabilised with 0.1 % (v/v) Triton X-100 in PBS for 5 min. The cells were again washed three times in PBS and then blocked in 5 % (v/v) FBS in PBS (hereafter referred to as blocking buffer) for 30 min at room temperature. The coverslips were then inverted and incubated on a 70 µl drop of primary Ab (see below) diluted in blocking buffer for 90 min in a moist chamber. The coverslips were washed three times in blocking buffer followed by incubation on a 70 µl drop of secondary Ab (see below) diluted in blocking buffer for 90 min in a moist chamber. The coverslips were then washed twice with blocking buffer and once with PBS. Finally the coverslips were dipped in distilled water to prevent the formation of PBS crystals, placed on to a slide prepared with a 30 µl drop of mounting medium (Mowiol 4-88, containing 4',6-diamidino-2-phenylindole (DAPI)) and allowed to set before storing at 4 ^{o}C. The cells were visualised using a Zeiss Pascal Confocal Microscope at 63X magnification and images were collected using Zeiss LSM Image Browser.

Antibody	Source	Dilution
Rabbit-anti-FLAG	Sigma (F7425)	1:300
Mouse-anti-HA	Cambridge Bioscience (MMS-101P)	1:200
Mouse-anti-p65	Santa Cruz (sc-8008)	1:50
Alexa Fluor 488 goat anti-rabbit IgG (H+L)	Invitrogen (A-11008)	1:500
Alexa Fluor 488 goat anti-mouse IgG (H+L)	Invitrogen (A-21202)	1:500
Alexa Fluor 546 goat anti-rabbit IgG (H+L)	Invitrogen (A-11010)	1:500
Alexa Fluor 546 goat anti-mouse IgG (H+L)	Invitrogen (A10036)	1:500

2.3.9 Conventional immunoprecipitation assays

Prior to harvesting, the cells were washed twice on ice with ice-cold PBS followed by scraping in an appropriate volume of immunoprecipitation (IP) buffer (150 mM NaCl, 20 mM Tris-HCl pH 7.4, 10 mM $CaCl_2$, 0.1 % (v/v) Triton-X, 10 % (v/v) glycerol, supplemented with protease inhibitors (Roche). The cells were collected in eppendorf tubes and the cell debris was collected by centrifugation at 14,000 x *g* for 20 min, 4 ^{o}C. Fifty µl of the cleared lysate was transferred to a tube (input) and the remainder transferred to another tube for the IP assay. Thirty µl of protein G sepharose beads (GE healthcare), anti-FLAG M2 agarose beads (Sigma) or strep-tactin beads (IBA) were prepared per IP by washing once with 1 ml water and twice with 1 ml IP buffer (centrifuging at 600 x *g* for 1 min per wash). The beads were resuspended in an appropriate volume of IP buffer and added directly to the cell lysates. For IP assays using the protein G sepharose beads the appropriate Ab (see below) was added to the lysate at the same time as the beads. The tubes were then incubated with rotating at 4 ^{o}C for 2 h. The beads were washed three times in pre-chilled IP buffer (centrifuging at 600 x *g* for 1 min per wash) and finally were resuspended in 20 µl 6x protein sample buffer for analysis by SDS-PAGE (see 2.3.3) and immunoblotting (see 2.3.5).

Antibody	Source	Dilution
Mouse-anti-HA	Cambridge Bioscience (MMS-101P)	1:200
Goat-anti-TANK	Santa Cruz (sc1997)	1:50
Mouse-anti-V5	AbD Serotec Ltd. (MCA1360GA)	1:300
Mouse-anti-DNA-PKcs	Thermo Fisher (LVMS423P1)	1:100
Rabbit-anti-SMARCC1	Abcam (ab72503)	1:100
Rabbit-anti-UBR1	Abcam (ab42420)	1:100

2.3.10 LUMIER assay

For luminescence-based mammalian interactome (LUMIER) assays HEK293 cells were prepared in 6-well plates and transfected with 1.5 µg of a plasmid expressing a renilla luciferase (LUC)-tagged protein and 1.5 µg of a plasmid expressing a FLAG-tagged protein using the calcium phosphate method (see 2.2.2). Prior to harvesting the cells were washed once on ice with ice-cold PBS followed by scraping in 250 µl IP buffer. The cells were collected in eppendorf tubes and the cell debris was removed by centrifugation at 14,000 x *g* for 20 min, 4 ^{o}C. Forty µl of the cleared lysate was transferred to a tube for immunoblotting

analysis, 20 µl was retained to measure total luminescence of the sample and the remainder was transferred to another tube for the IP assay. Thirty µl anti-FLAG M2 agarose beads (Sigma) were prepared per IP by washing three times in Tris-buffered saline (TBS) (2.5 mM Tris-HCl, 15 mM NaCl, 0.2 mM KCl) and once in IP buffer (centrifuging at 600 x *g* for 1 min per wash). The beads were resuspended in an appropriate volume of IP buffer and were added directly to the cell lysates. The tubes were then incubated with rotating at 4 ^{o}C for 2 h. The beads were washed three times in pre-chilled TBS (centrifuging at 600 x *g* for 1 min per wash) and the associated proteins were eluted by incubation with 50 µl 150 µg/ml FLAG peptide (Sigma) in 5x passive lysis buffer (Promega), incubated with rotating at 4 ^{o}C for 1 h. The beads were then collected by centrifugation at 14,000 x *g* for 1 min and 10 µl of the supernatant was analysed for luminescence by addition of 50 µl coelenterazine renilla luciferase substrate (1 mg/ml, Prolume Ltd.) using a FLUOstar luminometer (BMG). The luminescence after IP was normalised to the total luminescence of the sample. A fold binding was calculated by normalising to a FLAG-green fluorescent protein (GFP) control.

2.3.11 ELISA

For enzyme-linked immunosorbent assay (ELISA), PRO-BIND flat bottom 96-well assay plates (BD) were coated overnight at room temperature with 100 µl capture Ab (Murine CXCL-10 and IL-6 ELISA Duosets, R&D Systems) per well diluted in PBS. The plates were washed 3 times in PBST (PBS + 0.1% Tween) and then were blocked for 1 h at room temperature with 300 µl 1 % (w/v) BSA in PBS (hereafter termed diluent) per well. The plates were washed 3 times in PBST. The standards were prepared in duplicate (CXCL-10: 2000 pg/ml-31.3 pg/ml, IL-6: 500 pg/ml-7.8 pg/ml) by preparing a two-fold dilution in diluent. One-hundred µl un-diluted BAL supernatant, or cell culture supernatant was added per well and the mixture was incubated for 2 h at room temperature. The plates were washed again 3 times in PBST. The detection Ab (Murine CXCL-10 and IL-6 ELISA Duosets, R&D Systems) was prepared in diluent, 100 µl was added per well and the plate was incubated at room temperature for 2 h. The plates were washed 3 times in PBST. Streptavidin HRP (R&D systems) was diluted 1:200 in diluent, 100 µl was added per well and the plate was incubated at room temperature for 20 min. The plates were again washed 3 times in PBST and the ELISA substrate reagent (R&D systems) was prepared by mixing solutions A and B in a 1:1 ratio. One-hundred µl was added per well and the plate was incubated in the dark for 20 min.

The reaction was stopped by the addition of 100 µl 2N H_2SO_4 per well. The absorbance at 450 nm was measured, with 540 nm as a reference.

2.4 Functional assays

2.4.1. Reporter gene assay

For a reporter gene assay cells were seeded in 96-well plates and transfected at 70 % confluency (see 2.2.3). Transfection reactions contained 60 ng of a firefly luciferase reporter plasmid, 10 ng of renilla luciferase transfection control plasmid and varying quantities of a C6 expression plasmid or an empty vector (EV) plasmid (either pcDNA4/TO or pEF.puro) per well. The transfections were performed in triplicate and were added to cells in DMEM + 2 % (v/v) FBS + P/S. In each case the total amount of DNA transfected per well was made equal with empty vector plasmid. Twenty four h post-transfection the cells were stimulated with poly I:C (Autogen Bioclear), poly dA:dT (Sigma), IFNα (Peprotech) or IFNγ (R&D Systems) as described in the figure legends and the cells were then harvested in passive lysis buffer (Promega). For the stimulation of cells by ectopic expression of signalling molecules, plasmids expressing these molecules were included in the initial transfection mix and the cells were harvested approximately 30 h post-transfection. Non-stimulated cells were transfected with the empty vector control plasmid. Ten µl of lysate was used for luminescence measurements after the addition of 50 µl of firefly luciferase substrate (20 mM Tricine, 2.67 mM $MgSO_4.7H_20$, 0.1 mM EDTA, 33.3 mM DTT, 530 µM ATP, 270 µM acetyl coenzyme A, 132 µg/ml Luciferin (Prolume Ltd.), 5 mM NaOH, 0.26 mM $(MgCO_3)_4Mg(OH)_2.5H_20$) or coelenterazine renilla luciferase substrate (1 mg/ml, Prolume Ltd.) using a FLUOstar luminometer (BMG). The firefly luciferase activity in each sample was normalised to the renilla luciferase activity, and these data were further normalised to the un-stimulated EV control, or the un-stimulated control of each test plasmid, as indicated in the figure legends, to yield a fold induction.

2.4.2 RNA extraction and cDNA synthesis

RNA was extracted from cells using the QIAgen RNeasy RNA extraction kit according to the manufacturer's protocols. For 24- and 6-well plates the cells were harvested in 350 µl buffer

RNeasy lysis buffer (RLT). For reverse transcription to synthesize complementary DNA (cDNA), each reaction contained 1 µg RNA, 2.5 µM oligo dT, 500 µM dNTP, made up to 13 µl with nuclease-free water. These reactions were incubated at 65 ^{o}C for 5 min and then transferred directly to ice for 1 min. To each reaction was then added 4 µl 5x First-strand buffer (Invitrogen), 5 mM DTT, 40 U RNase OUT (Invitrogen), 50 U Superscript III reverse transcriptase (Invitrogen), made up to a total of 20 µl with nuclease-free water. The reactions were incubated at 50 ^{o}C for 1 h, followed by 70 ^{o}C for 15 min. cDNA was diluted 1:2 in nuclease-free water before quantitative reverse transcription-polymerase chain reaction (qRT-PCR) analysis (see 2.4.3).

2.4.3 qRT-PCR

Each qRT-PCR, performed in 96-well plates, in duplicate, contained 2 µl cDNA, 10 µl 2x SYBR® Green PCR master mix (Applied Biosystems), 0.5 µM of each primer, made up to 20 µl with water per well. A ΔΔCt relative quantity assay was then performed where the amplification of genes of interest was normalised to an endogenous control (GAPDH) on a 7900HT Real-Time PCR machine (Applied Biosystems) using the following programme:

2 min	50 ^{o}C	
10 min	95 ^{o}C	
15 s	95 ^{o}C	
1 min	60 ^{o}C	40 cycles

Data were analysed using the RQ Manager 1.2 software (Applied Biosystems).

Primer	**Sequence**
Human GAPDH FWD	5′ ACCCAGAAGACTGTGGATGG 3′
Human GAPDH REV	5′ TTCTAGACGGCAGGTCAGGT 3′
Human CCL-5 FWD	5′ CCCAGCAGTCGTCTTTGTCA 3′
Human CCL-5 REV	5′ TCCCGAACCCATTTCTTCTCT 3′

2.4.4. Statistical analysis

Statistical analysis of data was performed using GraphPad Prism 5 software. For reporter gene assays, qRT-PCR, ELISA, weight loss, signs of illness, lesion measurements and flow

cytometry, data were analysed using an unpaired Student's T-test, applying Welch's correction. For IMV plaque reduction neutralisation assays the data were analysed using a Mann-Whitney non-parametric test. * $P<0.05$, ** $P<0.01$, *** $P<0.001$

2.5 Tandem affinity purification

2.5.1. Plasmid construction

C6 amplified from WR genomic DNA by PCR (see 2.1.1) was cloned into the pcDNA4/TO tandem affinity purification (TAP) vectors (containing a zeocin resistance cassette, constructed by B. Ferguson) using the restriction enzymes *Xba*I and *Not*I for N-terminal TAP and *Kpn*I and *Not*I for C-terminal TAP (see Table 2.1 for oligonucleotide primers). The TAP tag consisted of two Streptavidin (Strep) epitopes fused to a FLAG epitope.

2.5.2 Construction of stable inducible cell lines

HEK293 T-REx cells grown in 10-cm dishes were transfected with 5 μg pcDNA4/TO C6-TAP or pcDNA4/TO TAP-C6 plasmids using Fugene-6 (see 2.2.3). Once confluent the cells were transferred into new dishes at varying dilutions in the presence of zeocin (100 μg/ml) to allow colony formation of zeocin-resistant cells. Colonies were then picked for amplification. Clonal cell lines were tested for inducible expression of TAP-tagged C6 by growth in the presence or absence of 2 μg/ml doxycycline for 24 h, followed by analysis of cell extracts by immunoblotting.

2.5.3. TAP assay

Prior to lysis, the cells were washed once with PBS and were removed from the flask by incubation for 3 min with 3 ml 0.05 % trypsin EDTA (Gibco) per 175 cm^2 flask. The cells were resuspended in 10 ml medium per flask, pooled and collected by centrifugation at 250 x *g* for 5 min. The pellet was washed in PBS and the cells were again collected as above. The cells were then lysed by resuspension in 1 ml TAP IP buffer (0.5 % NP-40 (v/v) in PBS supplemented with protease and phosphatase inhibitors (Roche)) per flask and incubated for 20 min, rotating at 4 ^{o}C. The cellular debris was collected by centrifugation at 1,000 x *g*, 10 min, 4 ^{o}C. The supernatant was removed and a sample was taken to analyse as 'input'. The

remaining cleared lysate was incubated with 100 µl strep-tactin beads (IBA) per condition (prepared by washing once in water and three times in wash buffer (0.1 % NP-40 (v/v) in PBS supplemented with protease and phosphatase inhibitors (Roche), centrifuging at 600 x *g* for 30 s per wash), with rotation at 4 ^{o}C for 1-2 h. The beads were collected by centrifugation at 600 x *g* for 5 min and washed three times in wash buffer by centrifugation at 600 x *g* for 30 s. The proteins were eluted from the strep-tactin beads by incubation with a des-thiobiotin solution (IBA, strep-tag elution buffer), with rotation for 30-60 min. The beads were then collected by centrifugation, the supernatants were transferred to clean eppendorfs and were incubated with 100 µl anti-FLAG M2 agarose beads (Sigma) per condition (prepared by washing once in water and three times in wash buffer) with rotation for 1-2 h at 4 ^{o}C. The beads were collected by centrifugation and washed three times in wash buffer. The proteins were eluted from the anti-FLAG beads by incubation with a 250 µg/ml FLAG-peptide solution (Sigma), rotating for 30-60 min. The beads were then collected by centrifugation and the supernatants were transferred to an Amicon Ultra centrifugal filter (3K membrane, Millipore) and were centrifuged at 14,000 x *g*, 4 ^{o}C until approximately 50 µl remained.

2.5.4. Mass spectrometry analysis

For the TAP assay using the HEK293 T-REx C6-TAP cell line the proteins in the final elution, or still associated with the beads, were separated by Nu-PAGE (see 2.3.4) and silver stained (see 2.3.7). The protein bands of interest were then excised carefully from the gel and sent for liquid chromatography-mass spectrometry (LC-MS/MS) analysis (Systems Biology Centre, Imperial College South Kensington Campus). For the TAP assay from HCT116 cells infected with vC6TAP (see 2.6.2) the final elution was sent to the Cambridge Centre for Proteomics (University of Cambridge) to be separated by PAGE. The lane of the gel was then cut into 16 equal slices and each one analysed by LC-MS/MS.

2.6 Construction of recombinant VACV

2.6.1 Plasmid construction

To construct the *C6L* deletion virus 300-350 bp of the left and right flanking regions of the C6 ORF were amplified by overlapping PCR from WR genomic DNA. Each PCR contained

100 ng WR genomic DNA, or 10 ng of PCR product and was performed according to 2.1.1 (see table 2.1 for oligonucleotide primers). To construct the revertant virus, the haemaglutinin (HA)-tagged revertant virus and the frame-shift revertant virus the C6 ORF, an HA-tagged version of the C6 ORF or the C6 ORF with an additional adenine nucleotide in the start codon, respectively, in addition to the 300-350 bp left and right flanking regions were amplified by overlapping PCR as described above (for schematics of the inserts see Figure 3.6A). PCR products were cloned into the Z11 plasmid (*Escherichia coli guanylphosphoribosyl transferase* (Ecogpt) (Boyle & Coupar, 1988) fused to *enhanced green fluorescent protein* (EGFP)) by digesting the PCR product and Z11 plasmid DNA with the restriction enzymes *Bam*HI and *Not*I (see 2.1.4) and then ligating the digestion products together (see 2.1.5). To construct the TAP-tagged revertant virus the left flanking region of C6 plus the C6 ORF was inserted upstream of the TAP tag in the pcDNA4/TO TAP vector using the restriction enzymes *Bam*HI and *Not*I. The right flanking region of C6 was then inserted downstream of the TAP tag in the resulting vector using the restriction enzymes *Sac*II and *Xba*I. The left flanking region of C6, the C6 ORF, the TAP tag and the right flanking region of C6 were then excised together and inserted into the pUC13 vector containing the Ecogpt fused with EGFP cassette (constructed by B. Bahsoun) using the restriction enzymes *Bam*HI and *Xba*I.

2.6.2 Infection/transfection protocol

C6 recombinant viruses were constructed using the transient dominant selection method (Falkner & Moss, 1988). For construction of vΔC6, a 25 cm^2 flask of CV-1 cells was infected with WR at 0.01 plaque forming units (p.f.u.) per cell for 90 min in infection medium (DMEM + 2.5 % (v/v) FBS + P/S). The cells were then transfected with 5 μg Z11ΔC6 plasmid using Fugene-6 (see 2.2.3) and were harvested after 48 h. The resulting virus was diluted in ten-fold steps and used to infect RK-13 cells in the presence of mycophenolic acid (MPA, 25 μg/ml), hypoxanthine (HX, 15 μg/ml) and xanthine (X, 250 μg/ml). Green plaques were picked and purified by three rounds of infection using RK-13 cells. The intermediate virus was resolved in BSC-1 cells by three rounds of infection in the absence of MPA, HX and X. The phenotype of resolved viruses was analysed by PCR (see 2.6.3). An intermediate virus that had resolved back to the wild-type phenotype was purified as the wild-type virus for *in vivo* work (vC6WR). For the construction of vC6Rev, vC6HA, vC6FS and vC6TAP,

CV-1 cells were infected with vΔC6, followed by transfection with Z11C6Rev, Z11C6HA, Z11C6FS or pUC13 C6TAP, respectively, as described above.

2.6.3 Screening plaques by PCR

To confirm the phenotype of plaques by PCR, plaques were picked directly into a well of a 24 well-plate of RK-13 cells. The cells were scraped 48 h later and the medium was transferred to a 2 ml tube and was sonicated well at 100 W. Ten µl of lysate was treated with proteinase K according to the manufacturer's instructions (Sigma) in a total of 50 µl. Each PCR contained 0.5 µl proteinase K-treated lysate, 10x GoTaq buffer (Promega), 2 mM $MgCl_2$, dNTPs (0.2 mM each), 0.2 µM of the primers used to construct Z11ΔC6 (see Table 2.1) and 1 U GoTaq polymerase (Promega), made up to a total volume of 30 µl with water. PCR was carried out in a thermo cycler using the following programme:

5 min 95 ^{o}C	
30 s 95 ^{o}C 30 s 50 ^{o}C 90 s 68 ^{o}C	5 cycles
30 s 95 ^{o}C 30 s 55 ^{o}C 90 s 72 ^{o}C	25 cycles
10 min 72 ^{o}C	

PCR products were separated by agarose gel electrophoresis (see 2.1.2).

2.6.4 Amplification of crude virus stocks

For the preparation of a master stock of crude virus, one 25 cm^2 flask of RK-13 cells per virus was infected at 0.1 p.f.u. per cell for 48 h. The cells were scraped in their medium, collected by centrifugation at 500 x *g* for 10 min and resuspended in 1 ml infection medium. For preparation of working stock crude virus, five 175 cm^2 flasks of RK-13 cells per virus were infected at 0.1 p.f.u. per cell for 48 h. The cells were collected as described above and resuspended in 5 ml infection medium. Recombinant viruses were stored at –80 ^{o}C.

2.6.5 Virus titration

Viruses were titrated by plaque assay, in duplicate, on monolayers of BSC-1 grown in six-well plates. The viruses were diluted in infection medium (10^{-5} to 10^{-9} dilutions, total volume 500 µl) and were incubated with the cells for 90 min at 37 ^{o}C, rocking the plate every 15 min. After this time the virus was removed and 2 ml 50% 2x MEM (supplemented with 5 % (v/v) FBS and 100 µg/ml P/S): 50% 3% (w/v) carboxy methyl cellulose (CMC) was added to each well. The cells were incubated for 48-72 h to allow for plaque formation. The MEM/CMC mix was then removed, the cells were washed once with PBS and were stained for 30 min with crystal violet (5 % (v/v) crystal violet solution (Sigma), 25 % (v/v) ethanol). The wells were then washed with water and the number of plaques was counted.

2.6.6 Virus purification by sedimentation through sucrose

Recombinant viruses were partially purified for *in vivo* use by sedimentation through two sucrose cushions. Ten 175 cm^2 flasks of RK-13 cells per virus were infected at 0.1 p.f.u. per cell for 48 h. The cells were then scraped, pooled (where appropriate) and collected by centrifugation at 500 x *g* for 5 min at 4 ^{o}C. The cell pellets were resuspended in 10 ml 10 mM Tris pH 9 for 10 min to allow the cells to swell and the cells were then disrupted by Dounce homogenisation on ice. The homogenised cells were transferred to a fresh tube and the nuclei and unbroken cells were collected by centrifugation at 250 x *g* for 5 min. The supernatant was transferred carefully to a fresh tube on ice and the pellet was resuspended in 5 ml 10 mM Tris pH 9 and homogenised again. The homogenates were combined and centrifuged at 500 x *g* for 30 min. Ultracentrifuge tubes (Beckman Coulter) were prepared with 18 ml 36 % (w/v) sucrose solution. The cytoplasmic extracts were sonicated at 100 W for 10 s and then layered carefully on the sucrose cushion. The supernatants were centrifuged at 32,900 x *g* for 80 min at 4 ^{o}C. The supernatants were discarded and the pellet containing the virus was resuspended in 1 ml 10 mM Tris pH 9 by sonicating briefly for 10 s as above, followed by incubation on ice for 30 s, repeated three times. Fresh ultracentrifuge tubes were prepared with 18 ml 36 % (w/v) sucrose solution and the resuspended virus pellet was layered on top. The samples were centrifuged a second time at 32,900 x *g* for 80 min at 4 ^{o}C. The supernatant was again discarded and the pellet was washed by resuspension in 36 ml 10 mM Tris pH 9. The tubes

were finally centrifuged at 26,000 x *g* for 50 min at 4 ^{o}C. The supernatant was discarded and the pellet was resuspended in 1 ml 10 mM Tris pH 9, aliquotted and stored at -80 ^{o}C.

2.7 Analysis of recombinant VACV

2.7.1 Infection of cells

For infection with VACV, the viruses were thawed in a 37 ^{o}C water bath and sonicated for 10-15 s at 100 W. The viruses were diluted in infection medium and added to cells in the minimal volume required to cover them. The cells were incubated with virus for 90 min at 37 ^{o}C, with rocking of the plate or dish every 15 min. After this time the unbound virus was removed and replaced with an appropriate volume of fresh infection medium. For infection of cells with NDV (provided by the laboratory of W. Barclay, Imperial College London), the virus was thawed and incubated with the cells as described above, without sonication.

2.7.2 Timing of C6 expression

To analyse the time p.i. at which C6 protein could be detected, BSC-1 cells that had been grown in 3.5-cm dishes were infected in the presence or absence of 40 μg/ml cytosine arabinoside (AraC) at 10 p.f.u. per cell of WR in 500 μl infection medium for 90 min, rocking on ice. After this time one dish of cells was harvested (0 h) and for the remaining dishes the unbound virus was removed by washing with infection medium, the cells were incubated in 2 ml infection medium (-/+ AraC where appropriate) and the dishes returned to 37 ^{o}C. The cells were harvested at various time points p.i. as described in 2.3.1.

2.7.3 Localisation by cellular fractionation

For cellular fractionation HeLa cells were prepared in 14.5-cm dishes and infected with recombinant viruses overnight at 5 p.f.u. per cell. The cells were washed twice in ice cold LS buffer (20 mM Hepes pH 7.8, 0.5 mM DTT, 0.5 mM $MgCl_2$) and allowed to swell in 20 ml LS buffer on ice for 20 min. The buffer was then removed and the cells were scraped gently. The cells were then disrupted by Dounce homogenisation on ice with 20 strokes with a loose homogeniser. The lysates were transferred to eppendorf tubes and were centrifuged at 600 x *g*

for 2 min at 4 ^{o}C to sediment the nuclei. The supernatant (cytoplasmic fraction) was transferred to a clean eppendorf tube. The nuclei were washed five times in PBS by gentle resuspension and re-collected by centrifugation at 600 x *g* for 2 min at 4 ^{o}C. Finally the nuclei were resuspended in 100 µl nuclei resuspension buffer (50 mM Tris/HCl pH 8, 0.5 mM $MgCl_2$, 20 mM iodoactetamide supplemented with protease inhibitor (Roche)) and sonicated until well disrupted.

2.7.4 Purification and digestion of viral genomic DNA

Viral genomic DNA was purified from IMV cores that had been purified by sucrose density ultracentrifugation. The sucrose gradients were prepared in 36 ml ultracentrifuge tubes (Beckman Coulter) the day before use and stored at 4 ^{o}C. The gradient was prepared by adding 5.8 ml 24 % (w/v) sucrose to the ultracentrifuge tube, followed by the drop-wise addition of 5.8 ml 28 % (w/v) sucrose, 5.8 ml 32 % (w/v) sucrose, 5.8 ml 36 % (w/v) sucrose and finally 5.8 ml 40 % (w/v) sucrose. Five-hundred µl of recombinant virus that had been sedimented through a 36 % (w/v) sucrose cushion (see 2.6.6) was carefully added to the top of the sucrose gradient and then centrifuged at 26,000 x *g* for 50 min, 4^{o}C. The sucrose above the white virus band was aspirated, the virus was removed carefully using a 5 ml pipette and was transferred to a clean ultracentrifuge tube. The virus was diluted 1:3 in 10 mM Tris pH 9 and was centrifuged at 32,900 x *g* for 80 min, 4 ^{o}C. Finally the viral pellet was finally resuspended in 600 µl 50 mM Tris pH 7.8. To extract viral DNA, proteinase K reactions were incubated at 37 ^{o}C for 4-6 h and consisted of 600 µl sucrose gradient-purified virus, 0.05 M Tris pH 7.8, 0.5 % (w/v) SDS, 6 % (w/v) sucrose and 4000 U proteinase K. Viral genomic DNA was then purified by phenol-chloroform extraction. One volume of phenol:chloroform:isoamyl alcohol was added to the proteinase K-treated virus, the sample was mixed and then centrifuged at 2,500 x *g* for 2 min. The aqueous phase was transferred to a clean eppendorf and one volume of phenol:chloroform:isolamyl alcohol was added and centrifuged as above. The aqueous phase was again transferred to a clean eppendorf and one volume of phenol:chloroform:isolamyl alcohol was added and the mixture was centrifuged as above. The aqueous phase was transferred to a clean eppendorf and one volume of chloroform:isoamyl alcohol was added and the mixture was centrifuged as above. The aqueous phase was transferred to a clean eppendorf tube and the DNA was precipitated by the addition of sodium acetate pH 7.0 (final concentration 0.1 M) and one volume of ice-cold

100 % ethanol and incubation at -20 °C for 30-60 min. The DNA was collected by centrifugation at 14,000 x *g* for 30 min at 4 °C. The pellet was washed with 1 ml 70 % ethanol and then centrifuged again at 14,000 x *g* for 10 min. The ethanol was removed completely and the pellet was allowed to air-dry for 15 min. Finally the pellet was dissolved in 100 µl water.

2.7.5 *In vitro* growth curves

For the single-step growth curves six 25 cm^2 flasks of BSC-1 cells per virus were infected at 10 p.f.u. per cell in 1.5 ml infection medium for 90 min. After this time the virus was removed and the cells were washed twice with fresh medium to remove any unbound virus. The cells were then incubated in 5 ml infection medium. At 0 h, 12 h and 24 h time points the medium was removed carefully and the cells were collected by centrifugation at 500 x *g* for 10 min. The supernatant (extracellular virus) was carefully removed and titrated immediately (see 2.6.5). The cells were then scraped in 3 ml fresh medium and added to the pellet from the first centrifugation step. The cells were collected as described above, resuspended in 500 µl infection medium and stored at -20 °C (intracellular virus). For the multi-step growth curve eight 25 cm^2 flasks of BSC-1 cells per virus were infected at 0.01 p.f.u. per cell as described above. Virus was harvested at 0 h, 12 h, 48 h and 72 h p.i. as described above. Harvested viruses were titrated on BSC-1 cells as described in 2.6.5.

2.7.6 Plaque size analysis

RK-13, BSC-1 and TK143 cells were prepared in six-well plates and infected in duplicate with virus at 50 p.f.u. per well. Plaques were allowed to form over a period of 72 h. The cells were washed once with PBS and stained for 60 min with crystal violet (5 % (v/v) crystal violet solution (Sigma), 25 % (v/v) ethanol). The wells were then washed with water and the size of six plaques per well measured using Axiovision 4.6 software and a Zeiss Axiovert 200M microscope.

2.8 Murine *in vivo* experiments

2.8.1 Intranasal infection

Groups of female BALB/c mice, aged 6-8 weeks old, were inoculated i.n. with 20 µl sucrose-purified recombinant VACV (see 2.6.6) diluted in PBS whilst under anaesthetic (Williamson et al, 1990). The titre of each inoculum was confirmed by plaque assay (see 2.6.5). The animals were weighed daily and scored for signs of illness as follows:

1 – hair ruffling
2 – back arching
3 – reduced mobility
4 – severe pneumonia

2.8.2 Preparation of cells from BAL

The bronchoalveolar lavage (BAL) was harvested in 1 ml PBS containing 10 U/ml heparin per animal. The cells were collected by centrifugation at 1,000 x *g* for 5 min and the supernatant was transferred to a clean tube for cytokine analysis by ELISA (see 2.3.11). The cells were resuspended in 500 µl ACK buffer (150 mM NH_4Cl, 10 mM $KHCO_3$, and 0.1 mM Na_2EDTA, pH 7.4) and incubated at room temperature for 3 min to lyse the red blood cells. Ten ml RPMI + 10 % (v/v) FBS + P/S (hereafter termed 'RPMI-10') was added and the cells were collected as above. The cells were then resuspended in 300 µl fluorescence-activated cell sorting (FACS) buffer (0.1 % (w/v) BSA, 0.1 % (w/v) sodium azide in PBS) and were enumerated by trypan blue exclusion.

2.8.3. Extraction of cells from lung

The lung tissue was cut into small pieces and incubated in 3 ml digestion medium (1 mg/ml collagenase, 30 µg/ml DNaseI in RPMI-10) for 30 min at 37 ^{o}C with periodic agitation. The lung homogenate was passed through a cell strainer into a 50 ml Falcon tube and 250 µl was retained for virus titration (see 2.8.6). The strainer was washed with 2 ml RPMI-10 and the cells were collected by centrifugation at 1000 x *g* for 5 min. The pellet was vortexed briefly,

the cells were resuspended in 1 ml ACK buffer and then incubated at room temperature for 3 min. Nineteen ml of RPMI-10 was added and the cells were collected as above. The pellet was resuspended in 5 ml 20 % Percoll (Sigma) in RPMI-10 and centrifuged at 1000 x *g* for 20 min. The cells were then resuspended in 2 ml FACS buffer and enumerated by trypan blue exclusion (using a 1:10 dilution).

2.8.4. Extraction of cells from spleen

A 10-cm dish was prepared with 5 ml RPMI-10 and a fine metal mesh was placed over the top. The spleen was cut into small pieces and then mashed on top of the mesh using the end of the plunger of a 10 ml syringe by the addition of 1 ml RPMI-10 at a time (5 ml in total). The cell suspension was passed through a cell strainer into a 50 ml Falcon tube and 500 µl was retained for virus titration (see 2.8.6). Ten ml of RPMI-10 was added to wash the cell homogenate and the cells were collected by centrifugation at 1,000 x *g* for 5 min. The pellet was resuspended in 4 ml ACK buffer and was incubated at room temperature for 3 min. Sixteen ml RPMI-10 was then added and the cells were collected as above. Finally the cells were resuspended in 10 ml FACS buffer and enumerated by trypan blue exclusion (using a 1:10 dilution).

2.8.5. Staining of cells and flow cytometry

Cells in FACS buffer were collected by centrifugation at 1,000 x g for 5 min, resuspended in an appropriate volume of FACS block (10 % (v/v) normal rat serum (AbD Serotec Ltd.), 1:500 anti-CD16/CD32 Fc gamma receptor (BD Biosciences) in FACS buffer) for the number of staining conditions required (100 µl per condition) and transferred into wells of a round-bottom 96-well plate. The plate was incubated at 4 ^{o}C for 30 min. The FACS Abs were prepared by diluting in FACS block (100 µl per well). Ab panel 1 included anti-CD3, anti-CD4, anti-CD8 and anti-CD69 or anti-CD44 Abs for T lymphocytes and anti-CD19 to stain for B lymphocytes (see below). Ab panel 2 included anti-F4/80 and anti-CD11b Abs to stain for macrophages, anti-Ly6G to stain for neutrophils and anti-DX5 to stain for NK cells (see below). The cells were collected by centrifugation as above, resuspended in the FACS stains and incubated at 4 ^{o}C for 30 min in the dark. The cells were collected as above and washed once with 200 µl PBS per well. The cells were again collected, resuspended in 100 µl

LIVE⁄DEAD® Fixable Aqua Dead Cell Stain (Invitrogen) per well, diluted 1:500 in PBS and incubated at 4 ^{o}C for 30 min in the dark. The cells were collected and washed with PBS as above and then were resuspended in 100 µl fixing solution (2 % (v/v) paraformaldehyde in PBS) per well, and incubated at room temperature for 30 min in the dark. The cells were collected and washed in PBS as above, resuspended in 200 µl FACS buffer per well and stored overnight at 4 ^{o}C. Stained cells were analysed on a BD FACS CantoII flow cytometer and these data were analysed using FlowJo software. Ab compensation was performed using rat/hamster Ab compensation beads (BD Biosciences). For BAL 10,000 events were analysed where possible and 100,000 events were analysed for the spleen and lung samples.

Antibody	Source	Dilution
rat-anti-CD3 APC-Cy7	BD Biosciences (560590)	1:50
rat-anti-CD4 APC	BD Biosciences (553051)	1:200
rat-anti-CD8 FITC	BD Biosciences (553031)	1:100
Armenian hamster-anti-CD69 PE	BD Biosciences (553237)	1:100
rat-anti-CD19 PE-Cy7	BD Biosciences (552854)	1:200
rat-anti-F4/80 APC	Serotec (MCA 497 APC)	1:20
rat-anti-CD11b APC-Cy7	BD Biosciences (557657)	1:100
rat-anti-Ly6G PE	BD Biosciences (551461)	1:100
rat-anti-DX5 FITC	BD Biosciences (553857)	1:100
rat-anti-CD44 PE	BD Biosciences (553135)	1:100

2.8.6. Virus titre analysis from infected tissue

Cell suspensions taken from the lung (see 2.8.3) and spleen (see 2.8.4) for viral titre analysis were subjected to three rounds of freeze-thawing and were sonicated briefly before titration on monolayers of BSC-1 cells as described in 2.6.5.

2.8.7 Intradermal infection

Groups of female C57BL/6 mice, aged 6-8 weeks old, were inoculated i.d. with 10 µl sucrose-purified recombinant VACV (see 2.6.6) diluted in PBS in both ear pinna whilst under anaesthetic (Tscharke & Smith, 1999). The titre of each inoculum was confirmed by plaque assay (see 2.6.5). The diameter of the resulting lesions was measured daily using a micrometer.

2.8.8. Vaccination and challenge experiment

Groups of female C57BL/6 mice, aged 6-8 weeks old, were vaccinated by i.d. infection in both ears, as described in 2.8.7. One month later the animals were challenged i.n. with 5×10^6 p.f.u. WR per animal, as described in 2.8.1. The animals were weighed daily. The titre of both vaccination and challenge inocula were confirmed by plaque assay (see 2.6.5).

2.8.9. IMV plaque reduction neutralisation assay

One month post-vaccination animals were sacrificed and the blood was taken. The blood was incubated at room temperature for 1 h to allow clotting to occur. The blood cells were then collected by centrifugation at 2,500 x *g* for 30 min. The serum was transferred to a clean eppendorf tube and was stored at -80 ^{o}C. Complement in the serum was inactivated by incubation at 56 ^{o}C for 30 min. Two-fold dilutions of serum were then prepared from 1:25-1:800, diluted in infection medium. The diluted serum was then incubated for 1 h at 37 ^{o}C with 100 p.f.u. sucrose purified WR per sample. The serum/virus mixes were then titrated in duplicate on monolayers of BSC-1 cells (see 2.6.5).

2.8.10. VACV ELISA

The VACV ELISA was performed in 96-well immunoplates (Nunc). The plates were coated overnight at 4 ^{o}C with antigen (1:500 dilution of a cell lysate of WR-infected cells (Putz et al, 2006), or 2 μg/ml BSA) diluted in 50 mM $NaHCO_3$ pH 9.6. The plates were washed three times in wash buffer (2 mM Tris-HCl, 154 mM NaCl, 0.2 % (v/v) Tween-20) and then blocked for 2 h at room temperature in 5 % (w/v) milk proteins in TBS. Two-fold dilutions of serum (1:100-1:12,800) were prepared in 1 % (w/v) milk proteins in TBS + 0.1 % (v/v) Tween-20 (TBST). Blocked plates were washed three times as above and were incubated with the diluted serum at room temperature for 90 min. The plates were again washed three times as above and were incubated at room temperature for 1 h with goat-anti-mouse IgGγ specific-alkaline phosphatase conjugate (Sigma) diluted 1:1000 in 1 % (w/v) milk proteins in TBST. The plates were washed three times as above and the revelation solution (1 Sigma FAST pNPP tablet and 1 Sigma FAST buffer tablet per 10 ml water) was added for 1 h. The absorbance was then measured at 405 nm, with 650 nm as a reference.

2.8.11 Chromium release cytotoxicity assay

EL-4 (murine T lymphoma cell line) target cells were infected with WR at 20 p.f.u. per cell for 2 h in RPMI infection medium (RPMI + 2.5 % (v/v) FBS + P/S). The cells were collected by centrifugation at 250 x *g* for 5 min, resuspended in ^{51}Cr solution supplemented with 30 % (v/v) FBS (150 μCi per 3 x 10^6 cells) and incubated at 37 ^oC for 2 h. Chromium-loaded cells were then washed three times in RPMI-10 by centrifugation at 250 x *g* for 5 min per wash. Finally the cells were resuspended in RPMI-10 at 10^6 cells/ml. Splenocytes (effector cells) from infected mouse spleens were prepared as described in 2.8.4. Two-fold dilutions of effector cells were prepared in RPMI-10 to give 100:1 to 2.5:1 effector cell:target cell ratios. The effector cells were then incubated with infected target cells for 6 h at 37 ^oC. The cells were collected by centrifugation at 250 x *g* for 5 min and 100 μl supernatant transferred to a LUMA plate (PerkinElmer) to quantify the radioactivity of the sample.

2.8.12 ELISPOT

Enzyme-linked immunosorbent spot (ELISPOT) plates were coated with IFNγ capture Ab overnight at 4 ^oC (Mouse IFNγ ELISPOT set, Beckton Dickenson). The wells were washed once in RPMI-10 and then blocked by incubating with RPMI-10 for 2 h at room temperature. Whole splenocytes were prepared from infected mouse spleens as described in 2.8.4. Two-fold dilutions of splenocytes were prepared from 2 × 10^6 cells/ml to 2.5 × 10^5 cells/ml in RPMI infection medium. The splenocytes were then stimulated overnight by incubation at 37 ^oC with VACV-specific peptide (TSYKFESV or VGPSNSPTF, 2 μg/ml) or with EL-4 cells that had been infected for 4 h with 20 p.f.u. per cell WR (50,000 cells per well). The cell suspensions were removed and the wells were washed twice with deionised water, allowing a 3-5 min incubation per wash. The wells were then washed three times with PBST, allowing a 1-2 min incubation per wash. The plate was incubated with IFNγ detection Ab (Mouse IFNγ ELISPOT set, Beckton Dickenson) diluted in PBS + 10 % (v/v) FBS and were incubated at room temperature for 2 h. The wells were then washed three times in PBST as above. The enzyme conjugate (Mouse IFNγ ELISPOT set, Beckton Dickenson) diluted in PBS + 10 % (v/v) FBS was added to wells and the mixture was incubated at room temperature for 1 h. Wells were then washed four times in PBST as above, and twice with PBS. Aminoethylcarbazole (AEC) substrate reagent (Beckton Dickenson) was added to each well

and spots were allowed to develop for 5 min. The substrate reaction was stopped by washing wells with deionised water. The plates were air-dried overnight in the dark and the spots were enumerated.

Chapter 3: Analysis of the VACV WR *022* ORF encoding protein C6

3.1 Bioinformatic analysis of the *022* ORF from VACV strain WR

ORF *022* of the WR strain of VACV (gene *C6L* in VACV strain Copenhagen and termed protein C6 from here on) is 456 bp in length and is situated at the left end of the genome. It is predicted to encode an uncharacterised polypeptide of 151 amino acids with a molecular mass of 17.3 kDa and a PI of 4.96. It is not predicted to have any coiled-coil segments and does not contain an obvious signal peptide sequence (www.poxvirus.org). Using the viral protein localisation algorithm Virus-mPLoc (www.csbio.sjtu.edu.cn/bioinf/virus-multi/), C6 is predicted to be cytoplasmic as it contains no obvious nuclear localisation sequence (NLS) (Shen & Chou, 2010).

The predicted C6 protein is highly conserved amongst VACV strains (>96 % amino acid identity), with differences in amino acid sequence at just six residues (Figure 3.1, highlighted in red). C6 is also highly conserved in MVA (97 % identity), except for an additional six amino acids present at the C terminus of both the sequenced strains of MVA. These extra residues are also present in VACV strain ACAM3000. The high level of conservation of C6 is also maintained within the OPV family (>88 % identity) with all sequenced OPVs encoding a C6 orthologue (Figure 3.2). Notably the C6 orthologue of RPXV strain Utrecht and C6 from all sequenced VACV strains are a few amino acids shorter in length compared to other OPVs, due to a 5 amino acid deletion at residue 146 close to the C terminus of the protein. Outside of the OPV family C6 orthologues are predicted to be encoded by members of the *Capripoxvirus* genus goatpox, sheepox and lumpy skin disease virus, and also by the unclassified mule deer poxvirus (www.poxvirus.org). C6 encoded by VACV WR shares between 46-50 % similarity and 26-27 % identity with these non-OPV orthologues.

Structural-based screens of the VACV genome have identified C6 as a member of the VACV Bcl-2-like Pfam (Finn et al, 2008) protein family. This family currently consists of 10 proteins; A46, A52, B14, C1, C6, C16/B22, F1, K7, N1 and N2 (Gonzalez & Esteban, 2010; Graham et al, 2008) with low amino acid sequence identity, but for A52, B14

Figure 3.1: Conservation of WR_022 amongst sequenced VACV strains. Orthologues of WR_022 in VACV strains were identified from www.poxvirus.org and the amino acid sequences were aligned using the online ClustalW2 multiple sequence alignment tool. Positions where the amino acid sequence differs between strains are indicated in red.

Figure 3.2: Conservation of WR_022 amongst the OPVs. Orthologues of WR_022 in OPV strains were identified from www.poxvirus.org and the amino acid sequences were aligned using the online ClustalW2 multiple sequence alignment tool. RPXV: rabbitpox virus, VACV: vaccinia virus, VARV: variola virus, TATV: taterapox virus, CMLV: camelpox virus, CPXV: cowpox virus, MPXV: monkeypox virus, HSPV: horsepox virus, ECTV: ectromelia virus.

(Graham et al, 2008), K7 (Kalverda et al, 2008; Oda et al, 2009), N1 (Aoyagi et al, 2007; Cooray et al, 2007) and F1 (Kvansakul et al, 2008) whose structures have been solved, a high level of structural similarity exists and this resembles the fold of the cellular Bcl-2 family of apoptotic regulators (Petros et al, 2004). The structure of C6 was modelled using MODELLER (Eswar et al, 2006), based on a sequence alignment with the VACV Bcl-2 family member B14 (Graham et al, 2008) (Figure 3.3). This algorithm predicted the structure of C6 to be highly similar to B14, adopting a Bcl-2 fold comprising of seven alpha helices. Subjecting this model to the Ramanchandran plot assessor RAMPAGE (Lovell et al, 2002) indicated that 95.5 % of the residues were in a favourable region of the plot, supporting the validity of this structural prediction. Notably the residues at which the VACV strains differ in sequence (Figure 3.1) are mainly found within alpha helices 3 and 4 in the C6 model.

The cellular Bcl-2 proteins have characterised roles in regulating apoptosis, but despite the high level of structural similarity between these cellular proteins and N1, F1, B14 and A52, only N1 and F1 are anti-apoptotic (Cooray et al, 2007; Graham et al, 2008). Cellular anti-apoptotic proteins exert their function via a groove on their surface that interacts with the BH3 peptide of pro-apoptotic family members (Youle & Strasser, 2008). This groove lies between alpha helices 2 and 4 of myxoma poxvirus protein M11, as demonstrated in the crystal structure of this protein in complex with the BH3 peptide of human Bak-2 (Douglas et al, 2007). Alpha helices 2 and 4 are also believed to form the BH3-binding groove in protein N1, based on model predictions (Cooray et al, 2007). Residues V64 and F65 in helix 2 of B14, as well as Y90 in helix 4 however are predicted to occlude this potential BH3 peptide binding groove and explain why this protein in not anti-apoptotic (Graham et al, 2008) (Figure 3.3). Similar bulky residues are also present at equivalent positions at the end of helices 2 and 4 in A52, which is also not able to inhibit apoptosis (Graham et al, 2008). N1 on the other hand is one turn shorter in helix 2 than B14 and A52 and does not have bulky residues protruding into the putative BH3 peptide binding groove, a potential explanation for how this member of the VACV Bcl-2 family has anti-apoptotic abilities (Figure 3.3). Like B14, C6 has an additional turn in helix 2 and at positions equivalent to V64 and F65 there are two tyrosine residues (Figure 3.3), which are also bulky and may occlude the putative BH3 peptide binding groove. From this structural model C6 is therefore not predicted to have anti-apoptotic ability, but this still remains to be confirmed experimentally.

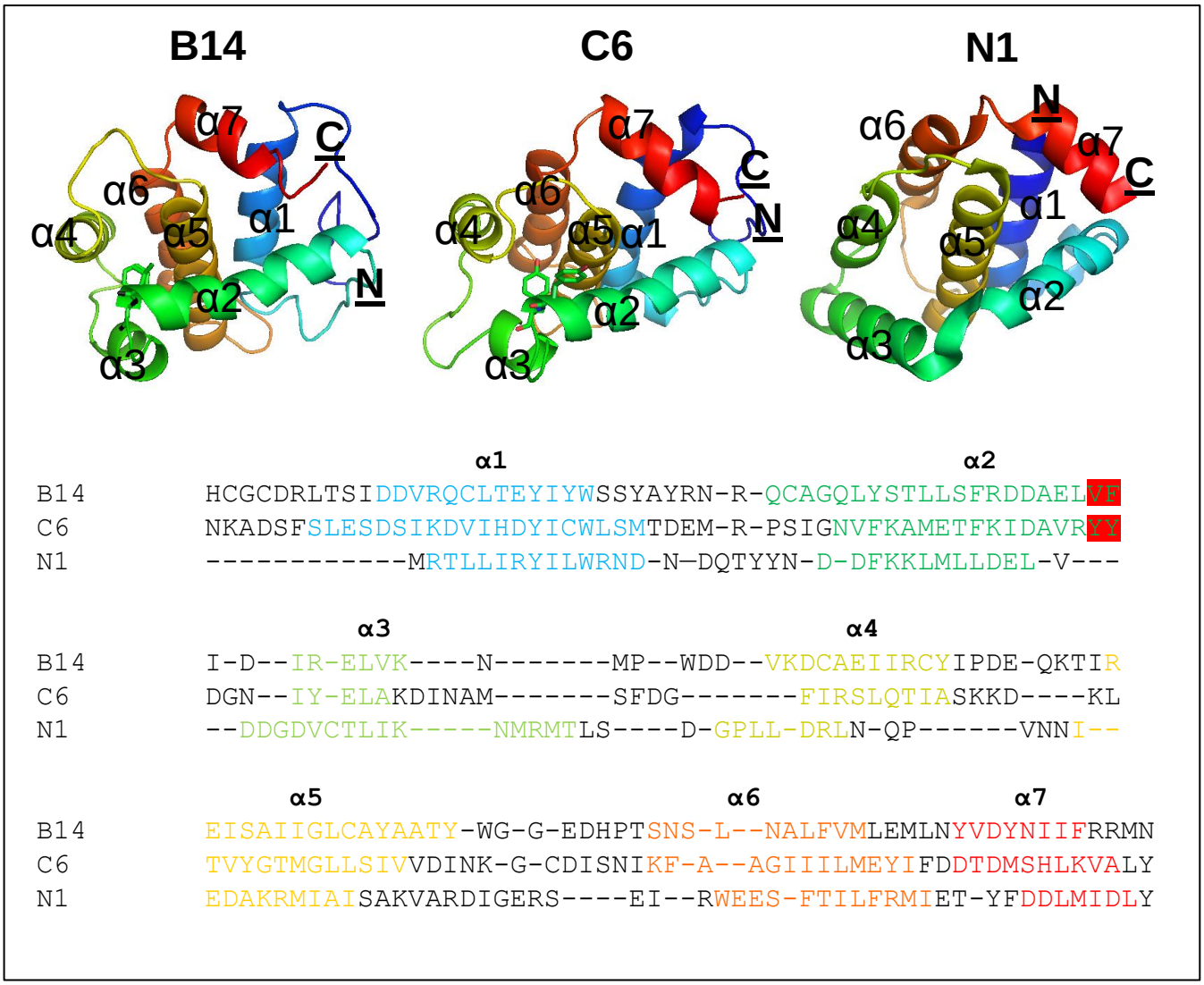

Figure 3.3: C6 predicted structure. The structure of C6 was modelled using MODELLER (Eswar et al, 2006) based on a sequence alignment with B14 (Graham et al, 2008). The side chains of the bulky residues (highlighted in red in the sequence alignment) predicted to protrude into the groove formed by alpha helices 2 and 4 and potentially prevent the binding of a BH3 peptide are shown. The structure of N1, which has an open groove, is also shown. The positions of the alpha helices (α) and the N (**N**) and C (**C**) termini are indicated

3.2 Expression of C6 protein

Peptides derived from C6 are presented to $CD8^+$ T cells during VACV infection (Oseroff et al, 2005) and therefore it is assumed that this protein is expressed during infection. To confirm this expression and to study the potential function of C6 the *022* gene was amplified from WR genomic DNA by PCR and inserted into the pcDNA3.1 expression vector with an N-terminal FLAG tag. The expression of FLAG-tagged C6 was confirmed by transfection of HEK293 cells and immunoblotting with a mouse-anti-FLAG monoclonal Ab (Figure 3.4A). This protein resolved to 17-18 kDa on a denaturing protein gel, as expected from C6 size predictions. To study C6 expression during virus infection a polyclonal serum was made by immunising rabbits with unfolded C6 that had been produced in *E. coli*. This serum recognised a protein that resolved to approximately 15 kDa on a denaturing protein gel from lysates of BHK cells infected with WR, but not mock-infected cells (Figure 3.4B). Immunoblotting of this lysate with an Ab against the late VACV protein D8 (Niles & Seto, 1988) served as a control in this experiment to confirm the infection of these cells. The serum was also capable of recognising plasmid expressed FLAG-tagged C6, which was slightly larger than virus-expressed C6, presumably due to the tag. In addition a protein of approximately 15 kDa was recognised by the C6 serum in lysates of BHK cells infected with VACV MVA. Again, this protein was slightly larger than WR C6, as MVA C6 is 6 amino acids longer.

Taken together these data indicated that a protein that resolves to approximately 15 kDa is expressed from the sequence of VACV WR gene *022* and a serum raised against this protein produced in *E. coli* is able to recognise C6 expressed from VACV strain WR. The predicted orthologue of C6 is also expressed by MVA and is recognised by the C6 polyclonal serum due to the high sequence conservation of these two proteins. This finding was mirrored very recently by Garcia-Arriaza et al who demonstrated that a polyclonal serum raised against MVA C6 also recognised C6 expressed by WR (Garcia-Arriaza et al, 2011).

3.3 Timing of C6 expression

A transcriptome-based analysis of VACV ORFs characterised *C6L* as an immediate-early transcript, with mRNA detected from as early as 30 min p.i. (Assarsson et al, 2008). To

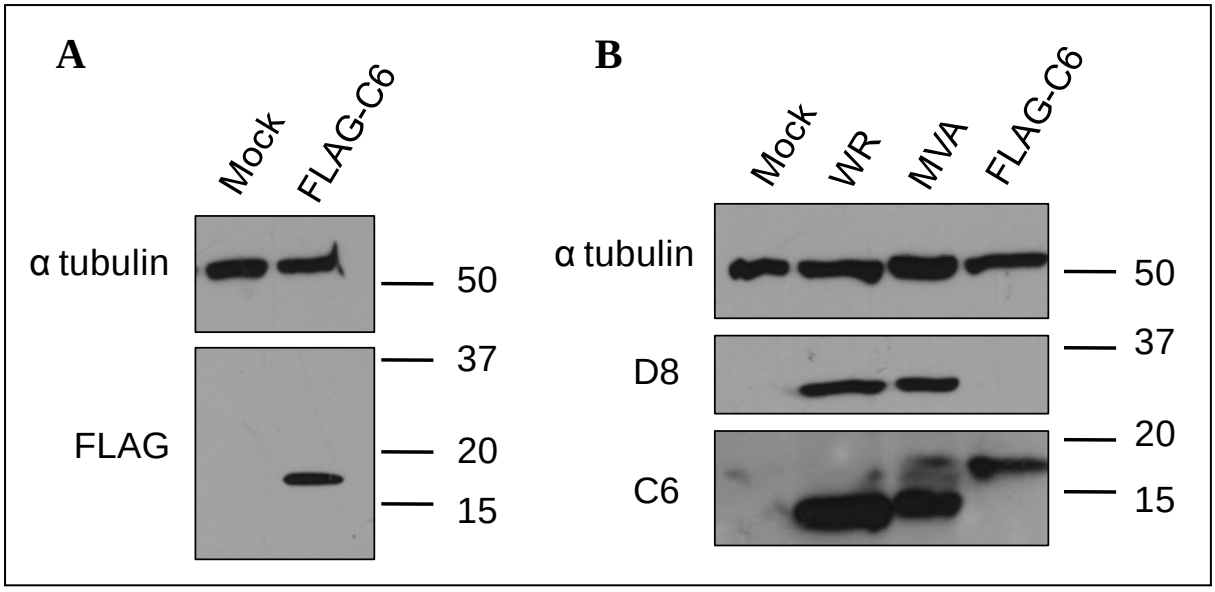

Figure 3.4: C6 expression by plasmid transfection and infection with VACV strains WR and MVA. (A) HEK293 cells were transfected for 24 h with a plasmid expressing FLAG-tagged C6 or were mock-transfected using calcium phosphate. (B) BHK cells were either mock infected or infected with VACV strains WR or MVA overnight with 2 p.f.u. per cell. The cells were harvested in cell lysis buffer, the proteins were separated by SDS-PAGE and then immunoblotted with mouse-anti-tubulin and mouse-anti-FLAG antibodies (A) or mouse-anti-tubulin, mouse-anti-D8 and rabbit-anti-C6 antibodies (B). The location of protein molecular mass markers is indicated (kDa).

confirm the early expression of C6 at the protein level, BSC-1 cells were infected with WR at 5 p.f.u. per cell in the presence or absence of AraC and whole cell lysates were prepared at various time points p.i. for immunoblotting analysis with the C6 serum (Figure 3.5). Expression of C6 protein was detected at two h p.i. with increased levels of protein detected at four h. The expression of C6 was affected only minimally by the presence of AraC, an inhibitor of viral replication and hence late gene expression. In contrast the expression of the late protein D8 was completely inhibited by this compound. These data confirmed expression of C6 from an early VACV promoter.

3.4 Construction of WR C6 recombinant viruses

To study the role of C6 for virus replication *in vitro* and assess its contribution to virulence *in vivo* a panel of recombinant viruses were constructed. For a virus lacking the *C6L* gene approximately 300-350 bp flanking the left and right of this gene was amplified by PCR from

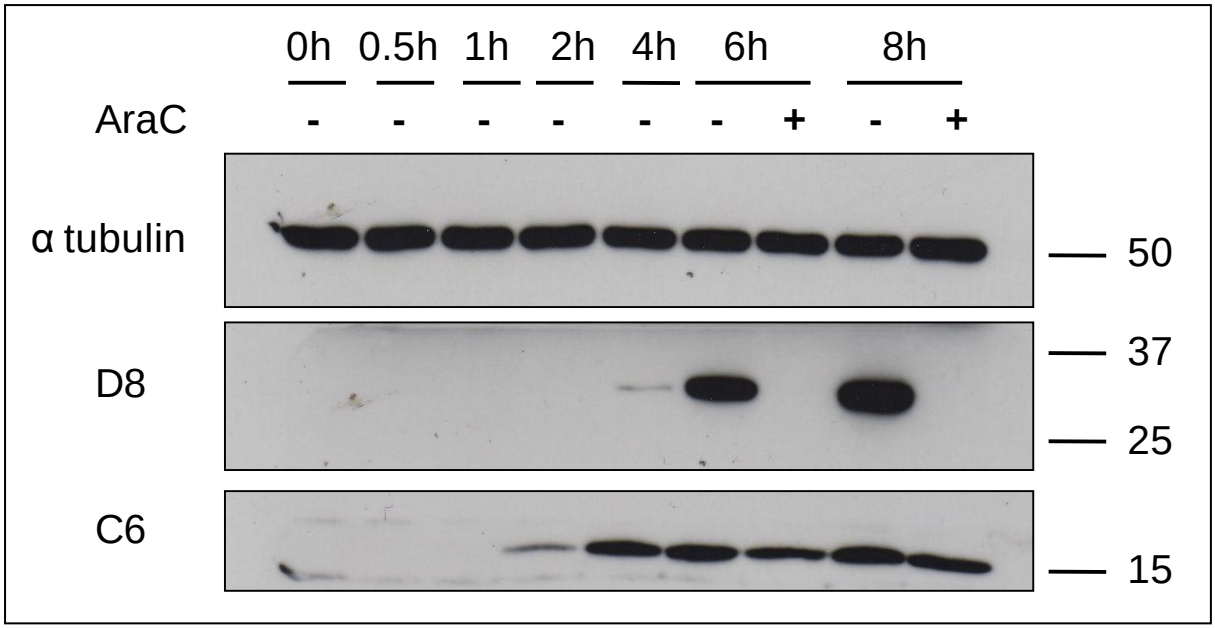

Figure 3.5: C6 is an early expressed VACV protein. BSC-1 cells were infected in the presence or absence of AraC at 5 p.f.u. per cell for 90 min on ice to allow viruses to adhere. The cells were then transferred to 37 ^{o}C and harvested at the indicated times p.i.. The proteins were separated by SDS-PAGE and immunoblotted with mouse-anti-tubulin, mouse-anti-D8 or rabbit-anti-C6 antibodies. The location of protein molecular mass markers is indicated (kDa).

WR genomic DNA and cloned into a plasmid containing *Ecogpt* (Boyle & Coupar, 1988) fused to *EGFP* (Z11ΔC6, Figure 3.6A). For the construction of a C6 revertant virus, the C6 ORF, in addition to the left and right flanking regions was amplified from genomic DNA by PCR and inserted into the Z11 plasmid (Z11C6Rev, Figure 3.6A). For *in vivo* analysis a revertant frame-shift plasmid was constructed where the C6 ORF was amplified with an additional adenine nucleotide to disrupt the translational initiation codon (i.e. ATAG) and hence the C6 protein cannot be expressed (Z11C6FS, Figure 3.6A). For localisation and binding partner studies revertant viruses expressing HA-tagged (Z11C6HA, Figure 3.6A) or TAP (comprising two Strep epitopes and one FLAG epitope, see Chapter 6)-tagged C6 (pUC13 C6TAP, Figure 3.6A) were also constructed. Digestion of these plasmids with *Bam*HI and *Not*I for the Z11 derivatives or with *Bam*HI and *Xba*I for the pUC13 derivative indicated all plasmids to contain an insert of the expected size (Figure 3.6B).

Recombinant viruses were generated using the transient-dominant selection method as described in Chapter 2 (Falkner & Moss, 1988). For the C6 deletion virus (vΔC6) CV-1 cells

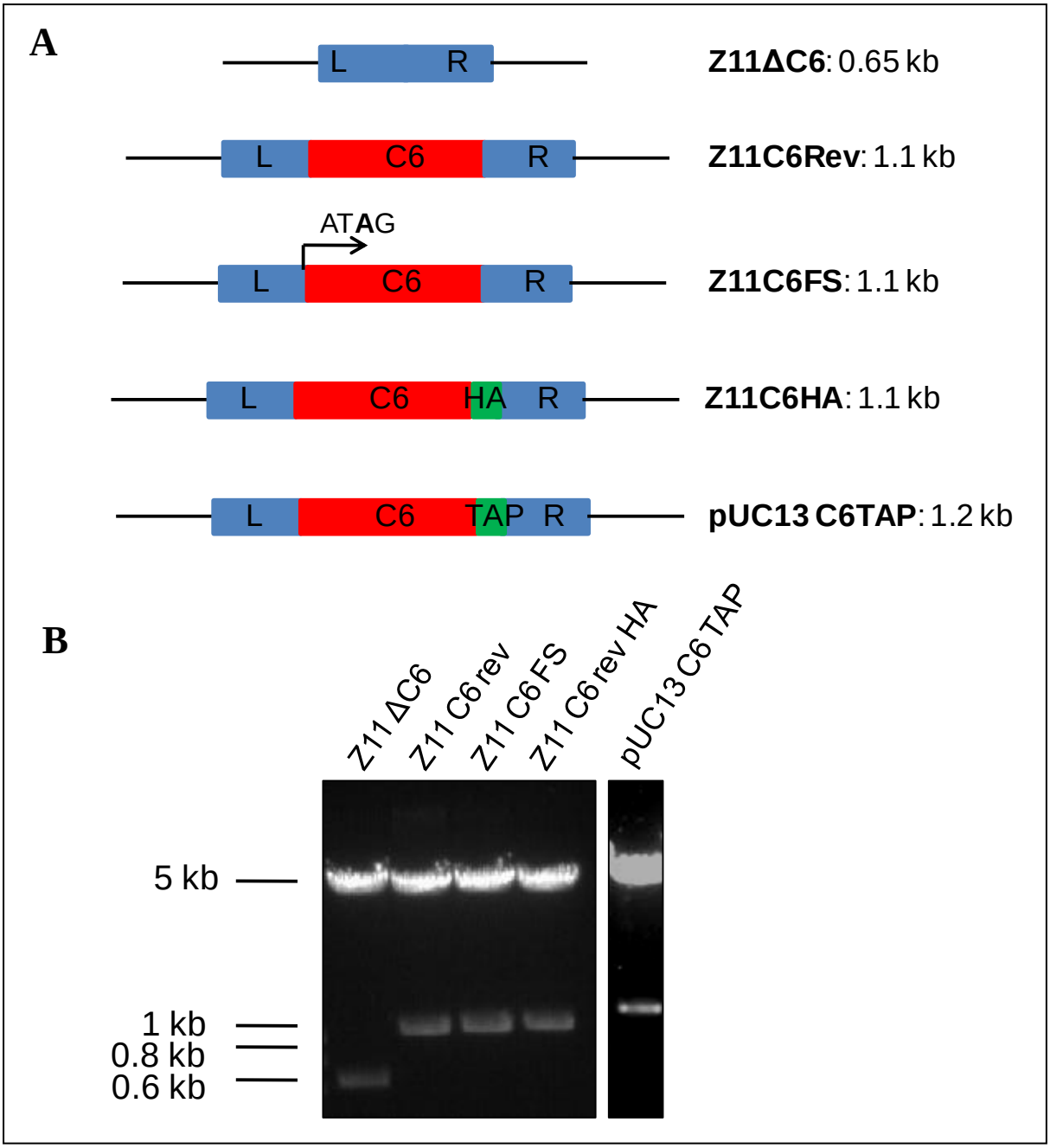

Figure 3.6: Plasmids for construction of the WR C6 recombinant viruses. (A) For construction of the C6 deletion virus (vΔC6) the left (L) and right (R) flanking regions of C6 were cloned into the Z11 plasmid containing the *Escherichia coli guanylphosphoribosyl transferase* (*Ecogpt*) gene fused in-frame with the *enhanced green fluorescent protein* (*EGFP)* gene (Z11 ΔC6). For the revertant (vC6Rev), revertant HA-tagged (vC6HA) or revertant frame-shift (vC6FS) viruses the C6 ORF, an HA-tagged version of the C6 ORF or a frame-shift version of the C6 ORF respectively were cloned between the L and R flanking regions in the Z11 plasmid (Z11 C6 rev, Z11 C6HA and Z11 C6FS). For the revertant TAP-tagged (vC6TAP) virus a TAP-tagged version of the C6 ORF was cloned between the L and R flanking regions in the pUC13 plasmid also containing *Ecogpt.EGFP* (pUC13 C6TAP). (B) Digestion with *Bam*HI and *Not*I for the Z11 derivatives and with *Bam*HI and *Xba*I for the pUC13 derivative indicated all plasmids contained an insert of the correct size as indicated in (A).

were infected with WR and then transfected with Z11ΔC6. A single recombination event between regions of homology in the plasmid and the virus allowed the plasmid, including the *Ecogpt-EGFP* locus, to be recombined into the virus genome (Figure 3.7). These viruses could be selected by growth in the presence of MPA, X and HX. MPA is an inhibitor of purine metabolism, which blocks the replication of wild type VACV in normal cell lines but can be overcome by expression of Ecogpt, in the presence of X and HPX. The presence of EGFP allowed plaques formed by these intermediate viruses to be visualised and selected with ease. Due to the instability of the resulting intermediate virus, a second recombination event, between repeated right of left flanking sequences, occurred when the drug selection was removed, resolving the virus and excising the inserted plasmid yielding either a wild-type virus (vC6WR) or vΔC6 (Figure 3.7). For the revertant viruses CV-1 cells were infected with vΔC6 and transfected with Z11C6Rev (for vC6Rev), Z11C6FS (for vC6FS), Z11C6HA (for vC6HA) or pUC13 C6TAP (for vC6TAP).

The genotype of the resolved recombinant viruses was confirmed by PCR analysis using the primers that had been used to amplify the flanking regions of the C6 gene. Virus-infected cells were subjected to proteinase K digestion and the resulting lysate containing viral DNA was used as a template for PCR (Figure 3.8). PCR analysis confirmed that the vΔC6 recombinant virus did not contain the C6 ORF, as indicated by a product of approximately 650 bp, indistinguishable from that obtained from the Z11ΔC6 plasmid (Figure 3.8). Conversely, PCR analysis of vC6WR, vC6Rev, vC6FS and vC6HA yielded PCR products of approximately 1.1 kb, indistinguishable from that obtained from the Z11C6Rev, Z11C6FS and Z11C6HA plasmids respectively, thus confirming the presence of the C6 ORF. PCR analysis of vC6TAP yielded a PCR product of the slightly larger size of 1.2 kb due to the presence of the TAP tag.

Expression of C6 from the various recombinant viruses was confirmed by infecting RK-13 cells overnight followed by SDS-PAGE of whole cell lysates and immunoblotting. All the C6 recombinant viruses expressed D8, but only vC6WR, vC6Rev, vC6HA and vC6TAP viruses expressed C6, detected using the C6 polyclonal antiserum (Figure 3.9). In addition C6 from vC6HA or vC6TAP were detected using monoclonal antibodies against HA or FLAG, respectively. Both HA-tagged and TAP-tagged C6 were detected at lower levels using the polyclonal antiserum, indicating either a lower expression, or instability of C6 from these

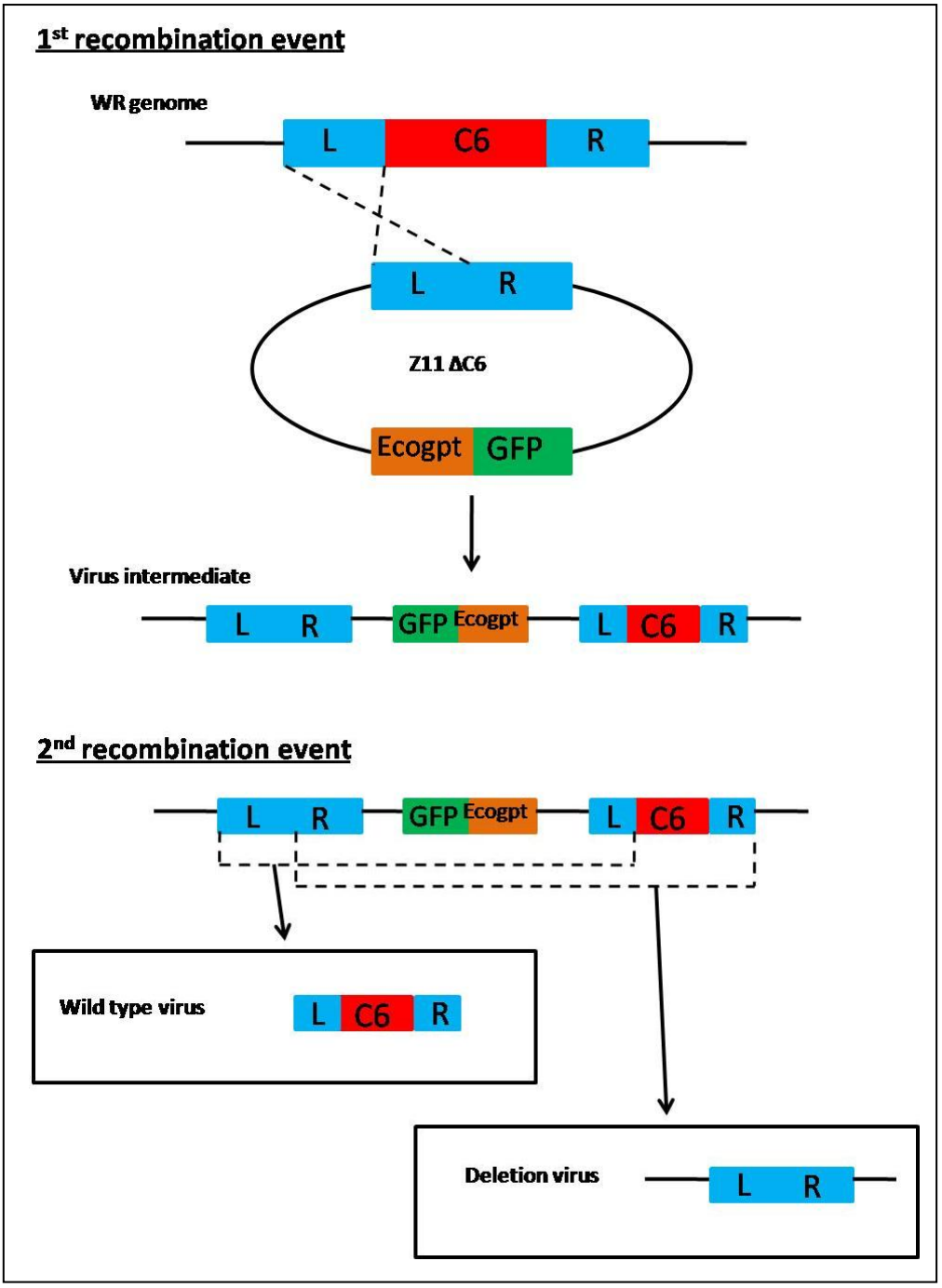

Figure 3.7: Schematic representation of the recombination events occurring during the construction of vΔC6. Recombinant viruses were constructed using the transient dominant selection method (Falkner & Moss, 1988). A single recombination event between the regions of homology in the plasmid and the virus genome allowed the plasmid, including the *Ecogpt-EGFP* locus, to be recombined into the virus genome. Due to the instability of the resulting intermediate virus a second recombination event occurs between the repeated left (L) or right (R) flanking regions when the drug selection is removed, resolving the virus and excising the inserted plasmid, yielding either a wild-type virus or deletion virus.

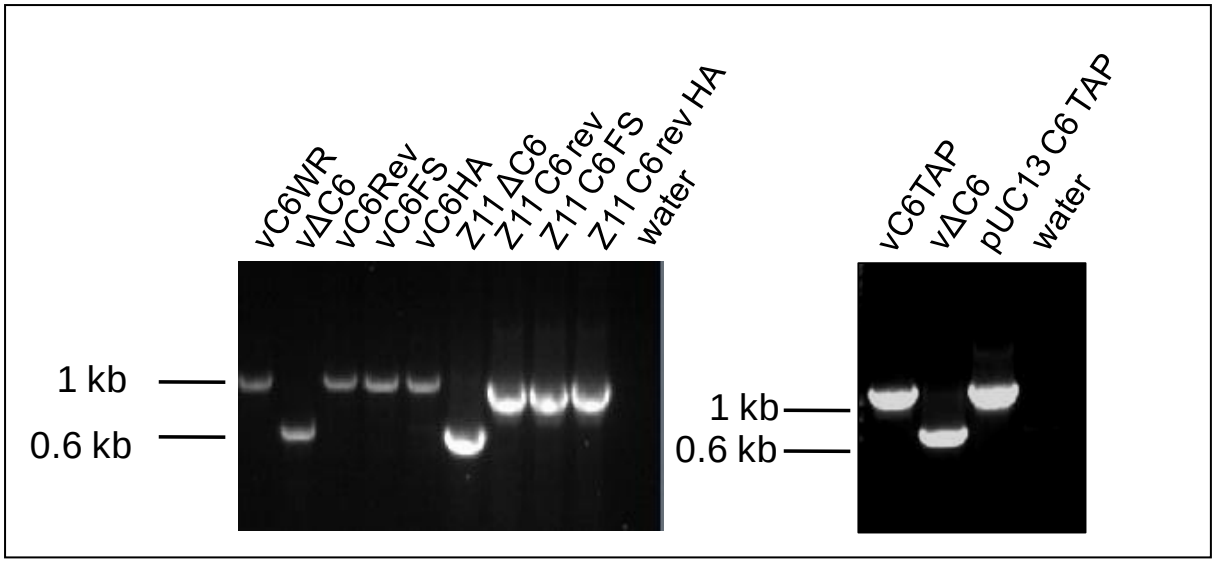

Figure 3.8: PCR analysis of WR C6 recombinant viruses. The phenotype of the recombinant viruses was confirmed by infecting RK-13 cells in a 24 well plate with the various recombinant viruses. Twenty four h later the cells were scraped in their medium, vortexed and 10 µl was used for a proteinase K digestion. One µl of digested lysate was used as a template for a PCR using primers specific for the left and right flanking regions of C6, and compared to the PCR product obtained from amplification of the plasmid used to construct each virus. The approximate sizes of DNA fragments were deduced from size markers run in parallel, as indicated.

viruses, or a diminished recognition of C6 tagged at the C terminus with these epitopes. As expected, C6 expression was not detected in whole cell lysates from cells infected with vΔC6 or vC6FS (Figure 3.9).

Further to the confirmation of C6 expression, the recombinant viruses to be used *in vivo* were subjected to genomic DNA digestion analysis to confirm that no major genomic rearrangements or deletions had occurred during their construction. Viral genomic DNA was purified from virion cores, digested with *Hin*dIII or *Xho*I and analysed by pulse-field agarose gel electrophoresis. As *C6L* lies within the *Hin*dIII C fragment, which is 22 kb in size, the loss of the 456-bp *C6L* gene is not visible on a 0.9 % agarose gel. Consequently digestion with this enzyme produced a similar pattern of DNA fragments in all the C6 recombinant and the parental WR strain, suggesting that no major rearrangements or deletions in the genome had occurred (Figure 3.10). Digestion of genomic DNA with *Xho*I confirmed that vΔC6 was lacking the C6 ORF, indicated by a difference of approximately 450 bp in the *Xho*I G fragment of vΔC6 compared to WR, vC6WR, vC6Rev and vC6FS, which all contain *C6L*.

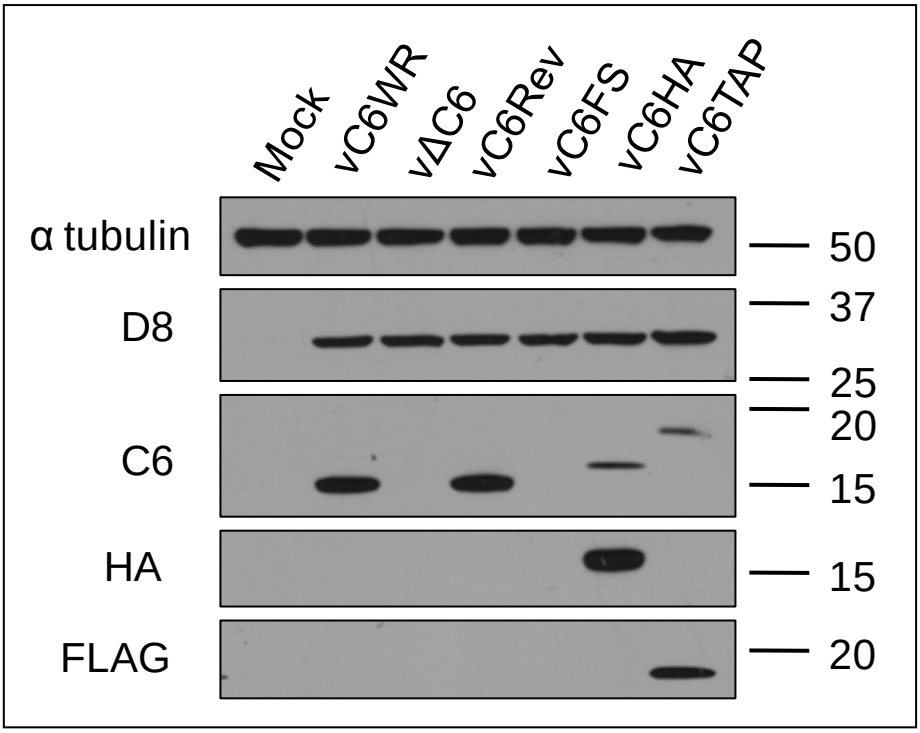

Figure 3.9: Expression of C6 by recombinant WR viruses. For immunoblotting RK-13 cells were infected overnight with the indicated viruses at 2 p.f.u. per cell. The cells were harvested in cell lysis buffer, the proteins were separated by SDS-PAGE and then immunoblotted with mouse-anti-tubulin, mouse-anti-D8, rabbit-anti-C6, rabbit-anti-HA or mouse-anti-FLAG antibodies. The location of protein molecular mass markers is indicated (kDa).

All other fragments resolved as expected, again indicating that no major rearrangements or deletions in the genome had occurred.

3.5 Analysis of C6 localisation

To determine the sub-cellular localisation of C6 during viral infection, HeLa cells were infected overnight with the various C6 recombinant viruses and the cells were harvested the next morning and carefully separated into nuclear and cytoplasmic fractions. These fractions were then analysed for C6 expression by SDS-PAGE and immunoblotting using the C6 polyclonal antiserum. Successful fractionation of cells was achieved using the method employed, with nuclear lamins A + C detected only in the nuclear fraction and α-tubulin detected only in the cytoplasmic fraction (Figure 3.11). C6 expression was found to be

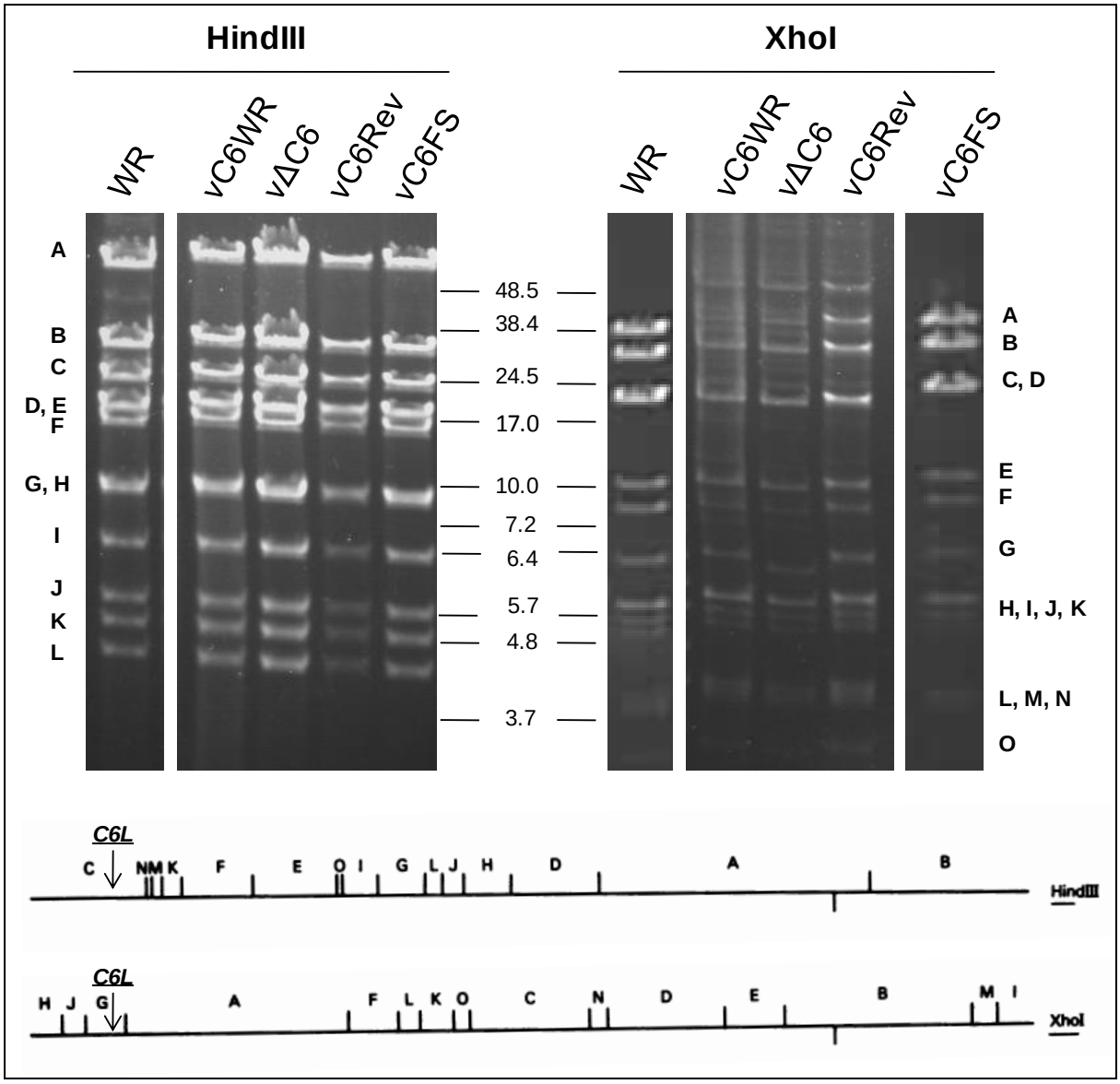

Figure 3.10: Restriction digestion of viral genomic DNA. One μg of genomic DNA purified from virion cores was subjected to digestion with the restriction enzymes *Hin*dIII or *Xho*I for 6 h. Restriction products were then separated by overnight pulse-field gel electrophoresis using a 0.9 % agarose gel. The expected restriction patterns for the WR genome with each restriction enzyme and the position of the *C6L* gene are shown below, with the corresponding fragments indicated beside the gels with letters. The location of a DNA size marker is indicated in the centre (kb).

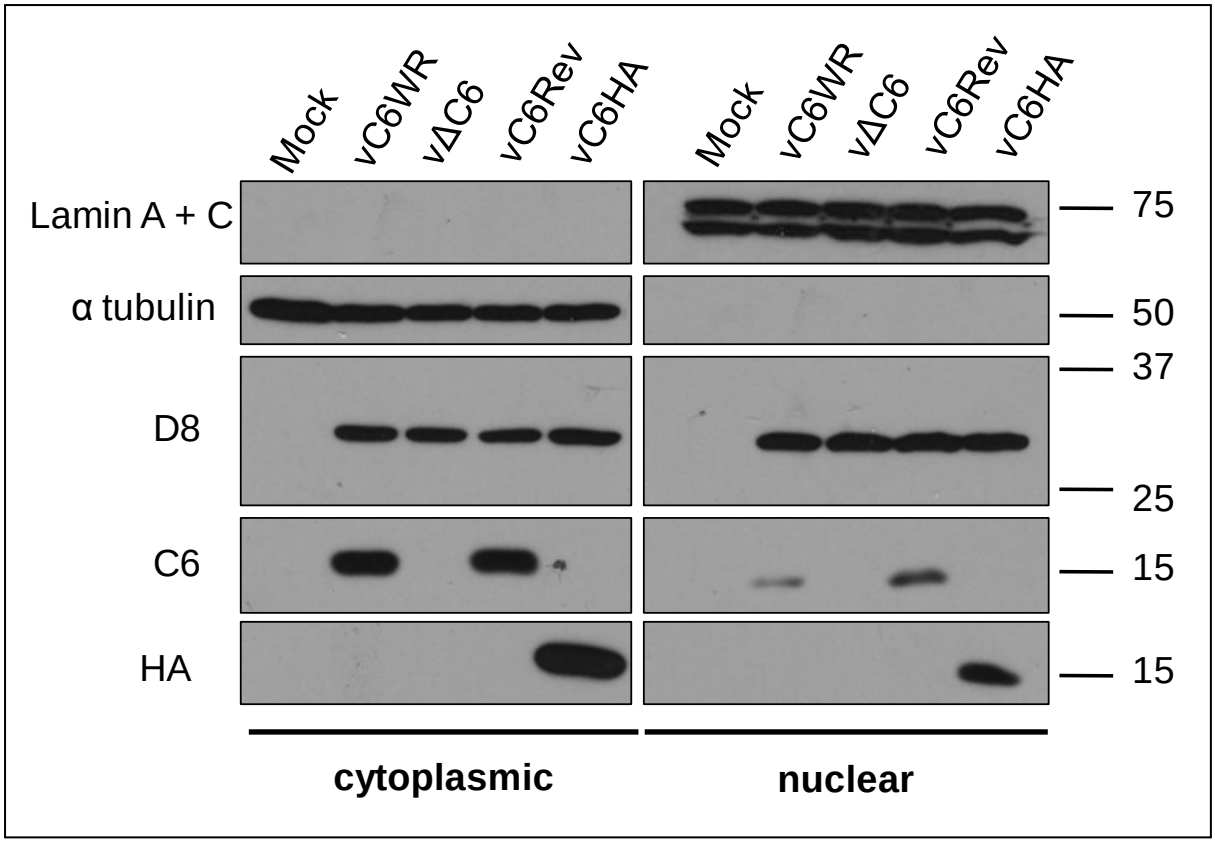

Figure 3.11: Localisation of C6 by cellular fractionation. HeLa cells were prepared in 14.5-cm dishes and infected overnight at 5 p.f.u. per cell. The cells were harvested in LS buffer and fractionated carefully into cytoplasmic and nuclear fractions by dounce homogenisation and centrifugation. The proteins were separated by SDS-PAGE and were analysed by immunoblotting with mouse-anti-tubulin, mouse-anti-lamin A + C, mouse-anti-D8, rabbit-anti-C6 or rabbit-anti-HA antibodies. Three-fold more of the total nuclear fraction was loaded compared to the total cytoplasmic fraction. The location of protein molecular mass markers is indicated (kDa).

predominantly cytoplasmic, but with some protein also detected in the nuclear fraction. Addition of the HA tag at the C terminus of C6 did not affect its localisation.

The localisation of C6 was also studied by immunofluorescence by both transfection with a plasmid expressing TAP-C6 and infection with vC6HA (Figure 3.12). Overnight transfection of HEK293 cells with a plasmid encoding TAP-C6 indicated both a cytoplasmic and nuclear localisation of C6, detected using a rabbit-anti-FLAG polyclonal Ab (Figure 3.12A). Infection of HeLa cells for 5 h with vC6HA also showed both a cytoplasmic and nuclear localisation of C6 (Figure 3.12B). A significant co-localisation of C6 with the DNA stain DAPI was observed in the cell nucleus. Mock-infected and vC6WR-infected cells had only

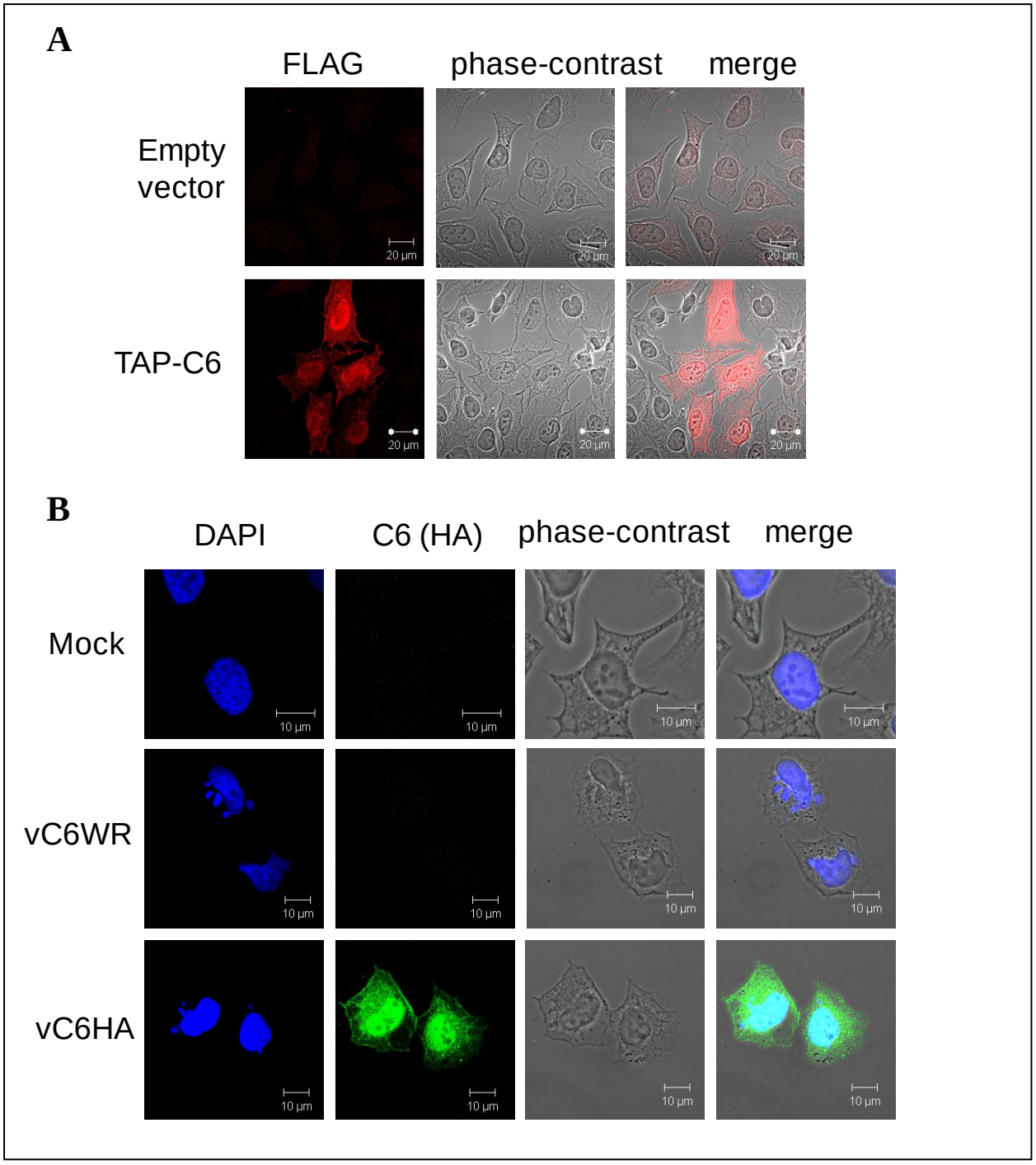

Figure 3.12: Localisation of C6 by immunofluorescence. (A) HEK293 cells were transfected overnight with a plasmid expressing TAP-C6 or empty vector control. Cells were then fixed and stained with a rabbit anti-FLAG Ab. The localisation of C6 (red), phase-contrast and merged images are shown. (B) HeLa cells were infected with the indicated viruses for 5 h with 5 p.f.u. per cell. The cells were then fixed and stained with a mouse anti-HA Ab. The localisation of C6 (green), nuclear and viral DNA stained with DAPI (blue), phase-contrast and merged images are shown.

background levels of fluorescence using the mouse-anti-HA Ab indicating specificity for C6-HA. Notably, the distribution of C6 in the cytoplasm of both transfected and infected cells was not diffuse, but rather showed an uneven distribution with greater staining in some regions of the cytoplasm than others (Figure 3.12).

An immunofluorescence time course showed expression of C6-HA as early as two h p.i. (Figure 3.13), in accordance with immunoblotting data of cells infected with WR (Figure 3.5). At all time points examined C6 was present in both the cytoplasm and the nucleus, with a similar distribution. The staining in the cytoplasm at all time points was again not diffuse, but rather C6 localised to an unknown sub-cellular structure.

Although both immunoblotting and immunofluorescence data agree both a cytoplasmic and nuclear localisation for C6, the relative distribution of protein in these two compartments is different. By immunoblotting both wild-type and HA-tagged C6 were predominantly cytoplasmic (Figure 3.11), whereas by immunofluorescence the localisation of C6 was more evenly distributed, regardless of the tag (Figures 3.12 and 3.13). One difference between these two experiments is the time of infection. Although a time course for immunofluorescence was performed this was only carried out up until 8 h p.i., whereas the cellular fractionation and immunoblotting analysis was carried out after an overnight infection. An overnight transfection with TAP-C6, however, still showed strong nuclear staining of C6 suggesting that the length of expression may not explain this difference (Figure 3.12A). Nevertheless it is still plausible that the presence of another viral protein may affect the localisation of C6 after longer periods of infection.

Although an obvious NLS is not present in the sequence of C6 (see 3.1) experiments were performed to confirm whether C6 was actively transported into the nucleus. HeLa cells were infected with vC6HA for 4 h and then incubated for a further 4 h in the presence of 20 ng/ml leptomycin B (LMB). LMB is an inhibitor of the nuclear export protein CRM1 (Kudo et al, 1999) and therefore proteins that are actively transported in and out of the nucleus accumulate in the nucleus in the presence of this compound. The localisation of C6 was unaltered by the presence of LMB (Figure 3.14A), whereas the cellular protein p65 (an NF-κB component), which is actively shuttled between the nucleus and cytoplasm and has a

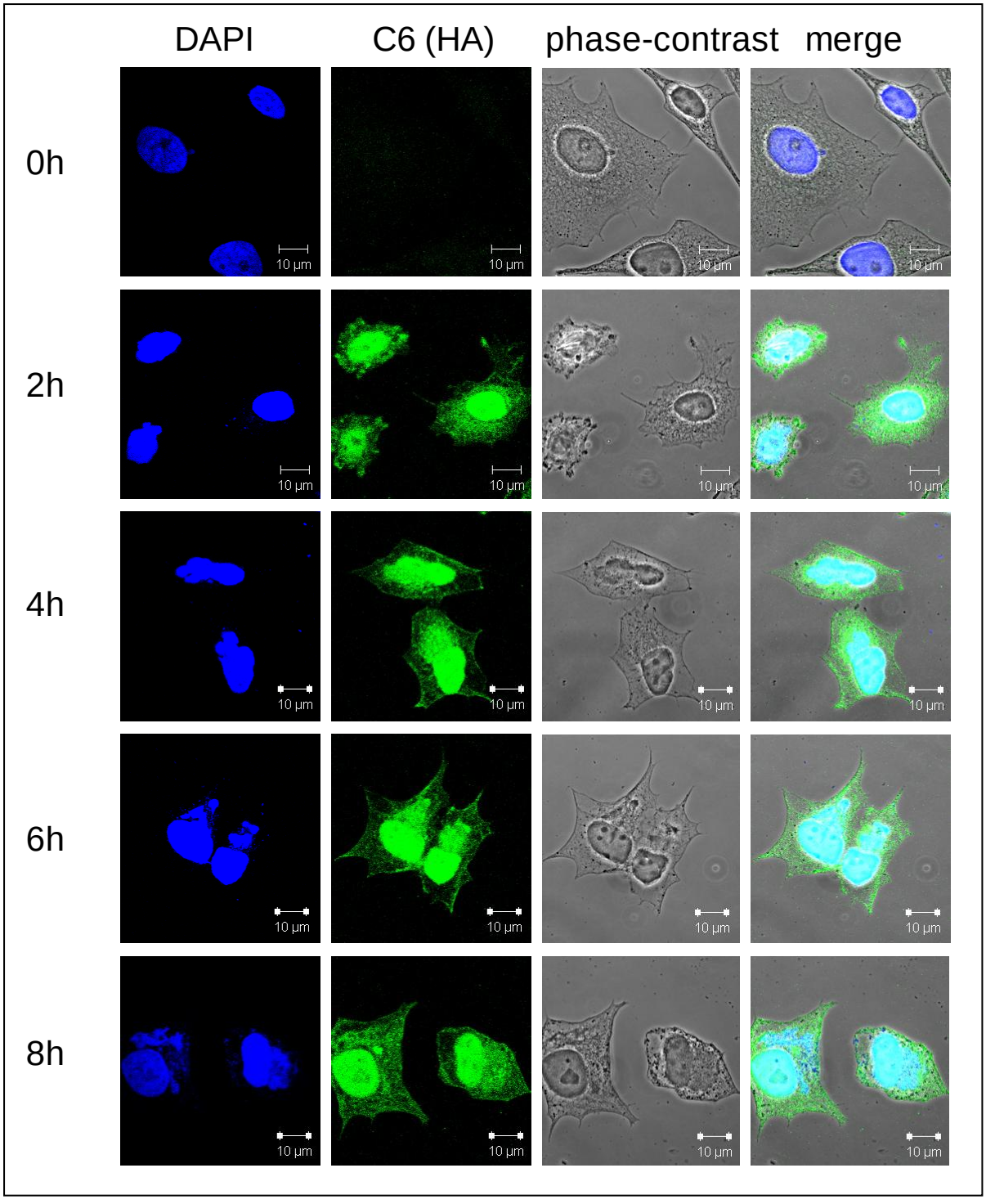

Figure 3.13: Time course of C6 localisation by immunofluorescence. HeLa cells were infected with 5 p.f.u. per cell of vC6HA for the times indicated. Cells were then fixed and stained with a mouse anti-HA Ab. The localisation of C6 (green), nuclear and viral DNA stained with DAPI (blue), phase-contrast and merged images are shown.

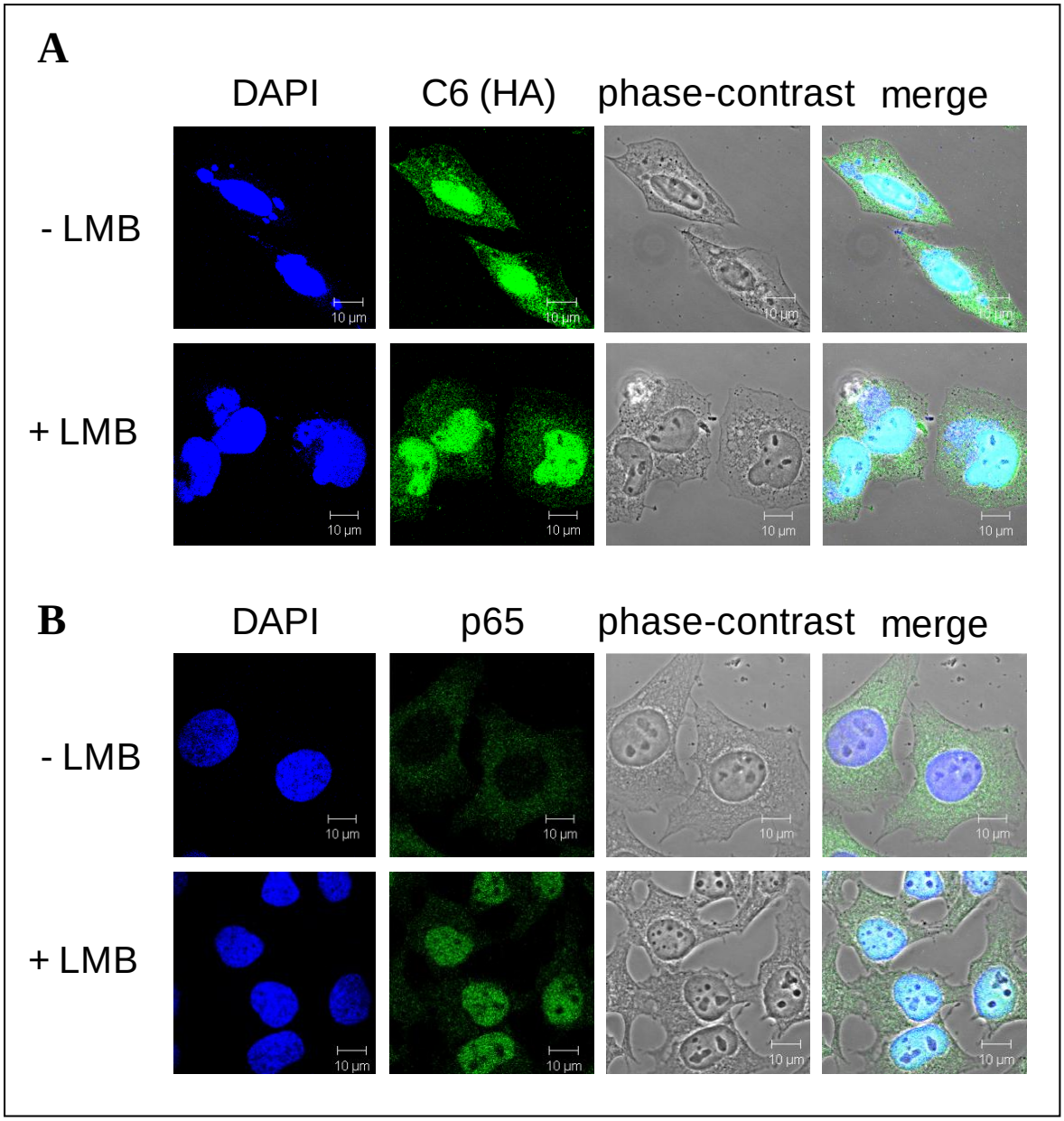

Figure 3.14: Localisation of C6 in the presence of leptomycin B. HeLa cells were infected with 5 p.f.u. per cell of vC6HA for 4 h for C6 localisation (A), or mock-infected for p65 localisation (B). The cells were then incubated in the presence or absence of 20 ng/ml leptomycin B (LMB) for a further 4 h. The cells were fixed and infected cells stained with a mouse anti-HA Ab (A) and mock-infected cells stained with a mouse-anti-p65 Ab (B). The localisation of C6 or p65 (green), nuclear and viral DNA stained with DAPI (blue), phase-contrast and merged images are shown.

predominantly cytoplasmic localisation (Birbach et al, 2002), was found to be nuclear in the presence of this compound (Figure 3.14B). These data indicated that C6 is not actively transported into the nucleus using the conventional importin/exportin system, but given its small size, is likely to do so by passive diffusion.

3.6 Dimerisation of C6

VACV Bcl-2-like family members N1 (Bartlett et al, 2002), B14 and A52 (Graham et al, 2008) have the ability to form homo-dimers. To test the ability of C6 to homo-dimerise an HEK293 T-REx cell line engineered to inducibly express C6-TAP (see Chapter 6) and HA-tagged C6 expressed from vC6HA were utilised. HEK293 T-REx C6-TAP cells were incubated for 24 h in the presence of 2 μg/ml doxycycline to induce the expression of TAP-C6 and then infected overnight with either vC6HA, or a recombinant WR virus expressing C-terminally HA-tagged B14 (vB14HA) as a control (Chen et al, 2008). An IP assay was then performed on cleared cell lysates using either a mouse-anti-HA Ab coupled to protein G sepharose beads (Figure 3.15A) or anti-FLAG agarose beads (Figure 3.15B). TAP-tagged C6 expressed from the cell line was found to co-immunoprecipitate with HA-tagged C6 expressed from the virus, but not with HA-tagged B14 (Figure 3.15A). Conversely when immunoprecipitating TAP-C6 from the cell line using the FLAG agarose beads virally expressed C6-HA was found to co-immunoprecipitate, whereas B14-HA did not, indicating a specificity of this interaction (Figure 3.15B). These data demonstrated that C6, like some other members of the VACV Bcl-2-like family, is able to homo-dimerise and this can occur in the context of a viral infection.

Additional evidence for C6 homo-dimerisation was obtained by a LUMIER assay. HEK293 cells were co-transfected with plasmids expressing LUC-tagged C6 and either FLAG-C6 or TAP-C6. The cleared cell lysates were then incubated with anti-FLAG agarose beads and the bound proteins eluted in a buffer containing 250 ng/ml FLAG peptide. The luminescence in this eluted sample was normalised to the total luminescence of the sample before IP. FLAG-GFP was used as a negative control and data for the other FLAG-tagged proteins were normalised to this protein and expressed as a fold binding relative to this. Both FLAG- and TAP-tagged C6 showed a 20-25 fold binding to LUC-C6 indicating the ability of C6 to

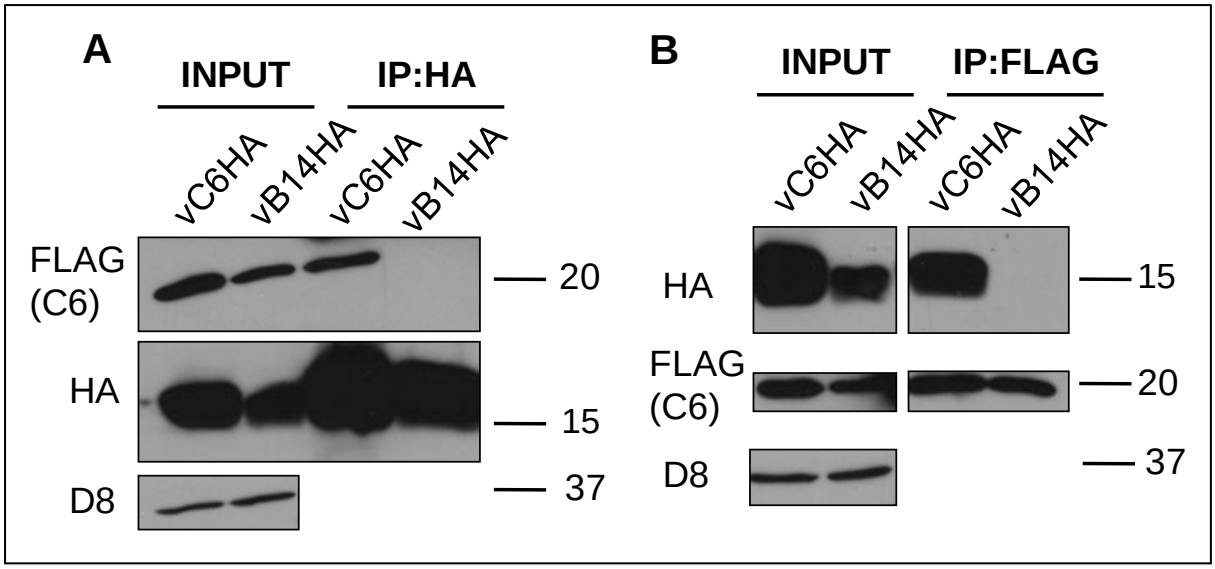

Figure 3.15: Dimerisation of C6 by immunoprecipitation assay. HEK293 T-REx TAP-C6 cells were incubated for 24 h in the presence of 2 μg/ml doxycycline to induce the expression of TAP-C6. The cells were then infected overnight at 5 p.f.u. per cell with either vC6HA or vB14HA. The cells were harvested in IP buffer (see Materials and Methods) and the cleared lysates were incubated with either a mouse-anti-HA Ab coupled to protein G sepharose beads (A) or FLAG agarose beads (B) to immunoprecipiatate the epitope-tagged proteins. Whole cell lysates (INPUT) and immunoprecipitated proteins (IP) were separated by SDS-PAGE and analysed by immunoblotting with mouse-anti-D8, mouse-anti-FLAG or rabbit-anti-HA antibodies. The location of protein molecular mass markers are indicated (kDa).

dimerise (Figure 3.16). Whether or not C6 dimers can be detected in virus-infected cells was not addressed and whether dimerisation is important for C6 function is currently not known.

3.7 Summary

Protein C6 encoded by gene *022* of the WR strain of VACV is an uncharacterised protein that is highly conserved amongst VACV strains (including MVA) and other OPVs. An orthologue of this protein is also predicted in the genomes of the more distantly related capripoxviruses and also in the uncharacterised mule deer poxvirus. Although the structure of this protein has not been solved, structural based alignments predict C6 to be a member of the VACV Bcl-2-like Pfam (Finn et al, 2008) protein family (Gonzalez & Esteban, 2010; Graham et al, 2008). Given the role of other members of this family in innate immune evasion and the high conservation of C6 in all sequenced OPVs this protein was chosen for further investigation.

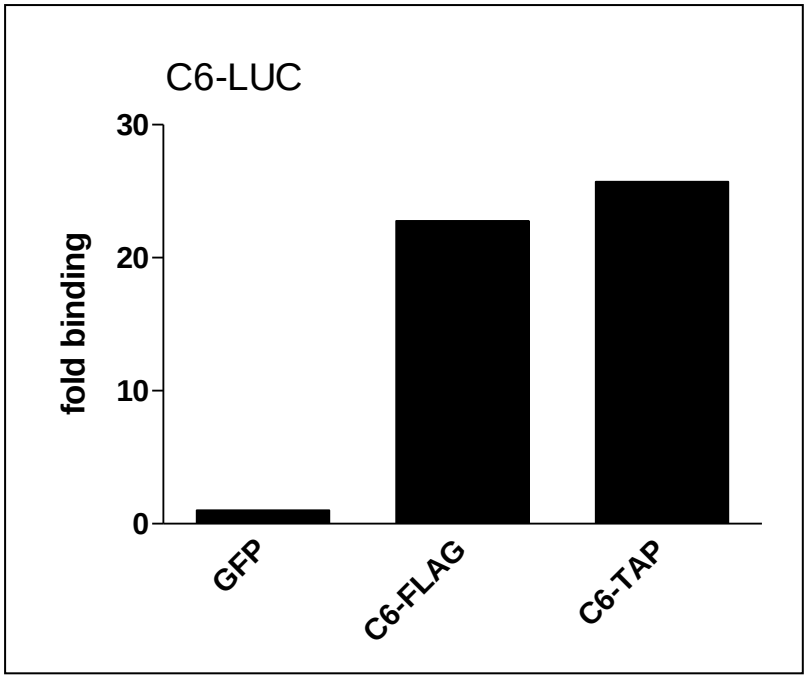

Figure 3.16: Dimerisation of over-expressed C6 by LUMIER assay. HEK293 cells were co-transfected with a plasmid expressing renilla luciferase(LUC)-tagged C6 and with plasmids expressing either FLAG-GFP, C6-FLAG or C6-TAP. The cells were harvested in IP buffer and the cleared lysates were incubated with FLAG agarose beads. The proteins bound to the beads were eluted in a buffer containing 250 ng/ml FLAG peptide. The luminescence in the samples was measured after elution from the beads and was normalised to the total luminescence in the whole cell lysate. Data are from one representative experiment of three and are presented as a fold binding normalised to the FLAG-GFP control.

Transcriptome analysis suggested C6 to be an immediate-early gene (Assarsson et al, 2008) and this was confirmed by both immunoblotting and immunofluorescence analysis of infected cells. C6 was found to be localised to both the cytoplasm and the nucleus of infected and transfected cells and its nuclear accumulation was unaffected by the nuclear export inhibitor LMB.

To study C6 both *in vitro* and *in vivo* a panel of recombinant viruses were constructed using the transient-dominant selection method (Falkner & Moss, 1988). This included a C6 deletion virus, a revertant virus, a frame-shift virus and two epitope-tagged C6 viruses. The successful construction of a virus lacking the C6 ORF indicated that C6 was a non-essential viral protein. Genomic DNA was purified from the recombinant viruses that were to be used for *in vivo* experiments and subjected to digestion with two restriction enzymes, followed by

agarose gel electrophoresis. All of the viruses showed the expected sizes of restriction fragments indicating that no major genomic rearrangements or deletions had occurred during their construction.

Co-IP and LUMIER assays using C6 tagged with two different epitopes/molecules demonstrated that C6 was able to dimerise, consistent with other members of the Bcl-2-like family N1 (Bartlett et al, 2002), B14 and A52 (Graham et al, 2008). The functional relevance of this dimerisation ability in the context of viral infection is currently unknown.

Chapter 4: Characterisation of C6 as an inhibitor of innate immune signalling

4.1 Inhibition of IFNβ induction by protein C6

Given the role of other Bcl-2-like VACV proteins in innate immune evasion, namely the inhibition of NF-κB by A46, A52 (Bowie et al, 2000), B14 (Chen et al, 2008) and N1 (Cooray et al, 2007; DiPerna et al, 2004) and the inhibition of the IRF3 intracellular immune signalling pathway by K7 (Schroder et al, 2008), it was hypothesised that C6 may function in a similar manner. IFNs play a very important role in the cellular defence against viruses, particularly IFNβ which is produced early in response to infection. The promoter of the IFNβ gene contains binding sites for the NF-κB, IRF3 and AP-1 transcription factors (Thanos & Maniatis, 1995; Visvanathan & Goodbourn, 1989) and therefore those Bcl-2 family members that inhibit the activation of these transcription factors ultimately reduce the induction of IFNβ.

To test the potential effect of C6 on IFNβ induction a dual luciferase reporter gene assay was performed in human HEK293ET cells. Unlike HEK293 cells that do not exhibit IFNβ induction when incubated with the dsRNA mimic poly I:C in the culture medium, the HEK293ET cell line is able to respond to RNA in this manner (Ryzhakov & Randow, 2007). The mechanism by which this occurs is not currently known, but it is believed to be via the cytoplasmic RNA sensors, as these cells, like HEK293T cells, do not express TLR3. These cells were transfected in 96-well plates with an IFNβ-promoter firefly luciferase reporter plasmid, where the expression of firefly luciferase is under the control of the IFNβ promoter, a renilla luciferase reporter plasmid whose expression is under the control of the thymidine kinase (TK) promoter and therefore acts as a transfection control, and 100, 200 or 300 ng of a plasmid expressing TAP-C6. Twenty four h later the cells were stimulated by incubation for 9 h in the presence of 20 μg/ml poly I:C in the overlay and then harvested for measurement of firefly and renilla luciferase activity. The firefly luciferase activity was normalised to renilla luciferase activity to account for transfection efficiency, and these data normalised to the un-stimulated EV control to give a fold induction relative to the control. Incubation of HEK293ET cells with poly I:C led to a 50-fold induction of the IFNβ-promoter and this was

inhibited in a concentration-dependent manner by the presence of C6 (Figure 4.1A). This inhibition was highly statistically significant ($P<0.001$) when analysed using the Student's T-test.

To understand whether the inhibition of IFNβ induction by C6 was specific to signalling downstream of RNA, other stimuli known to induce IFNβ promoter activity were tested by reporter gene assay. Transfection of cells with the dsDNA mimic poly dA:dT for 24 h led to a 3-fold induction from the IFNβ promoter, which was again inhibited in a concentration-dependent manner by C6 (Figure 4.1B). As with poly I:C, this inhibition was highly statistically significant ($P<0.001$). In HEK cells poly dA:dT is bound by RNA pol III and transcribed into RNA, which is sensed by RIG-I (Ablasser et al, 2009; Chiu et al, 2009), a cytoplasmic RNA sensor that signals via the canonical and non-canonical IKK complexes to induce IFNβ production (Sasai et al, 2006; Yoneyama et al, 2004). Consistent with the ability of C6 to inhibit the induction of IFNβ in response to poly dA:dT transfection, C6 was also found to be inhibitory following the infection of HEK293ET cells with Newcastle disease virus (NDV) with statistical significance (Figure 4.1C). NDV is an RNA virus of the *Paramyxoviridae* family and like poly dA:dT, is sensed by RIG-I (Kato et al, 2005).

In addition to inhibiting IFNβ induction in human cells, the ability of C6 to inhibit innate immune signalling in murine cells was also tested. Murine NIH3T3 cells were transfected with the same IFNβ reporter and renilla luciferase plasmids as described above and either 100 or 200 ng of a plasmid expressing TAP-C6. After 24 h the cells were stimulated by transfection with 800 ng poly I:C per well for a further 24 h. This stimulation induced a robust induction from the IFNβ promoter, which was again inhibited by the presence of C6 with high statistical significance ($P<0.01$) (Figure 4.1D). Poly I:C delivered to the cytoplasm by transfection is recognised by the cytoplasmic RNA sensor MDA-5 (Andrejeva et al, 2004; Kang et al, 2004; Kang et al, 2002). These data indicated that C6 was able to inhibit IFNβ induction downstream of both RIG-I and MDA-5, indicating that its method of inhibition was likely at a point of a signalling pathway common to these receptors. These data also indicated that the inhibitory function of C6 was conserved in both human and murine cells.

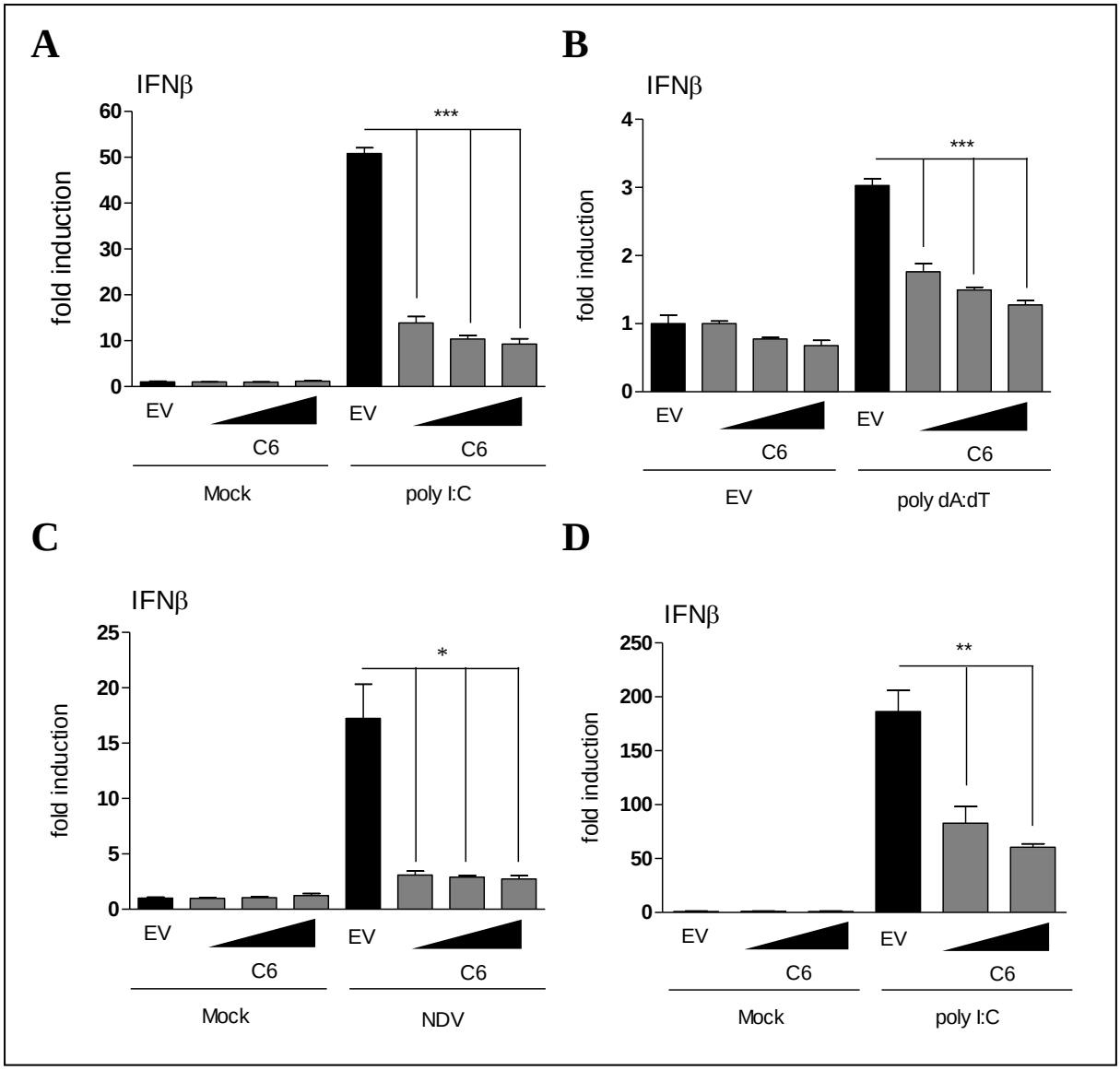

Figure 4.1: C6 inhibits IFNβ induction in human and murine cells. (A, B, C) HEK293ET cells were transfected in 96-well plates with 60 ng of IFNβ-promoter firefly luciferase reporter plasmid, 10 ng of renilla luciferase transfection control plasmid, 100, 200 or 300 ng of a C6 expression plasmid (C6) or empty vector control (EV) per well. After 24 h cells were stimulated for 9 h with 20 µg/ml poly(I:C) (A), transfected for 24 h with 800 ng poly(dA-dT) per well (B), or mock-infected or infected for 16 h with NDV (C). (D) Mouse NIH3T3 cells were transfected as above and stimulated by transfection for 24 h with 800 ng poly(I:C) per well. All cells were harvested in passive lysis buffer and the firefly luciferase activity was measured and normalised to the renilla luciferase activity. Data are from one representative experiment of at least three, with each being performed in triplicate. Data are represented as mean ± standard deviation (SD) normalised to the un-stimulated EV control. * P<0.05, ** P<0.01, *** P<0.001 analysed using the Student's T-test.

The inhibitory action of C6 was evident using a plasmid expressing TAP-C6. As recombinant viruses had been constructed with C-terminally tagged C6 (vC6HA and vC6TAP) for identification of novel binding partners, it was important to determine that epitope-tagging C6 in this manner would not affect its function. HEK293 cells were transfected with the IFNβ-promoter firefly luciferase reporter plasmid, the renilla luciferase transfection control and 250 ng of plasmids encoding un-tagged (Figure 4.2A), N- and C-terminally TAP-tagged C6 (Figure 4.2A), N- and C-terminally histidine (HIS)-tagged C6 (Figure 4.2B), frame-shift C6 (Figure 4.2B) and C-terminally HA-tagged C6 (Figure 4.2C). The cells were stimulated by co-transfection with a plasmid expressing the adaptor molecule TRIF lacking the RIP domain, as the RIP domain induces cellular apoptosis (Kaiser & Offermann, 2005) (TRIFΔRIP, Figures 4.2A & B) or with 40 μg/ml poly I:C in the overlay (Figure 4.2C). These stimuli induced a robust induction from the IFNβ promoter that was inhibited by C6 regardless of the tag or its location. As expected, the plasmid encoding frame-shift C6, which does not express C6 protein, was incapable of inhibiting IFNβ induction (Figure 4.2B).

4.2 Conservation of IFNβ inhibition by protein C6 expressed from MVA

Protein C6 from VACV strains WR and MVA (encoded by gene *019*) show 97 % amino acid sequence identity, but differ in their C termini where an additional six amino acids are present in 019, but not C6 (Figure 4.3A). MVA is a highly passaged and attenuated VACV strain. This attenuation is due to the deletion of large regions of non-essential genes from the genome (Meyer et al, 1991). In addition a number of proteins with a role in innate immune evasion have insertions or deletions within their coding sequence rendering them non-functional, including the soluble receptors for IFNγ, IFNα/β, TNF and CC chemokines (Blanchard et al, 1998) and MVA gene *183R*, encoding an orthologue of B14 (McCoy et al, 2010), a protein which when expressed full length has anti-NF-κB signalling activity (Chen et al, 2008).

To determine whether the additional six C-terminal amino acids in 019 rendered it non-functional, *019* was amplified from MVA genomic DNA by PCR and cloned into the pcDNA4/TO N-terminal TAP vector yielding a plasmid that expressed TAP-019. This plasmid was then analysed by IFNβ reporter gene assay in HEK293 cells stimulated by co-

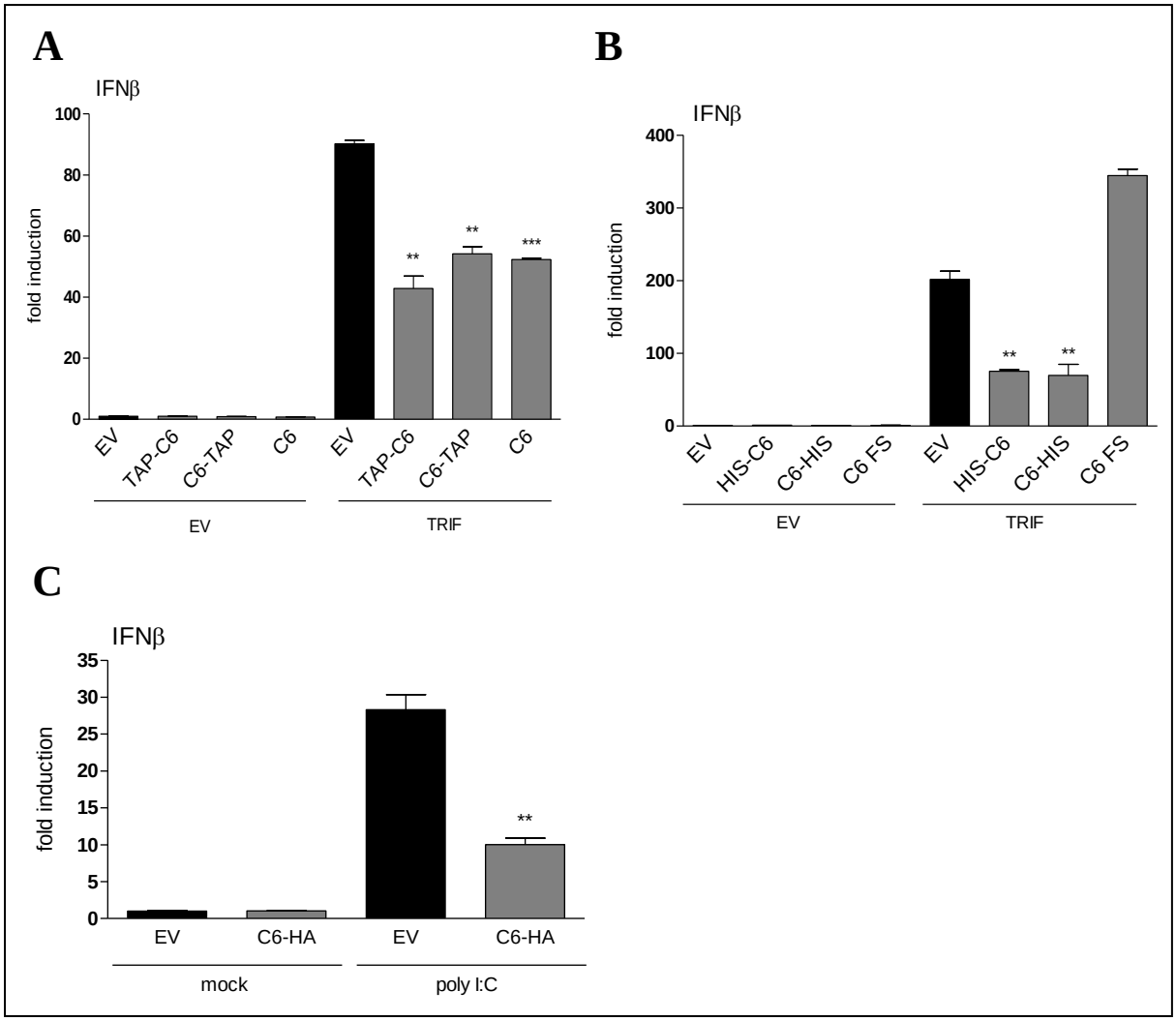

Figure 4.2: C6 epitope-tagged at either terminus inhibits IFNβ induction. (A, B) HEK293 cells were transfected in 96-well plates with 60 ng of IFNβ-promoter firefly luciferase reporter plasmid, 10 ng of renilla luciferase transfection control plasmid, 250 ng of un-tagged (C6) or TAP-tagged C6 (A), or frame-shifted C6 (C6 FS) or HIS-tagged C6 (B) or empty vector control (EV) expression plasmid and 70 ng of TRIFΔRIP expression plasmid per well. After 24 h the cells were harvested in passive lysis buffer and the firefly luciferase activity was measured and normalised to the renilla luciferase activity. (C) HEK293ET cells were transfected in 96-well plates with 60 ng of IFNβ-promoter firefly luciferase reporter plasmid, 10 ng of renilla luciferase transfection control plasmid, 250 ng of HA-tagged (C6-HA) or empty vector control (EV) expression plasmid. After 24 h the cells were stimulated by incubation with 40 μg/ml poly I:C in the overlay for 8 h. Data are from one representative experiment of at least three, each performed in triplicate. Data are represented as mean ± SD fold induction normalised to the un-stimulated (EV) control of each plasmid. ** P<0.01, *** P<0.001, analysed using the Student's T-test.

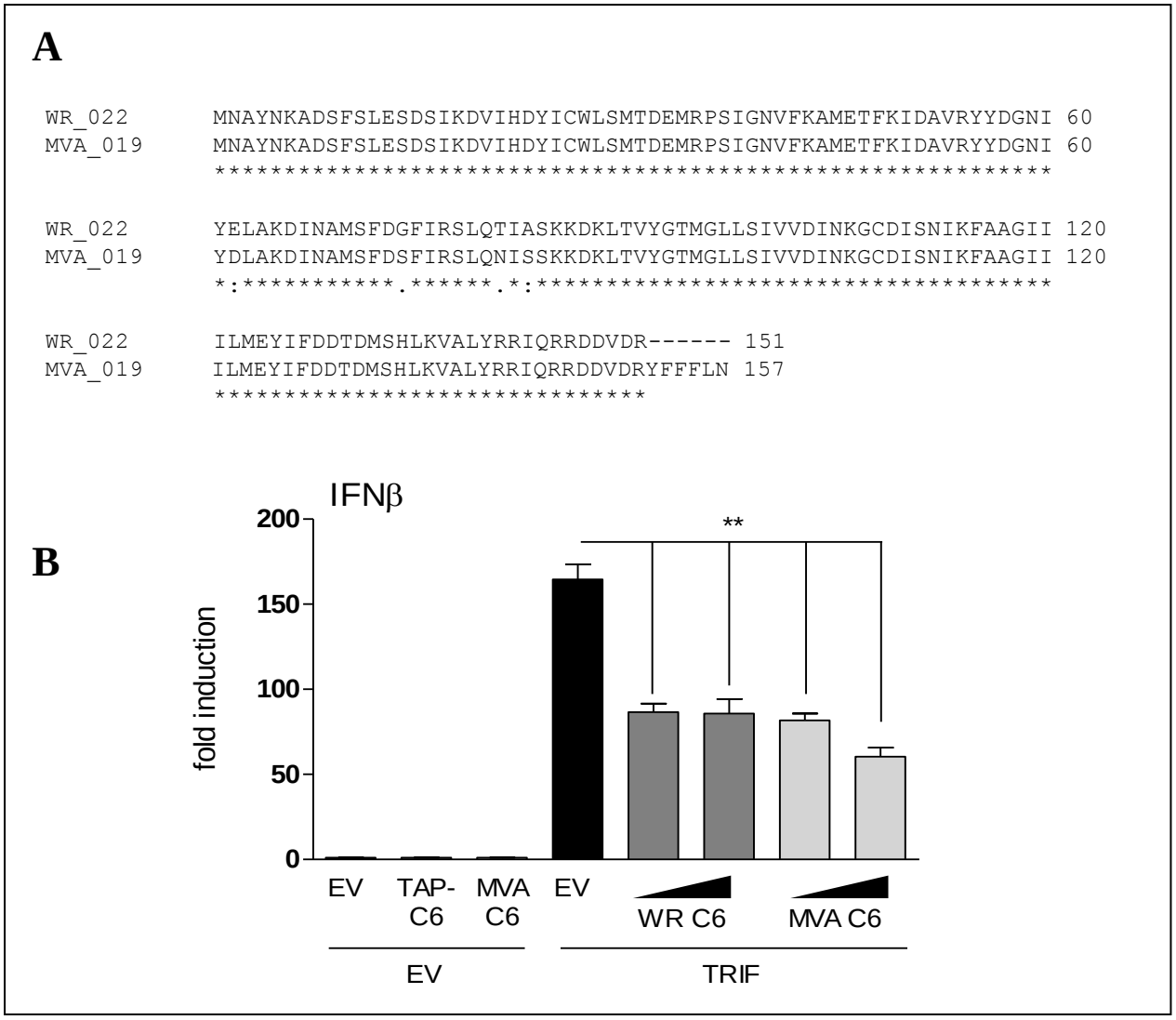

Figure 4.3: Conservation and functionality of C6 encoded by MVA. (A) Amino acid sequence alignment of the C6 protein from VACV strains WR and MVA. (B) HEK293 cells were transfected in 96-well plates with 60 ng of IFNβ-promoter firefly luciferase reporter plasmid, 10 ng of renilla luciferase transfection control plasmid, 100 or 250 ng of TAP-C6 from WR (WR C6) or TAP-019 from MVA (MVA C6) and 70 ng of TRIFΔRIP expression plasmid per well. After 24 h the cells were harvested in passive lysis buffer and the firefly luciferase activity was measured and normalised to the renilla luciferase activity. Data are from one representative experiment of at least three, each performed in triplicate. Data are represented as mean ± SD fold induction normalised to the un-stimulated control (EV) of each plasmid. ** $P<0.01$, analysed using the Student's T-test.

transfection with a plasmid expressing TRIFΔRIP. Both C6 and 019 inhibited IFNβ promoter activity in this assay with high statistical significance ($P<0.01$) indicating the conservation of function of this protein in MVA, despite the additional residues at the C terminus (Figure 4.3B).

The inhibition of IFNβ induction by C6 was also demonstrated to be conserved in the MPXV orthologue of this protein by collaborators in Professor Andrew Bowie's laboratory at Trinity College Dublin (Unterholzner et al, 2011). This protein differs from VACV C6 by just a few amino acids (Figure 3.2). The conservation of function in MPXV is also interesting as this is an emerging zoonotic pathogen (Parker et al, 2007).

4.3 C6 does not inhibit NF-κB signalling

As discussed in 4.1 the IFNβ promoter contains binding sites for the transcription factors NF-κB, IRF3 and AP1. To better understand how C6 might inhibit IFNβ promoter activity it was tested in an NF-κB reporter gene assay. HEK293 cells were transfected with an NF-κB-promoter firefly luciferase reporter plasmid, a renilla luciferase transfection control and 100 ng of a plasmid expressing C6, B14 or an empty vector control. After 24 h the cells were stimulated for 8 h with TNFα (50 ng/ml) or IL-1β (100 ng/ml). The binding of TNFα (DiDonato et al, 1997) and IL-1β (Woronicz et al, 1997) to their respective receptors induces independent signalling cascades which converge on the canonical IKK complex, consisting of the kinases IKKα, IKKβ (Zandi et al, 1997) and the regulatory subunit NEMO (Rothwarf et al, 1998). Activation of this complex leads to phosphorylation of IκBα and the subsequent release of NF-κB allowing it to translocate to the nucleus and bind to the promoter of NF-κB-responsive genes, such as IFNβ. Stimulation of HEK293 cells with TNFα induced an approximate 40-fold induction of NF-κB reporter activity, whilst stimulation with IL-1β induced a more modest 15-fold induction (Figure 4.4A). In both cases the presence of C6 was found not to affect this activation whereas protein B14 was a potent inhibitor, as expected (Chen et al, 2008).

The ability of C6 to inhibit NF-κB activity was also tested by immunoblotting the lysates of cells that had been stimulated with TNFα for total IκBα and its phosphorylated form. When

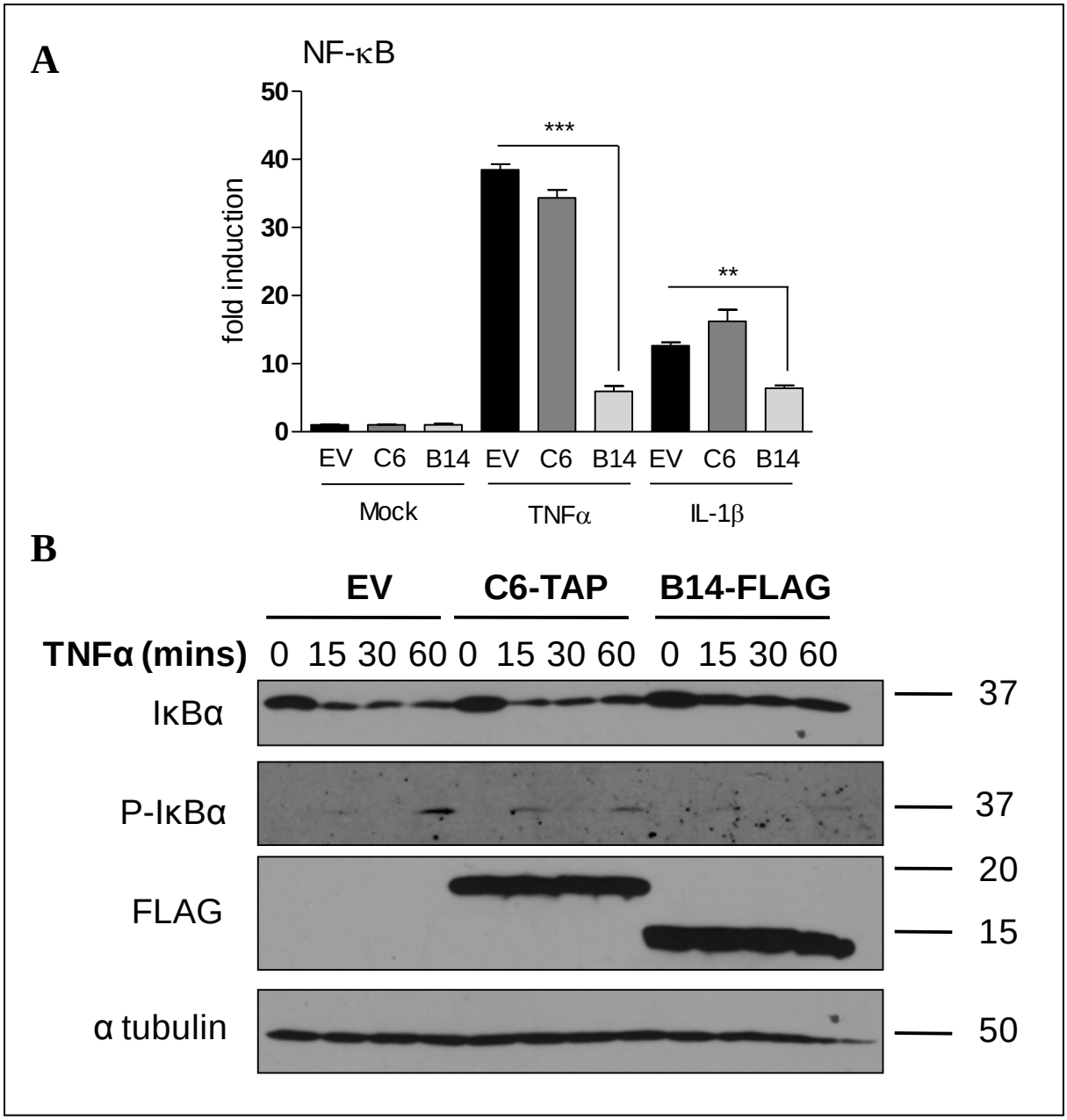

Figure 4.4: C6 does not inhibit NF-κB signalling. (A) HEK293 cells were transfected in 96-well plates with 60 ng of NF-κB-promoter firefly luciferase reporter plasmid, 10 ng of renilla luciferase transfection control plasmid and 100 ng of a C6, B14 or empty vector control (EV) expression plasmid per well. After 24 h the cells were stimulated for 8 h with TNFα (50 ng/ml) or IL-1β (100 ng/ml). The cells were harvested in passive lysis buffer and the firefly luciferase activity was measured and normalised to the renilla luciferase activity. Data are from one representative experiment of at least three, each performed in triplicate. Data are represented as mean ± SD normalised to the un-stimulated control (Mock) of each plasmid. ** $P<0.01$, *** $P<0.001$ analysed using the Student's T-test. (B) HEK293 cells were transfected with a TAP-C6, FLAG-B14 or empty vector (EV) control expression plasmid for 24 h. The cells were stimulated with 100 ng/ml TNFα and harvested at the indicated times. The whole cell lysates were analysed by immunoblotting with rabbit-anti-IκBα, mouse-anti-phospho-IκBα (P-IκBα), mouse-anti-FLAG or mouse-anti-tubulin antibodies. The location of protein molecular mass markers is indicated (kDa).

the canonical IKK complex becomes activated due to upstream signalling events, the IKK kinases cooperate to phosphorylate IκBα leading to its ubiquitination and subsequent degradation by the proteasome, thus releasing the NF-κB transcription factor (Beg et al, 1993). After incubation of HEK293 cells in the presence of TNFα for 15 min, a substantial decrease in total IκBα was observed in the empty vector control-transfected cells (Figure 4.4B). This was accompanied by the appearance of the phosphorylated form of this protein, with the highest levels detected after 60 min of stimulation. In contrast, levels of total IκBα were higher in cells expressing B14 and phosphorylated IκBα was only weakly detected. This is consistent with work published by our laboratory characterising the binding of B14 to IKKβ, inhibiting its kinase function and hence preventing the phosphorylation of IκBα (Chen et al, 2008). Both IκBα phosphorylation and degradation were observed in the presence of C6, confirming reporter gene assay data showing that C6 does not have a role in inhibiting NF-κB activation.

A third assay, namely a p65 translocation assay analysed by immunofluorescence, was also performed to assess the effect of C6 on NF-κB signalling. HeLa cells were transfected overnight with a plasmid expressing TAP-C6, FLAG-B14 or empty vector control and then stimulated with TNFα or IL-1β for 30 min. The cells were stained for the FLAG epitope of C6 and B14 and for endogenous p65, one of the subunits of the NF-κB heterodimer. In resting cells p65 was mainly cytoplasmic, regardless of the presence of C6 or B14 (Figure 4.5). When empty vector control – transfected cells were stimulated with either TNFα or IL-1β p65 was observed in the nucleus, co-localised with the DNA stain DAPI, suggesting translocation of this protein had occurred. This translocation induced by either stimulus was not affected by the presence of C6, but was prevented in both cases in cells expressing FLAG-B14, where p65 remained cytoplasmic.

These data indicated that C6 did not inhibit NF-κB signalling in a reporter gene assay (Figure 4.4A) and did not inhibit the translocation of p65 to the nucleus (Figure 4.5), whereas B14 had an inhibitory function in both of these assays. In addition, IκBα degradation was observed in the presence of C6 after stimulation of cells with TNFα and higher levels of phosphorylated IκBα were detected than cells expressing B14 (Figure 4.4B). Taken together, these data therefore indicated that C6 did not inhibit NF-κB signalling pathways.

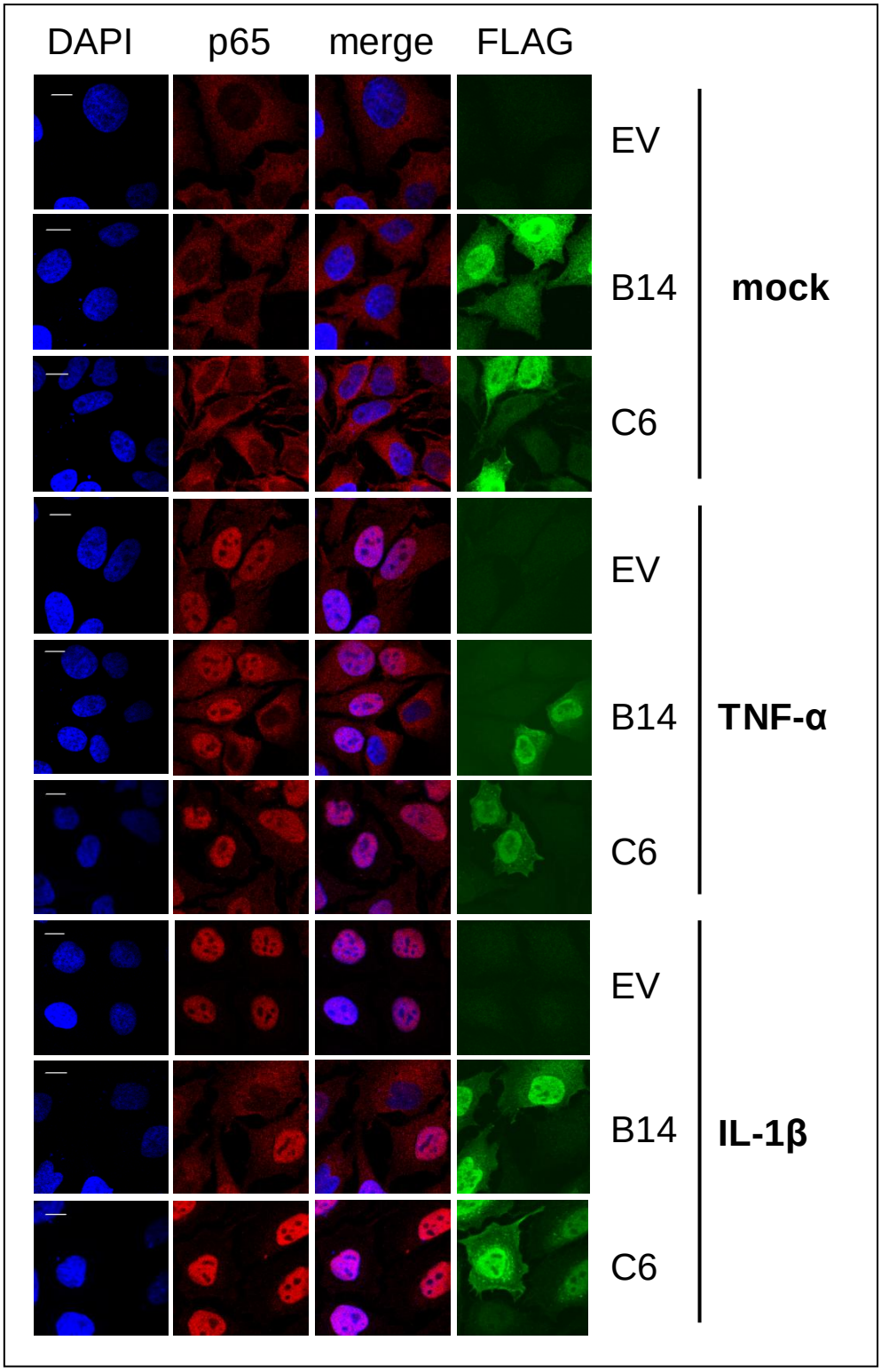

Figure 4.5: C6 does not inhibit p65 translocation. HeLa cells were transfected overnight with a plasmid expressing TAP-C6, FLAG-B14 or empty vector (EV) control. The cells were stimulated with TNFα (100 ng/ml) or IL-1β (250 ng/ml) for 30 mins, fixed and stained with rabbit anti-FLAG and mouse-anti-p65 antibodies. The localisation of C6 or B14 (green), endogenous p65 (red), nuclear DNA stained with DAPI (blue) and merged images are shown.

4.4 Inhibition of IRF3 activation by protein C6

In addition to testing the potential effect of C6 on the NF-κB signalling pathway, the effect of this protein on IRF3 signalling was also tested. To assess IRF3-specific promoter activity an ISG56.1-promoter firefly luciferase reporter plasmid was utilised. Transcription of this gene is highly dependent on, and specific for the IRF3 transcription factor (Grandvaux et al, 2002). HEK293ET cells were transfected with this reporter plasmid, the renilla luciferase transfection control and 100 ng of a C6, B14 or empty vector control expression plasmid. After 24 h cells were stimulated by transfection for 24 h with 800 ng poly I:C or poly dA:dT per well. Transfection with either of these stimuli induced an approximate 5-6 fold increase in IRF3 promoter activity, which was unaffected by the presence of B14 (Figure 4.6). In contrast the presence of C6 significantly reduced IRF3 induction in response to either stimulus ($P<0.01$).

The effect of C6 on IRF3 signalling was also tested at the mRNA and protein level by qRT-PCR and ELISA, respectively. HEK293ET cells were transfected in triplicate in 24-well plates with 1.5 μg of a TAP-C6, FLAG-GFP or empty vector control (EV) expression plasmid per well. After 24 h cells were stimulated by infection with NDV. For qRT-PCR analysis the cells were harvested 6 h p.i., the RNA was extracted, cDNA was synthesized and this was then used for qRT-PCR analysis using primers specific for human *CCL-5*, an IRF3-dependent gene (Lin et al, 1999a). Infection with NDV induced a relative 300-fold increase in CCL-5 mRNA, which was reduced by 50 % in cells expressing C6 (Figure 4.7A). Such an inhibition was not observed in the presence of GFP. For protein expression experiments the cell supernatants were harvested 24 h p.i. and were analysed for CXCL-10, a protein with IRF3-dependent expression (Ohmori & Hamilton, 1993), by ELISA. Approximately 120 pg/ml of CXCL-10 was detected in the supernatants of empty vector control – transfected cells infected with NDV (Figure 4.7B). In the presence of C6 however, CXCL-10 production was significantly reduced, a phenomenon that was again not observed in the presence of GFP.

Taken together these data demonstrated that C6 was an inhibitor of IRF3 activation. This inhibition was observed by reporter gene assay using the promoter of the IRF3-dependent gene *ISG56.1* fused to firefly luciferase, as well as by qRT-PCR and ELISA where C6 was

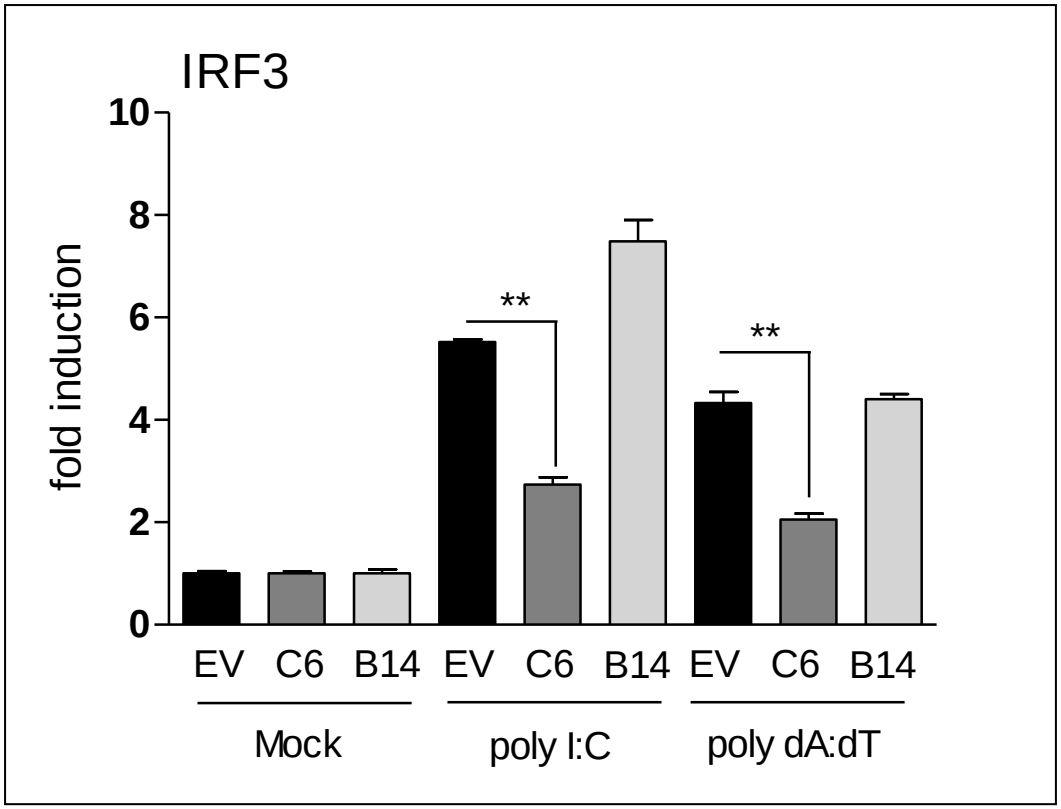

Figure 4.6: C6 inhibits IRF3 induction. HEK293ET cells were transfected in 96-well plates with 60 ng of ISG56.1-promoter firefly luciferase reporter plasmid, 10 ng of renilla luciferase transfection control plasmid and 100 ng of a C6, B14 or empty vector control (EV) expression plasmid per well. After 24 h the cells were stimulated by transfection for 24 h with 800 ng poly(I:C) or poly(dA-dT) per well. The cells were harvested in passive lysis buffer and the firefly luciferase activity was measured and normalised to the renilla luciferase activity. Data are from one representative experiment of at least three, each performed in triplicate. Data are represented as mean ± SD normalised to the un-stimulated control (Mock) of each plasmid. ** $P<0.01$, analysed using the Student's T-test.

able to inhibit the expression of an IRF3-dependent gene and protein in cells that had been infected with NDV. Further to this, collaborators in Andrew Bowie's laboratory demonstrated the ability of C6 to inhibit IRF3 translocation to the nucleus following the stimulation of cells with SeV (Unterholzner et al, 2011), a paramyxovirus that like NDV is sensed by RIG-I and induces IRF3 signalling and IFNβ production (Li et al, 2005).

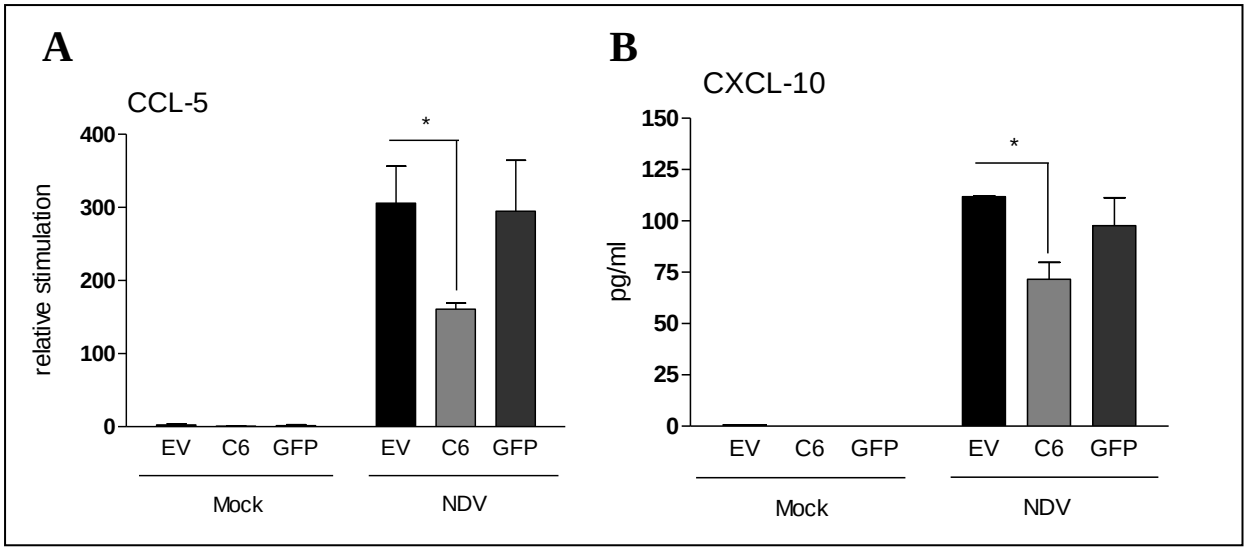

Figure 4.7: C6 inhibits IRF3-dependent gene expression and protein production. HEK293ET cells were transfected in triplicate in 24-well plates with 1.5 µg of a C6, GFP or empty vector control (EV) expression plasmid per well. After 24 h the cells were stimulated by infection with NDV for 6 h (A) or 24 h (B). (A) Following stimulation RNA was extracted from the cells, cDNA was synthesized and used for qRT-PCR analysis in duplicate using primers specific for human *CCL-5*. Data are represented as mean ± SD stimulation relative to sample one of the mock-treated EV control. (B) Following stimulation the culture supernatant was analysed for human CXCL-10 protein in duplicate by ELISA. Data are represented as mean ± SD. * $P<0.05$, analysed using the Student's T-test.

4.5 C6 inhibits IRF3 signalling downstream, or at the level of the non-canonical IKK complex

To gain an understanding of how C6 blocked the activation of IRF3, experiments were performed to determine the level at which it inhibited the IRF3 signalling cascade. The IRF3 translocation data from Professor Bowie's laboratory indicated that C6 was not inhibiting IRF3 activation in the nucleus, as its translocation was prevented in the presence of this protein (Unterholzner et al, 2011). This implied that C6 was abrogating IRF3 signalling within the cytoplasm of stimulated cells. The reporter gene assay data presented in Figure 4.1 demonstrated that C6 was able to inhibit IFNβ induction downstream of various stimuli that are sensed by different PRRs, suggesting C6 was unlikely to inhibit the receptors themselves. Further to this, C6 was found to inhibit the activation of IFNβ following the over-expression of TRIFΔRIP (Figure 4.2), therefore indicating that C6 acted downstream of this adaptor protein.

To further narrow down the point at which C6 inhibited IRF3 signalling, reporter gene assays were performed where IRF3 or IFNβ activation were induced by the over-expression of various proteins characterised to have a role in the IRF3 signalling cascade. In agreement with data presented in Figure 4.2, C6 was found to inhibit IRF-3 as well as IFNβ activation in cells over-expressing the TLR adaptor protein TRIF (Figure 4.8A). C6 was also able to inhibit IRF3 activation induced by the RIG-I adaptor molecule MAVS in a concentration-dependent manner. Moving further downstream in the signalling cascade C6 was found to inhibit IRF3-dependent transcription following the over-expression of the kinases TBK1 and IKKε (Figure 4.8B), both of which activated IRF3, albeit weaker than the adaptor molecules shown in Figure 4.8A. Finally, the over-expression of IRF3 itself was used to stimulate IFNβ induction, however C6 was found not to inhibit in this instance (Figure 4.8C).

In conclusion, these data demonstrated that C6 could inhibit IRF3 activation downstream of the adaptors TRIF and MAVS, as well as the kinases of the non-canonical IKK complex, but acted upstream of IRF3, as inhibition was no longer observed following the over-expression of this molecule. This implied that the likely level of inhibition of C6 was downstream, or at the level of the non-canonical IKK complex (Figure 4.8D).

4.6 C6 inhibits signalling downstream of IFNα but not IFNγ

Following the expression and secretion of IFNs in response to infection, these molecules act in a paracrine and autocrine manner to induce the expression of ISGs, causing an antiviral state in the cell. The binding of IFNs to their respective receptors induces intracellular signalling cascades involving the JAK kinases and STAT transcription factors, which ultimately translocate to the nucleus and bind to the promoters of IFN responsive genes, thus regulating their transcription (reviewed in (Takaoka & Yanai, 2006). The binding of the type I IFNs, IFNα and IFNβ to the IFNα/β receptor ultimately regulates the transcription of genes with an ISRE in their promoter. To investigate whether C6 was able to abrogate IFN signalling HEK293 cells were transfected with an ISRE-promoter firefly luciferase reporter plasmid, a renilla luciferase transfection control and 100 or 200 ng of a C6, B14 or empty vector control expression plasmid. After 24 h cells were stimulated for 8 h with 250 U/ml IFNα. IFNα treatment induced an approximate 120-fold activation of the ISRE reporter in

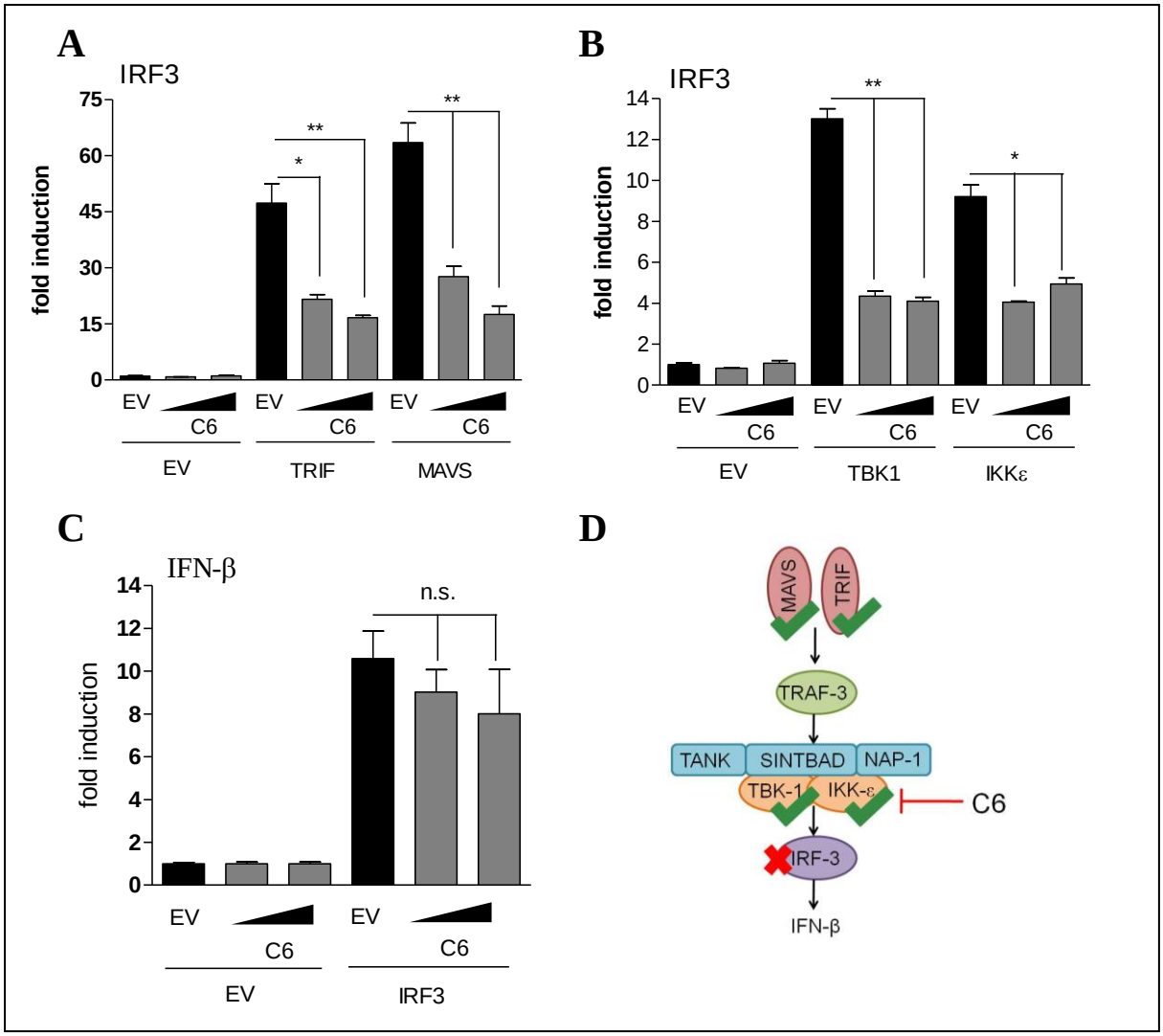

Figure 4.8: C6 inhibits IRF3 induction downstream, or at the level of the non-canonical IKK complex. HEK293 cells were transfected in 96-well plates with 60 ng of ISG56.1- (A, B) or IFNβ- (C) promoter firefly luciferase reporter plasmid, 10 ng of renilla luciferase transfection control plasmid, 100 ng or 200 ng of a C6 or empty vector control (EV) expression plasmid and 70 ng of TRIFΔRIP or MAVS (A), 200 ng of TBK1 or IKKε (B) or 200 ng of IRF3 (C) expression plasmid per well. After 24 h the cells were harvested in passive lysis buffer and the firefly luciferase activity was measured and normalised to the renilla luciferase activity. Data are from one representative experiment of at least three, each performed in triplicate. Data are represented as mean ± SD normalised to the un-stimulated EV control. n.s. Not significant, * $P<0.05$, ** $P<0.01$, analysed using the Student's T-test. (D) Summary of C6 inhibition in schematic form with green ticks indicating inhibition by C6 observed and the red cross indicating no inhibition by C6 after over-expression of this protein.

empty vector-transfected cells, which was reduced to less than 50-fold in cells transfected with a plasmid expressing C6 (Figure 4.9B). The same effect was not observed when cells were transfected with a plasmid expressing B14, as observed previously (Chen et al, 2008).

To understand if the inhibition of ISRE activation downstream of IFNα was the only IFN-induced signalling pathway that C6 had an effect on, signalling downstream of IFNγ was also tested. When IFNγ binds to the IFNγ receptor STAT1 is activated, translocates to the nucleus and regulates the transcription of genes with a GAS element in their promoter. To investigate IFNγ signalling HEK293 cells were transfected with a GAS-promoter firefly luciferase reporter plasmid, renilla luciferase transfection control and 200 ng of a C6, B14 or empty vector control expression plasmid. After 24 h cells were stimulated for 8 h with 1000 ng/ml IFNγ. Unexpectedly, this treatment did not induce any activation of the GAS reporter and thus HeLa cells were tested instead. In these cells treatment with 1000 ng/ml IFNγ induced an approximate 50-fold activation of the GAS reporter and this was unaffected by the presence of C6 or B14 suggesting that neither of these proteins were able to inhibit signalling downstream of IFNγ (Figure 4.9B).

These data indicated that C6 specifically inhibited signalling downstream of the type I IFNs and was unlikely to act on a protein that is common to both type I and type II IFN signalling pathways, for example STAT1, but was more likely to act on a protein unique to IFNα/β signalling. Incubation of cells with IFNλ also activates the transcription of genes with an ISRE in their promoter (Meager et al, 2005). It would therefore be interesting to determine whether C6 is able to inhibit ISRE-reporter plasmid activity downstream of these type III IFNs. If so, these data may indicate where C6 is likely to inhibit these signalling pathways. The mechanism by which C6 inhibits type I IFN signalling is currently unknown.

4.7 Summary

Given the role of many of the other VACV Bcl-2-like family members in evasion of innate immune signalling it was hypothesised that C6 may too have an immunodulatory function. To this end, C6 was found to inhibit IFNβ reporter activity in a concentration-dependent manner downstream of a number of stimuli, including infection with NDV. This inhibition

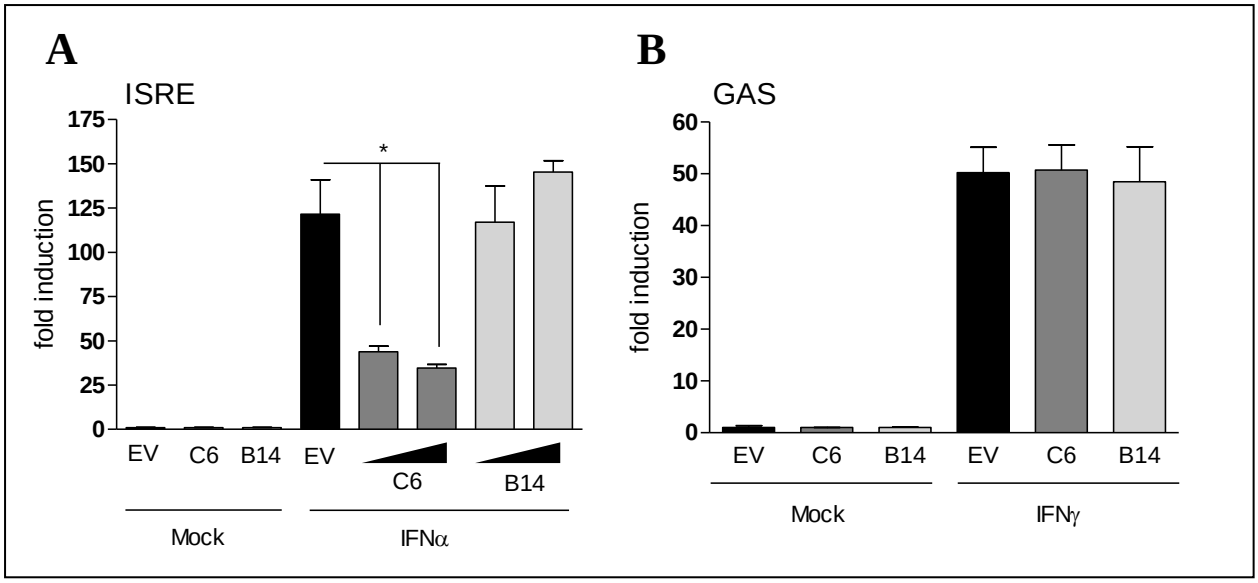

Figure 4.9: C6 inhibits signalling downstream of IFNα but not IFNγ. (A) HEK293 cells were transfected in 96-well plates with 60 ng of ISRE-promoter firefly luciferase reporter plasmid, 10 ng of renilla luciferase transfection control plasmid and 100 ng or 200 ng of a C6, B14 or empty vector control (EV) expression plasmid. After 24 h the cells were stimulated for 8 h with 250 U/ml IFNα. (B) HeLa cells were transfected in 96-well plates with 60 ng of GAS-promoter firefly luciferase reporter plasmid, 10 ng of renilla luciferase transfection control plasmid and 200 ng of a C6, B14 or empty vector control (EV) expression plasmid. After 24 h the cells were stimulated for 8 h with 1000 ng/ml IFNγ. The cells were harvested in passive lysis buffer and the firefly luciferase activity was measured and normalised to the renilla luciferase activity. Data are from one representative experiment of at least three, each performed in triplicate. Data are represented as mean ± SD normalised to the un-stimulated control (Mock) of each plasmid. * $P<0.05$, analysed using the Student's T-test.

was observed in both human and murine cells, and was unaffected by a number of epitope tags, located at either the N or C terminus of the C6 protein. The conservation of IFNβ inhibition was found in MVA 019 and MPXV, orthologues of protein C6.

Signalling downstream of the TLRs and RLRs activates multiple transcription factors including NF-κB, IRF3 and AP1. These transcription factors cooperate in activating the transcription of the IFNβ gene. The ability of C6 to inhibit IFNβ induction was not due to an effect on NF-κB because C6 was found not to inhibit NF-κB induction by reporter gene assay, analysing IκBα phosphorylation and degradation by immunoblotting, or p65 translocation to the nucleus by immunofluorescence. Instead, C6 was found to have an inhibitory role on the IRF3 signalling pathway. Reporter gene assay data obtained using the ISG56.1 promoter reporter plasmid, which has an IRF3 binding site indicated that C6

inhibited its activation downstream of both poly I:C and poly dA:dT in a concentration-dependent manner, whereas B14 did not. Further to this, C6 was found to inhibit the transcription of *CCL-5* and production of CXCL-10, both IRF3 specific genes, following infection of HEK293ET cells with NDV. The point at which C6 inhibited IRF3 signalling was also determined by over-expressing known proteins in the signalling pathway to drive activation of the ISG56.1 reporter plasmid. C6 was found to inhibit downstream, or at the level of the non-canonical IKK complex because it was able to inhibit IRF3 induction following over-expression of the kinases TBK1 and IKKε, but not the induction of IFNβ downstream of IRF3 itself.

Finally, in addition to the role of C6 in inhibiting IFNβ induction, this protein was found to inhibit signalling downstream of the IFNAR, reducing the activation of an ISRE reporter plasmid following the treatment of cells with IFNα. This inhibition was specific to signalling downstream of IFNα, as no such inhibition was observed on the activation of a GAS reporter plasmid following the treatment of cells with IFNγ. The mechanism by which C6 exerts this inhibitory action is currently unknown and warrants further investigation.

Chapter 5: Characterisation of the binding of C6 to the non-canonical IKK complex adaptor proteins TANK, SINTBAD and NAP1

5.1 C6 binds the non-canonical IKK complex adaptor protein TANK

Given that C6 was able to inhibit IRF3 signalling, and the level of this inhibition was determined to be at, or downstream of the non-canonical IKK complex, a LUMIER assay was used to screen for the binding of C6 to known components of this complex. HEK293 cells were co-transfected with a plasmid expressing a LUC – tagged prey protein, namely the two kinases of the non-canonical IKK complex IKKε and TBK1, and the three adaptor proteins TANK, SINTBAD and NAP1, and a plasmid expressing a FLAG-tagged bait protein. The cells were harvested 48 h later and cleared lysates were used for the LUMIER assay (see Chapter 2), and also separated by SDS-PAGE and analysed by immunoblotting for the expression of the FLAG-tagged protein.

In all instances the LUC-tagged prey proteins were found to co-immunoprecipitate with their respective positive control FLAG-tagged bait proteins, which was TBK1 for the adaptor proteins and TANK for the kinases (Figure 5.1). Expression of all FLAG-tagged proteins was detected by immunoblotting, except for FLAG-TBK1, a problem which was observed on a number of occasions, but given that all three LUC-tagged adaptor proteins were found to be co-immunoprecipitated in cells transfected with a plasmid expressing this protein, this problem was likely to be a detection issue rather than a problem with expression. TAP-C6 was found to co-immunoprecipitate LUC-TANK, but not LUC-tagged SINTBAD, NAP1 or IKKε, suggesting an interaction between these two proteins. A weak interaction was detected between TAP-C6 and LUC-TBK1, however this was probably background levels of binding, possibly mediated via the interaction of C6 with TANK.

To determine whether the interaction of C6 with TANK could be observed during the context of a viral infection HEK293 cells were either co-transfected with a plasmid expressing a LUC-tagged prey protein and FLAG-GFP, or transfected with a plasmid expressing a LUC-

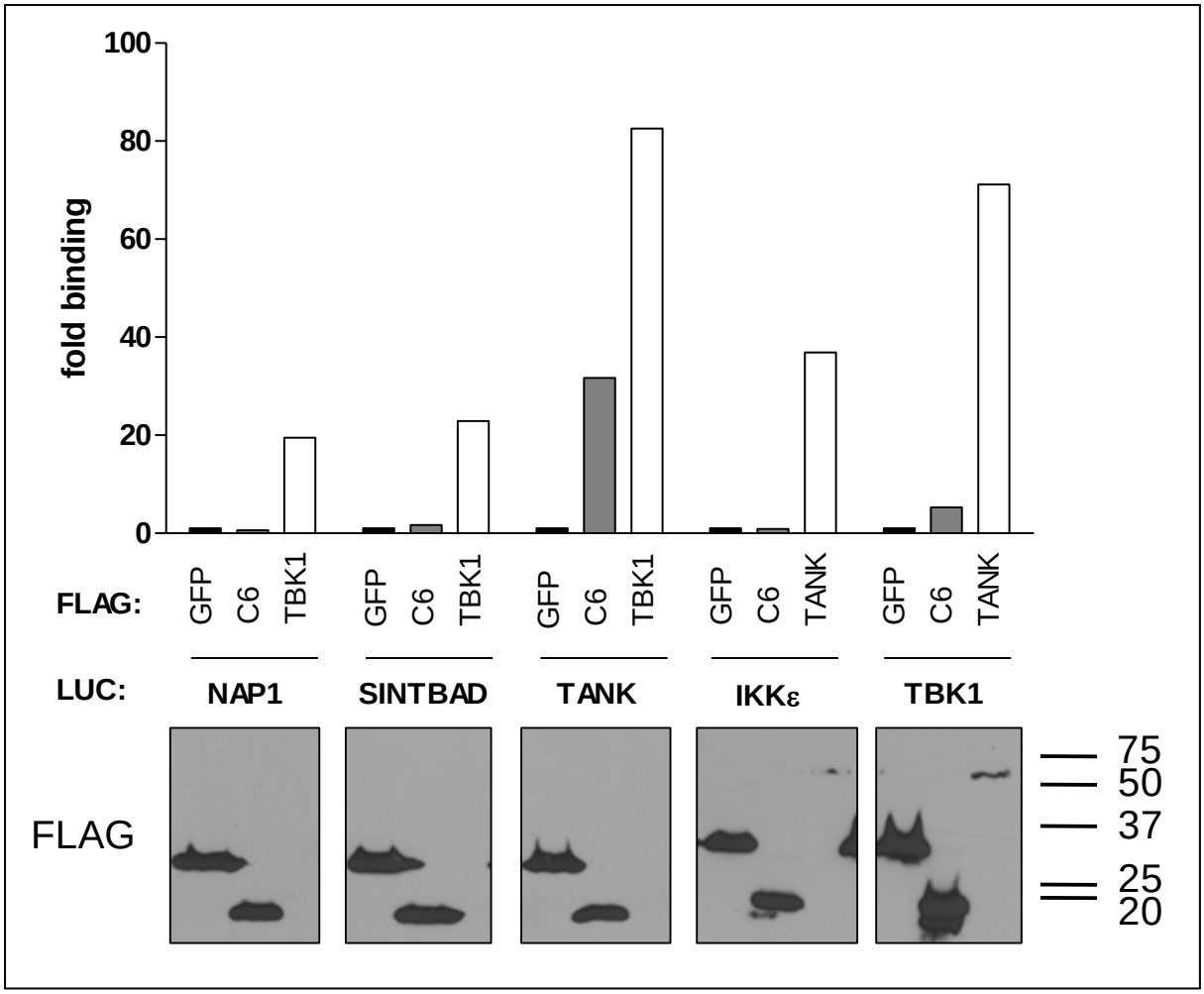

Figure 5.1: C6 interacts with TANK in a LUMIER assay. HEK293 cells were co-transfected with a plasmid expressing a renilla luciferase (LUC) – tagged prey protein and a plasmid expressing a FLAG-tagged bait protein (TAP-C6 for C6). The cells were harvested 48 h later in IP buffer and cleared lysates were incubated with FLAG agarose beads. A proportion of the whole cell lysate was analysed for total luminescence and also separated by SDS-PAGE and analysed by immunoblotting for the expression of the FLAG-tagged protein. The FLAG agarose beads were washed three times in IP buffer and the bound proteins were eluted using 150 ng/ml FLAG peptide. The luminescence after immunoprecipitation was measured and normalised to the total luminescence of the sample. A fold binding was calculated by normalising to a FLAG-GFP control. The location of protein molecular mass markers is indicated (kDa).

tagged prey protein and then infected with vC6TAP, or vΔC6 as a control. After the LUMIER assay was performed an equivalent level of background binding of the LUC-tagged prey proteins was observed in the cells transfected with FLAG-GFP, or infected with vΔC6, and thus only data for FLAG-GFP are presented in Figure 5.2. In agreement with LUMIER data obtained by over-expression of TAP-C6, LUC-TANK was co-immunoprecipitated with C6-TAP expressed by vC6TAP (Figure 5.2). No such binding was observed for the other proteins in the non-canonical IKK complex, or the proteins of the canonical IKK complex, namely IKKα, IKKβ and the regulatory subunit NEMO. All LUC-tagged proteins had been tested previously for binding to positive control FLAG-tagged molecules indicating their functionality in this assay (data not shown). The expression of FLAG-GFP or C6-TAP was confirmed in all samples by immunoblotting (Figure 5.2).

The binding of C6 to TANK in the context of a viral infection was also confirmed using conventional immunoprecipitation assays. HEK293 cells were transfected for 24 h with a plasmid expressing TANK and then infected for 4 h with 5 p.f.u. per cell of vC6WR, or vΔC6 as a control. Cleared lysates were incubated with the rabbit-anti-C6 serum coupled to protein G sepharose beads to immunoprecipitate C6 from the infected cells. Over-expressed TANK was found to co-immunoprecipitate with un-tagged C6 expressed from vC6WR but not in cells infected with vΔC6, indicating the specificity of this interaction (Figure 5.3A). In a converse experiment HEK293 cells were transfected with a plasmid expressing TANK and then infected with vC6HA, or vB14HA as a control and subjected to an immunoprecipitation with a goat-anti-TANK Ab coupled to protein G sepharose beads. In this instance C6-HA, but not B14-HA was found to co-immunoprecipitate with TANK, again indicating the specificity of the interaction (Figure 5.3B).

Taken together these data indicated that both over-expressed C6 and C6 expressed at natural levels from cells infected with VACV WR could interact with over-expressed TANK, and this was demonstrated following the immunoprecipitation of TANK or C6.

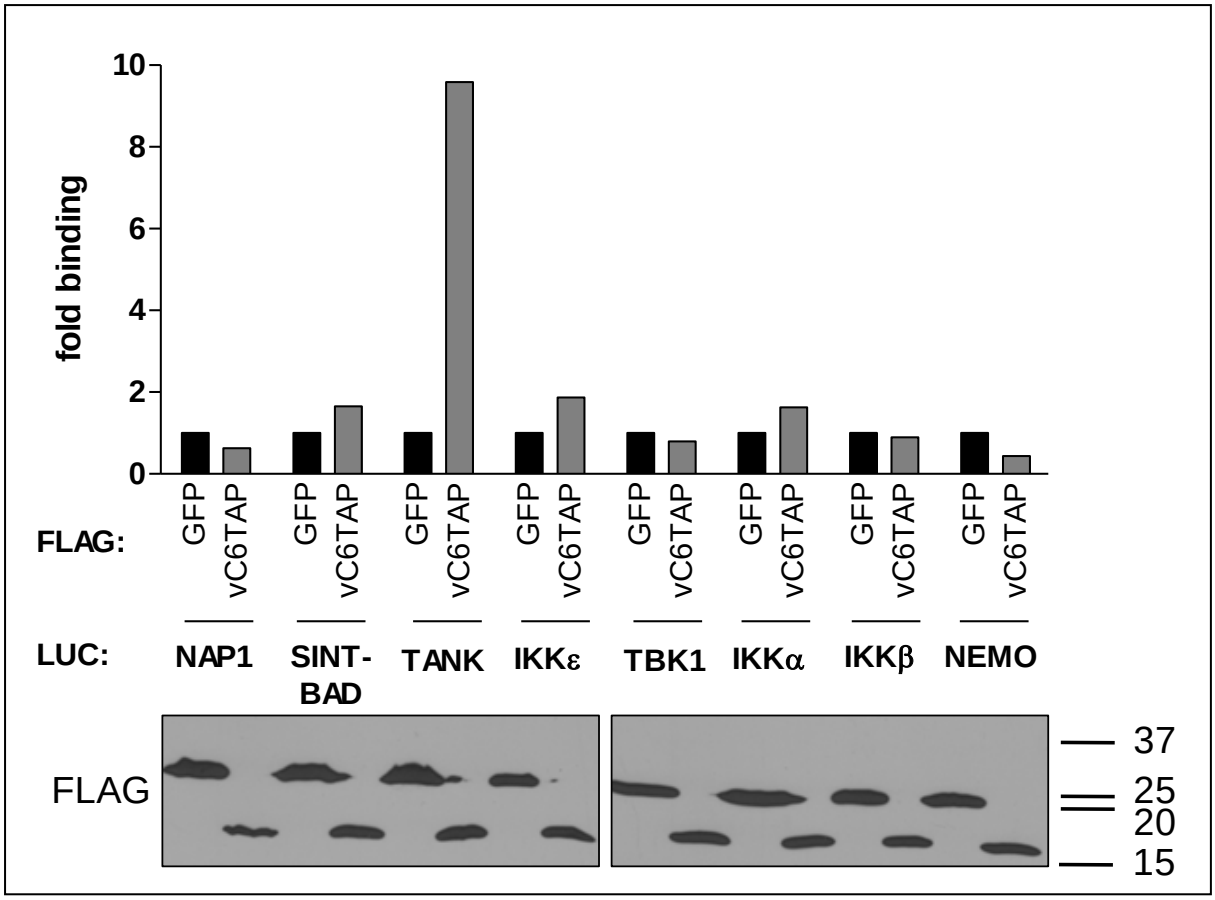

Figure 5.2: Virally expressed C6 interacts with TANK in a LUMIER assay. HEK293 cells were co-transfected with a plasmid expressing a LUC – tagged prey protein and a plasmid expressing FLAG-GFP or empty vector control. Thirty two h later empty vector-transfected wells were infected overnight with vC6TAP at 2 p.f.u. per cell. The cells transfected with FLAG-GFP were mock-infected overnight. The cells were harvested in IP buffer and cleared lysates were incubated with FLAG agarose beads. A proportion of the whole cell lysate was analysed for total luminescence and also separated by SDS-PAGE and analysed by immunoblotting for the expression of the FLAG-tagged protein. The FLAG agarose beads were washed three times in IP buffer and the bound proteins were eluted using 150 ng/ml FLAG peptide. The luminescence after immunoprecipitation was measured and normalised to the total luminescence of the sample. A fold binding was calculated by normalising to a FLAG-GFP control. The location of protein molecular mass markers is indicated (kDa).

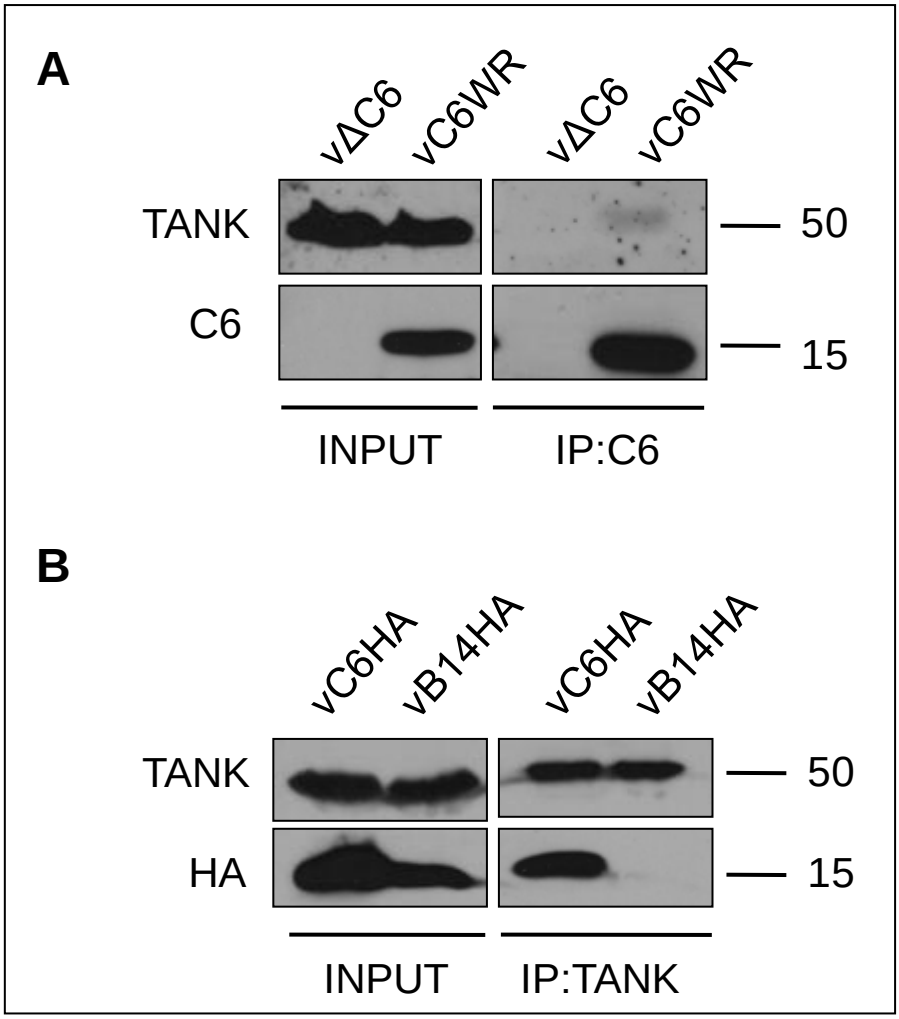

Figure 5.3: C6 interacts with over-expressed TANK in the context of a viral infection. HEK293 cells were transfected with a plasmid expressing TANK for 24 h and then infected for 4 h at 5 p.f.u. per cell with the viruses indicated. The cells were harvested in IP buffer and cleared lysates were incubated with either rabbit-anti-C6 serum coupled to protein G sepharose beads (A) or goat-anti-TANK Ab coupled to protein G sepharose beads (B). The whole cell lysates (INPUT) and immunoprecipitated proteins (IP) were separated by SDS-PAGE and analysed by immunoblotting with goat-anti-TANK, rabbit-anti-C6 or rabbit-anti-HA antibodies. The location of protein molecular mass markers is indicated (kDa).

5.2 C6 interacts with the N-terminal coiled-coil region, but not full length hTANK by LUMIER

To further characterise the interaction of C6 with TANK, a series of truncation mutants were designed with Dr. Felix Randow (MRC laboratory of Molecular Biology, Cambridge) based on the human sequence of TANK (hTANK). TANK is an adaptor molecule that has been described to interact with a number of proteins including TBK1 (Pomerantz & Baltimore, 1999), IKKε (Nomura et al, 2000), TRAF2 and TRAF3 (Cheng & Baltimore, 1996), NEMO (Chariot et al, 2002), IRF3 (Guo & Cheng, 2007) and it also has the ability to homo-dimerise (Chin et al, 1999). The structure of this protein has not been solved, but several domains have been predicted based on its amino acid sequence and biochemical analysis (see Figure 1.4). At the N terminus there is a coiled-coil domain, a domain with an important role in protein-protein interactions (Figure 5.4A). Between residues 135 and 173 there is the TBD, an α-helical region responsible for interactions with the kinases TBK1 and IKKε (Ryzhakov & Randow, 2007). At the C terminus of the protein there is a zinc-finger domain, a region which in addition to the N terminus is required for binding to NEMO (Bonif et al, 2006). Based on these domains a set of 7 truncation mutants were constructed with an N-terminal renilla luciferase tag, for use in LUMIER assays. The expression of the truncation mutants was confirmed by immunoblotting. HEK293 cells were transfected with the LUC – tagged hTANK truncation mutants. The cells were harvested 24 h later, the cleared lysates were separated by SDS-PAGE and these were analysed by immunoblotting with mouse-anti-renilla luciferase and mouse-anti-tubulin antibodies. All of the truncation mutants were expressed (indicated by the white arrows, Figure 5.4B), although the expression of 1-135, 1-173 and to some extent 1-69 was found to be weaker than the other mutants. The mouse-anti-renilla luciferase Ab was found repeatedly to react non-specifically with proteins of approximately 80 kDa and 100 kDa.

The interaction of TAP-C6 with the hTANK truncation mutants was then tested by LUMIER assay in HEK293 cells. Somewhat surprisingly, unlike full length murine TANK (mTANK), which had been previously identified as a binding partner for C6 (Figures 5.1, 5.2 and 5.3), full length hTANK did not co-immunoprecipitate with C6 (Figure 5.5A). This molecule however did show strong binding to TBK1 indicating that this protein was expressed and had folded correctly, or at least sufficiently to bind TBK1. This result was unexpected because

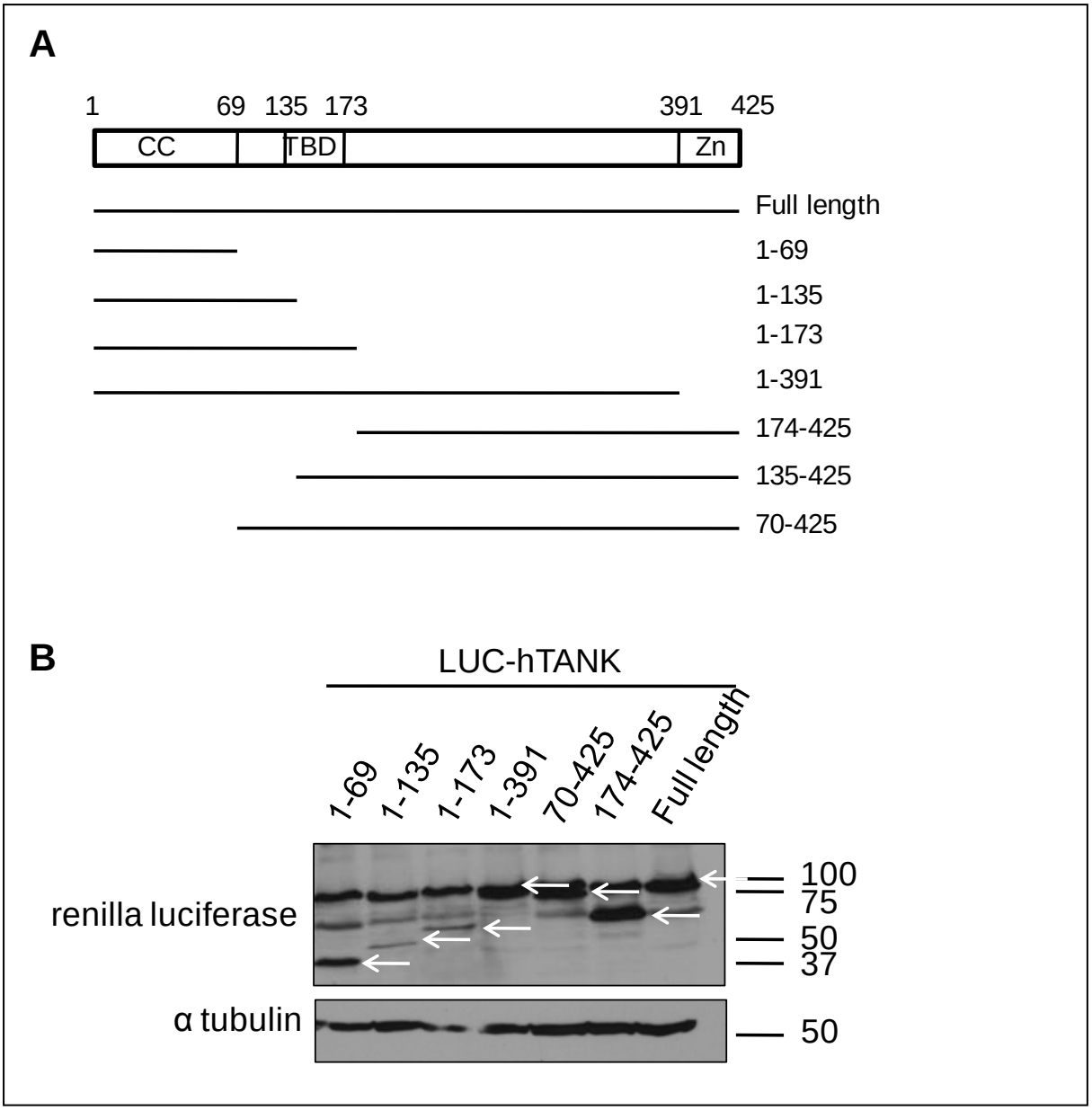

Figure 5.4: Human TANK truncation mutants. (A) Schematic representation of hTANK and the truncation mutants with the locations of the coiled-coil domain (CC), TBK1-binding domain (TBD) and Zinc finger domain (Zn) indicated. (B) Expression of truncation mutants. HEK293 cells were transfected with LUC – tagged hTANK truncation mutants. The cells were harvested 24 h later in cell lysis buffer and cleared lysates were separated by SDS-PAGE and analysed by immunoblotting with mouse-anti-renilla luciferase and mouse-anti-tubulin antibodies. The location of the LUC – tagged proteins is indicated with a white arrow. The location of protein molecular mass markers is indicated (kDa).

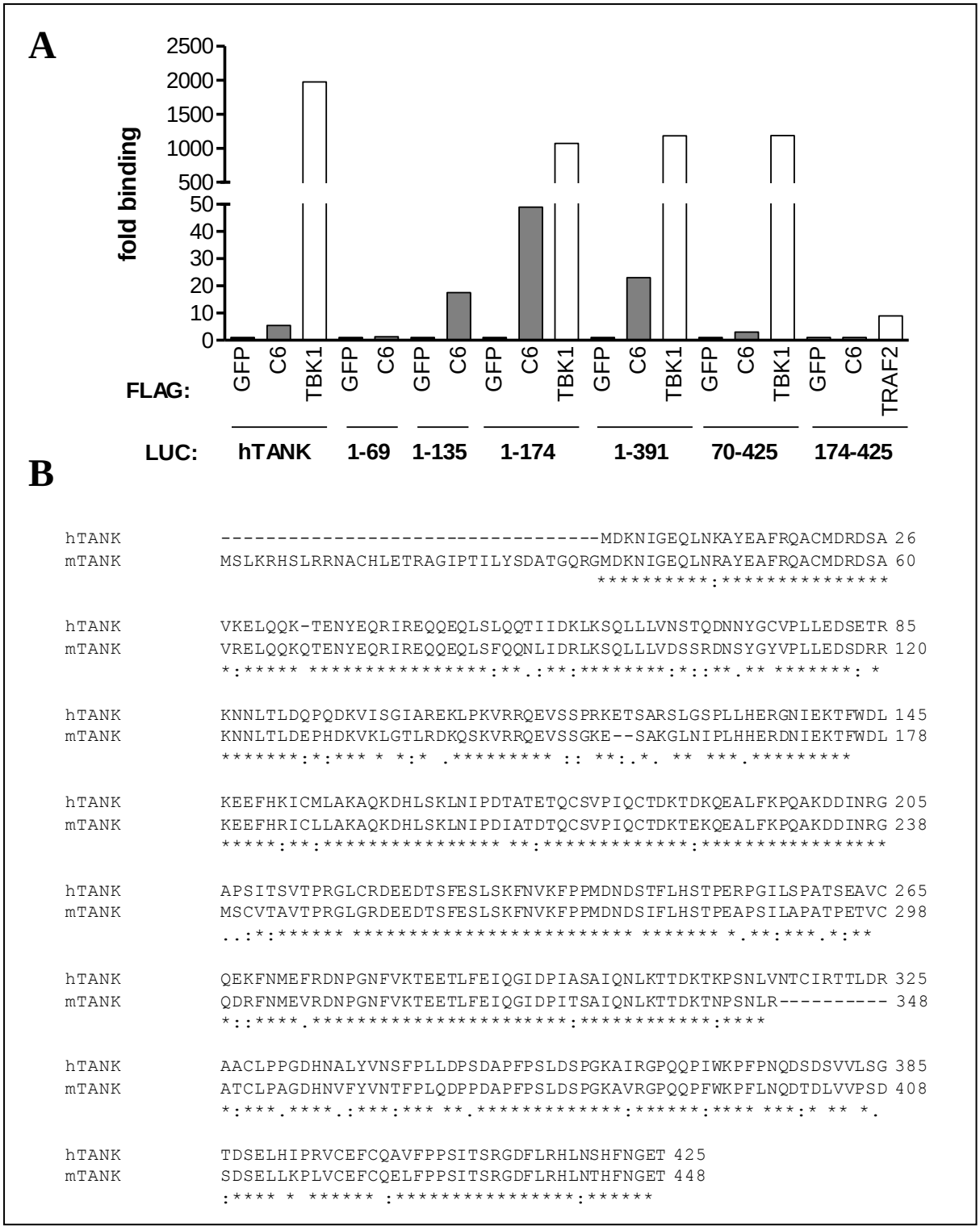

Figure 5.5: C6 interaction with hTANK truncation mutants. (A) HEK293 cells were co-transfected with a plasmid expressing a LUC – tagged hTANK prey protein and a plasmid expressing a FLAG-tagged bait protein. The cells were harvested 48 h later in IP buffer and cleared lysates were incubated with FLAG agarose beads. A proportion of the whole cell lysate was analysed for total luminescence. The FLAG agarose beads were washed three times in IP buffer and the bound proteins were eluted using 150 ng/ml FLAG peptide. The luminescence after immunoprecipitation was measured and normalised to the total luminescence of the sample. A fold binding was calculated by normalising to a FLAG-GFP control. (B) Amino acid sequence alignment of hTANK and murine TANK (mTANK).

murine and human TANK share high amino acid sequence identity (80 %) (Figure 5.5B). Notably there is an N-terminal extension in the sequence of mTANK and a ten amino acid deletion in this protein at residue 348 compared to hTANK. These differences may explain why C6 is able to interact with mTANK by LUMIER assay and not hTANK.

Despite the lack of binding of full length hTANK to C6 it was surprising to observe twenty fold more luminescence of mutant 1-135 in the immunoprecipitation of this protein with TAP-C6 than FLAG-GFP, suggesting a possible interaction between these molecules (Figure 5.5A). Due to the lack of known binding partners that interact solely with the N-terminal region of TANK, mutants 1-69 and 1-135 did not have positive controls for this assay. Mutant 1-69 is particularly small and may not fold correctly when fused to the large 36 kDa renilla luciferase tag. This could therefore explain the lack of interaction with C6. An interaction between TAP-C6 and mutants 1-173 and 1-391 was also observed in this assay. Both of these molecules showed positive binding to TBK1 as they included the TBD. Mutant 70-425 did not show an interaction with C6, but did bind TBK1, which acted as a positive control for this molecule. Mutant 174-425 also did not bind C6, and because it did not contain the TBD TRAF2 was used as a positive control since the binding of TANK to this molecule has been characterised to be between residues 173 and 191 (Cheng & Baltimore, 1996). Mutant 174-425 did show some binding to FLAG-TRAF2, although this interaction was weak.

In conclusion these data indicated that C6 interacted with the N terminus of hTANK, as truncations removing the C terminus were still able to bind. The smallest region found to bind C6 was residues 1-135, which included the coiled-coil domain. When the coiled-coil domain was not present, such as in mutant 70-425, C6 was no longer able to interact with hTANK, suggesting that this region is essential for binding. The coiled-coil domain alone (mutant 1-69) was not found to interact with C6, but it is not known if this domain of hTANK folded correctly when fused to the large LUC tag.

The finding that C6 interacted with mTANK and some of the truncation mutants of hTANK, but not full length hTANK was unexpected. It is possible that with full length hTANK the LUC tag obscures the N-terminal coiled-coil domain in some manner, thus preventing the

interaction with C6. Of note, the N terminus of mTANK is 34 amino acids longer than hTANK (Figure 5.5B), which may provide a spacer between the LUC tag and the domain that interacts with C6. In the context of full length hTANK fused to the LUC tag, it is further possible that the C terminus of the protein folds incorrectly, potentially precluding the binding of C6 to the coiled-coil domain at the N terminus. This may explain why mutants where C-terminal regions of the protein are removed show a positive interaction with C6. Supporting this hypothesis, the existence of intramolecular interactions between the N and C termini of TANK has previously been suggested (Chin et al, 1999), as has an intramolecular interaction within the signalling adaptor TRIF (Tatematsu et al, 2010). Of note mutant 1-391 is still able to interact with C6, suggesting that any preclusion of binding caused by the C terminus of the protein would be due to the Zinc finger region.

5.3 C6 interacts with hTANK by co-immunoprecipitation assay

To determine if the presence of the LUC tag was preventing the binding of hTANK to C6, a conventional immunoprecipitation assay was performed using FLAG-tagged hTANK. HEK293ET cells were transfected with plasmids encoding FLAG-tagged GFP, mTANK, or hTANK and TAP-C6. After 48 h the cells were harvested and cleared lysates were subjected to immunoprecipitation with Strep agarose beads to purify TAP-C6. Both FLAG-tagged murine and human TANK were found to co-immunoprecipitate with C6, although the interaction with hTANK appeared weaker (Figure 5.6). FLAG-GFP was not found to co-immunoprecipitate with C6 in this assay indicating the specificity of the interaction of C6 with TANK. These data indicated that over-expressed FLAG-hTANK was able to interact with C6 and that the LUC-hTANK molecule used in the LUMIER assay was not folded appropriately to support this interaction.

5.4 C6 interacts with the N-terminal coiled-coil region of mTANK

To confirm those data obtained by LUMIER assay using the hTANK mutants, four LUC-tagged mTANK truncation mutants were constructed (Figure 5.7A). As with the hTANK mutants the expression of the mTANK truncations was confirmed by transfecting HEK293 cells and immunoblotting cell lysates with a mouse-anti-renilla Ab. All four mutants were found to express a protein of the expected size, although as with the hTANK truncations this

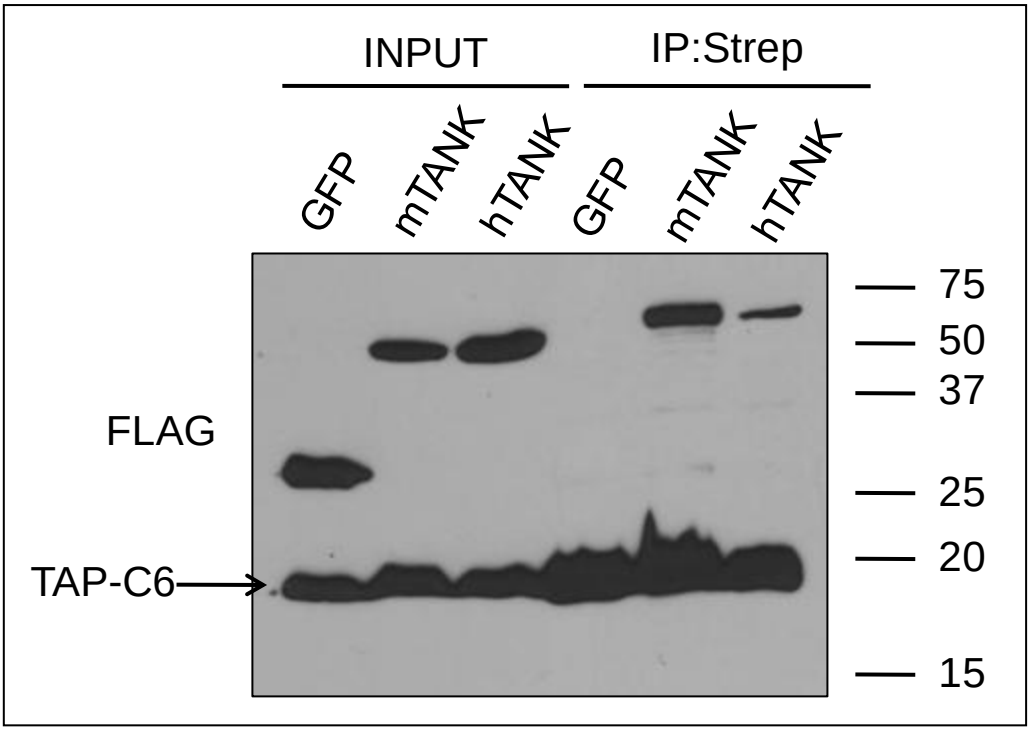

Figure 5.6: C6 interacts with over-expressed hTANK by conventional IP. HEK293ET cells were grown in 10-cm dishes and transfected with 5 μg of plasmids encoding FLAG-tagged GFP, mTANK or hTANK and 5 μg of TAP-tagged (consisting of FLAG and Strep epitopes) C6 as indicated. After 48 h the cells were harvested in IP buffer and cleared lysates (INPUT) were subjected to immunoprecipitation (IP) with Streptavidin agarose beads. The proteins were separated by SDS-PAGE and detected by immunoblotting with a mouse-anti-FLAG Ab. The location of protein molecular mass markers (kDa) and TAP-C6 are indicated.

expression varied between the mutants (Figure 5.7B). The interaction of the mTANK truncations with C6 was then tested by LUMIER assay. Consistent with data obtained with the hTANK truncations, mTANK truncations including the coiled-coil domain (1-120 and 1-165) interacted with TAP-C6, but those lacking this domain (120-448 and 162-448) did not (Figure 5.8 and data not shown). Truncation 120-448 was presumed to be functional by LUMIER assay because it was able to interact with TBK1 as a positive control. These data confirm previous findings that C6 binds the N-terminal coiled-coil region of TANK, and that this region is essential, because when it is deleted C6 is no longer able to interact. Further supporting this hypothesis, in the case of mTANK, C6 was found to interact with the coiled-coil region expressed alone, encoded by residues 1-120.

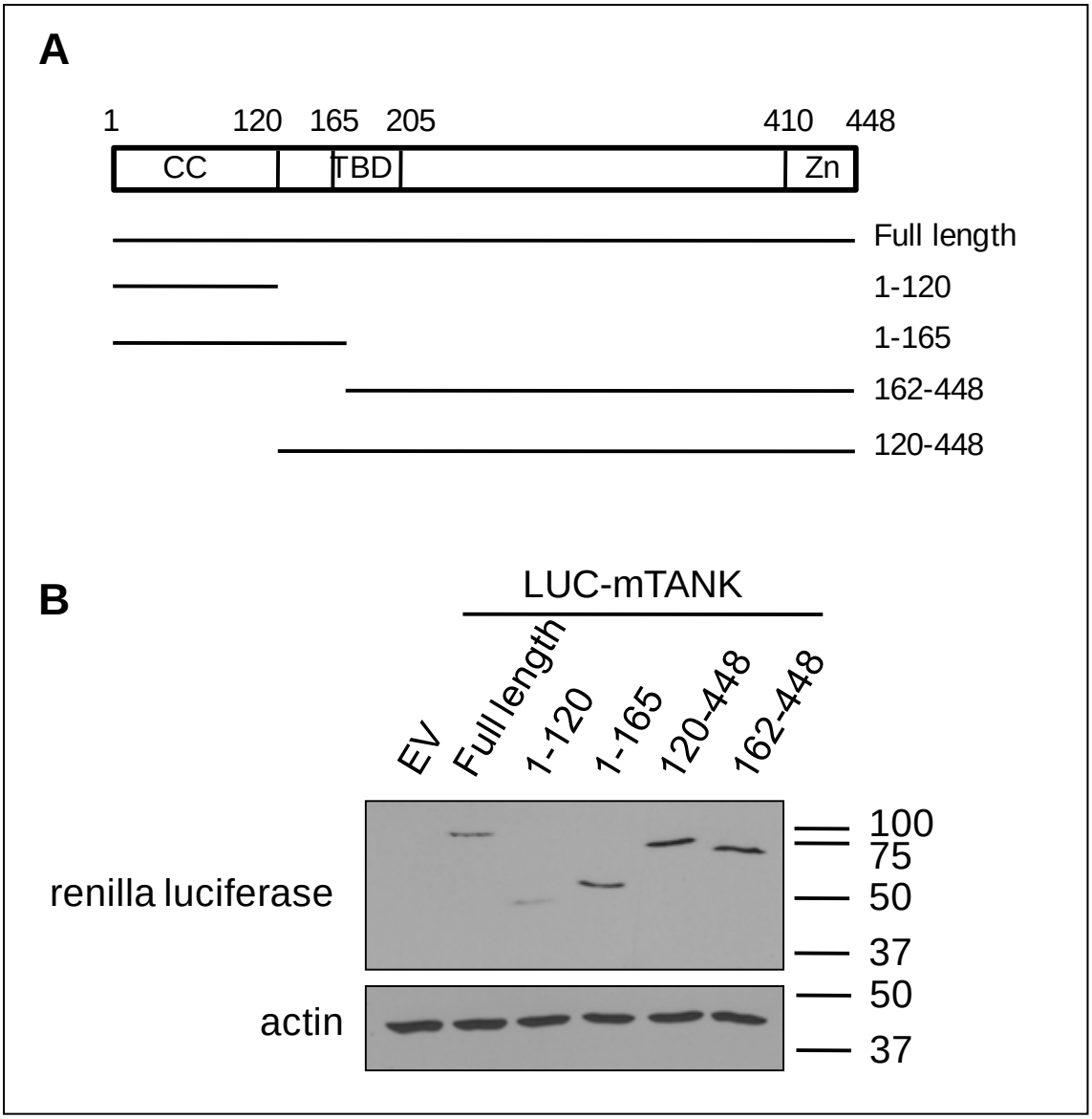

Figure 5.7: mTANK truncation mutants. (A) Schematic representation of mTANK and the truncation mutants with the locations of the coiled-coil domain (CC), TBK1-binding domain (TBD) and Zinc finger domain (Zn) indicated. (B) Expression of truncation mutants. HEK293 cells were transfected with LUC – tagged mTANK truncation mutants. The cells were harvested 24 h later in cell lysis buffer and the cleared lysates were separated by SDS-PAGE and analysed by immunoblotting with mouse-anti-renilla luciferase and rabbit-anti-actin antibodies. The location of protein molecular mass markers is indicated (kDa).

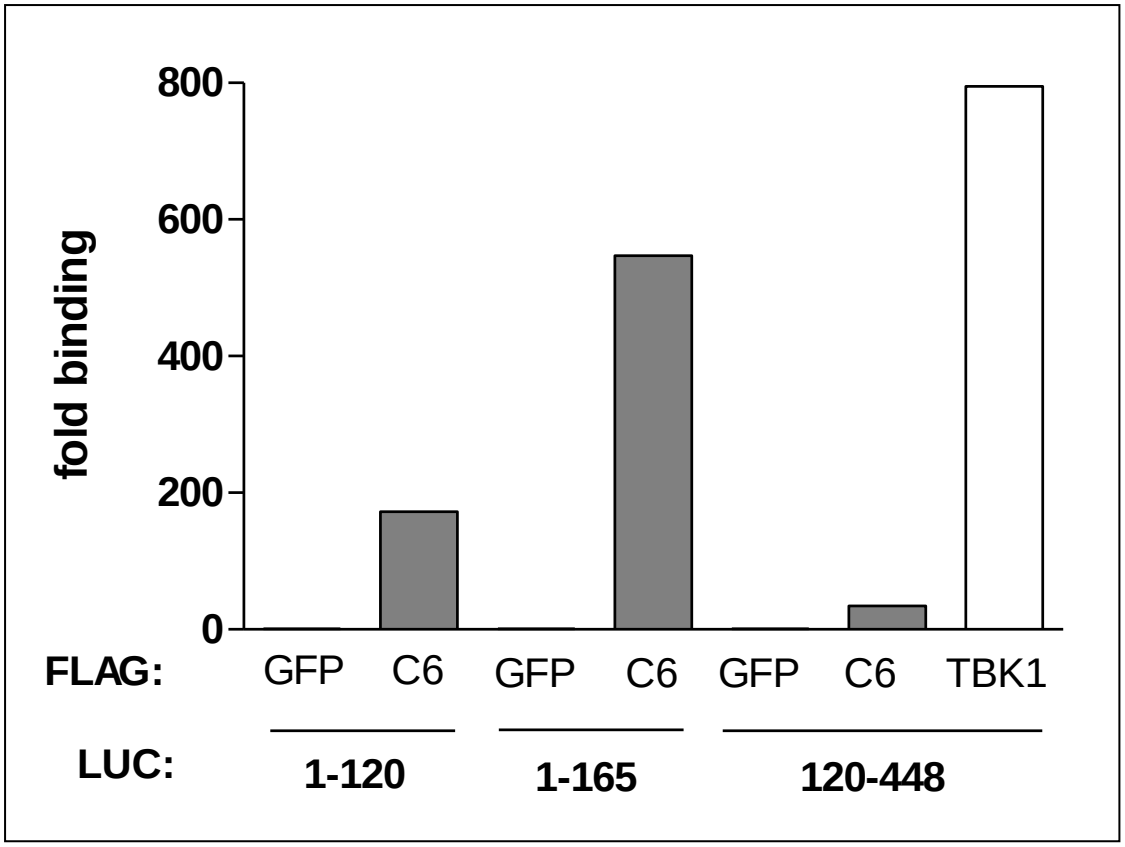

Figure 5.8: C6 interaction with mTANK truncation mutants. HEK293 cells were co-transfected with a plasmid expressing LUC – tagged mTANK prey protein and a plasmid expressing a FLAG-tagged bait protein. The cells were harvested 48 h later in IP buffer and cleared lysates were incubated with FLAG agarose beads. A proportion of the whole cell lysate was analysed for total luminescence. The FLAG agarose beads were washed three times in IP buffer and the bound proteins were eluted using 150 ng/ml FLAG peptide. The luminescence after immunoprecipitation was measured and normalised to the total luminescence of the sample. A fold binding was calculated by normalising to a FLAG-GFP control.

5.5 C6 is still able to inhibit IFNβ induction in TANK-null cells

To determine whether the binding of C6 to TANK could explain mechanistically how this VACV protein was able to inhibit IRF3 signalling and hence IFNβ induction, TANK-null cells were obtained from the laboratory of Dr. Felix Randow to use in a reporter gene assay. HCT116 TANK +/+ or TANK -/- cells were transfected with the IFNβ-promoter firefly luciferase reporter plasmid, the renilla luciferase transfection control plasmid, 100 ng of a C6 expression plasmid or empty vector (EV) control and 70 ng of TRIFΔRIP expression plasmid to induce IFNβ reporter activation. Over-expression of the adaptor molecule TRIF induced an approximate nine-fold activation of the IFNβ promoter in the HCT116 parental cell line

(HCT116 TANK +/+) and this induction was significantly inhibited by the expression of C6, as expected (Figure 5.9). The lack of TANK did not prevent IFNβ induction in the HCT116 TANK -/- cell line following over-expression of TRIFΔRIP, but this activation was significantly (P<0.01) reduced, indicating an important contribution of TANK to this signalling pathway, as previously observed in the context of viral infection (Guo & Cheng, 2007). Interestingly C6 was also found to significantly (P<0.01) inhibit IFNβ activation in the TANK-null cell line, indicating that the binding of C6 to TANK was not the cause of IRF3 signalling abrogation, or this binding alone was not sufficient to explain the inhibition.

5.6 Renilla luciferase-tagged C6 failed to interact with TANK

The fact that C6 was able to inhibit IFNβ induction in TANK-null cells suggested that C6 might interact with other proteins in addition to TANK. Data obtained with the TANK truncation mutants identified the coiled-coil region as the binding site for C6 on TANK. This region is shared amongst the three non-canonical IKK adaptor proteins TANK, SINTBAD and NAP1, with a single coiled-coil domain in TANK and three present in SINTBAD and NAP1 (Ryzhakov & Randow, 2007). If C6 had evolved to bind the coiled-coil domain of TANK, it may also be able to interact with this region of SINTBAD and NAP1. Given the overlapping role of these adaptors in the IRF3 signalling pathway (Guo & Cheng, 2007; Ryzhakov & Randow, 2007; Sasai et al, 2006), targeting all three adaptors could be highly beneficial to the virus and an effective way of abrogating IRF3 activation.

LUMIER data obtained in Figures 5.2 and 5.3 indicated that C6 was not able to interact with LUC-tagged SINTBAD or NAP1. However, as previously discussed, the renilla luciferase tag used in the LUMIER assay is very large and may preclude the binding of some pairs of proteins, or may prevent their correct folding. It was observed, for example, that C6 did not interact with LUC-hTANK (Figure 5.5A), but did interact with FLAG-hTANK (Figure 5.6), perhaps due to the considerably smaller size of the FLAG epitope. In order to screen the interaction of C6 against signalling molecules with a smaller tag (the FLAG epitope), C6 was renilla luciferase tagged at either the N or the C terminus for use in the LUMIER assay.

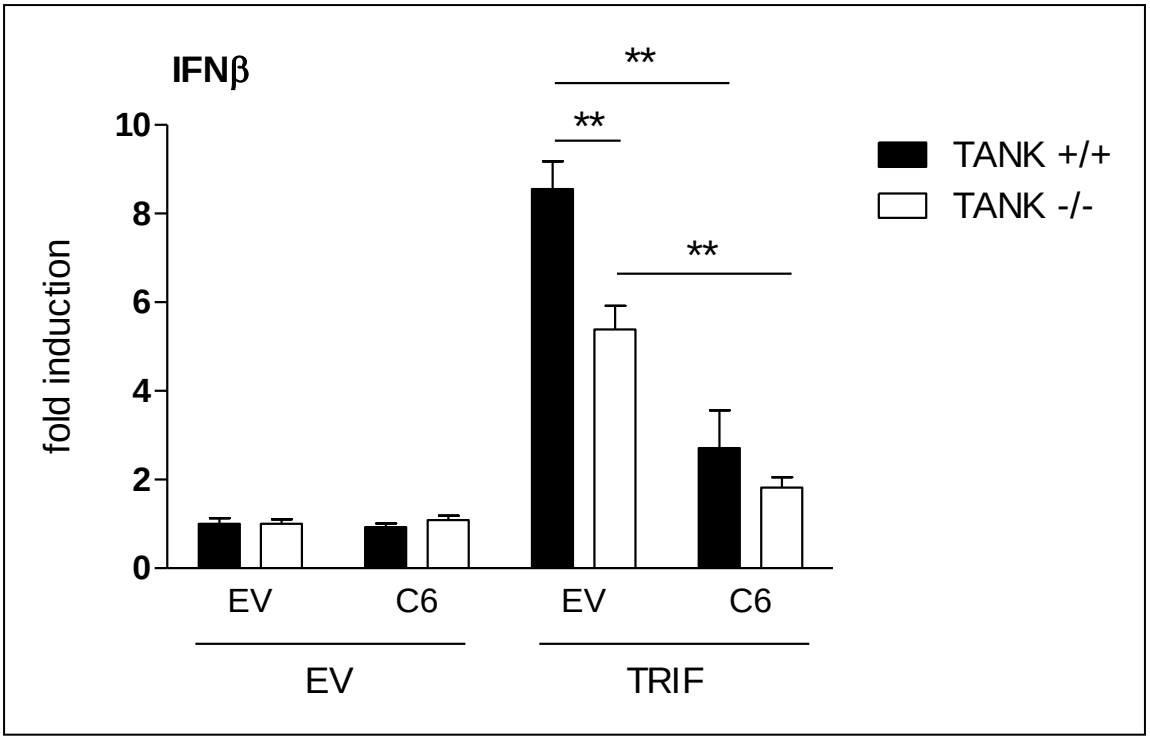

Figure 5.9: C6 inhibits IFNβ induction in TANK-null cells. HCT116 TANK +/+ or TANK -/- cells were transfected in 96-well plates with 60 ng of IFNβ-promoter firefly luciferase reporter plasmid, 10 ng of renilla luciferase transfection control plasmid, 100 ng of a C6 expression plasmid (C6) or empty vector control (EV) and either 70 ng of TRIF expression plasmid (TRIFΔRIP) or EV per well using JetPrime. Thirty h after transfection the cells were harvested in passive lysis buffer and the firefly luciferase activity was measured and normalised to the renilla luciferase activity. Data are from one representative experiment of at least three, each performed in triplicate. Data are represented as mean ± SD. ** $P<0.01$, analysed using the Student's T-test.

HEK293 cells were co-transfected with a plasmid expressing LUC-C6 (Figure 5.10A) or C6-LUC (Figure 5.10B) prey protein and a plasmid expressing a FLAG-tagged bait protein. The cells were harvested 48 h later and a LUMIER assay was performed. The homo-dimerisation of C6 was used as a positive control in this assay (see Chapter 3) and accordingly both LUC-C6 and C6-LUC were found to interact with TAP-C6 (Figure 5.10). These data indicated that C6 tagged at either end with renilla luciferase was sufficiently folded to support its dimerisation. In both cases, however, C6 was found not to interact with any of the non-canonical IKK complex proteins, including human and murine TANK. The lack of interaction with mTANK, which had previously been demonstrated by LUMIER assay using LUC-mTANK (Figures 5.1 and 5.2) implied that LUC-tagged C6 was not sufficiently folded

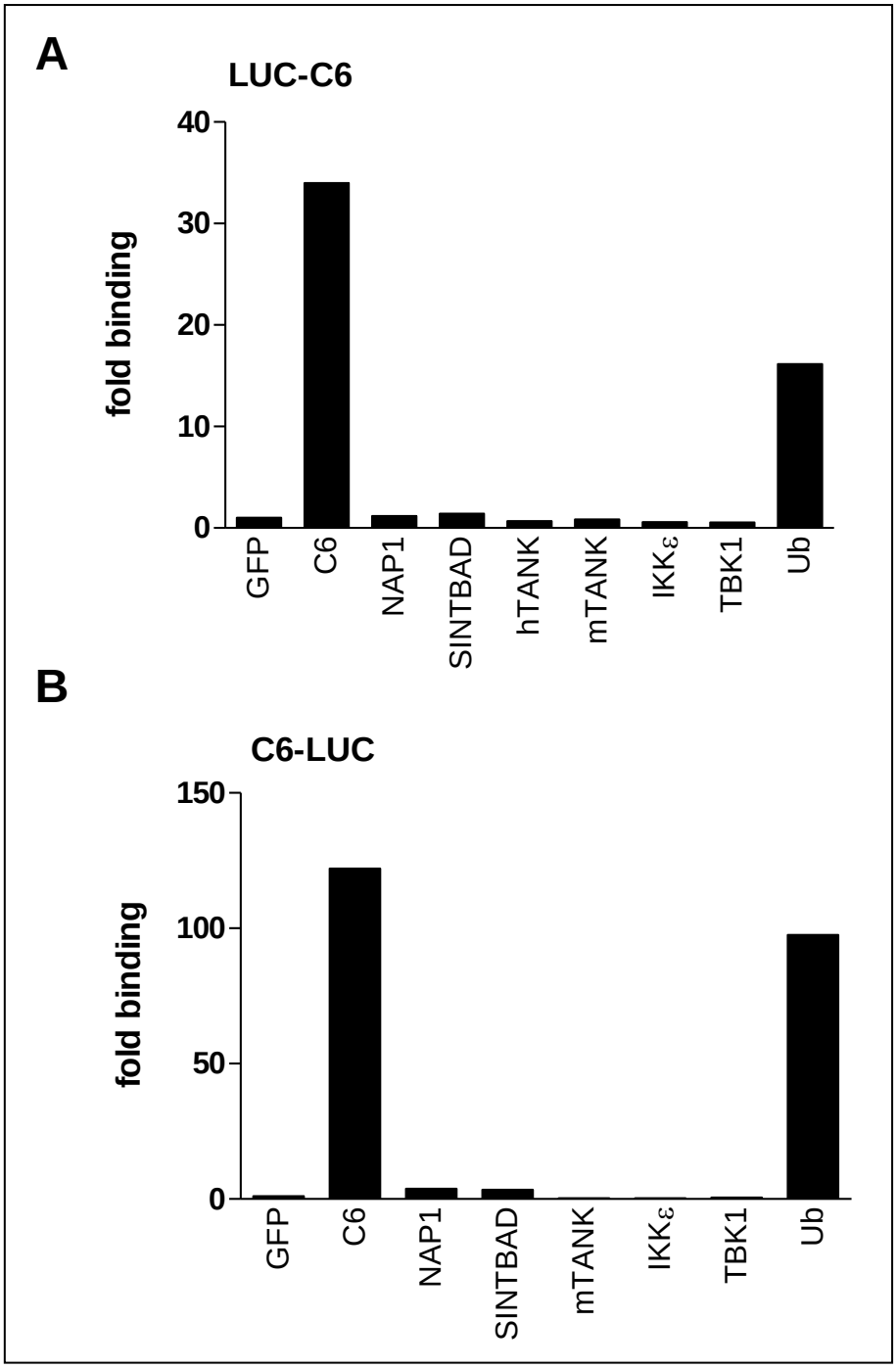

Figure 5.10: Interaction of LUC-tagged C6 with FLAG-tagged proteins. HEK293 cells were co-transfected with a plasmid expressing an N-terminal (A) or C-terminal (B) LUC – tagged C6 prey protein and a plasmid expressing a FLAG-tagged (or TAP-tagged in the case of C6) bait protein. The cells were harvested 48 h later in IP buffer and cleared lysates were incubated with FLAG agarose beads. A proportion of the whole cell lysate was analysed for total luminescence. The FLAG agarose beads were washed three times in IP buffer and the bound proteins were eluted using 150 ng/ml of FLAG peptide. The luminescence after immunoprecipitation was measured and normalised to the total luminescence of the sample. A fold binding was calculated by normalising to a FLAG-GFP control.

to allow this interaction, or the binding surface was not accessible. These data again highlight the limitations of the LUMIER assay and the use of large tags.

The interaction of C6 with FLAG-Ub was also tested in these assays, because data collected by members of the laboratory had shown an interaction between this molecule and other Bcl-2 family members (unpublished results). C6 LUC-tagged at either end was found to interact with FLAG-Ub (Figure 5.10). It is not possible to conclude from this assay whether this interaction is non-covalent or whether C6 itself is ubiquitinated and therefore the functional relevance of this interaction is currently unknown, but given the importance of ubiquitination in innate immune signalling (Chau et al, 2008) and the fact that TANK has been shown to be ubiquitinated (Gatot et al, 2007), this finding is very interesting.

5.7 C6 interacts with NAP1 and SINTBAD in addition to TANK by conventional IP

A number of problems had been encountered using the LUMIER assay to probe for interactions between C6 and innate immune signalling molecules, and therefore their potential interaction was investigated by conventional IP using signalling proteins tagged with the small FLAG epitope. HEK293 cells were transfected with plasmids encoding FLAG-tagged NAP1, SINTBAD, TANK or GFP as a negative control and 48 h later the cells were infected with vC6HA (2 p.f.u. per cell) for 16 h. The cells were then harvested in IP buffer and cleared lysates were subjected to immunoprecipitation with anti-FLAG agarose beads. Using this method C6-HA expressed by vC6HA was found to co-immunoprecipitate with FLAG-tagged NAP1, SINTBAD and TANK, but not GFP (Figure 5.11A).

To perform a reciprocal immunoprecipitation assay HEK293 cells were co-transfected with the same plasmids as above encoding FLAG-tagged NAP1, SINTBAD, TANK or GFP, in addition to TAP-tagged C6. After 48 h the cells were harvested and cleared lysates were subjected to immunoprecipitation with Streptavidin agarose beads to purify TAP-C6. In agreement with data presented in Figure 5.11A, an interaction was detected between C6 and NAP1, SINTBAD and TANK, but not GFP, confirming the specificity of this interaction (Figure 5.11B).

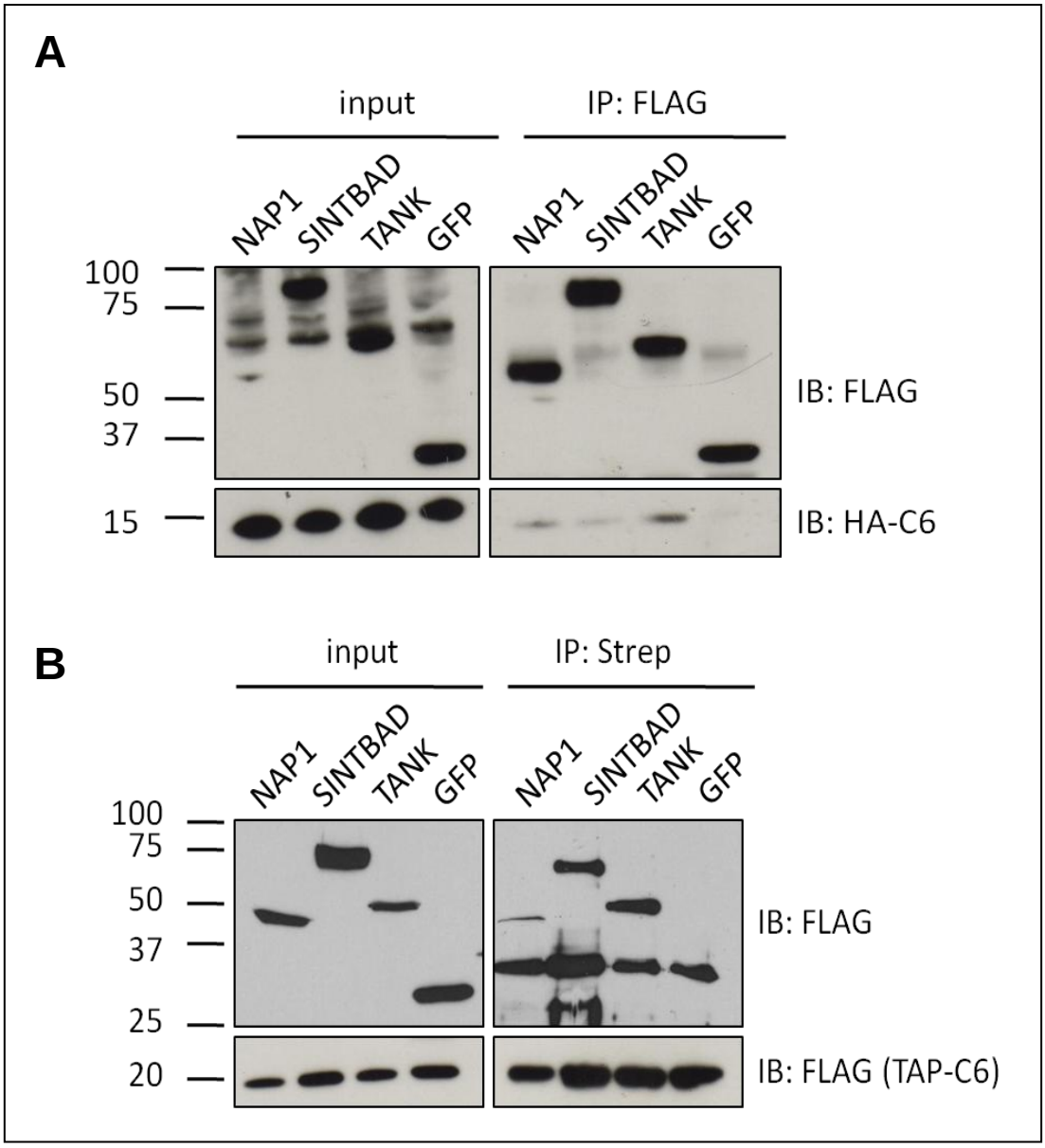

Figure 5.11: C6 interacts with NAP1, SINTBAD and TANK. (A) HEK293 cells were grown in 10-cm dishes and transfected with 10 μg of plasmids encoding FLAG-tagged NAP1, SINTBAD, TANK or GFP as indicated. After 48 h the cells were infected with vC6HA (2 p.f.u. per cell) for 16 h. The cells were harvested in IP buffer and the cleared lysates (input) were subjected to IP with anti-FLAG agarose beads. The proteins were separated by SDS-PAGE and detected by immunoblotting as indicated on the right. (B) HEK293 cells were grown in 10-cm dishes and transfected with 5 μg of plasmids encoding FLAG-tagged NAP1, SINTBAD, TANK or GFP and 5 μg of TAP-tagged (consisting of FLAG and Strep epitopes) C6 as indicated. After 48 h the cells were harvested in IP buffer and the cleared lysates (input) were subjected to IP with Streptavidin agarose beads. The proteins were separated by SDS-PAGE and detected by immunoblotting with antibodies, as indicated on the right. The location of protein molecular mass markers is also indicated (kDa).

Taken together these data indicated that despite the failure to find an interaction between C6 and SINTBAD and NAP1 by LUMIER assay, these molecules did in fact interact when tagged with smaller epitope tags. This interaction was observed with C6 tagged in two different ways suggesting the interaction was not an artefact of the epitope tag and was also observed in the context of a viral infection where C6 was expressed at natural levels (Figure 5.11A). Importantly, the interaction was also observed when immunoprecipitating either the adaptor proteins or C6, and FLAG-GFP was not found to interact.

5.8 The expression of C6 did not prevent the non-canonical IKK adaptor proteins from binding to TBK1

To gain a mechanistic understanding of how the interaction between C6 and the non-canonical IKK adaptor proteins NAP1, SINTBAD and TANK might inhibit IRF3 signalling, assays were performed to investigate whether the expression of C6 might prevent the interaction of these adaptors with known binding partners. This was achieved using two methods; the LUMIER assay and conventional immunoprecipitation assays using the inducible HEK293 T-REx TAP-C6 cell line (see Chapter 6).

TANK is known to interact with both TRAF3 and TBK1, thus forming a trimeric complex (Gatot et al, 2007). One possibility is that the binding of TANK to these two proteins links signalling upstream of TRAF3 to the non-canonical IKK complex, leading to TBK1 activation and the subsequent phosphorylation and activation of IRF3. As all three adaptors bind constitutively to TBK1 and IKKε, one hypothesis is that C6 may prevent this interaction and disconnect the link between upstream signalling molecules and the non-canonical IKK complex, preventing the activation of these kinases. To test this hypothesis HEK293 cells were co-transfected with a plasmid expressing LUC-TANK prey protein, a plasmid expressing a FLAG-tagged TBK1 or IKKε and varying quantities of a plasmid expressing un-tagged C6. After 48 h the cells were harvested for a LUMIER assay. In the absence of C6 both TBK1 and IKKε were found to interact with LUC-TANK, as expected (Figure 5.12A). The fold binding between TBK1 and TANK was slightly reduced by the presence of C6, although increasing quantities did not reduce this interaction further. The presence of C6 did not reduce the interaction of IKKε with TANK until 1500 ng of plasmid was transfected in a well of a six-well plate, and again this interaction was not reduced greatly.

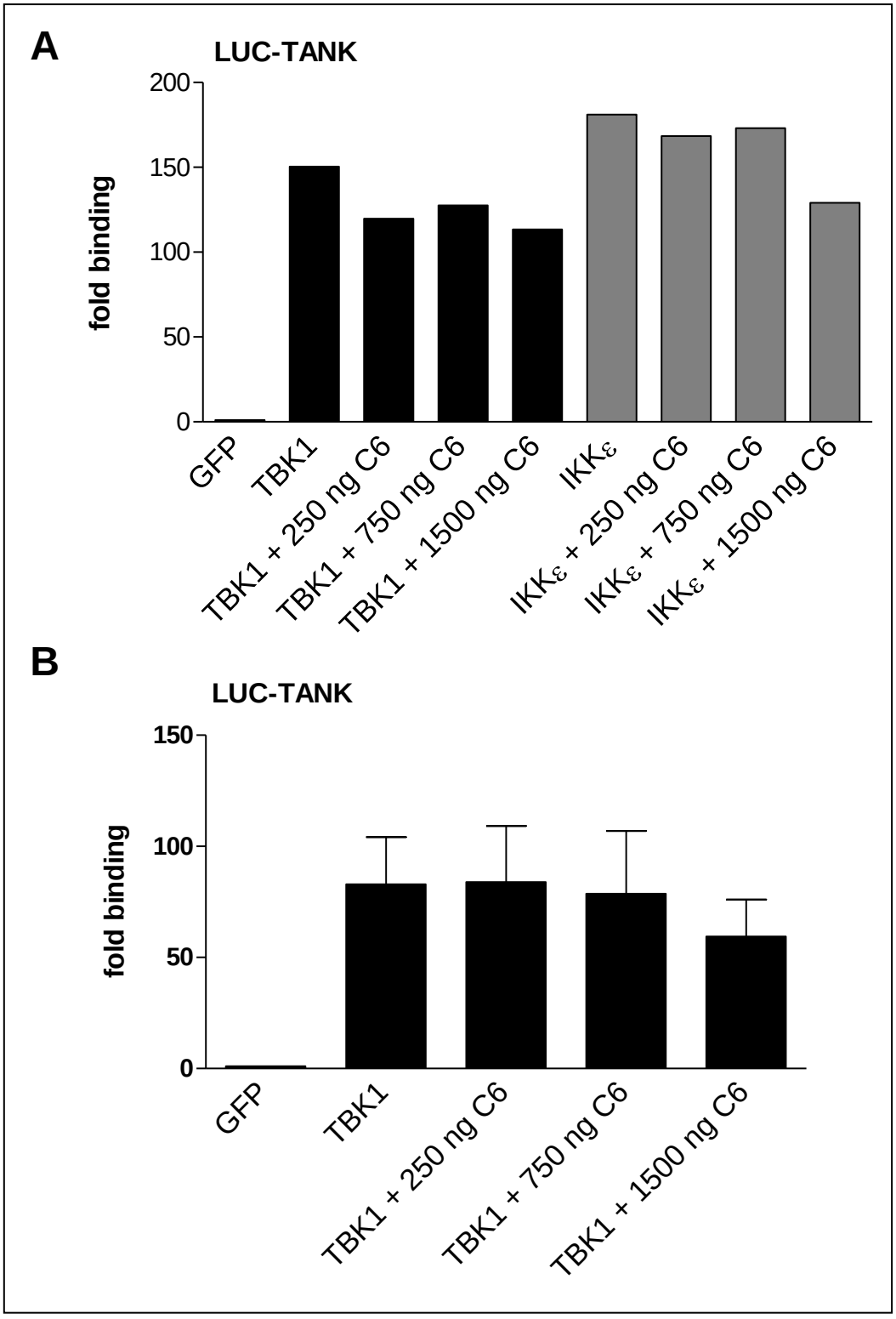

Figure 5.12: Interaction of TANK with TBK1 and IKKε in the presence of C6. HEK293 cells were co-transfected (A) or co-transfected in triplicate (B) with a plasmid expressing LUC – tagged TANK prey protein, a plasmid expressing a FLAG-tagged bait protein and varying quantities of a plasmid expressing un-tagged C6, as indicated. The cells were harvested 48 h later in IP buffer and the cleared lysates were incubated with FLAG agarose beads. A proportion of the whole cell lysate was analysed for total luminescence. The luminescence after immunoprecipitation was measured and normalised to the total luminescence of the sample. A fold binding was calculated by normalising to a FLAG-GFP control.

It was unclear from the data presented in Figure 5.12A whether the observed reduction in fold binding was significant, particularly because the LUMIER immunoprecipitation was performed from a single transfected well of a six-well plate. To allow for some statistical analysis to be performed the experiment was repeated for the TBK1-TANK interaction in triplicate. Upon averaging the fold bindings between LUC-TANK and TBK1 from three separate LUMIER immunoprecipitation assays no difference was found for these molecules in the presence or absence of C6 (Figure 5.12B). A small reduction was observed when cells were transfected with 1500 ng of a plasmid expressing C6, but this was not significant due to the size of the error bars.

A major advantage of the LUMIER assay is that to some extent it is a quantitative assay, particularly when comparing the interaction of the same molecules in various conditions, such as in the presence of varying quantities of C6. A major disadvantage of this assay, however, is achieving replicate fold binding data with a small standard deviation. This is challenging due to the number of steps in the protocol where variability between immunoprecipitations can occur. As such it is unlikely that statistically significant data will be achieved when only small differences in fold binding are observed, such as that presented in Figure 5.12. An additional disadvantage of this approach is that the cells were co-transfected with three different plasmids. Inevitably not all cells would be transfected will all three and not all cells would express C6. To overcome this non-uniform expression of C6 a conventional immunoprecipitation assay was performed using the inducible HEK293 T-REx TAP-C6 cell line. The advantage of this cell line was the fact that in the presence of doxycycline all cells would express C6.

To further investigate the interaction of TANK and the other two adaptor proteins with TBK1 HEK293 T-REx TAP-C6 cells were transfected in duplicate with a V5-TBK1 expression plasmid and a plasmid expressing HA- NAP1, - SINTBAD, - TANK or - N1 as a negative control. One dish per transfection was transfected in the presence of 2 μg/ml doxycycline to induce TAP-C6 expression. The cells were harvested 24 h later and cleared lysates were subjected to immunoprecipitation with mouse-anti-HA Ab coupled to protein G sepharose beads. In this assay V5-TBK1 was observed to co-immunoprecipitate with HA-NAP1, - SINTBAD and - TANK, but not HA-N1, indicating a specificity of the interaction between the adaptors and this kinase (Figure 5.13). Of note, N1 had been previously described to

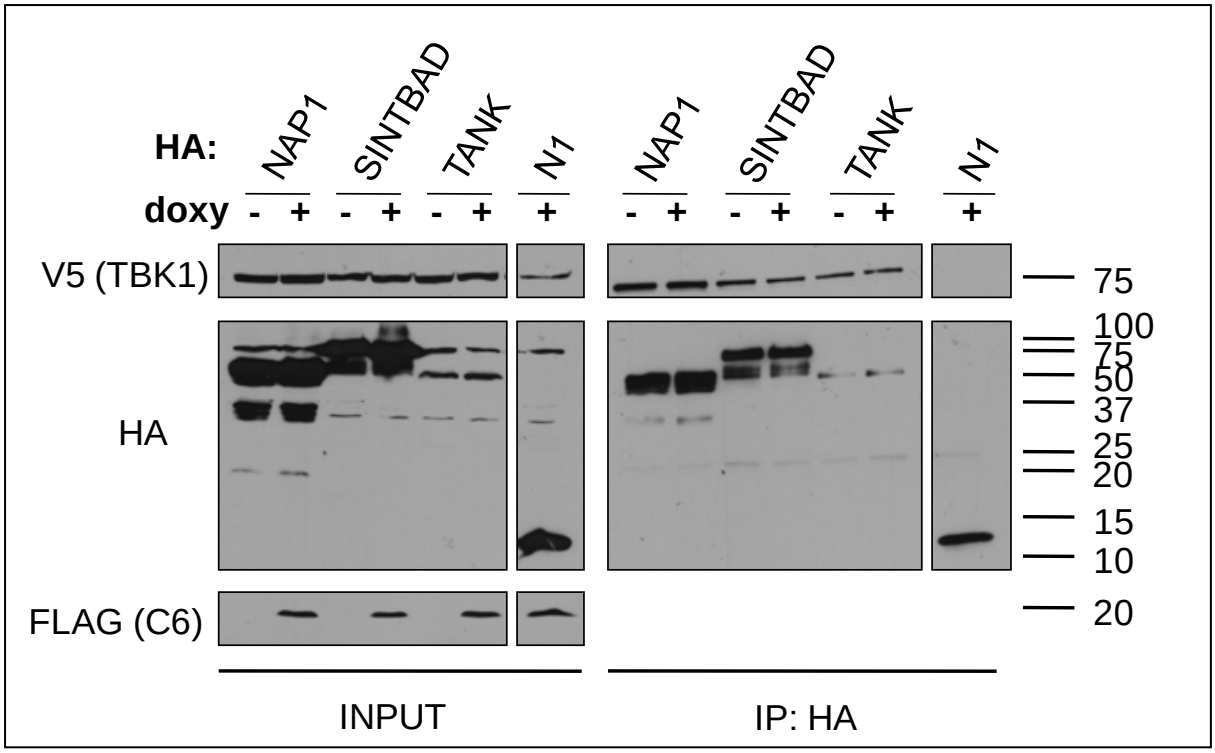

Figure 5.13: Interaction of TBK1 adaptor proteins with TBK1 in the presence of C6. (A) HEK293 T-REx TAP-C6 cells were grown in 10-cm dishes and transfected in duplicate with 5 μg of V5-TBK1 expression plasmid and 5 μg of a plasmid expressing HA- NAP1, - SINTBAD, - TANK or - N1 control. One dish per transfection was transfected in the presence of 2 μg/ml doxycycline (doxy) to induce TAP-C6 expression. The cells were harvested 24 h later in IP buffer and cleared lysates (INPUT) were subjected to IP with mouse-anti-HA Ab coupled to protein G sepharose beads. The proteins were separated by SDS-PAGE and detected by immunoblotting as indicated on the left. The location of protein molecular mass markers is indicated (kDa).

interact with TBK1 (DiPerna et al, 2004), but this interaction has not been repeated by members of our laboratory. In the presence of C6 the amount of TBK1 co-immunoprecipitated with the adaptor proteins was highly similar, indicating that the interaction of these molecules is not inhibited by the presence of C6, in agreement with data obtained by LUMIER assay (Figure 5.12).

5.9 The expression of C6 did not prevent binding of TANK to TRAF3, IRF3 or its homo-dimerisation

Given that the mechanism of C6 inhibition was unlikely to be due to it preventing the interaction between the kinases and the adaptor proteins, the known interaction of TANK

with other signalling molecules was tested. TANK was chosen as it was the best characterised adaptor molecule of the three. Since C6 was found to interact with the coiled-coil region of TANK (Figures 5.5 and 5.8), and this domain had been reported to be involved in the oligomerisation of TANK (Chin et al, 1999), it was hypothesised that the binding of C6 to this domain may preclude TANK homo-dimerisation. To test this, HEK293 cells were co-transfected with a plasmid expressing LUC-TANK prey protein, a plasmid expressing FLAG-TANK and varying quantities of a plasmid expressing un-tagged C6. The cells were then harvested 48 h later and a LUMIER assay was performed. An approximate 180-fold binding was observed between LUC- and FLAG-tagged TANK and this was not affected significantly by the presence of increasing amounts of C6 (Figure 5.14).

To confirm the result of the LUMIER assay HEK293 T-REx TAP-C6 cells were transfected in duplicate with a V5-TANK expression plasmid and a plasmid expressing HA - TANK or - N1 as a negative control. As for the experiment presented in Figure 5.13, one dish per transfection was transfected in the presence of 2 μg/ml doxycycline to induce TAP-C6 expression. The cells were then harvested 24 h later and cleared lysates were again subjected to immunoprecipitation with mouse-anti-HA Ab coupled to protein G sepharose beads. In agreement with the data obtained by LUMIER assay, the amount of V5-TANK co-immunoprecipitated with HA-TANK was similar in the presence or absence of C6, indicating that TANK homo-dimerisation can occur, and is not reduced by the presence of C6 (Figure 5.15). V5-TANK was not found to co-immunoprecipitate with HA-N1, as only a band corresponding to the Ab heavy chain at approximately 50 kDa (a little smaller than the size of V5-TANK) was observed.

As discussed previously, TANK has been proposed to link upstream signalling events to the non-canonical IKK complex by interacting with both TRAF3 and TBK1 to form a complex. Although the binding sites for TRAF3 and C6 on TANK do not overlap the structure of TANK has not been solved and therefore it is not possible to conclude from the primary sequence which domains of this protein would be in close proximity in three dimensional space. As such, the binding of C6 to TANK may preclude its interaction with TRAF3 which theoretically could then break the link between the non-canonical IKK complex and upstream signalling events. To test this hypothesis HEK293 cells were co-transfected with a plasmid expressing LUC-TANK prey protein, a plasmid expressing FLAG-TRAF3 bait protein and

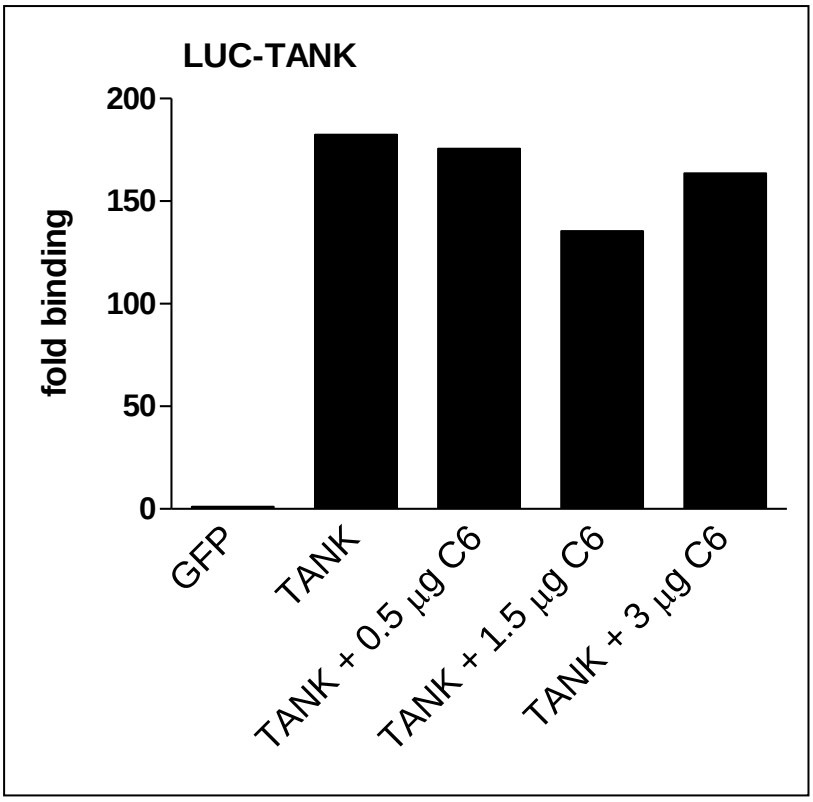

Figure 5.14: Homo-dimerisation of TANK in the presence of C6. HEK293 cells were co-transfected with a plasmid expressing LUC – tagged TANK prey protein, a plasmid expressing a FLAG-tagged bait protein and varying quantities of a plasmid expressing un-tagged C6, as indicated. The cells were harvested 48 h later in IP buffer and the cleared lysates were incubated with FLAG agarose beads. A proportion of the whole cell lysate was analysed for total luminescence. The luminescence after immunoprecipitation was measured and normalised to the total luminescence of the sample. A fold binding was calculated by normalising to a FLAG-GFP control.

varying quantities of a plasmid expressing un-tagged C6. The cells were then harvested 48 h later for a LUMIER assay. As expected, LUC-TANK was found to interact with FLAG-TRAF3 by LUMIER assay in the absence of C6, and this interaction was largely unaffected by the presence of this VACV protein (Figure 5.16). This interaction was also investigated by transfecting HEK293 T-REx TAP-C6 cells in duplicate in the presence or absence of C6 expression with a V5-TANK expression plasmid and a plasmid expressing FLAG-TRAF3 or N1-TAP as a negative control for the FLAG epitope. The cells were harvested 24 h later and cleared lysates were subjected to immunoprecipitation with mouse-anti-V5 Ab coupled to protein G sepharose beads. FLAG-TRAF3, but not N1-TAP was immunoprecipitated with V5-TANK and this interaction was not reduced in the presence of C6 (Figure 5.17). These

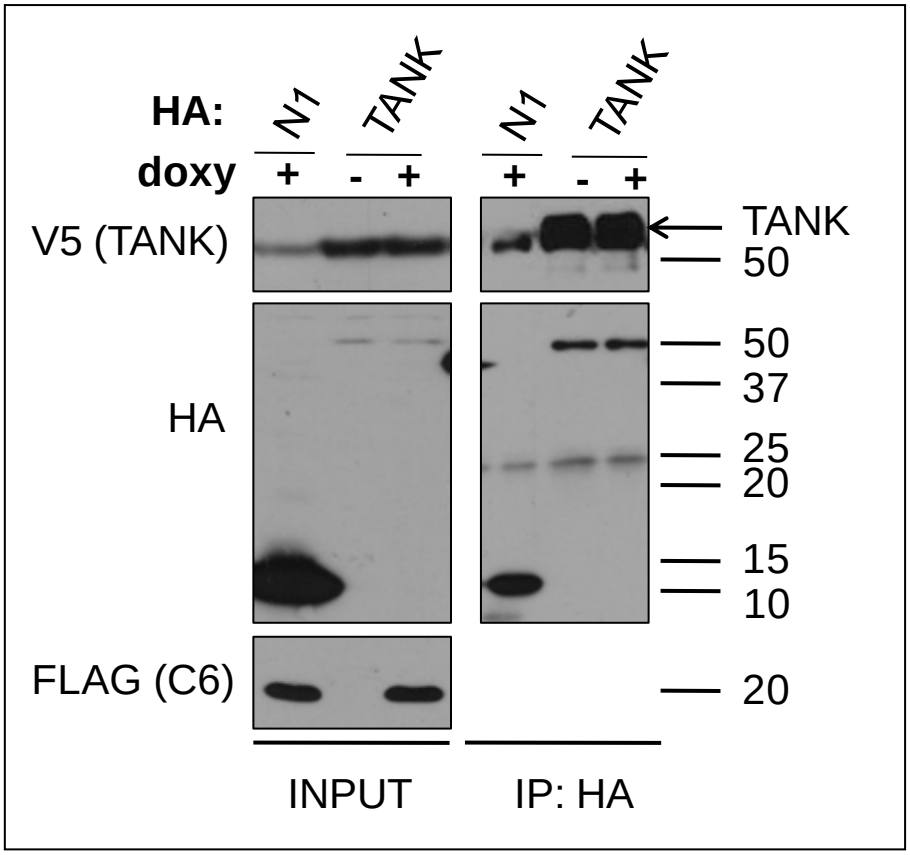

Figure 5.15: Homo-dimerisation of TANK in the presence of C6. (A) HEK293 T-REx TAP-C6 cells were grown in 10-cm dishes and transfected in duplicate with 5 μg of V5-TANK expression plasmid and 5 μg of a plasmid expressing HA - TANK or - N1 control. One dish per transfection was transfected in the presence of 2 μg/ml doxy to induce TAP-C6 expression. The cells were harvested 24 h later in IP buffer and the cleared lysates (INPUT) were subjected to IP with mouse-anti-HA Ab coupled to protein G sepharose beads. The proteins were separated by SDS-PAGE and detected by immunoblotting as indicated on the left. The location of protein molecular mass markers is indicated (kDa). The location of co-immunoprecipitated V5-TANK is indicated by the arrow.

data are in agreement with the LUMIER data presented in Figure 5.16 and indicated that the binding of C6 to TANK did not prevent this adaptor molecule from interacting with TRAF3.

Finally, an interaction between TANK and IRF3 had been described previously by Gatot and colleagues (Gatot et al, 2007). The binding of TANK to this transcription factor may bring it into proximity of the non-canonical IKK kinases, aiding the phosphorylation and activation of IRF3 by these kinases. Preventing the recruitment of IRF3 to this complex by inhibiting its interaction with TANK might inhibit IRF3 signalling and be beneficial to a virus. Because a FLAG-IRF3 plasmid was not available the interaction of TANK with IRF3 could not be

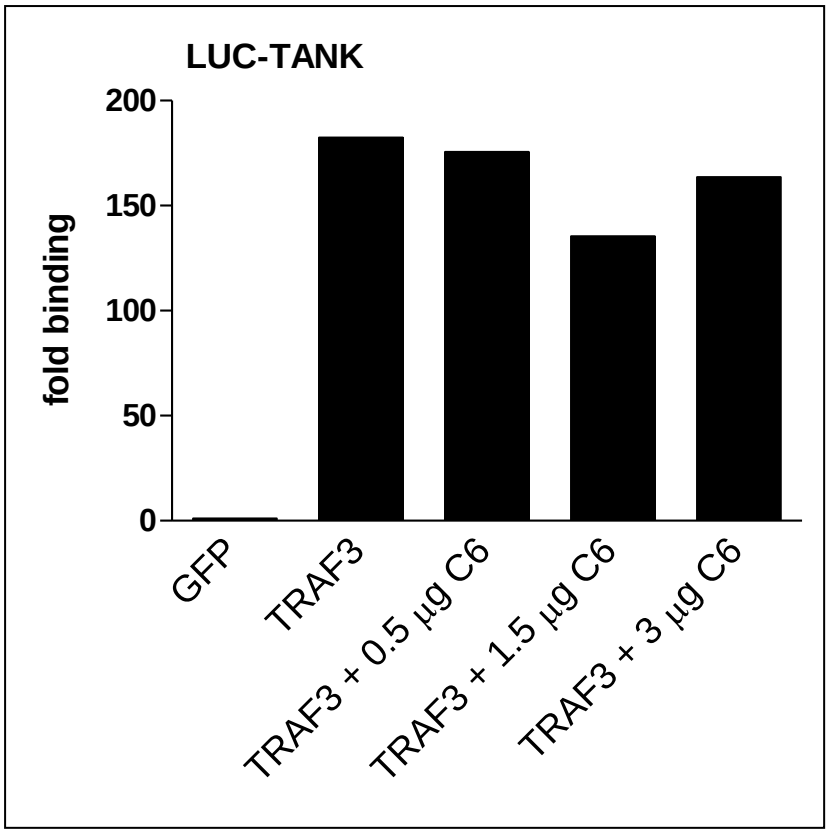

Figure 5.16: Interaction of TANK with TRAF3 in the presence of C6. HEK293 cells were co-transfected with a plasmid expressing LUC – tagged TANK prey protein, a plasmid expressing a FLAG-tagged bait protein and varying quantities of a plasmid expressing un-tagged C6, as indicated. The cells were harvested 48 h later in IP buffer and the cleared lysates were incubated with FLAG agarose beads. A proportion of the whole cell lysate was analysed for total luminescence. The luminescence after immunoprecipitation was measured and normalised to the total luminescence of the sample. A fold binding was calculated by normalising to a FLAG-GFP control.

investigated by LUMIER assay. Instead, HEK293 T-REx TAP-C6 cells were transfected in duplicate in the presence or absence of TAP-C6 with a V5-TANK expression plasmid and a plasmid expressing HA – IRF3 or - N1 negative control. The cells were then harvested 24 h later for an anti-V5 IP. Only very small amounts of HA-IRF3 were co-immunoprecipitated with V5-TANK, but this was a specific interaction as HA-N1 was not co-immunoprecipitated in this assay despite being well expressed (Figure 5.18). The interaction of IRF3 with TANK was not demonstrated by Gatot et al to be direct, but rather as part of a complex including TRAF3, TANK, TBK1 and IRF3. It is not known if TANK and IRF3 therefore interact directly and this may explain the weak binding observed in Figure 5.18. The presence of C6 nevertheless did not prevent this interaction.

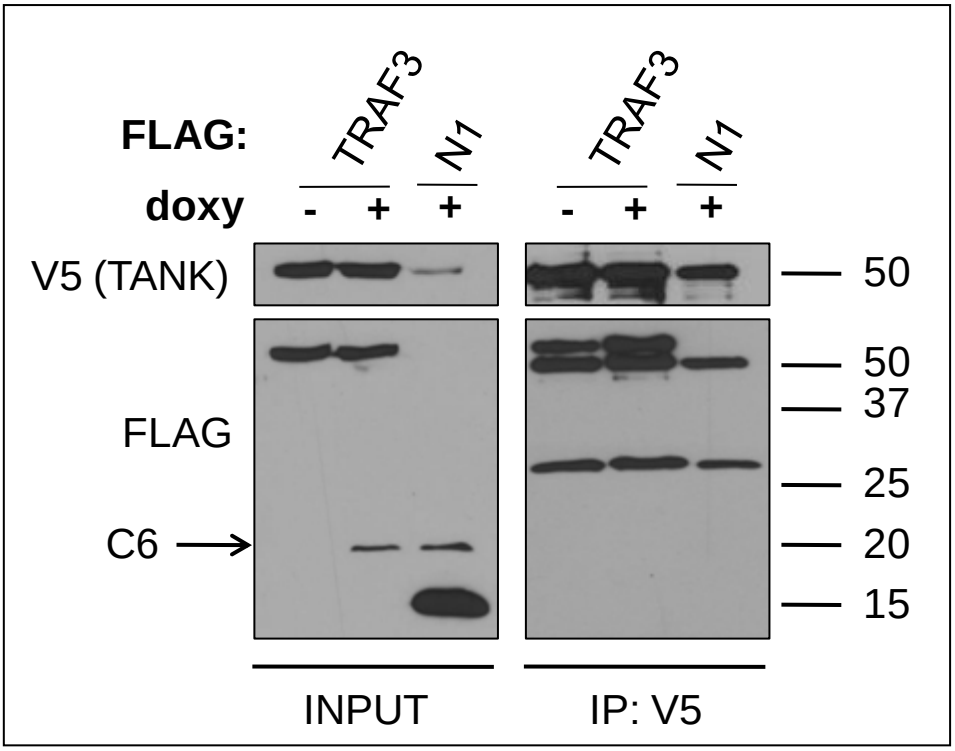

Figure 5.17: Interaction of TANK with TRAF3 in the presence of C6. HEK293 T-REx TAP-C6 cells were grown in 10-cm dishes and transfected in duplicate with 5 μg of V5-TANK expression plasmid and 5 μg of a plasmid expressing FLAG-TRAF3 or TAP-N1 control. One dish per transfection was transfected in the presence of 2 μg/ml doxy to induce TAP-C6 expression (indicated by the arrow). The cells were harvested 24 h later in IP buffer and cleared lysates (INPUT) were subjected to IP with mouse-anti-V5 Ab coupled to protein G sepharose beads. The proteins were separated by SDS-PAGE and detected by immunoblotting as indicated on the left. The location of protein molecular mass markers is indicated (kDa).

5.10 Summary

C6 was found to inhibit the IRF3 signalling pathway downstream, or at the level of the non-canonical IKK complex (Chapter 4) and therefore the potential binding of C6 to the known proteins of this complex was investigated by LUMIER assay. Using this method TANK was identified as an interaction partner for C6 and this was confirmed by conventional immunoprecipitation assay in the context of a viral infection. By constructing a set of TANK truncation mutants the binding site for C6 on TANK was identified as the N-terminal coiled-coil domain, because mutants lacking this domain failed to interact with C6 by LUMIER assay. In the case of mTANK, the coiled-coil domain alone was sufficient for binding to C6. Intriguingly, LUC-tagged full length hTANK was not found to interact with C6 by LUMIER assay, but a FLAG-tagged version of this protein was found to interact by conventional IP.

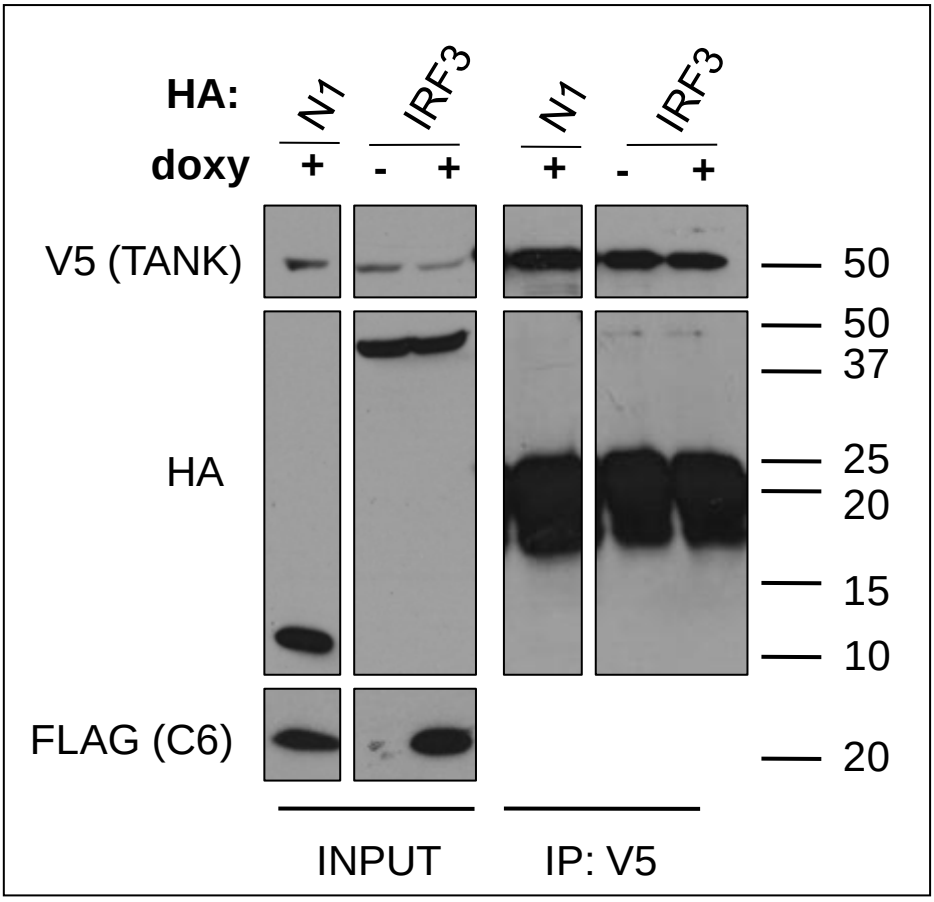

Figure 5.18: Interaction of TANK with IRF3 in the presence of C6. (A) HEK293 T-REx TAP-C6 cells were grown in 10-cm dishes and transfected in duplicate with 5 μg of V5-TANK expression plasmid and 5 μg of a plasmid expressing HA – IRF3 or - N1 control. One dish per transfection was transfected in the presence of 2 μg/ml doxy to induce TAP-C6 expression. The cells were harvested 24 h later in IP buffer and the cleared lysates (INPUT) were subjected to IP with mouse-anti-V5 Ab coupled to protein G sepharose beads. The proteins were separated by SDS-PAGE and detected by immunoblotting as indicated on the left. The location of protein molecular mass markers is indicated (kDa).

To link the binding of C6 to TANK to its ability to inhibit IRF3 signalling, an IFNβ reporter gene assay was performed in a TANK-null cell line. C6 was found to inhibit IFNβ induction in these cells and thus the binding of C6 to other proteins in this pathway was investigated further. To do this, plasmids expressing LUC-C6 and C6-LUC were constructed but these failed to interact with TANK, although they were able to dimerise with TAP-C6 suggesting they were folded to some degree. Interestingly LUC-tagged C6 was found to interact with FLAG-Ub in this assay. Given the possibility of the large luciferase tag precluding the interactions of some pairs of proteins, conventional immunoprecipitation assays were

performed with small epitope tags. Using this method NAP1 and SINTBAD, in addition to TANK, were found to interact with C6, and this occurred in the context of a viral infection.

Finally, to provide a mechanistic understanding of how the binding of C6 to the non-canonical IKK complex adaptor proteins might inhibit IRF3 signalling, LUMIER and immunoprecipitation assays were performed to investigate whether C6 expression could prevent, or reduce the interaction of these adaptors with other signalling molecules. C6 was found not to affect the interaction of any of the three adaptors with TBK1 and did not prevent the interaction of TANK with IKKε. In addition an effect of C6 on the interaction of TANK with TRAF3, IRF3 or TANK homo-dimerisation was not observed. Further assays are needed to fully understand the mechanism of IRF3 inhibition by C6.

Chapter 6: An un-biased approach for the identification of C6 binding partners

6.1 Construction of stable inducible cell lines expressing TAP-tagged C6

Data presented in Chapter 5 identified three novel binding partners for C6 using a directed approach based on knowledge of the function of this protein presented in Chapter 4. At the same time an un-biased method was also utilised for the discovery of novel binding partners. This approach was based on a TAP protocol described by Gloeckner and colleagues (Gloeckner et al, 2007). In that study proteins of interest were tagged with a TAP tag consisting of two StrepII epitopes and a FLAG epitope in tandem (Figure 6.1A) at either the N or C terminus of the protein. A stable HEK293 cell line was then constructed and cell lysates were subjected to a double purification protocol, first by incubation with strepactin superflow resin and then with FLAG agarose beads. The proteins eluted from the FLAG agarose beads were then separated by SDS-PAGE and silver stained so that proteins of interest could be identified and sent for mass spectrometry analysis.

The TAP protocol has a number of advantages for identifying novel protein-protein interactions. Firstly this a non-directed and hence non-biased approach, since the purification is performed from a large pool of proteins expressed by the cell. Secondly, this approach has been demonstrated to yield minimal false positives due to two rounds of purification and the choice of the Strep and FLAG epitopes, which both have a high affinity for the resin or beads used in this experiment (Gloeckner et al, 2007). Thirdly, the size of the tag is considerably smaller than those used in original TAP experiments where two IgG binding domains of protein A were fused to a calmodulin binding peptide domain, yielding a tag of 21 kDa (Rigaut et al, 1999). A tag of this size may preclude the correct folding of the protein being tagged and its presence may prevent potential protein-protein interactions.

To construct a stable inducible cell line expressing TAP-tagged C6, the C6 ORF was cloned using restriction enzyme digestion into pcDNA4/TO vectors previously engineered with either an N- or C-terminal TAP tag (designed by Brian Ferguson). This plasmid also contained a zeocin resistance cassette. Digestion of the N-terminal tag TAP-C6 plasmid with

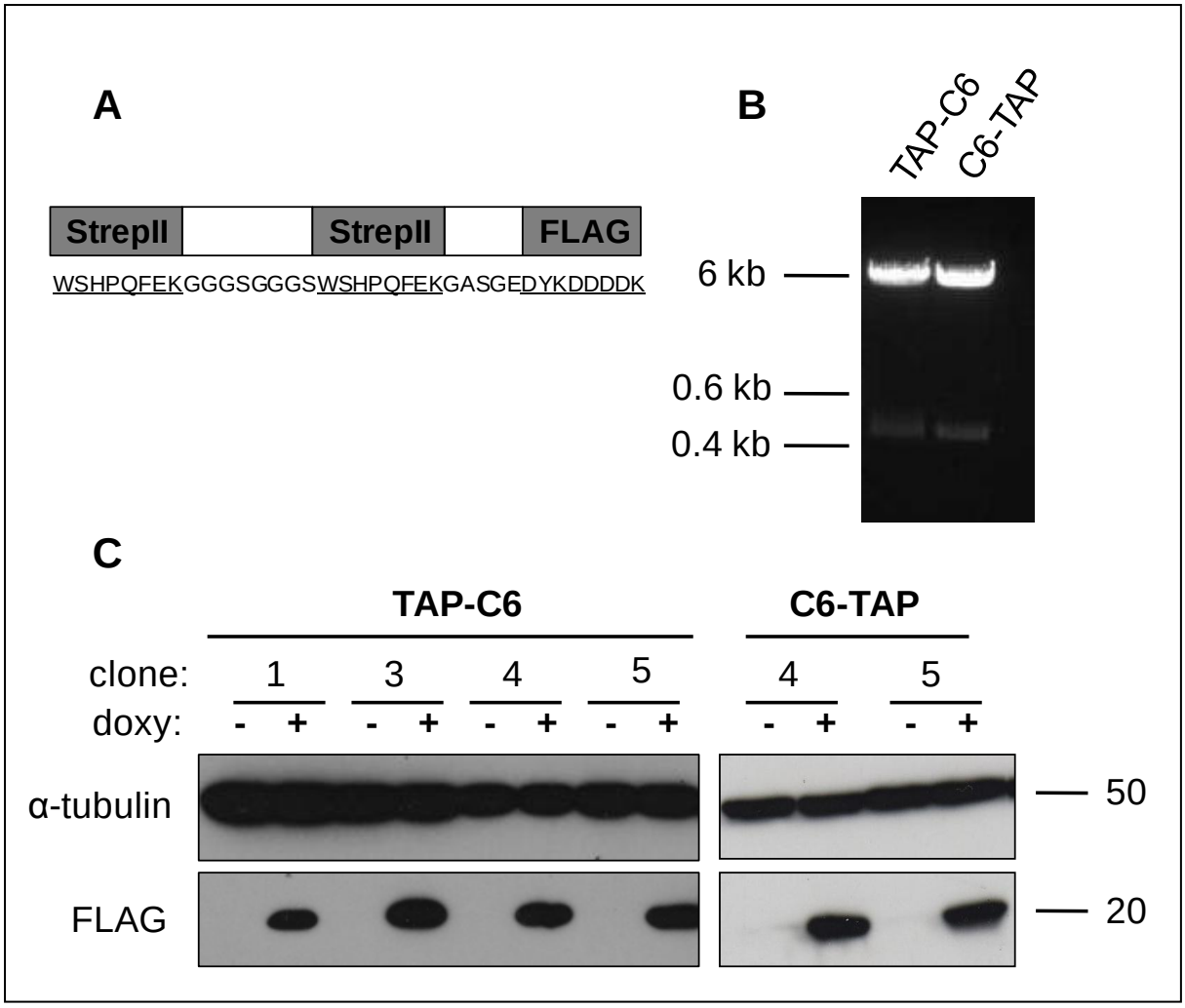

Figure 6.1: Construction of TAP-tagged C6 cell lines. (A) Tandem affinity purification (TAP) tag sequence and schematic. (B) C6 was cloned into the pcDNA4/TO TAP vectors using the restriction enzymes *Xba*I and *Not*I for N-terminal TAP and *Kpn*I and *Not*I for C-terminal TAP. To confirm the presence of the C6 ORF in these plasmids 1 μg of DNA was subjected to restriction enzyme digestion with the above enzymes and digestion products were separated by agarose gel electrophoresis on a 1 % gel. (C) Stable inducible cell lines were constructed by transfection of HEK293 T-REx cells followed by selection of clones in the presence of zeocin. The clones were tested for inducible expression of TAP-tagged C6 by growth for 24 h in the presence of 2 μg/ml doxycycline. Whole cell lysates were prepared, the proteins were separated by SDS-PAGE and then immunoblotted with mouse anti-tubulin or mouse anti-FLAG antibodies. The location of protein molecular mass markers is indicated (kDa).

*Xba*I and *Not*I, and the C-terminal tag C6-TAP plasmid with *Kpn*I and *Not*I excised an insert of approximately 450 bp, corresponding to the size of C6 (Figure 6.1B). These plasmids were then used to transfect HEK293 T-REx cells and stable clones were selected by growth in the presence of zeocin. The HEK293 T-REx cell line expresses the tetracycline repressor protein. Therefore, to induce expression of C6 from the stably transfected clones the cells were incubated in the presence of the tetracycline analogue doxycycline for 24 h. The cells were then harvested and the lysates subjected to SDS-PAGE and immunoblotting analysis using an anti-FLAG Ab, which binds to the FLAG epitope in the TAP tag. Four clones were selected for the TAP-C6 cell line and two were tested for the C6-TAP cell line. Expression of C6 was not observed in the absence of doxycycline in any clone, confirming that there was no leaky expression of this protein (Figure 6.1C). In the presence of doxycyline a band of approximately 20 kDa was observed for all tested clones, which corresponded to the expected size of C6 plus the 4.6 kDa TAP tag (Gloeckner et al, 2007). Clone 3 for the TAP-C6 cell line and clone 4 for the C6-TAP cell line were found to express slightly higher levels of TAP-tagged C6 and hence were selected for further analysis, although all clones were found to express good levels of this protein.

6.2 Mass spectrometry analysis of proteins purified with C6 from the HEK293 T-REx C6-TAP stable inducible cell line

As the HEK293 T-REx C6-TAP cell line was constructed first this was the one used for tandem affinity purification assay analysis. For a pilot experiment to optimise the TAP protocol 20 T175 flasks of HEK T-REx C6-TAP cells were prepared and half were induced to express C6-TAP by treatment with 2 μg/ml doxycycline for 24 h. The cells were then harvested and cleared lysates were subjected to a tandem affinity purification experiment, with samples taken at multiple steps during purification to analyse C6 expression and the efficiency of binding to and elution from the beads. These protein samples were subjected to SDS-PAGE using an Invitrogen NuPAGE 4-12% Bis-Tris polyacrylamide gel and immunoblotting analysis using an anti-FLAG Ab.

A band corresponding to the size of C6-TAP was present in the whole cell lysate (INPUT) from cells incubated in the presence of doxycycline but not in its absence, indicating expression of C6-TAP from the stable inducible cell line (Figure 6.2). Some C6-TAP was

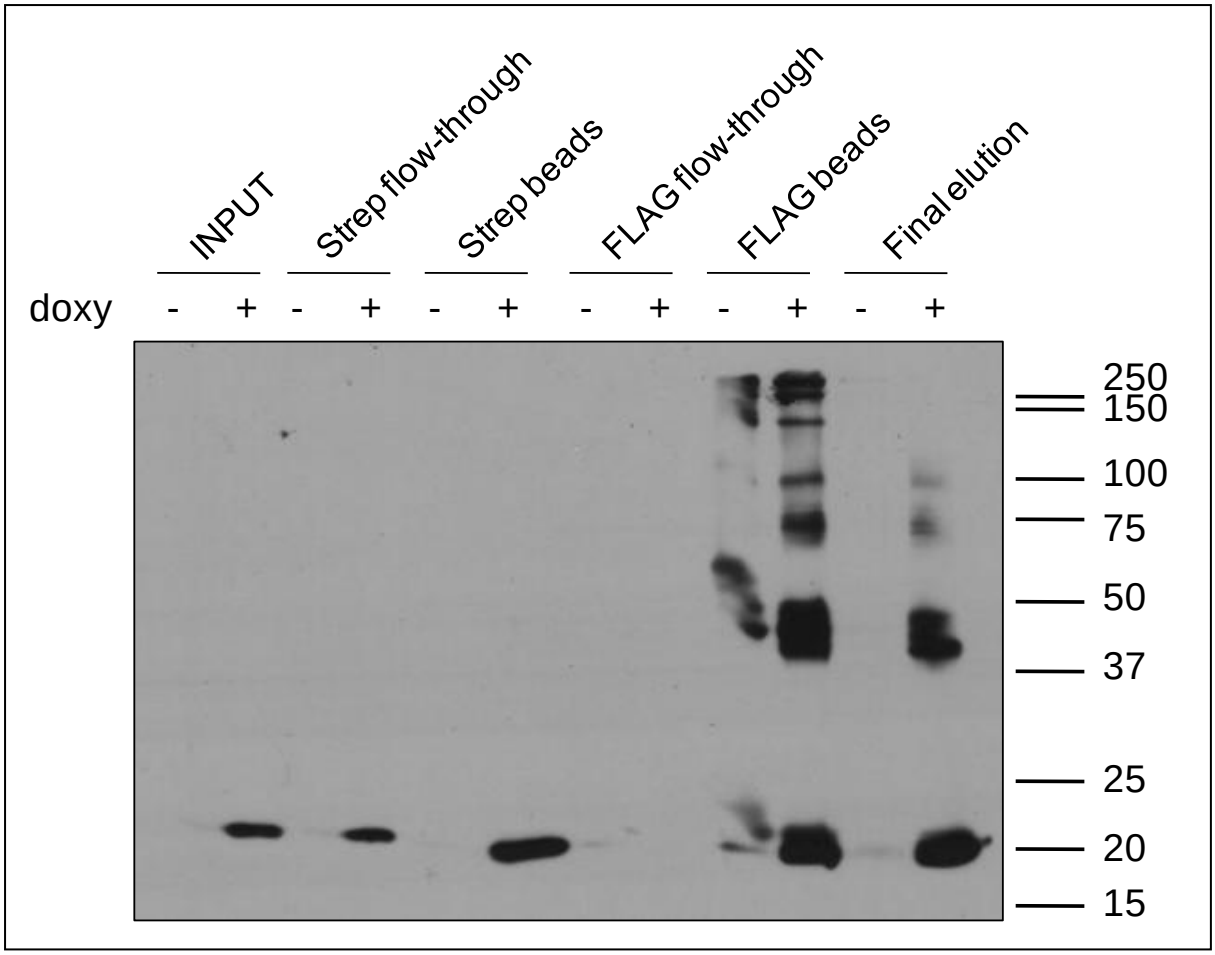

Figure 6.2: Immunoblot analysis of the tandem affinity purification assay using HEK293 T-REx C6-TAP cell line. Fractions of the tandem affinity purification assay were separated by SDS-PAGE and analysed by immunoblotting using a mouse-anti-FLAG Ab. Five times more Strep flow-through was loaded than INPUT sample. For the beads, the remaining protein associated with the beads after washing was eluted by boiling for 5 mins in the presence of protein sample loading buffer. One-fifth of the total final elution volume was used for immunoblotting analysis. The location of protein molecular mass markers is indicated (kDa).

detected in the streptactin bead flow-through suggesting that not all C6 had been captured by these beads. This was a step in the protocol that required optimisation and was later solved by incubating the whole cell lysate with more streptactin beads. Some C6-TAP was also associated with the streptactin beads following elution in the presence of des-thiobiotin. Again, this step required optimisation and two rounds of elution with des-thiobiotin was sometimes found to enhance the dissociation of C6 at this step. No C6-TAP was found in the FLAG bead flow-through indicating the efficient capture of this protein by the beads at this step. As with the strepactin beads a proportion of C6-TAP was still associated with the FLAG beads after elution in the presence of FLAG peptide and this was not improved by incubation

with a higher concentration of FLAG peptide, or two rounds of elution. A similar pattern of proteins was found in the final elution to those still associated with the FLAG beads. The band at approximately 20 kDa was presumed to be C6, and given data presented in Chapter 1 the band of approximately 40 kDa was thought to correspond to dimeric C6. A number of larger proteins were also present which could have been multimeric forms of C6, or C6 associated with potential interaction partners, because the NuPAGE buffer used for loading the samples in the Invitrogen NuPAGE 4-12% Bis-Tris polyacrylamide gels was not found to be as efficient at reducing samples as the protein sample buffer containing BME.

Following the optimisation of the TAP protocol the experiment was repeated and the proteins in the final elution and associated with both sets of beads were separated by SDS-PAGE as described above and the proteins were stained using the Invitrogen SilverQuest silver staining kit. Four main bands were identified that corresponded to proteins purified from cells incubated in the presence of doxycycline but not in its absence, as indicated by the black arrows in Figure 6.3. Three of these bands were present in the final elution and one was found still associated with the FLAG beads, presumably because this particular protein had not eluted well during the final incubation in the presence of FLAG peptide. These four bands were carefully excised and the proteins were identified by LC-MS/MS mass spectrometry at a service in Imperial College. The band at approximately 20 kDa was identified as VACV protein C6, indicating that C6 had been purified from the HEK293 T-REx cell line using this protocol. Unfortunately, only keratin contamination that appears in all mass spectrometry analysis was identified in the remaining three bands, presumably because the proteins present in these slices were below the limit of mass spectrometry detection and identification.

6.3 Mass spectrometry analysis of proteins purified with C6 from vC6TAP-infected cells

Two major disadvantages of using a stable inducible cell line for TAP experiments involving a viral protein are that the protein is expressed out of the context of other viral proteins, and protein-protein interaction analysis may be limited by the cell line chosen, for example by the lack of expression of the potential interaction partners in particular cell lines. To avoid these potential problems a recombinant virus expressing C6-TAP was constructed (see Chapter 3). This virus allowed protein-protein interaction analysis to be performed in multiple cell lines

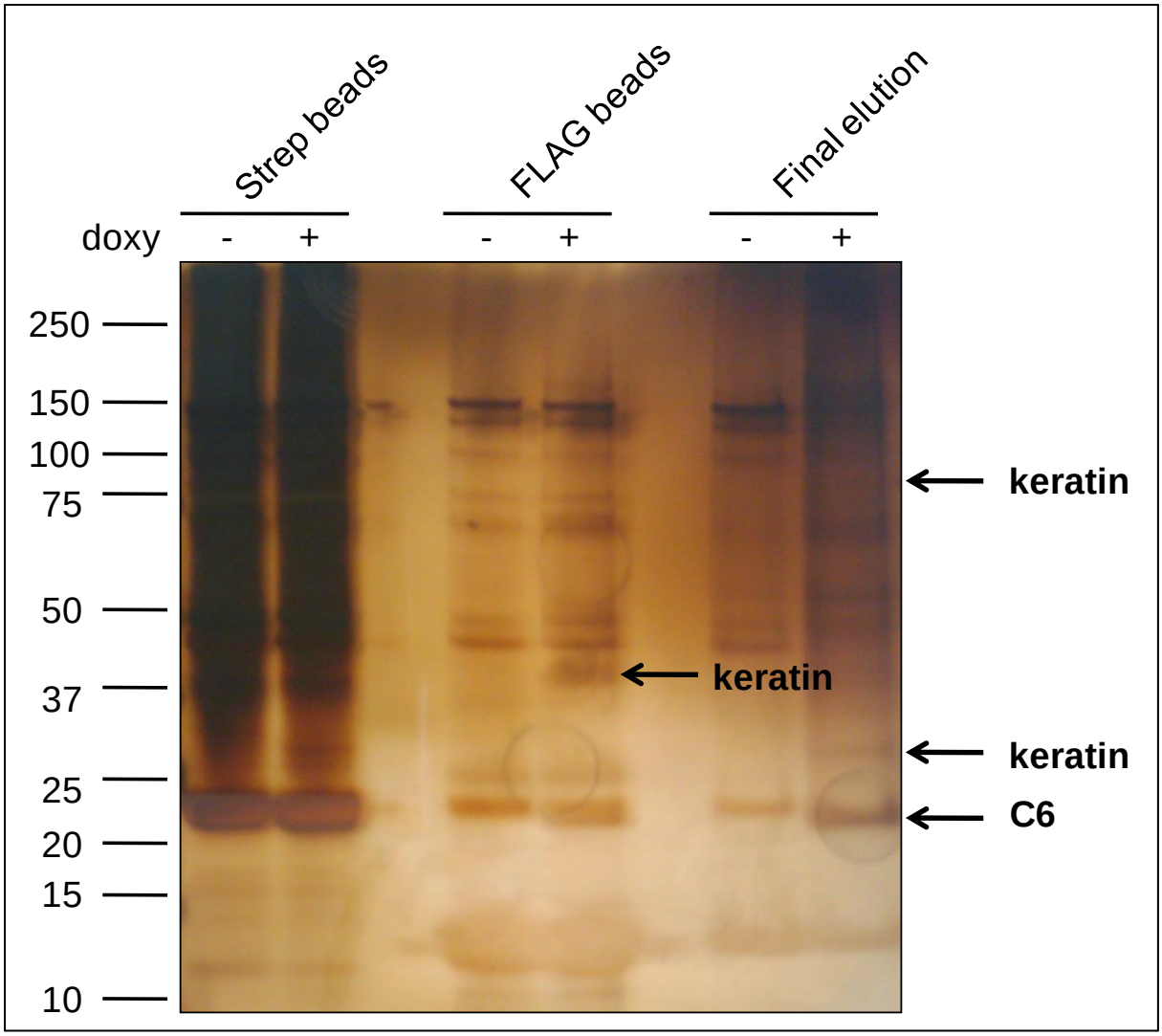

Figure 6.3: Tandem affinity purification assay using HEK293 TRex C6-TAP cell line. Twenty T175 flasks of HEK T-REx C6-TAP cells were prepared and half were induced to express C6-TAP by treatment with 2 μg/ml doxycycline (doxy) for 24 h. The cells were then harvested and cleared lysates were subject to a tandem affinity purification experiment. Proteins were separated by SDS-PAGE and stained using the Invitrogen SilverQuest silver staining kit. The bands of interest (indicated by arrows) were excised and sent for LC-MS/MS mass spectrometry analysis. The proteins that were identified are indicated. The location of protein molecular mass markers is also indicated (kDa).

where the expression of C6 would be in the context of a viral infection. This method would also potentially identify novel interactions between viral proteins.

To ascertain whether the pattern of bands observed in the final elution from the cell line would be similar to that obtained using the C6-TAP virus, 30 T175 flasks of HEK293 cells were prepared, half of which were infected overnight with 2 p.f.u. per cell of vΔC6 and the other half with vC6TAP. The cells were then harvested and the cleared lysates were subjected to a TAP experiment. The proteins in the final elution were separated by SDS-PAGE and stained using the Invitrogen SilverQuest silver staining kit as described above for the HEK293 T-REx C6-TAP cell line. Using this protocol a large number of proteins were purified with C6-TAP that were not purified from cells infected with the vΔC6 control, and this exceeded the number observed from the cell line (Figure 6.4A). This may have been because more C6-TAP was expressed from 15 flasks infected with vC6TAP than 10 flasks of the HEK293 T-REx C6-TAP cell line, or it could have been due to the presence of other viral proteins. As a direct comparison of expression from the virally-infected cells and the cell line was not made, it is not possible to conclude why more proteins were purified with virally expressed C6-TAP. Importantly however, proteins of a similar size to those sent for mass spectrometry analysis from the C6 cell line were also purified from vC6TAP infected cells (black arrows, Figure 6.4A).

To determine whether the pattern of proteins observed from infected HEK293 cells was unique to these cells or whether the pattern from other infected human cells might be similar, the tandem affinity purification assay was repeated using HCT116 cells. Whilst investigating the interaction of C6 with endogenous TANK, NAP1 and SINTBAD it was noted that TANK and NAP1 were more easily detected by immunoblotting from HCT116 lysates than HEK293 lysates, perhaps indicating that in this cell line the endogenous expression levels were higher (data not shown). The overall pattern of proteins purified with C6-TAP from vC6TAP-infected HCT116 cells was found to be highly similar to that from vC6TAP-infected HEK293 cells and, importantly, the amount of protein purified was higher, as indicated by the darker silver stained bands (Figure 6.4B). Although the pattern of proteins was similar, one notable difference was the relative intensities of the bands in the final elution, which seemed to differ between the two cell lines. For example, the protein of approximately 37 kDa which was hypothesised to be dimeric C6 was more abundant in infected HCT116 cells

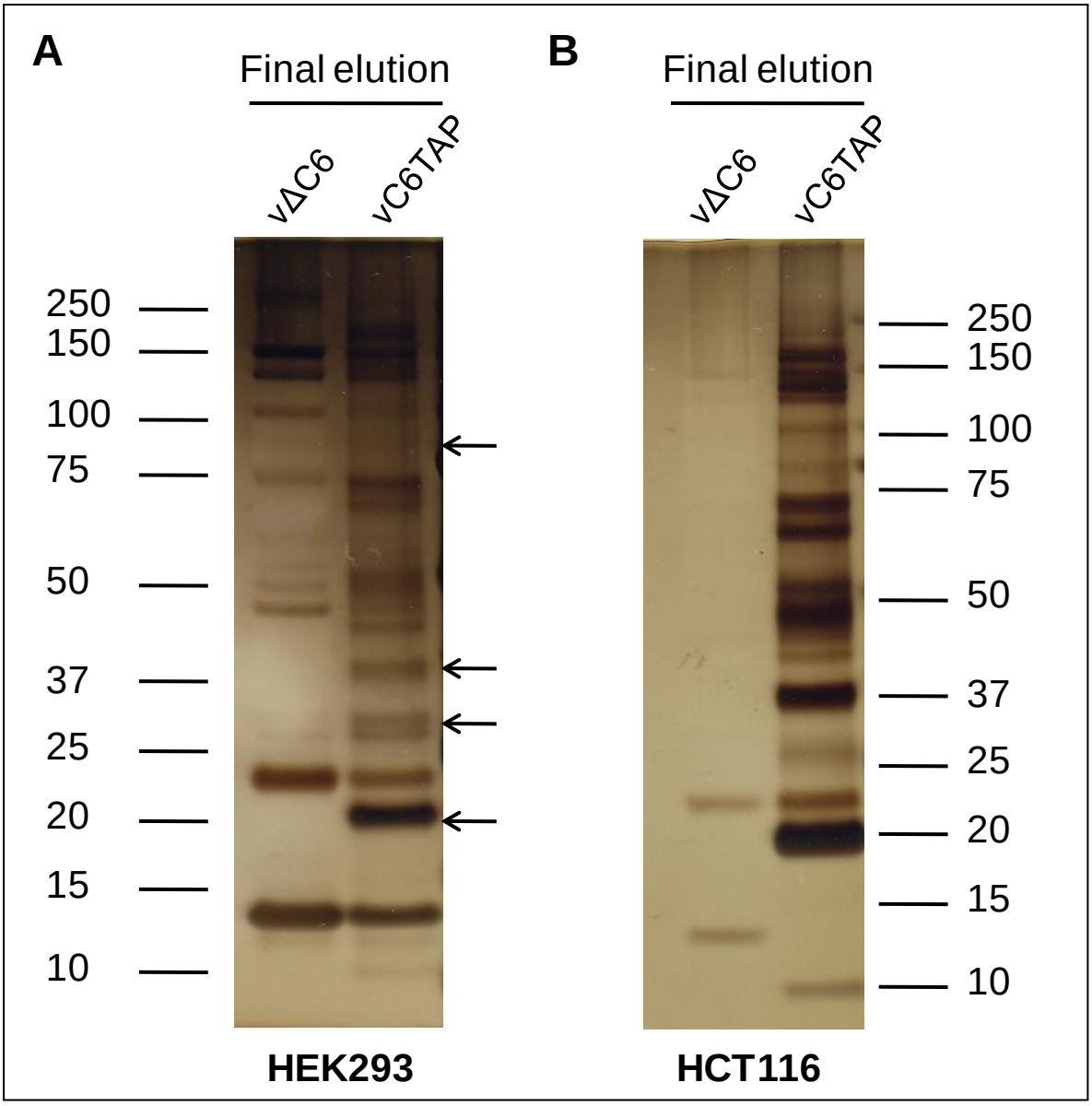

Figure 6.4: Tandem affinity purification assay following infection of cells with vC6TAP. Thirty T175 flasks of HEK293 (A) or HCT116 (B) cells were prepared, half of which were infected overnight with 2 p.f.u. per cell vΔC6 and the other half with vC6TAP. The cells were harvested and cleared lysates were subjected to a tandem affinity purification experiment. The proteins in the final elution were separated by SDS-PAGE and stained using the Invitrogen SilverQuest silver staining kit. The location of protein molecular mass markers is indicated (kDa). The black arrows indicate the size of the bands sent for mass spectrometry analysis from the HEK 293 T-REx cell line (Figure 6.3).

than HEK293 cells. A prominent protein of approximately 50 kDa was also visible in the HCT116 cell final elution that was present in much smaller quantities in the HEK293 cell elution. This band was of particular interest as it corresponded to the size of TANK. Given this finding and the fact that there was more protein overall in the final elution of the infected HCT116 cells, the experiment was repeated using these cells to send for LC-MS/MS mass spectrometry analysis.

For the mass spectrometry analysis 15 T175 flasks of HCT116 cells were infected overnight with vC6TAP and 15 were infected with a recombinant virus expressing TAP-tagged N1 (vN1TAP, Carlos Maluquer de Motes, unpublished results). The final elution was then sent to an LC-MS/MS mass spectrometry service at the University of Cambridge where the proteins were separated by SDS-PAGE and the gel cut into 16 equal slices per lane for identification of proteins in the individual slices. A small proportion of the final elution was retained, separated by SDS-PAGE and silver stained to visualise the proteins that had been purified with C6-TAP and not N1-TAP (Figure 6.5).

As with mass spectrometry analysis from the HEK293 T-REx cell line, the protein of approximately 20 kDa from vC6TAP-infected HCT116 cells was identified as VACV protein C6 (Figure 6.5). In addition to C6, 6 other proteins were identified as potential interacting partners. At the top of the gel a large protein of 450 kDa was identified as DNA-PKcs. This protein has a characterised role in DNA repair (Finnie et al, 1995), and more recently has been described as a DNA sensor as part of a complex with Ku70 and Ku80, with roles in the detection of foreign DNA and activation of IRF3 signalling ((Zhang et al, 2011), B. Ferguson et al, submitted). The proteins of 200 kDa, 70 kDa and 37 kDa were identified as Ub protein ligase E3 component n-recognin (UBR)1, heat shock protein (Hsp)70 and UBR2 respectively. These proteins form a complex that has a role in the N-end rule pathway of protein degradation (Nillegoda et al, 2010). This complex is responsible for the addition of a Ub moiety at the N terminus of target proteins marking them for degradation by the proteasome. This complex is important for the degradation of mis-folded cellular proteins and also viral proteins such as Sindbid virus RNA polymerase (de Groot et al, 1991) and HIV-1 integrase (Mulder & Muesing, 2000). A protein of approximately 150 kDa was identified as SWI/SNF related, matrix associated, actin dependent regulator of chromatin, subfamily c, member 1 (SMARCC1), also known as BAF155. This protein is a member of the SWI/SNF

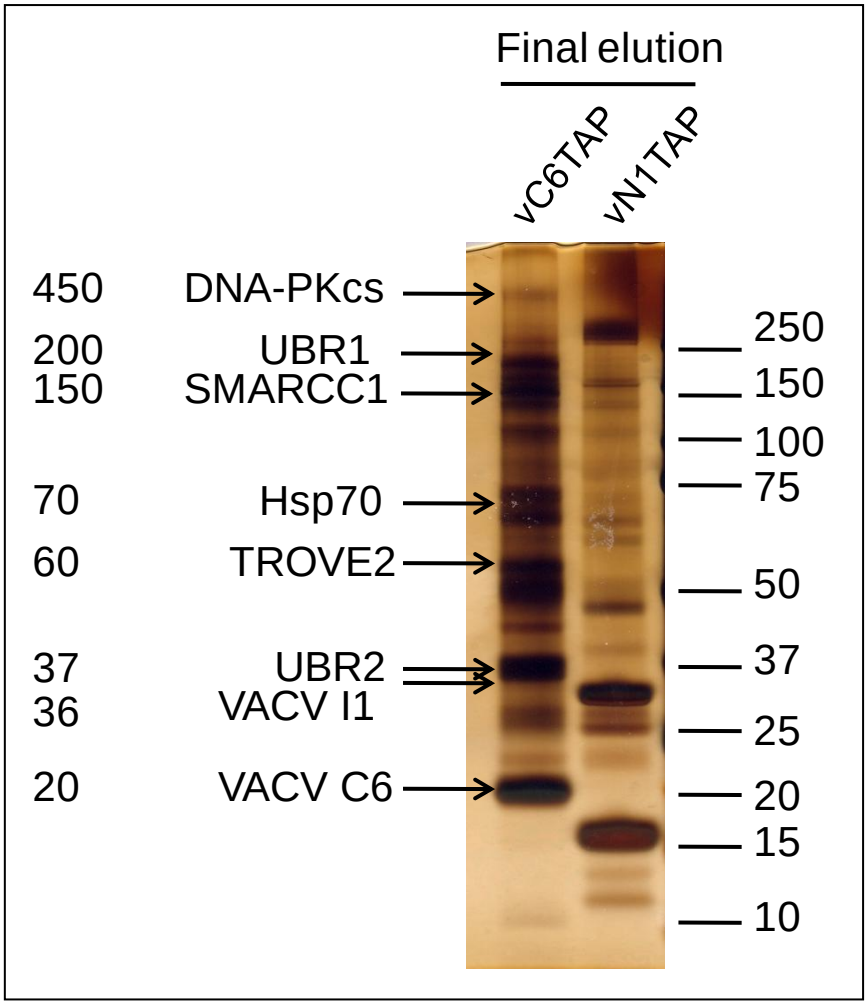

Figure 6.5: Potential C6 interaction partners identified by mass spectrometry. Thirty T175 flasks of HCT116 cells were prepared, half of which were infected overnight with 2 p.f.u. per cell of vC6TAP and the other half with vN1TAP. The cells were harvested and cleared lysates were subjected to a tandem affinity purification experiment. The final elution was sent for separation by SDS-PAGE and subsequent LC-MS/MS mass spectrometry analysis following the cutting of each lane of the gel into 16 equal slices. A proportion of the final elution was also separated by SDS-PAGE and stained using the Invitrogen SilverQuest silver staining kit. The proteins that were identified in the vC6TAP lane and not the vN1TAP lane, and their expected sizes (kDa), are indicated on the left. The location of protein molecular mass markers is indicated on the right (kDa). DNA-PKcs: DNA-protein kinase catalytic subunit, UBR: Ub protein ligase E3 component n-recognin, SMARCC1: SWI/SNF related, matrix associated, actin dependent regulator of chromatin, subfamily c, member 1, Hsp70: heat shock protein 70, TROVE2: TROVE domain family member 2.

family whose members possess ATPase and helicase activities and have roles in transcriptional regulation by chromatin remodelling (Wang et al, 1996). Gastric cancer MDR protein variant, or TROVE domain family member 2 (TROVE2), a protein of approximately 60 kDa was also identified as a potential C6 binding partner. TROVE2 is a ribonucleoprotein with the ability to bind several small cytoplasmic Y RNAs, potentially stabilising them from degradation (Deutscher et al, 1988). Finally a protein of 36 kDa was identified as VACV protein I1. I1 is a late expressed protein found in the virion core with DNA binding ability (Klemperer et al, 1997). Importantly, the identification of VACV I1 supports the use of this method for identifying novel viral protein-viral protein interactions. Further, this interaction was not identified in a large yeast two-hybrid screen of vaccinia virus protein-protein interactions (McCraith et al, 2000).

Given its mass the protein of approximately 37 kDa was hypothesised to be dimeric C6. This hypothesis was supported by the fact that C6 was shown to co-immunoprecipitate with another molecule of C6 (Chapter 3) and a protein of approximately 37 kDa was identified by a FLAG Ab from a previous TAP assay (Figure 6.3). Nevertheless mass spectrometry analysis did not identify protein C6 in the gel slice containing proteins of this mass (Figure 6.5). A potential reason for this is that dimeric C6 may be a very small component of the protein band observed at approximately 37 kDa. Indeed, VACV protein I1 is 36 kDa and may represent the majority of protein in the band of this size. Supporting this hypothesis is the fact that the protein samples are prepared with Nu-PAGE buffer that contains some reducing agent and thus prevents proteins from resolving by PAGE as complexes. Further, the protein band corresponding to dimeric C6 in immunoblotting data presented in Figure 6.3 is less strong than the band for monomeric C6, indicating substantially less dimeric C6 in this gel.

Interestingly, TANK, NAP1 and SINTBAD were not identified by mass spectrometry as interacting partners of C6. Given that confirming an endogenous interaction between C6 and these signalling adaptor molecules was problematic it may be that these proteins are not expressed at sufficient levels for identification by mass spectrometry. As a direct interaction between C6 and TANK, NAP1 or SINTBAD has not been demonstrated, it is possible that these proteins interact as part of a complex and again sufficient amounts of this complex may not have been purified for successful mass spectrometry analysis. It is also possible that the

interaction is weak or transient, or it may only occur at certain time points p.i., for example very early.

6.4 An interaction between C6-TAP and DNA-PKcs could not be confirmed by conventional IP

Following the identification of potential interaction partners by tandem affinity purification and mass spectrometry analysis it is important to confirm these interactions by other methods. To confirm the interaction between C6 and DNA-PKcs HCT116 cells were infected overnight with vC6TAP, or vN1TAP as a negative control. The cells were harvested and cleared lysates were subjected to IP with Streptactin beads to purify the TAP-tagged protein. Using this method DNA-PKcs was co-immunoprecipitated with both C6TAP and N1TAP, suggesting that this result may have been a false positive (Figure 6.6A). To further investigate this a reciprocal IP assay was performed where lysates of HCT116 cells infected with vC6TAP or vN1TAP were incubated with a DNA-PKcs Ab coupled to protein G sepharose beads. DNA-PKcs was immunoprecipitated from these lysates in the presence of the DNA-PKcs Ab, but not by the protein G sepharose beads alone (Figure 6.6B). In addition Ku70, a known interaction partner of DNA-PKcs (Gottlieb & Jackson, 1993) was co-immunoprecipitated in this assay, but neither C6 nor N1 were co-purified. Taken together these data indicated that DNA-PKcs did not interact specifically with C6 and may have been purified non-specifically during the TAP assay. By conventional IP DNA-PKcs was found to co-immunoprecipitate with both C6-TAP and N1-TAP, but it was not identified in the N1 lane by mass spectrometry. A potential explanation for this is that it was present, but was below the limit of detection.

6.4 An interaction between C6-TAP and SMARCC1 was confirmed by conventional IP

To confirm the interaction between C6 and SMARCC1 HEK293 cells were infected overnight with vC6TAP or vN1TAP. The cells were then harvested and cleared lysates were subjected to IP with protein G sepharose beads coupled with rabbit-anti-SMARCC1 Ab or with anti-FLAG agarose beads. Endogenous SMARCC1 was detected in the cell lysate using

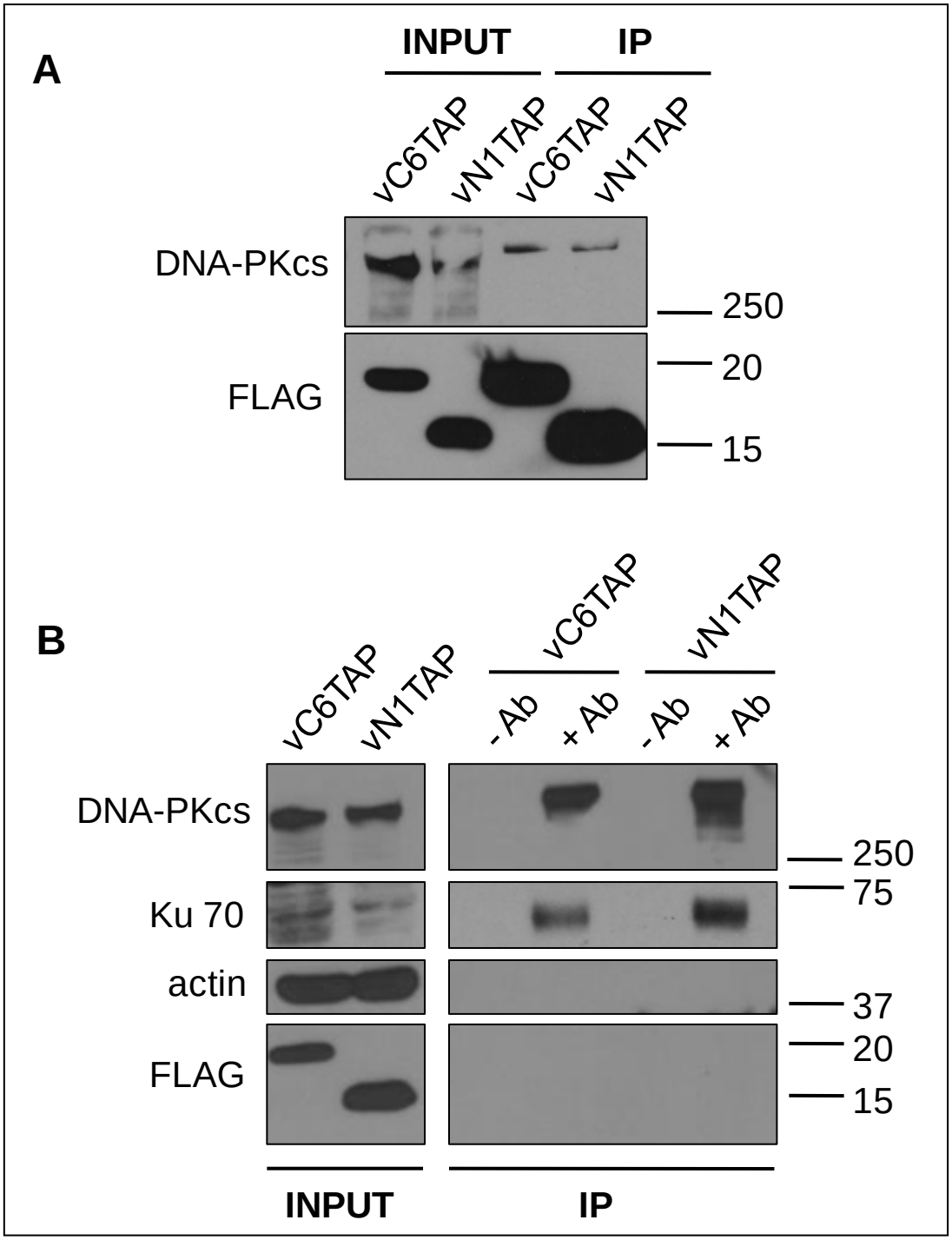

Figure 6.6: C6-TAP does not interact with DNA-PKcs. HCT116 cells were infected overnight with vC6TAP or vN1TAP (2 p.f.u. per cell). The cells were harvested in TAP IP buffer and cleared lysates (INPUT) were subjected to IP with Streptactin beads (A) or protein G sepharose beads coupled (+ Ab) or not coupled (- Ab) to mouse-anti-DNA-PKcs Ab. The proteins were separated by SDS-PAGE and detected by immunoblotting as indicated on the left. The location of protein molecular mass markers is indicated on the right (kDa).

the rabbit-anti-SMARCC1 Ab, and this Ab was also suitable to IP SMARCC1 (Figure 6.7). SMARCC1 was not immunoprecipitated with the rabbit-anti-HA control Ab demonstrating the specificity of this IP. Although SMARCC1 was found to co-immunoprecipitate with C6-TAP purified using FLAG agarose beads and not N1-TAP, C6-TAP was not co-immunoprecipitated with SMARCC1 purified using the SMARCC1 Ab coupled to protein G beads. These data confirmed the mass spectrometry data, but an interaction was not observed when purifying SMARCC1 rather than C6. A different SMARCC1 Ab may need to be tested to observe this interaction.

6.5 An interaction between C6-TAP and UBR1 was confirmed by conventional IP

In a similar experiment to the one described in section 6.4, UBR1 was found to co-immunoprecipitate with C6-TAP purified from the lysate of HEK293 cells infected with vC6TAP (Figure 6.8). This interaction was specific as UBR1 was not observed to interact with N1-TAP expressed by vN1TAP. A reciprocal IP experiment was performed purifying UBR1 from lysates using a rabbit-anti-UBR1 Ab coupled to protein G sepharose beads. A small amount of UBR1 was immunoprecipitated in this assay, but C6 was not co-immunoprecipitated. These data confirmed the mass spectrometry data, but in order to observe the interaction in the reciprocal IP, again, another Ab more suitable for the IP of UBR1 may be required.

6.6 Summary

As a non-biased approach to identify novel C6 interaction partners, cell lines expressing TAP-tagged C6 were constructed by stable transfection of HEK293 T-REx cells. The HEK293 T-REx C6-TAP cell line was used for a TAP assay and 4 protein bands from an SDS-PAGE protein gel were sent for LC-MS/MS mass spectrometry analysis. The band of 20 kDa was identified as VACV protein C6, but only keratin contamination was identified in the other three bands.

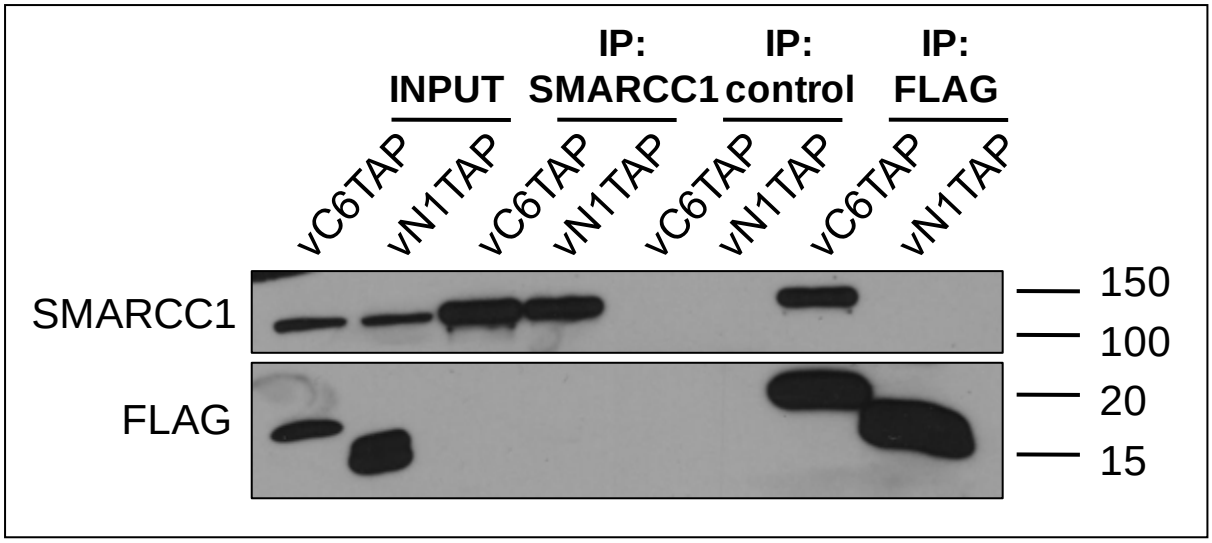

Figure 6.7: C6-TAP interacts with SMARCC1. HEK293 cells were infected overnight with vC6TAP or vN1TAP (2 p.f.u. per cell). The cells were harvested in TAP IP buffer and cleared lysates (INPUT) were subjected to IP with protein G sepharose beads coupled with rabbit-anti-SMARCC1 or rabbit-anti-HA (control) Ab or with anti-FLAG agarose beads, as indicated. The proteins were separated by SDS-PAGE and detected by immunoblotting as indicated on the left. The location of protein molecular mass markers is indicated on the right (kDa).

To identify novel interaction partners using other cell types and in the context of a viral infection, the recombinant virus expressing C6-TAP (vC6TAP, see Chapter 3) was used to infect HEK293 or HCT116 cells and a TAP assay was performed. The pattern of proteins observed in the final elution was highly similar between the two cell types, but the relative abundance of each protein differed somewhat. Proteins in the final elution of the TAP experiment performed from lysates of HCT116 cells infected with vC6TAP were analysed by mass spectrometry and compared to proteins purified by this method from cells infected with vN1TAP. From this experiment DNA-PKcs, UBR1, UBR2, Hsp70, TROVE2 and VACV protein I1 were identified as potential C6 binding partners. The interaction of C6 with UBR1 and SMARCC1 was confirmed by conventional IP, but the interaction between C6 and DNA-PKcs was found to be non-specific, because this protein also co-immunoprecipitated with N1-TAP. DNA-PKcs was therefore likely to be a false positive hit and thus highlights the importance of confirming mass spectrometry data by another method such as a conventional IP assay. Further assays need to be performed to confirm the interaction of C6 with the other identified proteins and to understand the biological relevance of these interactions.

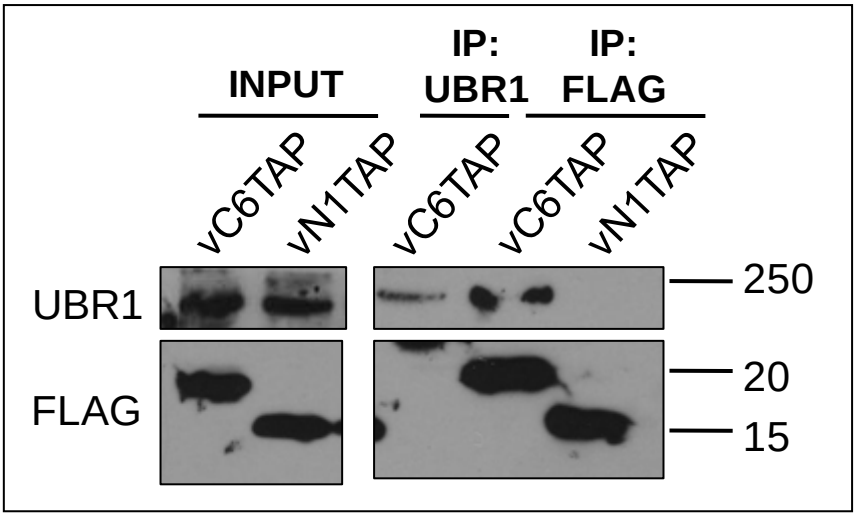

Figure 6.8: C6-TAP interacts with UBR1. HEK293 cells were infected overnight with vC6TAP or vN1TAP (2 p.f.u. per cell). The cells were harvested in TAP IP buffer and cleared lysates (INPUT) were subjected to IP with protein G sepharose beads coupled with rabbit-anti-UBR1 Ab or with anti-FLAG agarose beads, as indicated. The proteins were separated by SDS-PAGE and detected by immunoblotting as indicated on the left. The location of protein molecular mass markers is indicated on the right (kDa).

Chapter 7: Contribution of C6 to VACV virulence

7.1 Deletion of C6 has no effect on viral replication or spread *in vitro*

Before investigating the role of C6 during infection *in vivo*, the recombinant viruses were analysed *in vitro* to ascertain whether the deletion of C6 had an effect on viral replication and spread. The effect of C6 on viral spread was tested using three cell lines of different animal origin; African green monkey kidney BSC-1 cells, rabbit kidney RK-13 cells and human osteosarcoma TK143 cells. These cells were infected at low p.f.u. per cell with the C6 recombinant viruses (vC6WR, vΔC6, vC6Rev and vC6FS) for 72 h and the size of the resulting plaques was measured by microscopy. The plaque size of the viruses expressing or lacking C6 was found to be similar in all of the cell types tested suggesting that the deletion of *C6L* had no effect on viral spread *in vitro* (Figure 7.1).

In addition to analysing the plaque size of the C6 recombinant viruses, single- and multi-step growth curves were generated using BSC-1 cells. For the single-step growth curve to analyse viral replication, the cells were infected in duplicate with 10 p.f.u. per cell and the virus was harvested at 12 h and 24 h p.i., with careful separation of the intracellular and extracellular viral components, and was titrated on monolayers of BSC-1 cells. The production of both intracellular (predominantly IMV, Figure 7.2A) and extracellular (predominantly EEV, Figure 7.2B) virus was found to be similar amongst the four recombinant viruses indicating that the deletion of *C6L* did not affect viral replication *in vitro*.

For the multi-step growth curve to analyse viral spread, the cells were infected in duplicate with 0.01 p.f.u. per cell and the virus was harvested at 24 h, 48 h and 72 h p.i., again with careful separation of intracellular (Figure 7.2C) and extracellular (Figure 7.2D) viral components, and was titrated. As with the single-step growth curves, the multi-step growth curves for both IMV and EEV were found to be similar, demonstrating that the lack of C6 did not affect viral spread, in agreement with data presented in Figure 7.1.

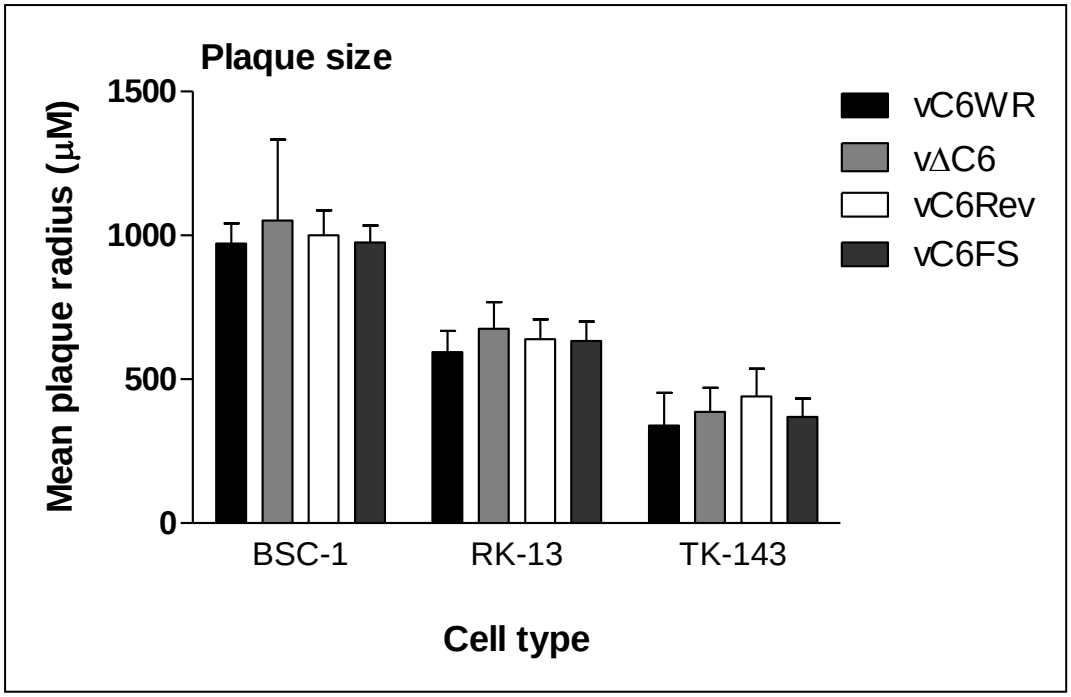

Figure 7.1: Plaque size analysis of C6 recombinant viruses *in vitro*. Six-well plates of BSC-1 (African green monkey), RK-13 (rabbit) and TK143 (human) cells were infected for 72 h at 50 p.f.u. per well. The cells were stained with crystal violet and the plaque size was measured using Axiovision 4.6 software and a Zeiss Axiovert 200M microscope. Results are expressed as the mean plaque radius (μM) ± SD.

7.2 Purification of C6 recombinant viruses for *in vivo* characterisation

Other members of the VACV Bcl-2 family have been characterised as virulence factors *in vivo*. This includes proteins A46 (Stack et al, 2005), A52 (Harte et al, 2003), B14 (Chen et al, 2006a), K7 (S. Lucas and A. Fahy, unpublished data) and N1 (Bartlett et al, 2002), where in all cases deletion of the encoding gene from WR led to the attenuation of the virus in at least one model of murine infection. Outside of the Bcl-2 family other VACV immunomodulatory proteins have also been demonstrated to be virulence factors *in vivo*, for example proteins C16 (Fahy et al, 2008), E3 (Brandt & Jacobs, 2001) and B8 (Symons et al, 2002) to name but a few. To test the contribution of C6 to VACV virulence vC6WR, vΔC6, vC6Rev and vC6FS recombinant viruses (see Chapter 3) were amplified to high titre in RK-13 cells and partially purified for *in vivo* experiments by sedimentation of cytoplasmic extracts through two sucrose cushions (see Chapter 2 for methods details). These viruses were titrated at least three times on monolayers of BSC-1 cells and the titres were found to be similar for all four viruses (Figure 7.3A). The expression of C6 from these partially purified viruses was confirmed by

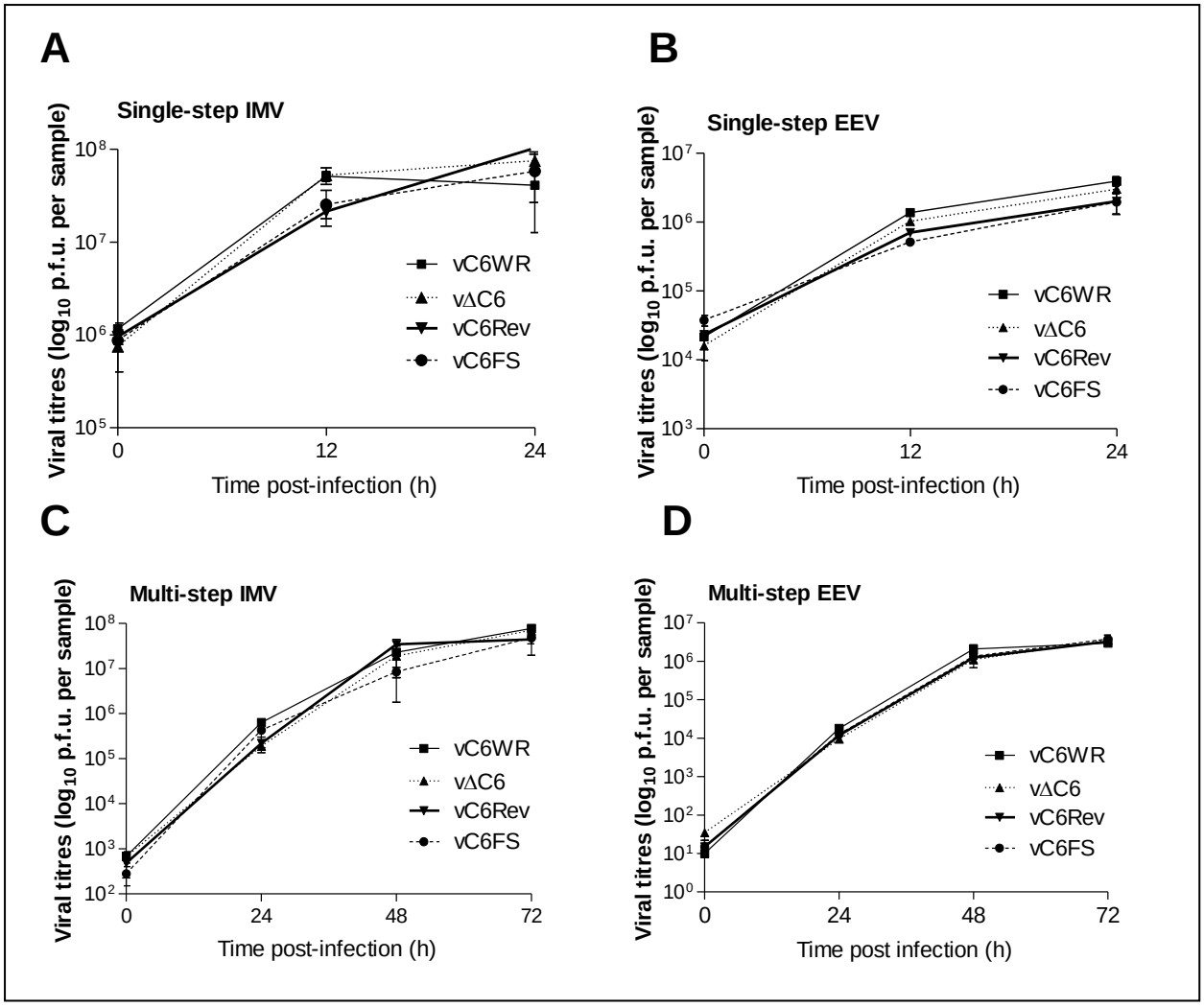

Figure 7.2: Replication and spread of C6 recombinant viruses *in vit*ro. For construction of single- (A and B) and multi-step (C and D) growth curves T25 flasks of BSC-1 cells were infected in duplicate at 10 p.f.u. per cell and 0.01 p.f.u. per cell, respectively, for 90 min. The unbound virus was then washed off and cells were harvested at the time points indicated with careful separation of intracellular (A and C) and extracellular virus (B and D) components. The harvested viruses were titrated in duplicate on confluent monolayers of BSC-1 cells. Results are expressed as the mean titre per sample ± SD.

infecting BSC-1 cells overnight and subjecting whole cell lysates to immunoblotting analysis. As expected, both vC6WR and vC6Rev expressed C6 but vΔC6 and vC6FS did not, while all viruses expressed D8 to equivalent levels (Figure 7.3B).

A

Virus	Titre (p.f.u./ml)
vC6WR	1.43×10^{10}
vΔC6	1.25×10^{10}
vC6Rev	1.59×10^{10}
vC6FS	1.41×10^{10}

B

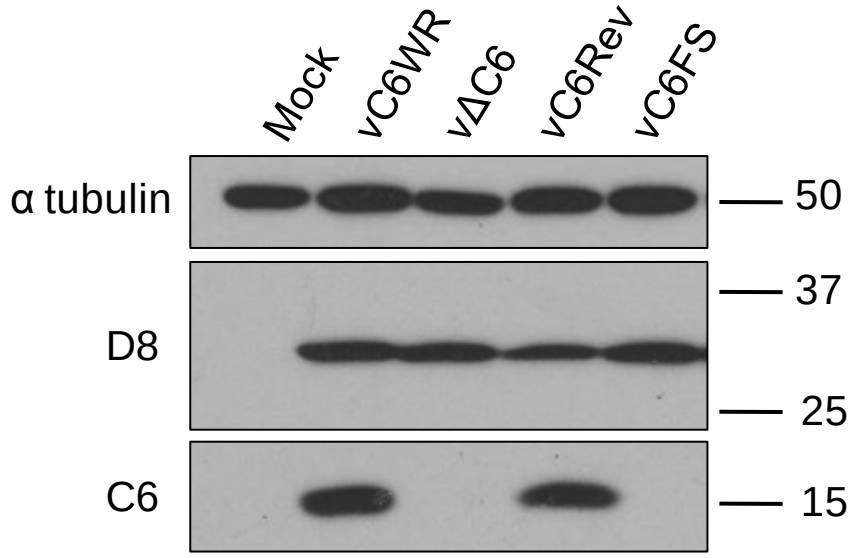

Figure 7.3: Partially purified recombinant viruses. Recombinant viruses were purified for *in vivo* experiments by sedimentation through two sucrose cushions. (A) Viral titres were calculated by plaque assay on confluent monolayers of BSC-1 cells. Data are from one representative experiment of three. (B) The expression of C6 was confirmed by infecting BSC-1 cells overnight with 5 p.f.u. per cell of recombinant virus. The cells were then lysed, the proteins were separated by SDS-PAGE and immunoblotted with mouse anti-tubulin, mouse anti-D8 or rabbit anti-C6 antibodies. The location of protein molecular mass markers is indicated (kDa).

7.3 A virus lacking C6 is attenuated in the VACV i.n. model of murine infection

To assess the contribution of C6 to VACV virulence the C6 recombinant viruses were first tested in the i.n. model of murine infection. Groups of ten female BALB/c mice were infected i.n. with 5×10^3 p.f.u. of virus per animal and their weights and signs of illness were monitored daily. Infection with vC6WR induced weight loss in these animals starting between days 4 and 5 p.i., with the maximal weight loss observed at days 7-8, followed by a period of recovery (Figure 7.4A). Between days 6 and 12 p.i. the mice that were infected with a virus lacking C6 expression (vΔC6 and vC6FS) lost significantly less weight than those animals that had been infected with a virus expressing C6 (vC6WR and vC6Rev). The maximal weight loss of these animals was also smaller (approximately 15 % for vΔC6 and vC6FS, and 20 % for vC6WR and vC6Rev) and this was reached one day earlier (day 7 for vΔC6 and vC6FS compared to day 8 for vC6WR and vC6Rev) indicating that these animals recovered from infection sooner.

Importantly, the weight loss observed in mice infected with vC6WR and vC6Rev was similar, supporting data presented in Figure 3.10 demonstrating that no major rearrangements or deletions of the genome had occurred during transient-dominant selection. Furthermore, the weight loss observed in animals infected with vΔC6 was similar to those infected with vC6FS, again indicating that these viruses are phenotypically alike and that the attenuation observed in the absence of the C6 ORF was due to the lack of expression of the C6 protein and not due to the lack of the DNA sequence or a non-coding RNA.

In agreement with the weight loss data, mice infected with a virus lacking the expression of C6 showed significantly fewer signs of illness between days 5 and 12 p.i. (Figure 7.4B). Further, the maximum signs of illness score was lower for those animals infected with vΔC6 or vC6FS, peaking at day 7 p.i., corresponding to the maximal weight loss of these animals (Figure 7.4A). For the animals infected with a virus retaining C6 expression the maximum signs of illness score was higher and recorded at days 8-9 p.i. (Figure 7.4B), again coinciding with the maximal weight loss of these animals (Figure 7.4A). Taken with the weight loss measurements, these data indicated that a virus lacking C6 expression was attenuated *in vivo,* and this protein was therefore a virulence factor.

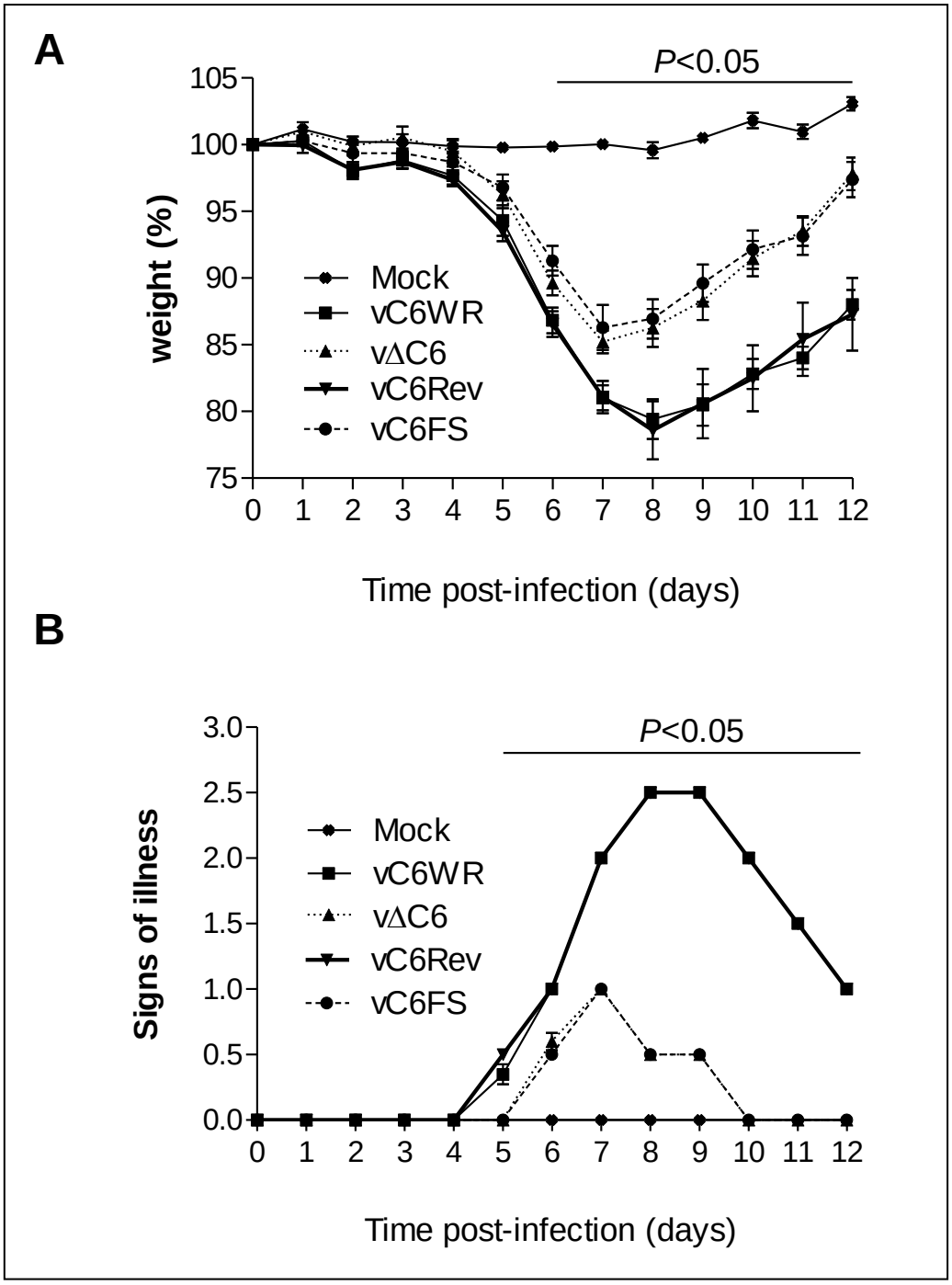

Figure 7.4: Virulence of C6 recombinant viruses in the murine i.n. model of infection. Female BALB/c mice (n=10) were infected with 5×10^3 p.f.u. of the indicated viruses and their weights (A) and signs of illness (B) were monitored daily. Data are from one representative experiment of two. Weight data (A) are expressed as the percentage ± standard error of the mean (SEM) of the mean weight of the same group of animals on day 0. Signs of illness data (B) are expressed as the mean score ± SEM. The horizontal bar indicates the days on which the weight loss or signs of illness induced by vΔC6 and vC6FS were statistically different (P<0.05) from both vC6WR and vC6Rev, analysed using the Student's T-test.

7.4 Mice infected with vΔC6 have more neutrophils and macrophages in the spleen early after infection

To gain a mechanistic understanding of why animals infected i.n. with vΔC6 lost significantly less weight than animals infected with the wild-type or revertant virus, BAL fluid, the lungs and the spleen were harvested from these animals at various time points p.i.. These samples were analysed for levels of cytokines and chemokines and for measurement of infiltrating immune cells by flow cytometry.

As C6 was found to be an inhibitor of the IRF3 signalling pathway, and *in vitro* the ectopic expression of this protein was able to suppress the production of CXCL-10 in response to NDV infection (Chapter 4), it was hypothesised that in the absence of C6 an enhanced production of CXCL-10 might be observed in the lungs mice infected i.n.. The BAL fluid was harvested from groups of 5 mice on days 2, 4, 7 and 12 p.i., the cells were collected by centrifugation and the supernatant was analysed for CXCL-10 (Figure 7.5A) and the NF-κB-dependent cytokine IL-6 as a negative control (Figure 7.5B) by ELISA. Small amounts of both CXCL-10 and IL-6 were detected in the BAL fluid of mice that had been infected i.n. with 5×10^3 p.f.u. of virus, but no differences were observed between infection with vC6WR, vΔC6 or vC6Rev. The highest levels of these proteins were measured at early time points p.i. (days 2 and 4), diminishing at later time points (days 7 and 12), as expected for a cytokine and chemokine that play a crucial role in the early inflammatory innate immune response. These inflammatory mediators function to recruit immune cells to the site of infection, and thus if C6 had had an effect on the production of these proteins in the lungs of infected animals this may have impacted on the total number of infiltrating cells. Although there was a trend for more cells infiltrating the airways of the lungs of animals infected with vΔC6 at early time points p.i. this was not statistically significant and the error bars were large (Figure 7.5C).

To determine whether the lack of C6 expression had an effect on the types of cells that were infiltrating the lungs, the cells that had been isolated from the BAL fluid were stained for lymphocyte markers and analysed by flow cytometry. To analyse T cell populations $CD3^+$ cells were gated and analysed further for CD4 and CD8 expression, as well as the expression of the early activation marker CD69 (Testi et al, 1988). At days 2 (Figure 7.6A), 4 (Figure

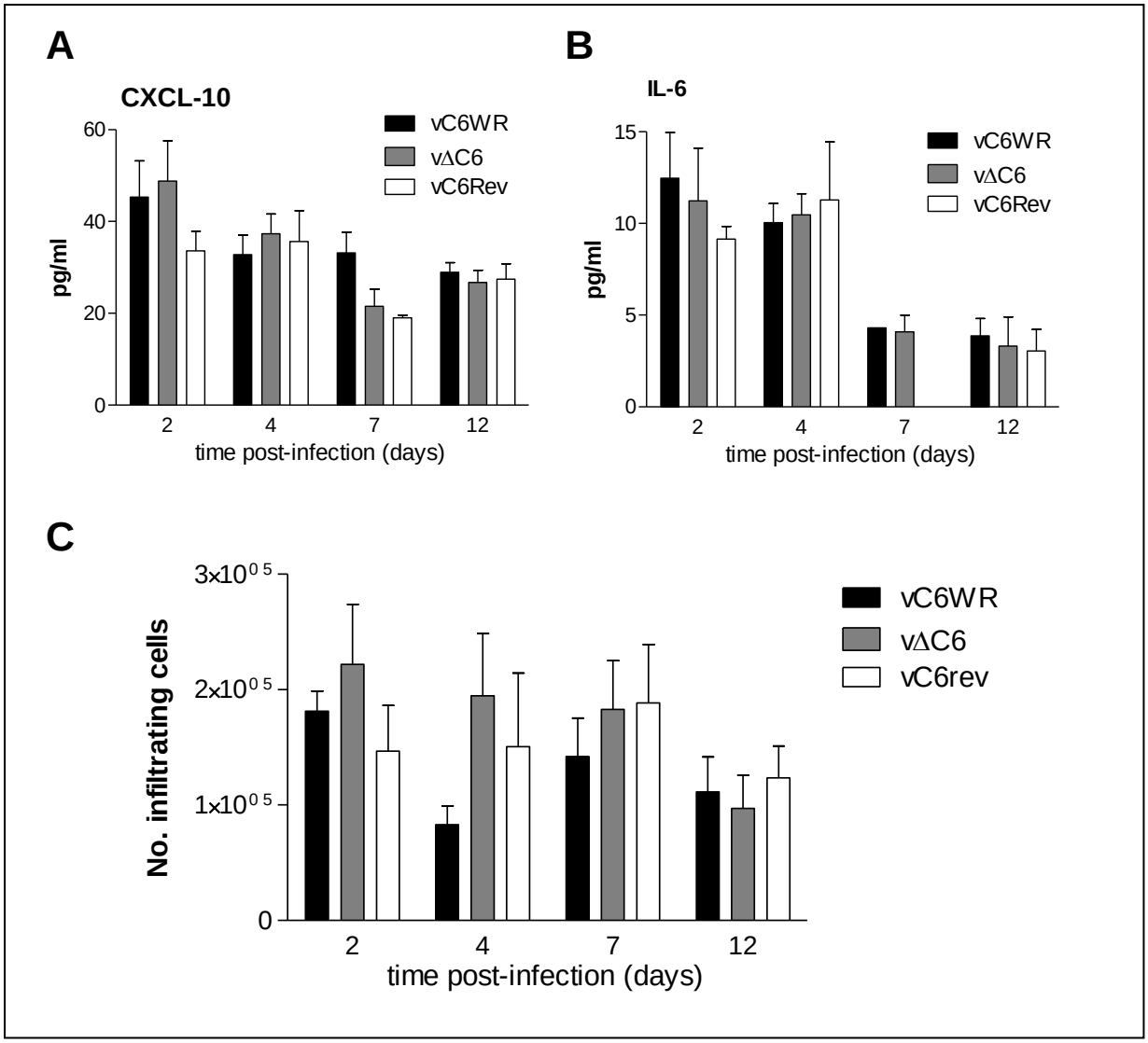

Figure 7.5: BAL fluid cytokine, chemokine and cell analysis. Female BALB/c mice were infected i.n. with 5×10^3 p.f.u. of the C6 recombinant viruses and five animals per virus were sacrificed and BAL fluid taken on the days indicated. Quantities of CXCL-10 chemokine (A) and IL-6 cytokine (B) in the BAL fluid were measured by ELISA. Data from a single experiment and are presented as mean ± SEM. The total number of viable cells in the BAL fluid were enumerated by the trypan blue exclusion method (C). Data are from a single experiment and are presented as mean number of infiltrating cells ± SEM.

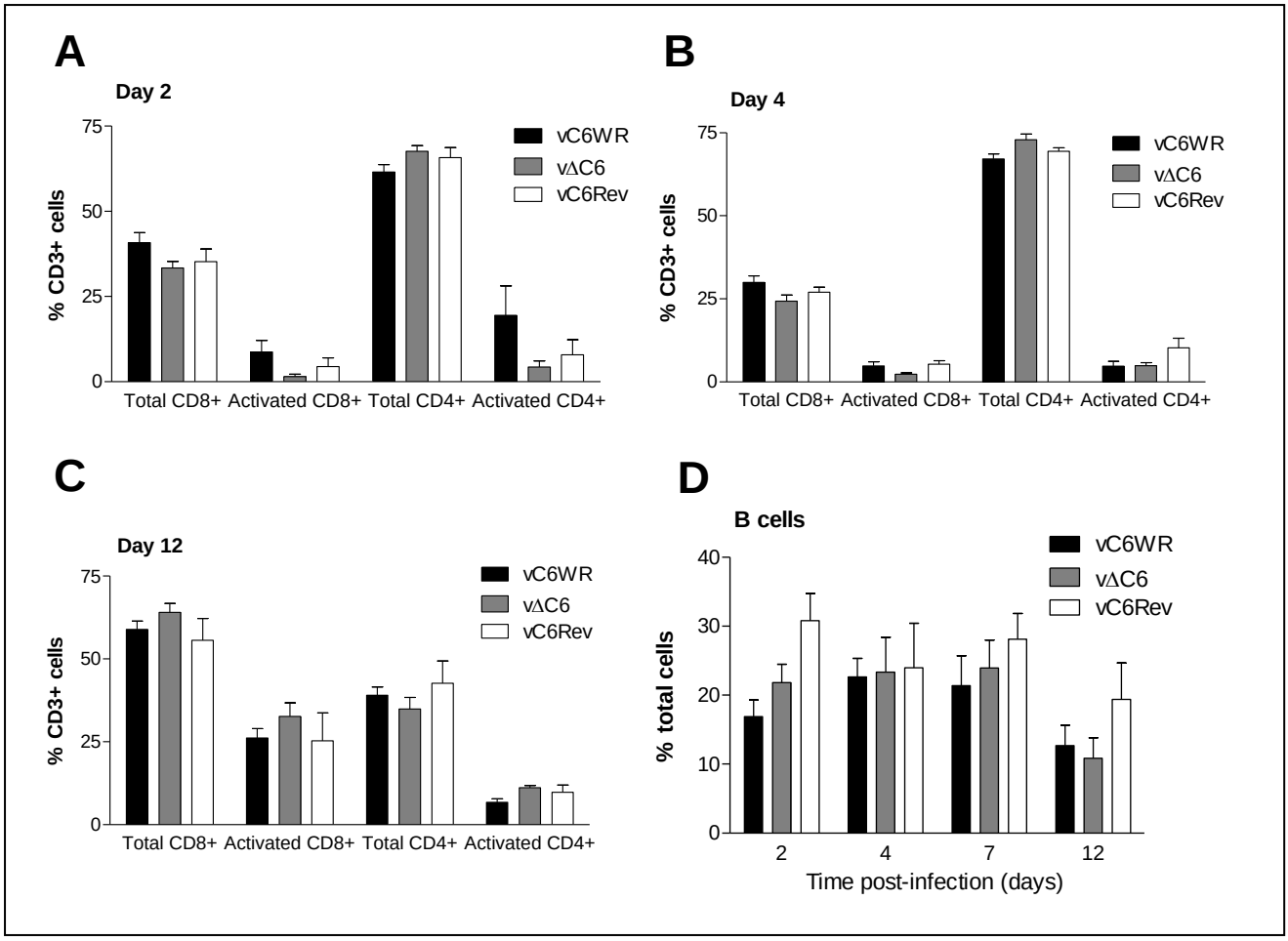

Figure 7.6: Flow cytometry analysis of cells in the BAL fluid. Female BALB/c mice were infected i.n. with 5×10^3 p.f.u. of the C6 recombinant viruses and five animals per virus were sacrificed and broncho-alveolar lavage (BAL) fluid taken on the days indicated. The cells were stained for CD3, CD4, CD8, CD69 (activated) (A, B and C) and CD19 (B cells) (D), and were analysed by flow cytometry. Data are from a single experiment and are presented as mean percentage of CD3-positive cells (A, B, C) or mean percentage total cells (D) ± SEM.

7.6B) and 12 (Figure 7.6C) p.i. no significant differences were observed in the proportion of cells that were $CD4^+$ or $CD8^+$, or the proportion of these cells that were activated from animals that had been infected with vΔC6 compared to vC6WR or vC6Rev. For all three viruses the proportion of T cells that were $CD4^+$ compared to $C8^+$ was higher on days 2 and 4 p.i., but by day 12 this proportion was observed to be more equivalent, with slightly more cells expressing the CD8 marker. In addition, the percentage of activated $CD8^+$ cells had increased greatly by this time point. Data for day 7 p.i. were unfortunately not available due to a technical problem with the staining for CD3. Finally, the cells in the BAL fluid were also stained for CD19, a marker of B cells (Stamenkovic & Seed, 1988), but no significant differences were observed in the number of these cells in mice infected with the three C6

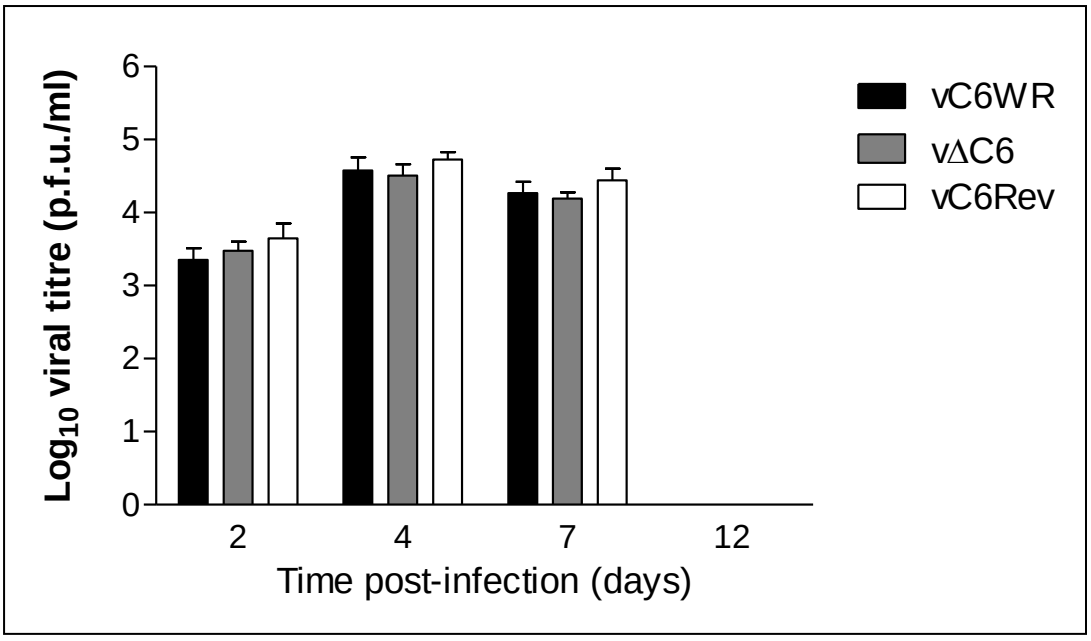

Figure 7.7: Viral titres in the lungs of i.n.-infected mice. Female BALB/c mice were infected i.n. with 5×10^3 p.f.u. of the C6 recombinant viruses and five animals per virus were sacrificed and the lungs were taken on the days indicated. The lungs were homogenised and virus titres were deduced by plaque assay in duplicate on confluent mono-layers of BSC-1 cells. Data are from a single experiment and are presented as the mean viral titre ± SEM .

recombinant viruses (Figure 7.6D). Due to the lack of cells, flow cytometry analysis of myeloid and NK cells in the BAL fluid was not possible.

To understand whether differences in the burden of virus in the lungs might account for the reduced weight loss in animals infected with vΔC6, virus isolated from lung homogenates was titred by plaque assay on BSC-1 cells. At days 2, 4 and 7 p.i. virus was detectable in the lungs of infected mice, but no differences were observed between the titres obtained for the three recombinant viruses (Figure 7.7). No virus was detected in the lung at day 12 p.i., presumably because it had been cleared by this time point, and no virus was detected in the spleen of these animals at any time point tested (data not shown).

The cells isolated from lung homogenates at the various time points p.i. were stained for both lymphoid and myeloid cell markers. As observed for the BAL fluid, the proportion of $CD4^+$ and $CD8^+$ cells, as well as their activation state ($CD69^+$) was similar between mice infected with the three C6 recombinant viruses at all time points tested (Figures 7.8A, B and C). Also in concordance with analysis of the T cells in the BAL fluid, the proportion of $CD4^+$ cells was

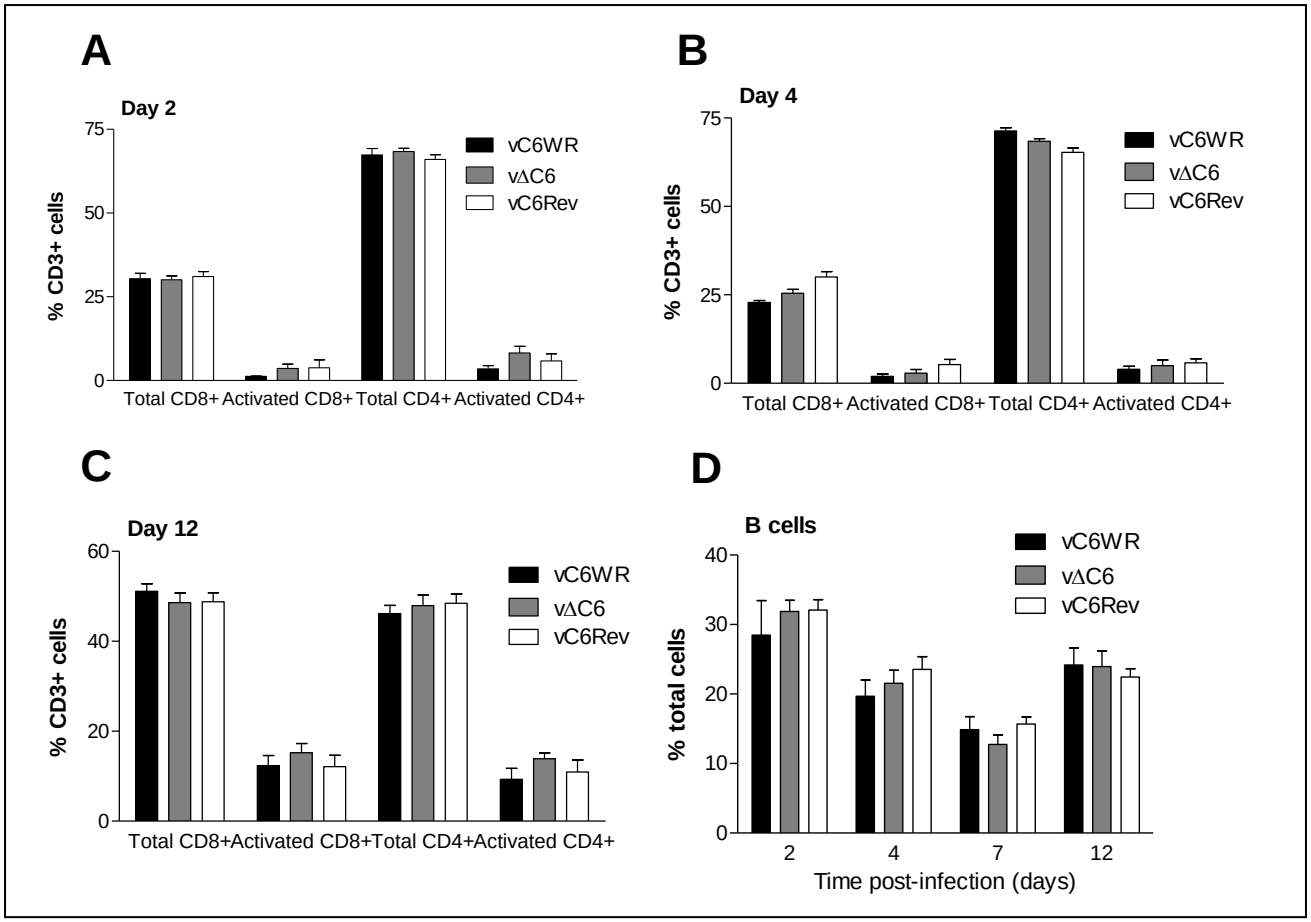

Figure 7.8: Lung lymphocytes flow cytometry analysis. Female BALB/c mice were infected i.n. with 5×10^3 p.f.u. of the C6 recombinant viruses and five animals per virus were sacrificed and the lungs were taken on the days indicated. The lungs cells were stained for CD3, CD4, CD8, CD69 (activation marker) (A, B and C) and CD19 (B cells) (D), and analysed by flow cytometry. Data are from a single experiment and are presented as the mean percentage of CD3-positive cells (A, B, C) or mean percentage of total cells (D) ± SEM .

higher at early time points p.i. but equal to the proportion of $CD8^+$ cells by day 12 p.i.. No differences in the proportion of B cells between the viruses were also observed (Figure 7.8D).

To analyse myeloid and NK cells in the lungs of infected mice the cells were stained for Ly6G (Fleming et al, 1993) to identify neutrophils (Figure 7.9A), DX5 (Arase et al, 2001) to identify NK cells (Figure 7.9B) and F4/80 (Austyn & Gordon, 1981) to stain for macrophages (Figure 7.9C). Macrophages were also stained for CD11b (Springer et al, 1979) but data obtained were similar to that obtained with an Ab against F4/80 (data not shown). At all the time points tested, no significant differences in the percentage of the various myeloid or NK cells was observed in the lungs of mice infected with the three C6 recombinant viruses.

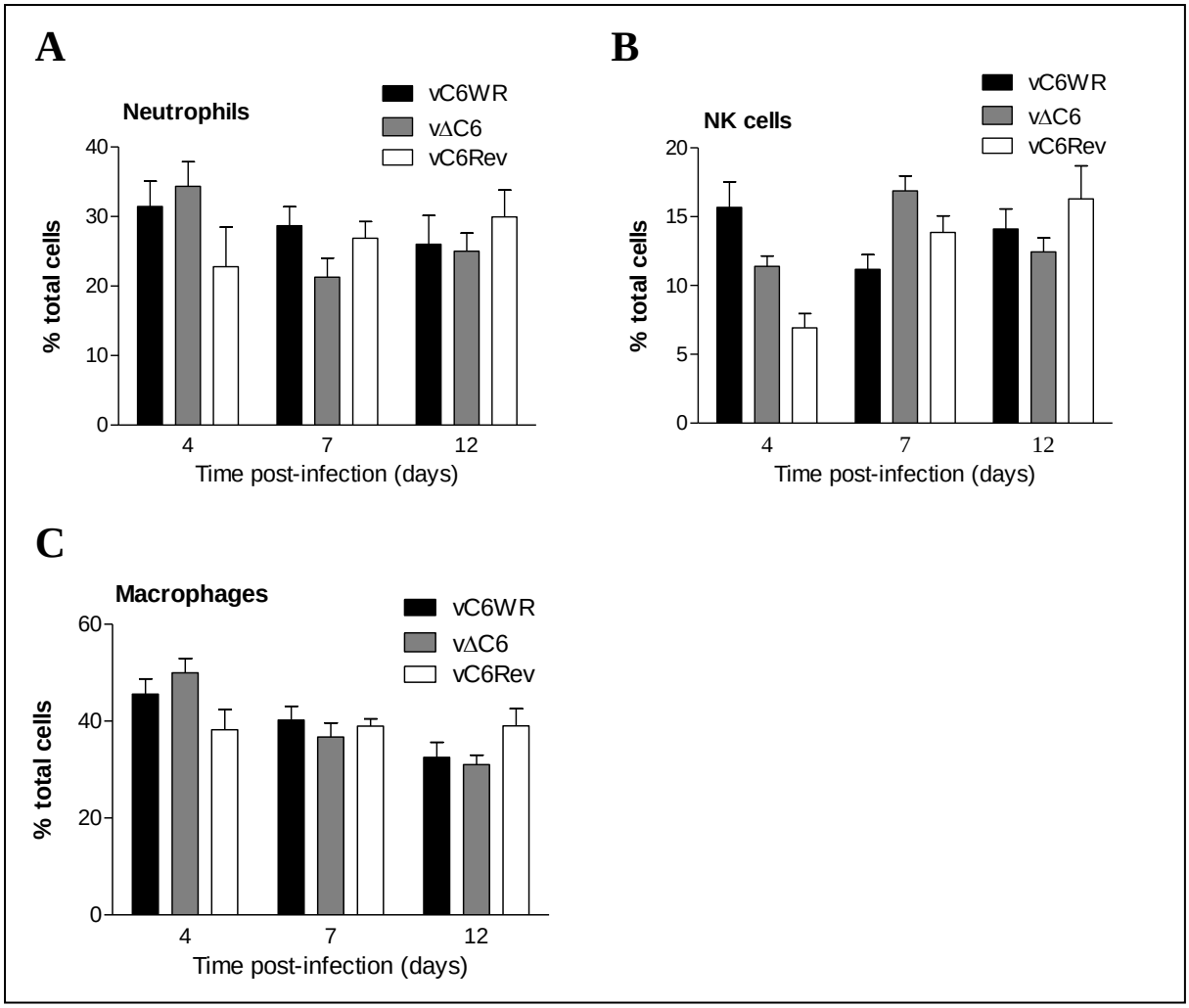

Figure 7.9: Lung myeloid and NK cell flow cytometry analysis. Female BALB/c mice were infected i.n. with 5×10^3 p.f.u. of the C6 recombinant viruses and five animals per virus were sacrificed and the lungs were taken on the days indicated. The lungs cells were stained for Ly6G (neutrophils, A), DX5 (NK cells, B), and F4/80 (macrophages, C), and analysed by flow cytometry. Data are from a single experiment and are presented as mean percentage of total cells ± SEM .

The spleen was also harvested from the animals used in the experiments above to analyse both lymphoid and myeloid cell populations. No differences were observed in the proportion of T cells that were $CD4^+$ or $CD8^+$, or activated at days 2 (Figure 7.10A), 4 (Figure 7.10B) or 12 (Figure 7.10C) p.i., or the percentage that were B cells (Figure 7.10D). In contrast to data obtained from the lung and BAL, $CD4^+$ cells were the more abundant type of T lymphocyte in the spleen at all time points tested. A difference was observed, however, in the percentage of neutrophils (Figure 7.11A) and macrophages (Figure 7.11C) in the spleen at day 2 p.i. where animals infected with vΔC6 had significantly higher numbers of these cell types. No

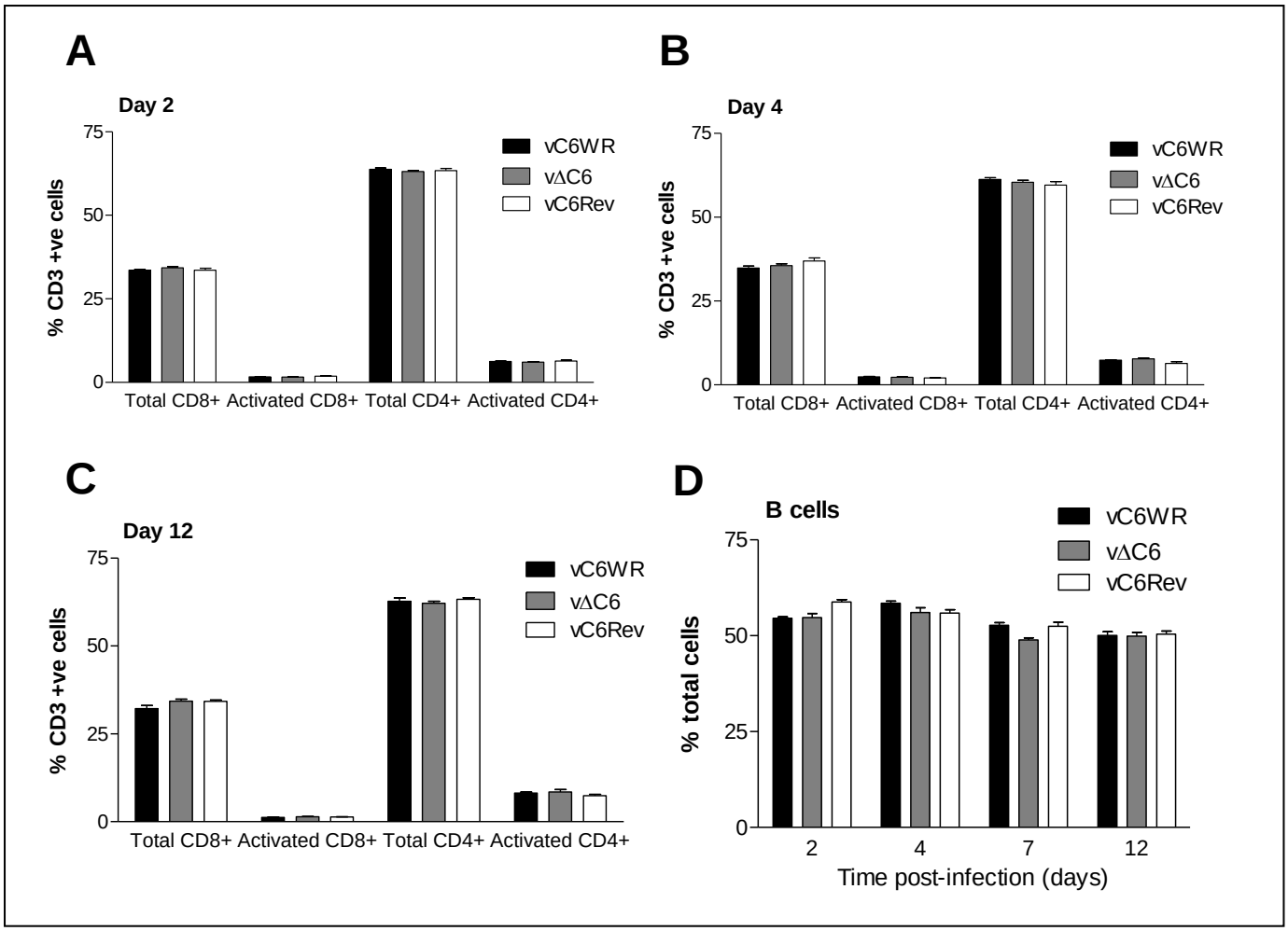

Figure 7.10: Spleen lymphocytes flow cytometry analysis. Female BALB/c mice were infected i.n. with 5×10^3 p.f.u. of the C6 recombinant viruses and five animals per virus were sacrificed and the spleen was taken on the days indicated. The spleen cells were stained for CD3, CD4, CD8, CD69 (activation marker) (A, B and C) and CD19 (B cells) (D), and were analysed by flow cytometry. Data are from a single experiment and are presented as mean percentage of CD3-positive cells (A, B, C) or mean percentage total cells (D) ± SEM .

significant difference was observed in the proportion of NK cells in the spleen (Figure 7.11B).

Taken together these data indicated that although no differences were observed in the type of lymphoid cells in the BAL, lung or spleen, or the proportion of myeloid and NK cells measured in the lungs, more neutrophils and macrophages were observed in the spleens of vΔC6-infected animals at day 2 p.i.. These innate immune effector cells have crucial roles at very early time points p.i.. Increased numbers of these cells may aid in the clearance of a viral infection and could in some part explain why a virus lacking C6 is attenuated in the i.n.

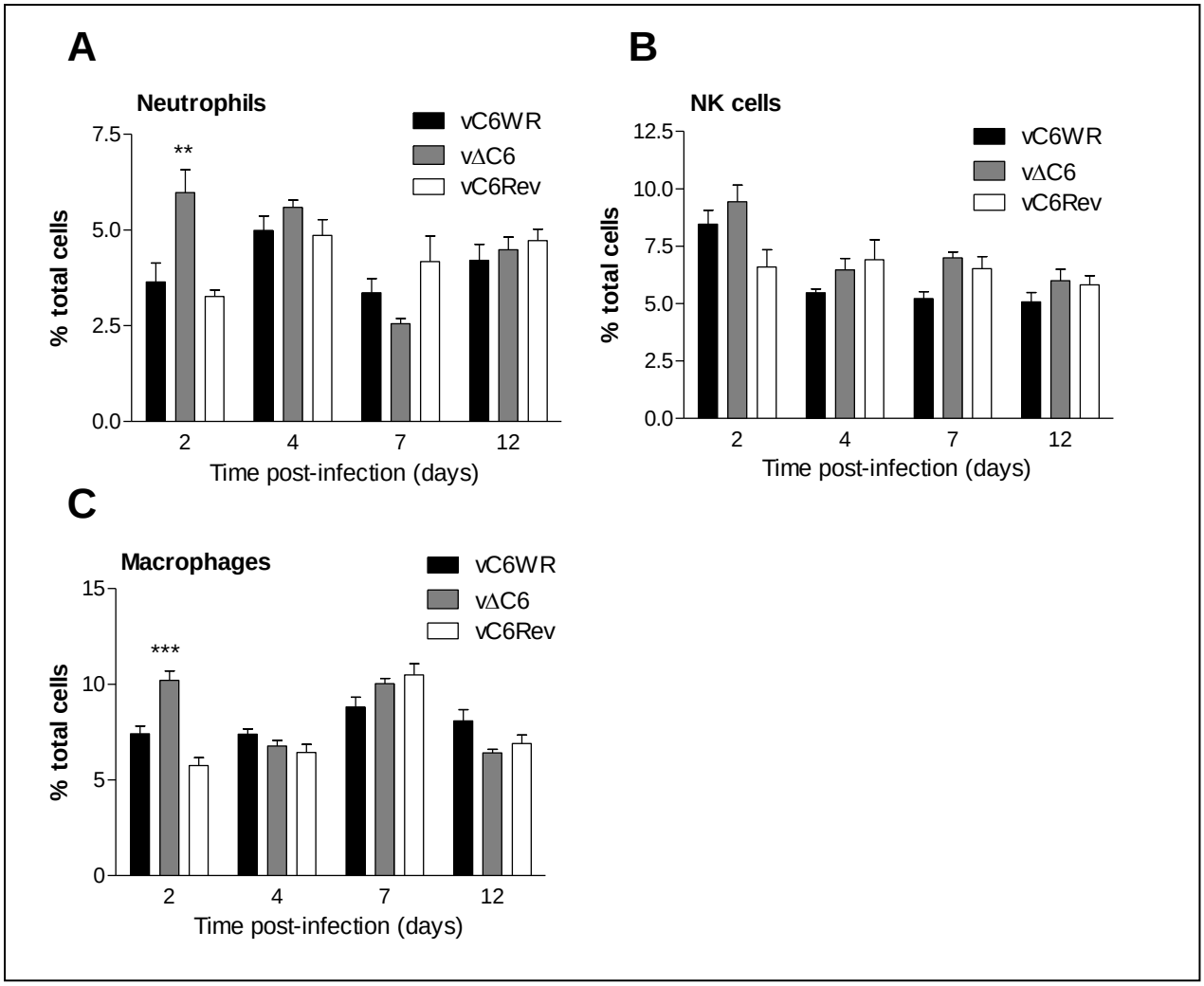

Figure 7.11: Spleen myeloid and NK cell flow cytometry analysis. Female BALB/c mice were infected i.n. with 5×10^3 p.f.u. of the C6 recombinant viruses and five animals per virus were sacrificed and the spleen was taken on the days indicated. The spleen cells were stained for Ly6G (neutrophils, A), DX5 (NK cells, B), and F4/80 (macrophages, C), and were analysed by flow cytometry. Data are from a single experiment and are presented as mean percentage of total cells ± SEM . ** $P<0.01$, *** $P<0.001$, analysed using the Student's T-test.

model of infection. It would be very interesting to investigate whether the proportion of these cells would also be increased in the lung and BAL fluid of animals infected with vΔC6 at day 2 p.i..

7.5 A virus lacking C6 is attenuated in the VACV i.d. model of murine infection

The contribution of C6 to VACV virulence was also tested in the murine i.d. model of infection. Groups of ten female C57BL/6 mice were infected with 10^4 p.f.u. of the C6 recombinant viruses per ear, in both ears, and the resulting lesions were measured daily with a micrometer. Measurable lesions were detectable from day 5 p.i., reaching their maximal size between days 11 to 14 p.i. and having completely healed by one month p.i. (Figure 7.12). Between days 5 and 23 p.i. the lesions caused by infection with vΔC6 or vC6FS were significantly smaller than those induced by vC6WR and vC6Rev. In addition, the lesions induced by the viruses lacking C6 expression had a smaller maximal size and began healing 3 days sooner (day 11 for vΔC6 and vC6FS compared to day 14 for vC6WR and vC6Rev) than the lesions caused by the viruses expressing C6. Similar to the results obtained in the i.n. model of infection, the size of the lesions induced by infection with the viruses expressing C6 was similar, as were the lesion sizes induced by infection with the viruses lacking C6 expression, again indicating that the attenuation observed was attributable to the lack of C6 protein expression and not due to the aberration of other viral genes.

7.6 Vaccination of animals with a virus lacking C6 expression provides enhanced protection against a lethal dose of virus

The strength and type of innate immune response mounted against a pathogen impacts greatly on the adaptive response that follows. As such, proteins that are known to dampen the innate response may have a negative impact on the adaptive immune response and thus may reduce the efficacy of vaccination. VACV was used as a vaccine in the eradication campaign against smallpox (Fenner et al, 1988) and is being investigated as a vector for the immunisation against a wide range of pathogens and cancer (Gomez et al, 2008). To investigate whether the deletion of C6 from WR had an effect on its efficacy as a vaccine, groups of 5 female C57BL/6 mice were vaccinated i.d. with 10^4 p.f.u. of the C6 recombinant viruses in both ears. One month later the animals were challenged i.n. with a lethal dose (5×10^6 p.f.u. per animal) of WR and their weights were monitored daily. The onset of weight loss in response to a lethal dose of virus post-vaccination occurred much sooner than that observed during a primary VACV infection and recovery began at just 2 days p.i. (Figure 7.13). Between days 2

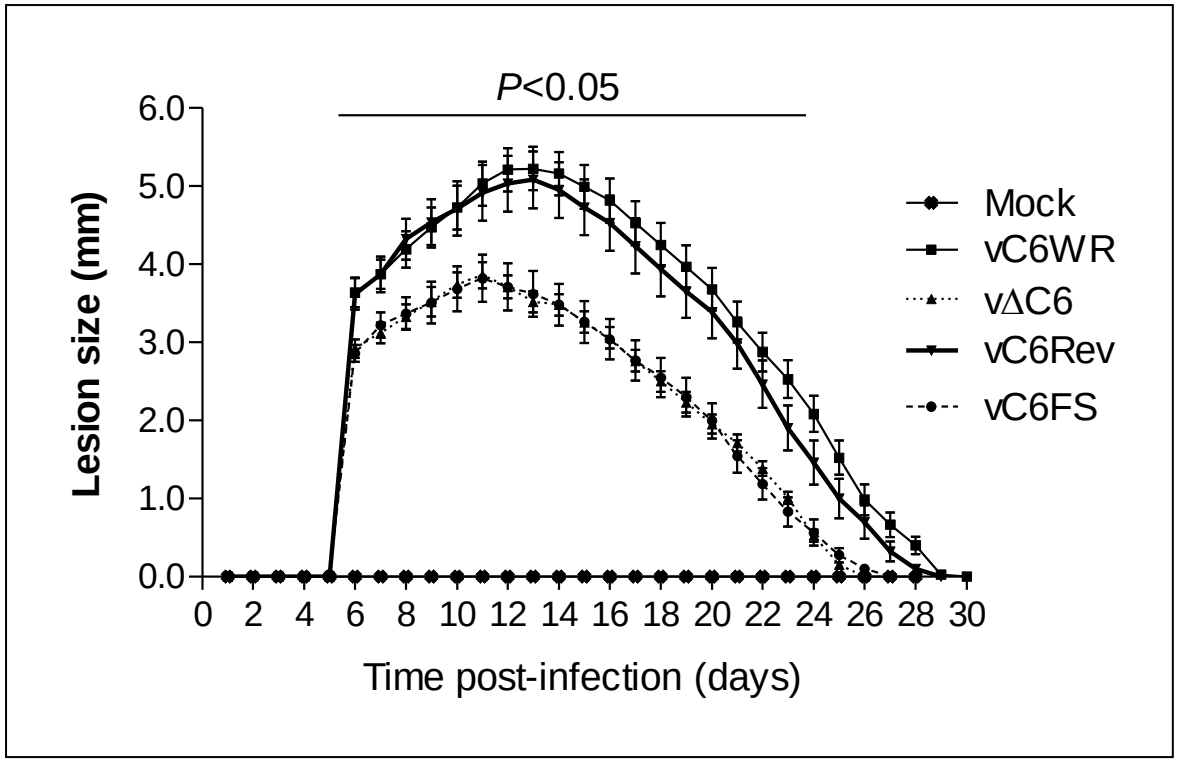

Figure 7.12: Virulence of C6 recombinant viruses in the murine i.d. model of infection. Female C57BL/6 mice (n=10) were infected i.d. with 10^4 p.f.u. of the indicated viruses in both ears and the resulting lesions were measured daily with a micrometer. Data are from a representative experiment of two and are expressed as the mean lesion size ± SEM. The horizontal bar indicates the days on which the lesion size caused by vΔC6 and vC6FS were statistically different (P<0.05) from both vC6WR and vC6Rev.

and 4 p.i. the weight loss observed when mice were vaccinated with a virus lacking C6 expression was found to be significantly less than that of mice that had been vaccinated with a virus expressing C6 (Figure 7.13). These data indicated that although all mice were protected against the lethal challenge, better protection was afforded by the viruses lacking C6 expression and that this virus was therefore a better vaccine. As observed in both the i.n. and i.d. models of infection, the viruses lacking and retaining C6 expression were grouped together.

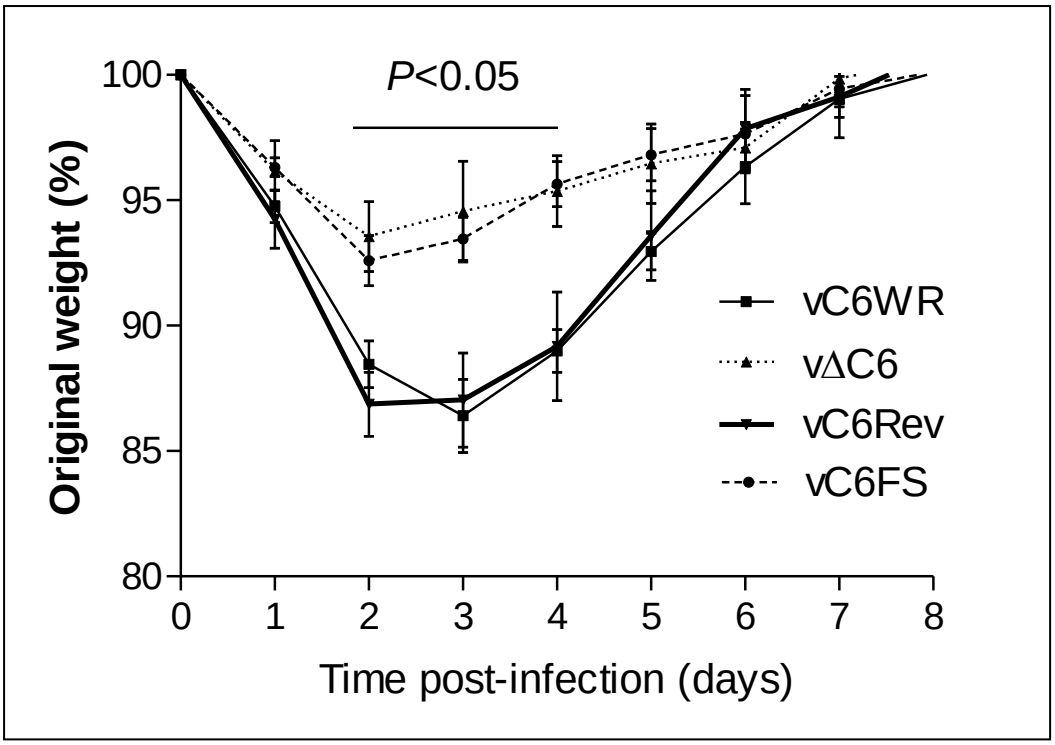

Figure 7.13: Challenge study following i.d. infection of mice with the C6 recombinant viruses. Female C57BL/6 mice (n=5) were infected i.d. with 10^4 p.f.u. of the indicated viruses in both ears. One month later the animals were challenged i.n. with 5×10^6 p.f.u. WR per animal and their weights were monitored daily. Data are from a representative experiment of two and are expressed as the percentage ± SEM of the mean weight of the same group of animals on day 0. The horizontal bar indicates the days on which the weight loss of the vΔC6- and vC6FS-vaccinated animals was statistically different (P<0.05) from both vC6WR- and vC6Rev-vaccinated animals.

7.7 The enhanced protection observed after vaccination of mice with a virus lacking C6 expression was not attributable to an enhanced Ab response

To understand how mice infected with a virus lacking C6 expression were better protected against a lethal dose of VACV, the blood was taken from mice one month post-vaccination for serum Ab analysis. Antibody neutralisation was first analysed by an IMV plaque reduction neutralisation assay. Somewhat surprisingly, antibodies in the serum of animals that had been vaccinated with either vΔC6 or vC6FS were found to have a significantly lower ND50 than the antibodies in the serum of animals that had been vaccinated with vC6WR or vC6Rev, indicating a poorer neutralisation capacity (Figure 7.14A). In each assay a positive control serum was included from a human vaccinated multiple times (GLS03). The ND50

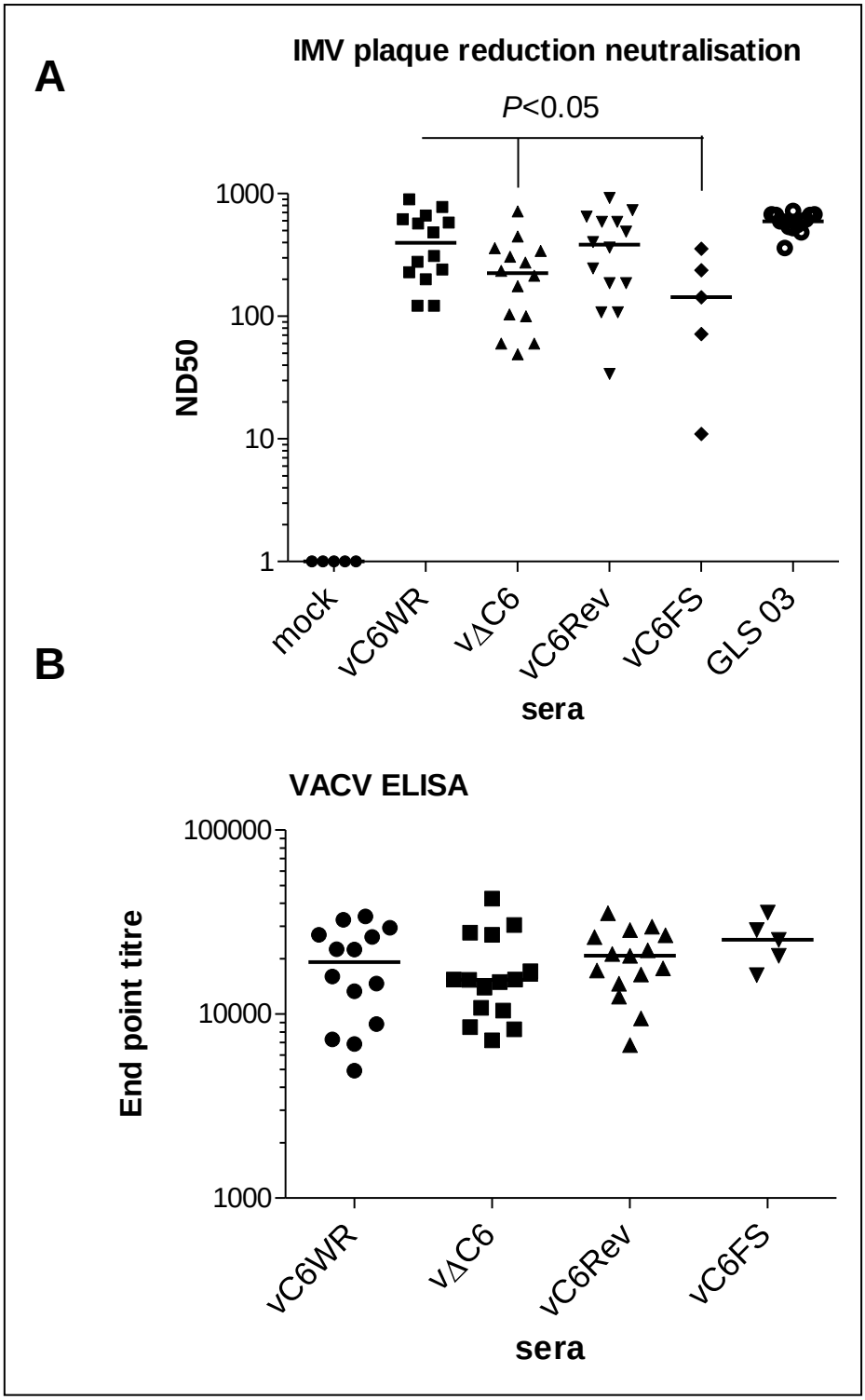

Figure 7.14: Antibody analysis of mice one month post - i.d. infection. Groups of female C57BL/6 mice (n=5) were infected i.d. with 10^4 p.f.u. of the indicated viruses in both ears. One month later animals were sacrificed and their blood was taken. Blood serum was analysed for Ab neutralisation by an IMV plaque reduction neutralisation assay (A) and Ab binding to VACV epitopes by ELISA (B). Data are from a total of three experiments and are presented as ND50 values (A) or end point titres (B) with the median indicated by a horizontal line. Neutralisation data were analysed by a Mann-Whitney test and indicated that the Ab neutralisation from animals vaccinated with vΔC6 or vC6FS were statistically different (P<0.05) from animals vaccinated with vC6WR.

data obtained from this serum were similar between assays, confirming reproducibility between experiments.

To determine whether the antibodies from animals vaccinated with a virus lacking C6 expression had a poorer neutralisation capacity because the titres of VACV-specific antibodies were lower, an ELISA was performed against whole cell lysates of cells that had been infected with WR. The end point titre of WR-specific antibodies was found to be similar between the vaccinated animals, indicating that the poorer neutralisation was not due to the presence of fewer VACV-specific antibodies (Figure 7.14B).

Given that the enhanced protection of vΔC6 as a vaccine could not be explained by enhanced VACV-specific Ab titres or enhanced Ab neutralisation it was hypothesised that the increased protection might be T cell-mediated. To investigate this, spleens were harvested from mice one month post-vaccination and the cells were analysed by flow cytometry. The overall proportion of T cells ($CD3^+$) and B cells ($CD19^+$) in the spleens of vaccinated animals was found to be similar (Figure 7.15A). In addition, the proportion of T cells that were $CD4^+$ or $CD8^+$, or were expressing CD44, a marker of T cell long-term activation and memory (Baaten et al, 2010) was also found to be equivalent (Figure 7.15B). These data indicated that the enhanced protection could not be attributed to differences in the relative quantities of these cell types or their activation.

To test the ability of the T cells from vaccinated animals to kill VACV-infected cells, a chromium release cytotoxicity assay was performed. One month post-vaccination spleens were harvested from groups of 5 animals for cytotoxicity analysis, whilst another 5 animals per group were challenged i.n. with 5×10^6 p.f.u. WR per animal and sacrificed 8 days later for subsequent T cell cytotoxicity analysis. The percentage specific lysis of WR-infected EL-4 cells by splenic T cells isolated from vaccinated animals was not found to be significantly different between the four C6 recombinant viruses, either before (Figure 7.16A), or after challenge (Figure 7.16B). As expected, the percentage specific lysis was higher after challenge than before challenge, and T cells from mock-infected animals did not have any lytic activity.

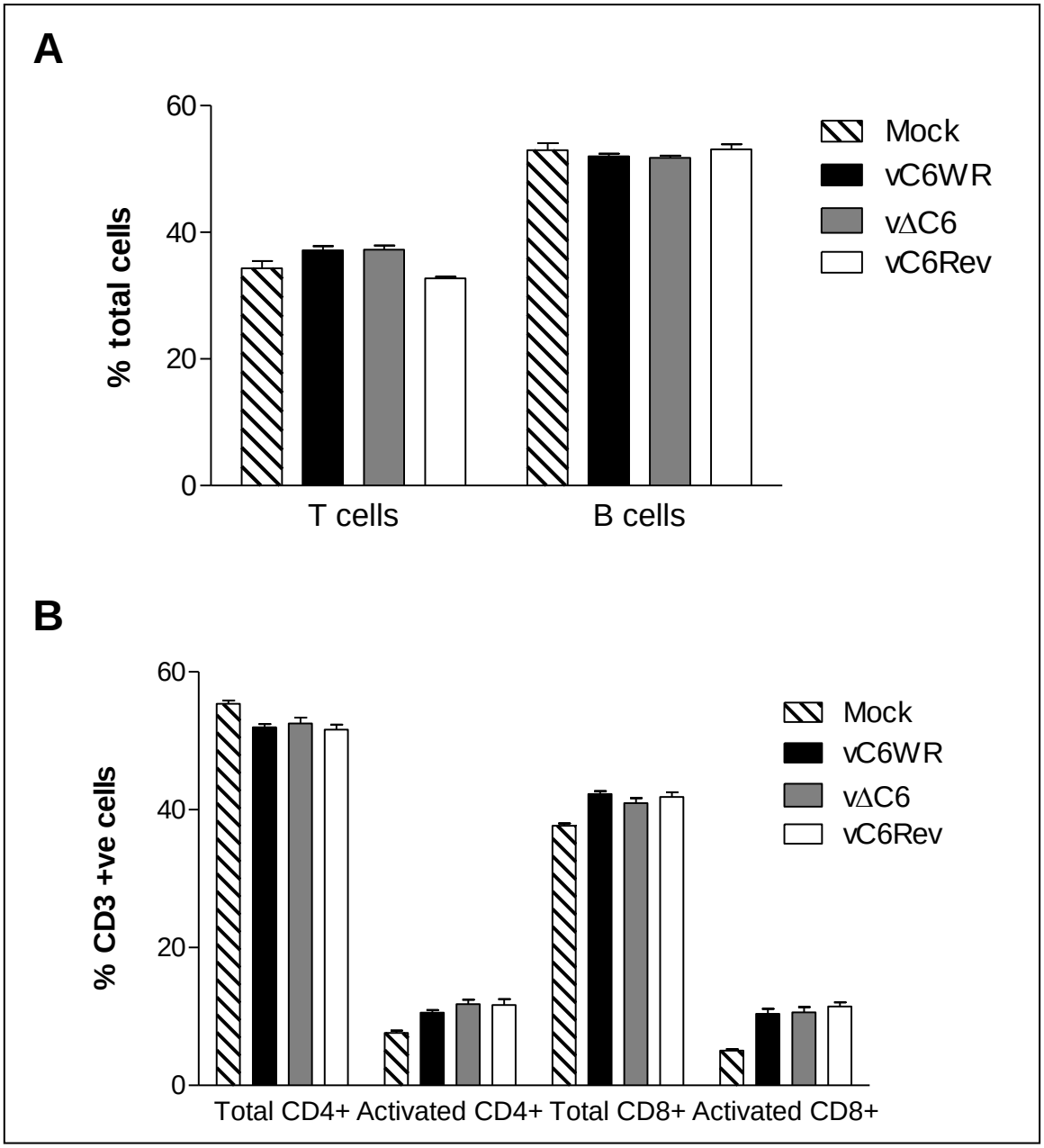

Figure 7.15: Spleen lymphocyte analysis one month post-i.d. infection by flow cytometry. Female C57BL/6 mice (n=5) were infected i.d. with 10^4 p.f.u. of the indicated viruses in both ears. One month p.i. the animals were sacrificed and the spleen was taken. The spleen cells were stained for CD3 (T cells) and CD19 (B cells) (A), and also CD4, CD8 and CD44 (activated) (B), and were analysed by flow cytometry. Data are from a representative experiment of two and are presented as the mean percentage of of total cells (A) or CD3-positive cells (B) ± SEM .

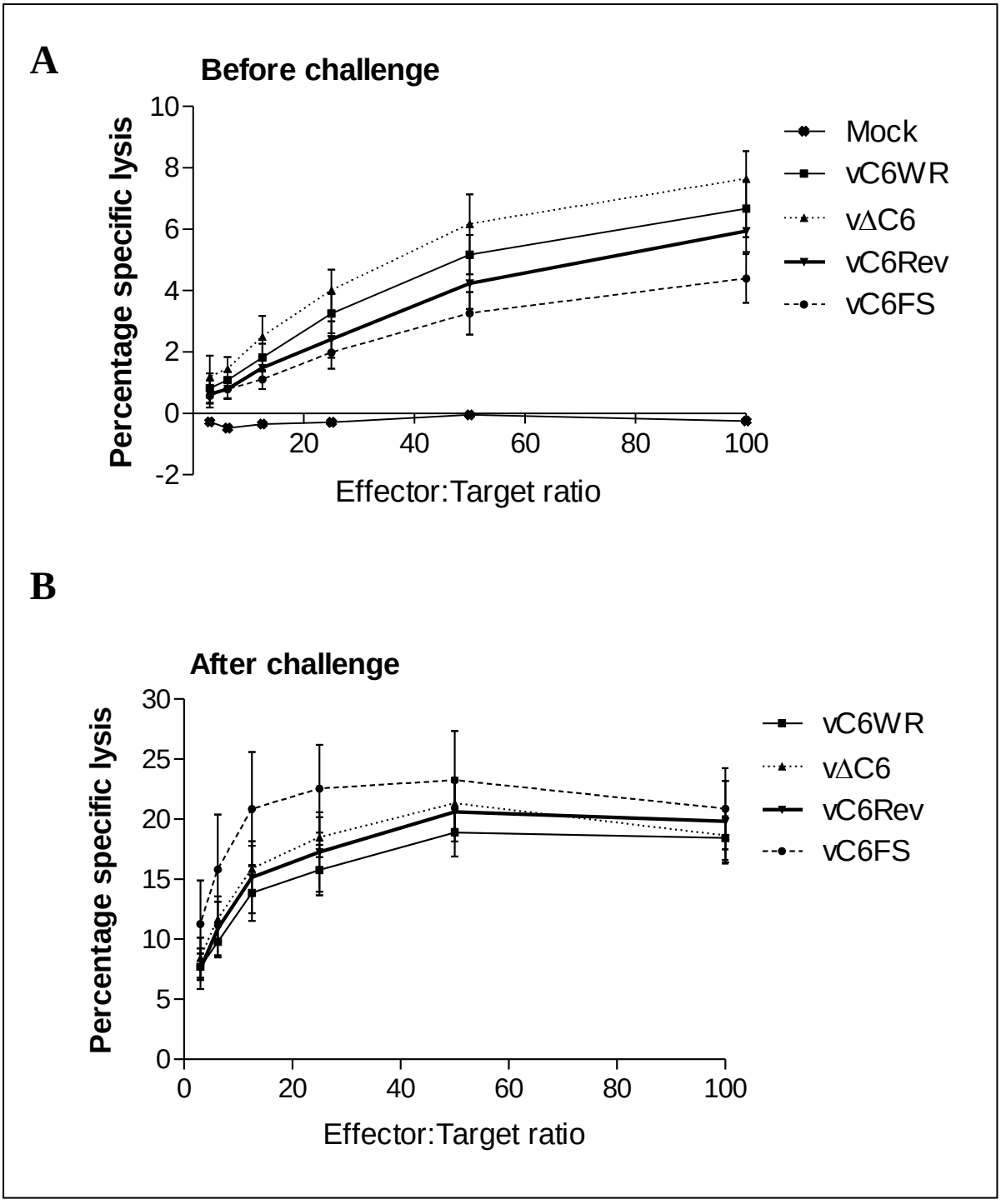

Figure 7.16: Splenic T cell cytotoxicity before and after challenge of i.d.-infected mice. Female C57BL/6 mice (n=10) were infected i.d. with 10^4 p.f.u. of the indicated viruses in both ears. One month p.i. 5 animals per group were sacrificed and the spleen taken for cytotoxicity analysis. The other 5 animals per group were challenged i.n. with $5x10^6$ p.f.u. WR per animal and sacrificed 8 days later for splenic T cell cytotoxicity analysis. Specific lysis of EL-4 cells by T cells was assessed by ^{51}Cr-release assay. Data are from a single experiment and are presented as the mean ± SD.

IFNγ produced by T cells is a very important cytokine for the immune defence against viral infection (Schroder et al, 2004). To analyse IFNγ release by T cells from vaccinated animals in response to exposure to VACV-specific antigens, an ELISPOT assay was performed. One month post-vaccination the mice were sacrificed and the spleen was harvested. The splenocytes were stimulated overnight with a CD8-specific peptide characterised to be immunogenic in C57/BL6 mice (TSYKFESV, (Tscharke et al, 2005)) or as a negative control a CD8-specific peptide characterised to be immunogenic in BALB/c mice (VGPSNSPTF, (Tscharke et al, 2006)), or they were incubated with EL-4 cells that had been mock-infected or infected with WR. As expected, minimal IFNγ release was observed from splenic T cells that were stimulated with the BALB/c-specific peptide or mock-infected EL-4 cells. The release of IFNγ in response to VACV-specific antigens was not enhanced in vΔC6-vaccinated animals, again providing no mechanistic explanation for the improved protection observed with this virus (Figure 7.17).

7.8 Summary

Prior to the characterisation of the C6 recombinant viruses *in vivo*, the effect of C6 deletion from WR on virus replication and spread was assessed *in vitro*. C6 was found not to contribute to replication or spread in cell culture as the viruses lacking C6 expression replicated to equivalent titres in both a single- and multi-step growth curve, performed using BSC-1 cells and formed similar size plaques in three cell types of different species origin. In contrast, a virus lacking C6 was attenuated in both the murine i.n. and i.d. models of infection *in vivo*. Mice infected i.n. with either vΔC6 or vC6FS lost significantly less weight and showed fewer signs of illness than mice infected with vC6WR or vC6Rev, and the lesions induced by i.d. infection of the viruses lacking C6 expression were significantly smaller and healed quicker.

Although C6 inhibited CXCL-10 production in response to NDV infection *in vitro*, no difference in the amount of this chemokine in the BAL fluid of i.n.-infected mice was observed *in vivo* at the times points measured. No difference was also observed in the total number of infiltrating cells in the lungs, or the types of immune cells measured in either the BAL fluid or the lung tissue. Interestingly, although the populations of T cells and NK cells in the spleen were unaltered between mice that had been infected with the various C6

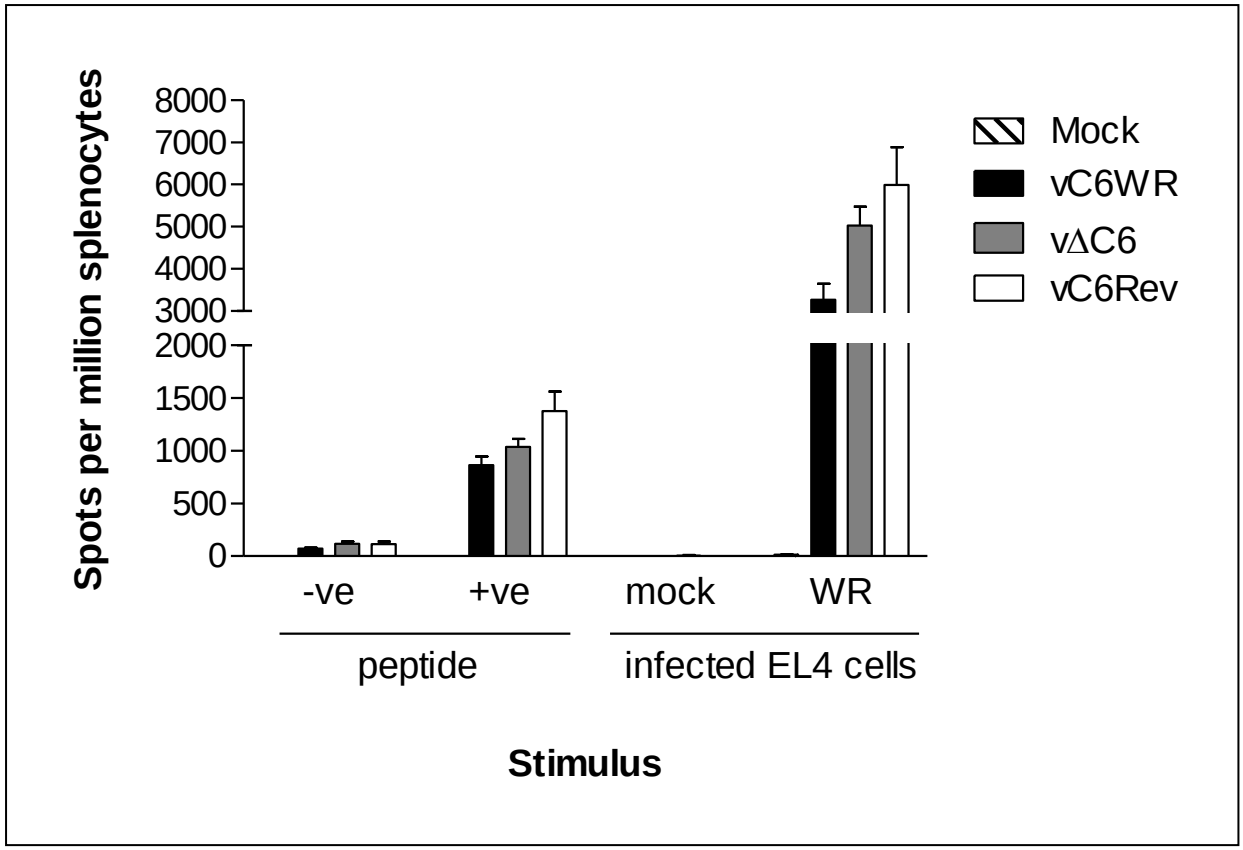

Figure 7.17: ELISPOT analysis of IFNγ-producing splenic T cells one month post-i.d. infection. Female C57BL/6 mice (n=5) were infected i.d. with 10^4 p.f.u. of the indicated viruses in both ears. One month p.i. the animals were sacrificed and the spleen taken for ELISPOT analysis. The splenocytes were stimulated with TSYKFESV peptide (+ve) or VGPSNSPTF peptide (-ve) or were incubated with EL-4 cells that had been mock-infected or infected with WR. Data are from one representative experiment of two and are presented as the mean spots per million splenocytes ± SEM.

recombinant viruses, more neutrophils and macrophages were present at 2 days p.i. with vΔC6. These data indicated that the presence of C6 had a negative effect on the number of these myeloid cells in the spleens of infected animals. As these cells are crucial for the early immune response against viral infection this finding might contribute to the attenuated phenotype observed in the absence of C6 expression.

In addition, a virus lacking C6 expression provided enhanced protection against a lethal challenge of mice with WR. This protection could not be attributed to enhanced titres of WR-specific antibodies in the serum, or enhanced Ab neutralisation capacity. In fact, antibodies isolated from vΔC6- or vC6FS-vaccinated animals had poorer neutralisation abilities against

IMV WR. Given these data it was hypothesised that the enhanced protection afforded by vΔC6 would be due to an enhanced T cell response and/or memory. No differences in the types of T cells, including memory T cells were observed in the spleen one month post-vaccination of mice with the various C6 recombinant viruses and the splenic T cells from vΔC6-vaccinated animals were found not to have enhanced killing capacity or release of IFNγ in response to VACV antigens. Further analysis of the immune response to infection with vΔC6 needs be undertaken to fully understand this phenotype.

Chapter 8: Discussion

8.1 Basic characterisation of VACV WR protein C6

To establish a productive infection pathogens must counteract the innate immune response. Viruses have evolved many mechanisms to achieve this and studying these not only enhances our knowledge of viral pathogenesis but also adds to our understanding of the immune system and how it functions. As such this continues to be a field of active research. VACV strain WR ORF *022* encodes protein C6, a predicted member of the VACV Bcl-2 family of proteins, whose other characterised members have roles in innate immune modulation. Together with the fact that C6 was identified from a screen performed in Prof. Bowie's lab at Trinity College Dublin of VACV proteins with the ability to inhibit IFNβ induction in HEK cells, this protein was selected for further investigation.

Orthologues of C6 were found to be highly conserved amongst the OPVs and counterparts were even identified in some *Capripoxvirus* genus members. The high conservation of C6 suggested an important function for this protein. An orthologue of C6 is also expressed by MVA, which differs from WR C6 by an additional 6 amino acids at the C terminus. These residues did not prevent this protein from inhibiting IFNβ however (Figure 4.3). This is in agreement with the work of Garcia-Arriaza et al who found that human macrophages and monocyte-derived macrophages infected with a strain of MVA lacking C6 expression (MVA-BΔC6) produced more IFNβ than wild-type MVA-B (Garcia-Arriaza et al, 2011). The ability of MVA C6 to inhibit ISRE induction or bind to UBR1 or SMARCC1 was not addressed in this study and would be interesting future work to understand whether all functions of this protein are conserved. Given that enhanced expression of IFIT1 and IFIT2, two IFNα/β-inducible genes, was measured in human macrophages infected with MVA-BΔC6 compared to wild-type MVA-B, MVA C6 may also have an immunomodulatory role downstream of the IFNAR (Garcia-Arriaza et al, 2011).

MVA is a highly attenuated virus that has been passaged more than 500 times in CEFs. Large portions of the genome are missing and many immune modulators have been found to be deleted or are no longer functional, for example protein 183, the MVA counterpart of VACV

WR B14 (McCoy et al, 2010). The recombinant WR virus lacking C6 (vΔC6) showed no defect in replication or spread *in vitro* (Figures 7.1 and 7.2) and therefore it is interesting that it is retained in the MVA genome. It is possible that in the absence of other genes, MVA C6 may contribute to viral replication. This however is unlikely as another highly attenuated VACV strain being tested in vaccine trials, NYVAC, lacks C6 and MVA-BΔC6 was found to replicate to identical titres as MVA-B, at least for a multistep growth curve (Garcia-Arriaza et al, 2011). A single-step growth curve for these viruses was not constructed by the authors. MVA does not replicate in mammalian cells and is normally grown in avian cells such as CEFs and DF1 cells. It is possible that the immunomodulatory function of C6 is highly beneficial to the virus in these cells *in vitro*, or another uncharacterised role for this protein provides some essential function.

The structural model of C6, predicted using MODELLER and based on a structural alignment between C6 and B14, demonstrated that C6 folds favourably as a Bcl-2 scaffold and is highly similar structurally to B14 (Figure 3.3). Like other members of this family C6 is an inhibitor of innate immune signalling. The amino acid sequence identity of this family of VACV Bcl-2 proteins is less than 20 % (Graham et al, 2008), demonstrating that structure is more highly conserved than sequence. The Bcl-2 fold may provide a stable structure or platform for protein-protein interactions.

The expression of C6 was observed from 2 h p.i. and occurred without the need for DNA replication, confirming it as an early gene (Figure 3.5). This in agreement with a recent study using WR and also MVA, where the orthologue of C6 is also expressed early and without the need for replication (Garcia-Arriaza et al, 2011). Many other innate immune modulators, including other members of the VACV Bcl-2 family are expressed early and this is consistent with a role for C6 as an immunomodulator. Viral detection by PRRs may occur very early after infection, or even at the point where the virus encounters the cell membrane and thus the rapid expression of proteins that can dampen the immune response is critical to the virus. Protein VH1 for example is packaged into virions and is able to de-phosphorylate STATs and prevent the expression of ISGs prior to viral gene transcription (Najarro et al, 2001). It may be interesting to put the expression of an immune modulator such as C6 under the control of a late VACV promoter and determine *in vivo* whether this virus is attenuated, and if so to what

extent compared to the knockout virus. This would give an indication to the importance of the early expression of a protein that counteracts the innate immune response.

Although lacking an obvious NLS, C6 was found to be both cytoplasmic and nuclear (Figure 3.11 and 3.12). TANK, SINTBAD and NAP1 are cytoplasmic proteins and therefore it would be interesting to investigate whether co-localisation of C6 and these proteins occurs in infected cells. Within the cytoplasm C6 is not diffuse, but rather localises to punctuate structures. It is unclear whether these structures are cellular organelles and therefore immunofluorescence experiments could be repeated with markers of organelles, such as MitoTracker for mitochondria, to look for co-localisation. The function of nuclear C6 is not yet known, although this may have something to do with the nuclear protein SMARCC1 that was identified by mass spectrometry as a potential binding partner for C6 (Figure 6.5). A recent study using a polyclonal antiserum raised against MVA C6 for immunofluorescence found C6 expressed by either WR or MVA to be localised to a distinct structure in the cytoplasm, which the authors suggested to be a viral factory, although co-localisation with DAPI was not presented (Garcia-Arriaza et al, 2011). A possible explanation for the difference in localisation observed is that Garcia-Arriaza et al used chicken DF1 cells for localisation studies whereas human HeLa and HEK293 cells were used in this study. Further, Garcia-Arriaza et al did not present data on C6 localisation by any method other than immunofluorescence.

Like A52, B14 and N1, C6 was also shown by both conventional IP assays (Figure 3.15) and LUMIER (Figure 3.16) to have dimerisation abilities. Whether dimers form in cells during the course of an infection or whether dimerisation is required for C6 function is currently unknown and warrants further investigation. In the case of B14, dimerisation is not required for function and in fact the dimerisation interface formed by alpha helices 1 and 6 is also the interface for binding to IKKβ (Benfield et al, 2011). The same interface is also used by N1 for dimerisation (Cooray et al, 2007) and by K7 for binding to DDX3 (Oda et al, 2009). This hydrophobic interface may provide a favourable platform for binding to cellular proteins and in the absence of ligand, dimersation occurs to prevent the exposure of hydrophobic residues to the solvent. Recent studies using a mutant N1 that is unable to dimerise found that this protein no longer inhibited NF-κB activation and was attenuated *in vivo* (Maluquer de Motes et al, 2011). What is not clear from this study is whether dimerisation is required for N1

function, or whether N1, like B14 and K7 uses the alpha helix 1-6 interface to interact with a cellular protein. In this case the mutation introduced in N1 may not only prevent dimerisation, but may also prevent binding to an unidentified cellular protein involved in the NF-κB pathway.

Whilst data presented in this study indicate an interaction between C6 molecules it cannot be ruled out that this is via an intermediate cellular protein and thus indirect. In order to confirm that C6 forms dimers mutations would need to be designed that interfere with the dimer interface and prevent an interaction from occurring, akin to what has been demonstrated for N1 (Maluquer de Motes et al, 2011), or an immunoprecipitation assay could be performed using C6 protein expressed and purified from bacteria.

Although the VACV Bcl-2 proteins have a similar fold and many have the ability to homo-dimerise they do not seem to form hetero-dimers. This was demonstrated for C6 and B14 in this study (Figure 3.15), and has also been shown for C6 and N1 (C. Maluquer de Motes, unpublished results). Of note, although dimerisation using the interface of helices 1 and 6 is conserved in A52, B14 and N1, the rotation of the individual monomers at this interface differs between the proteins by up to 57 ° (Graham et al, 2008), potentially explaining the lack of hetero-dimerisation.

Recently a role for the cellular Bcl-2 proteins in inflammation has been discovered. The pro-apoptotic Bcl-2 protein BID was found to interact with NOD1, NOD2 and the canonical IKK complex, influencing both NF-κB and MAPK signalling (Yeretssian et al, 2011). A further link between mechanisms of apoptosis and immunity was demonstrated by Ferrer et al. In that study the induction of Noxa-mediated apoptosis induced by MVA infection was found to be dependent on viral recognition by the cytosolic RIG-I-like helicases and subsequent activation of IRF3, leading to the upregulation of Noxa itself (Ferrer et al, 2011).

8.2 Functional characterisation of C6

C6 was identified in a functional screen of VACV proteins that could inhibit IFNβ induction (Unterholzner et al, 2011) and this ability was confirmed in this study (Figure 4.1). IFNs play

a crucial role in the defence against viral infection and therefore viruses have evolved numerous mechanisms to inhibit their production or counteract their functions (Fensterl & Sen, 2009). Many NF-κB-specific inhibitors expressed from VACV have been described (Bowie et al, 2000; Chen et al, 2008; DiPerna et al, 2004; Gedey et al, 2006; Myskiw et al, 2009; Shisler & Jin, 2004), but C6 did not inhibit NF-κB (Figure 4.4 and 4.5) and instead inhibited the activation of IRF3 (Figure 4.6), consistent with its ability to inhibit IFNβ induction. The site of action of C6 was found to be quite downstream in the signalling pathway (downstream of the non-canonical kinases, but upstream of IRF3, Figure 4.8), likely explaining how this protein is able to inhibit IRF3 activation downstream of various stimuli. In addition, work performed in Prof. Bowie's laboratory found C6 to inhibit non-canonical IKK-dependent, but not -independent activation of IRF7, further explaining its ability to inhibit IFNβ induction (Unterholzner et al, 2011). The inhibition of IFNβ induction by C6 is supported by a recent study demonstrating that human macrophages and monocyte-derived DCs upregulate the expression of and secrete more IFNβ in response to infection with MVA-BΔC6 compared to wild-type MVA-B, suggesting that C6 acts to dampen this production (Garcia-Arriaza et al, 2011).

A number of the other characterised IRF3 inhibitors expressed by VACV act upstream in the signalling pathway. Both C16 (which binds the Ku complex, N. Peters, manuscript in preparation) and E3 (which inhibits the activation of DAI (Wang et al, 2008), and the RLRs and PKR (Chang et al, 1992) and also RNA polymerase III-mediated dsDNA-sensing (Valentine & Smith, 2010)) act on the PRRs themselves and A46 binds to PRR adaptors. This means that these proteins inhibit signalling downstream of specific stimuli only. K7, however is a broader inhibitor of IFNβ induction and is believed to exert its effects by binding to DDX3. It is currently unclear which signalling pathways converging on the non-canonical IKK complex DDX3 plays a role in, but as K7 can inhibit IRF3 activation downstream of multiple TLRs and RLRs it is presumed to contribute to a number of pathways.

An important question therefore is why does VACV require so many proteins that apparently inhibit the activation of the same transcription factors and genes? There are a number of potential explanations for this, although testing them experimentally is currently challenging. First VACV is known to activate multiple signalling pathways and is recognised by numerous PRRs including MDA5, NALP3 (Delaloye et al, 2009), IFI16 (Unterholzner et al,

2010) and DNA-PK (B. Ferguson et al, submitted), and therefore all arms of the innate immune response need to be inhibited. Secondly there appears to be a lot of redundancy in the innate immune response, particularly amongst adaptor proteins and this may explain why VACV targets immune signalling pathways at multiple points. Further, the position in the pathway where the protein acts determines which downstream signalling events are inhibited and thus which transcription factor activation is prevented. For example B14 is a potent inhibitor of NF-κB activation as it inhibits the canonical IKK complex where multiple signalling pathways converge downstream of various PRRs (Chen et al, 2008). On the other hand, A52 binds IRAK2 and TRAF6 (Harte et al, 2003), thus inhibiting NF-κB activation downstream of certain PRRs only, but allowing this protein to also inhibit MAPK activation (Maloney et al, 2005). Thirdly the innate response is activated shortly after infection, at which point the level of expression of a single immunomodulator may not be sufficient to completely inhibit NF-κB and IRF3 activation. Finally the importance of the immunomodulators may be very cell-type specific, depending on the PRRs activated by the virus in that particular cell.

The finding that C6 binds to TANK, SINTBAD and NAP1 (Figure 5.11) corroborates data demonstrating that C6 inhibits IRF3 activation downstream of multiple stimuli, as the pathways activating IRF3 converge on the non-canonical IKKs via these adaptor proteins. It is interesting however that C6 inhibited IRF3 activation after the over-expression of either TBK1 or IKKε (Figure 4.8). Although it is not understood mechanistically how the over-expression of these kinases drives IRF3 reporter activity, it is presumed that the high concentration of protein allows auto-phosphorylation of the kinases and activation to occur, with the subsequent phosphorylation of IRF3. These data might therefore indicate that the adaptors in fact act downstream of the non-canonical IKKs or rather as a large multi-protein signalling complex linking upstream and downstream signalling. TANK, for example has been described to interact with IRF3 and IRF7 (Gatot et al, 2007) and thus may be required to bring these transcription factors in the vicinity of the activated non-canonical IKKs for their phosphorylation to occur. If the presence of C6 prevents the formation of this multi-protein complex in some manner, then despite the kinases being activated they may not be brought in proximity of the IRFs and thus C6 still inhibits the pathway. Analysis of whether TBK1 and IKKε are phosphorylated in the presence of C6 has not been performed and could be an

informative experiment. In addition, although IRF3 does not translocate to the nucleus in the presence of C6 (Unterholzner et al, 2011), its phosphorylation status is yet to be investigated.

In vitro, C6 inhibited IRF3-dependent gene expression and protein production in response to infection with NDV (Figure 4.7). In both cases this inhibition was not complete, but this may be explained by insufficient concentrations of C6 and/or the NF-κB dependency of both CXCL-10 (Ohmori & Hamilton, 1993) and CCL5 (Danoff et al, 1994) in addition to IRF3. This experiment however was performed by over-expressing C6 out of the context of a viral infection. Attempts were made to measure IFNβ and IRF-3-dependent gene expression following the infection of cells with the recombinant C6 viruses however little or no induction of these genes was observed, seemingly because WR expresses sufficient immunomodulatory proteins to prevent their activation. Indeed Delaloye et al noted that although pro-inflammatory cytokines, chemokines and IFNβ were readily detectable in response to MVA infection in macrophages, such a response to VACV WR was not detected and they attributed this finding to the presence of immune modulators in the WR genome (Delaloye et al, 2009). A recent study also found that myxoma virus-infected DCs produced IFN, whereas in an identical experiment using VACV WR no IFN induction was detected (Dai et al, 2011). The recent study from Garcia-Arriaza et al found that human macrophages infected with MVA-BΔC6 had increased expression of CCL5 compared to MVA-B, supporting the role of C6 as an IRF3 inhibitor (Garcia-Arriaza et al, 2011).

In vivo small amounts of CXCL-10 and IL-6 were found in the BAL of i.n.-infected animals but no differences were observed between viruses that did or did not express C6 (Figure 7.5). IL-6 is an NF-κB-dependent gene and thus acted as a negative control in this assay, however CXCL-10 is both IRF3- and NF-κB-dependent, and given that an effect *in vitro* was observed in the presence of C6, an effect *in vivo* may also have been expected. A possible explanation for the *in vivo* data is that any differences expected in the absence of C6 may have been masked by the presence of other viral immunomodulators. Further, human macrophages infected with MVA-BΔC6, despite showing increased expression of IFNβ and other IRF3-dependent genes, did not show increased expression of CXCL-10 (Garcia-Arriaza et al, 2011). Other IRF3-dependent genes that are less dependent on NF-κB may need to be measured *in vivo* to observe differences between viruses lacking or retaining C6 expression.

As C6 inhibits IFNβ induction *in vitro* the production of IFNβ protein was also measured in the BAL of infected mice by ELISA, but none was detected. Cytokine and chemokine levels in the BAL were found to be very low and higher levels may be measureable from homogenised lungs. As the production of these inflammatory mediators occurs very soon after infection it may also be worthwhile investigating their production at earlier time points p.i. such as at 2, 6, 12 or 24 h. In cell culture, differences with MVA-BΔC6 were observed at 6 h p.i. for example (Garcia-Arriaza et al, 2011). In order to test a broader range of IRF3-dependent gene induction qPCR could be performed on infected tissue such as the lungs and trachea for the i.n. model of infection, or the ear following i.d. infection and the differences between an infection with a virus expressing or lacking C6 could be assessed.

In this study the ability of C6 to inhibit IFNβ induction has been largely attributed to its ability to inhibit IRF3, and not NF-κB activation. The absence of anti-NF-κB activity by C6 is supported by findings that human macrophages infected with MVA-BΔC6 failed to show enhanced expression of IL-8, an NF-κB-, but not IRF3-dependent gene (Mukaida et al, 1990), compared to a wild-type MVA-B infection (Garcia-Arriaza et al, 2011). The IFNβ promoter however, in addition to NF-κB and IRF3 binding sites also has an AP-1 binding site and it is currently unknown whether C6 has any effect on the activation of this transcription factor. Reporter gene assays were performed with an AP-1-specific reporter, however the fold induction obtained following the treatment of cells with various stimuli was found to be poor and inconsistent. An alternative would be to assess AP-1-specific gene activation by qPCR, perform an AP-1-specific electrophoretic mobility shift assay, or assess the phosphorylation of the MAPKs in the presence and absence of C6. It remains possible therefore that C6 may inhibit IFNβ induction by more than one method. Opposing the possibility that C6 inhibits AP-1 activation is the finding that MVA-BΔC6 infection did not induce enhanced IL-8 activation, as expression of this cytokine is also dependent on AP-1 in addition to NF-κB (Yasumoto et al, 1992).

In addition to inhibiting IRF3 activation, C6 was also observed to inhibit an ISRE-specific reporter following the stimulation of cells with the type I IFN IFNα (Figure 4.9A). This finding is supported by the work of Garcia-Arriaza et al where it was observed that human macrophages infected with MVA-BΔC6 showed enhanced expression of IFIT1 and IFIT2, two IFNα/β-inducible genes, compared to infection with wild-type MVA-B (Garcia-Arriaza

et al, 2011). Thus far TANK, SINTBAD and NAP1 have not been characterised to contribute to the JAK-STAT signalling pathway downstream of the IFNAR. Consequently C6 may have a second function in inhibiting this pathway independent of its binding to the three non-canonical IKK adaptor proteins. However, given that IRF3 and ISGF3 have largely overlapping DNA recognition sequences (Fujii et al, 1999) it would be interesting to investigate whether IRF3 contributes to the activation of ISRE-dependent ISGs downstream of the type I IFNs. For example, the transcription of type I IFN-dependent genes, such as IFIT1 and IFIT2 could be measured in TBK1-null, or IRF3-null MEFs following the treatment of cells with IFNα and compared to wild-type cells. If IRF3 activation contributes to both IFNβ induction and ISRE induction this may explain how C6 inhibits both pathways.

The mechanism by which C6 inhibits ISRE induction is currently unknown, but is specific for the type I IFN signalling pathway because no effect was observed in GAS-specific reporter activity following the stimulation of cells with IFNγ (Figure 4.9B). As such it is unlikely that C6 acts on a molecule common to both pathways such as STAT1, but rather on a molecule unique to the pathway downstream of the IFNAR. The signalling pathway downstream of type III IFNs binding the type III IFN receptor is considered indistinguishable from that downstream of type I IFNs (Fensterl & Sen, 2009), therefore it is expected that C6 would also inhibit ISRE activation following the treatment of cells with a type III IFN, although this remains to be tested. Assays assessing the levels of STAT phosphorylation and subsequent translocation may indicate whether C6 is inhibiting this pathway within the cytoplasm or further downstream in the nucleus. Although many VACV proteins have been identified to inhibit the production of IFNs, or to bind and neutralise the activation of secreted IFNs, only VH1 has been identified to inhibit IFN-induced intracellular signalling (Najarro et al, 2001). It has been observed that VACV also has the ability to block the transcription of some STAT1-independent genes by a currently unknown mechanism (Mann et al, 2008) and it is plausible that C6 may contribute to this ability.

8.3 Identification of TANK, SINTBAD and NAP1 as C6 binding partners

Although TANK, SINTBAD and NAP1 were found to interact with C6 and it is presumed that this binding mechanistically explains how this VACV protein is able to inhibit IRF3 activation this hypothesis remains to be confirmed experimentally. Cells deficient is all three

adaptor proteins are currently not available, but would be very useful to test whether C6 is still able to inhibit IRF3 in their absence. It is possible that the activation of IRF3 is completely abrogated in the absence of these three adaptors as it is currently unclear whether some redundancy between these molecules and DDX3, or other unidentified adaptor proteins exists. In the absence of null cell lines an alternative would be to knockdown the expression of these proteins by RNAi, which may be challenging for three proteins simultaneously.

The binding of C6 to three non-canonical IKK adaptors is presumably an effective method for the virus to inhibit IRF3 activation by these kinases. It is currently not clear exactly which signalling pathways each adaptor is critical for and to what extent their functions are redundant, but clearly some non-redundant functions exist as the activation of IFNβ by TRIF over-expression was reduced in HCT116 cells lacking TANK (Figure 5.9). Thus by targeting all three adaptors the virus has evolved a method to inhibit IRF3 activation downstream of a number of stimuli. This is the first viral protein described to target these three adaptor molecules and this highlights an important role for these proteins in the host defence against viral infection. The severe acute respiratory syndrome (SARS) coronavirus M protein was recently described to inhibit type I IFN induction by preventing the formation of a ternary complex consisting of TRAF3, TANK and TBK1, and was found to physically associate with RIG-I, TRAF3, TBK1 and IKKε (Siu et al, 2009). In this study the M protein inhibited ISRE induction following the treatment of cells with dsRNA, or overexpression of RIG-I, MDA5, MAVS, TBK1 and IKKε, but not following the overexpression of IRF3 or IRF7, indicating that this protein exerts its function at a point in the signalling pathway similar to that of C6. These data further support an important role for this signalling pathway in host antiviral defence.

Mechanistically it is still not clear how the binding of C6 to TANK, SINTBAD and NAP1 inhibits IRF3 activation. An attractive hypothesis is that like SARS coronavirus M protein, C6 prevents the formation of a multimeric cellular signalling complex. This was tested by both LUMIER assay and conventional IP assays in the presence of over-expressed C6, but no disruption of complex formation was observed (Figures 5.12-5.18). However, there may be technical reasons for this (below) and no conclusions could be made from these experiments. One major limitation of these types of experiments is that all molecules are over-expressed outside the context of a viral infection. It is possible that the levels of over-expressed C6 were

not sufficient to interfere with the interaction between over-expressed cellular signalling molecules. For example in Figure 5.17 the expression level of TAP-C6 from the HEK293 T-Rex TAP-C6 cell line was significantly lower than over-expressed FLAG-TRAF3 or N1-TAP, all probed using an anti-FLAG monoclonal Ab.

It is unlikely that C6 requires other viral proteins to exert its function because C6 inhibits IFNβ (Figure 4.1) and IRF3 (Figure 4.6) activation in a reporter gene assay when it is over-expressed in the absence of a viral infection. It is possible however that the IRF3 signalling pathway needs to be activated, for example by infecting the cells with VACV, or NDV, or by treating them with poly I:C for C6 to exert its function. Clearly over-expressed C6 interacts with over-expressed TANK, NAP1 and SINTBAD without the need for activating the IRF3 pathway, but activation may induce protein conformational changes and/or post-translational modifications that are required to observe the mechanism of C6 inhibition. C6 may indeed affect the post-translational modifications of signalling proteins and this remains to be investigated. Infecting cells with VACV or NDV to stimulate the pathway may complicate the experiment due to the presence of other immunomodulatory viral proteins, although infection with vΔC6 may act as a good control for experiments using wild-type VACV WR infection.

It was not tested in this study whether the presence of C6 interfered with the interaction between TANK and NEMO, which would be particularly interesting as the N-terminal region where C6 interacts with TANK is important for its binding to NEMO. Although this binding has previously been shown to have a role in NF-κB activation rather than IRF3 signalling (Chariot et al, 2002), more recent work has indicated that cross-talk between the canonical and non-canonical IKKs exists and that the canonical IKKs play an important role in TBK1 and IKKε activation (Clark et al, 2011). Whether this involves TANK is currently unclear and as yet no interaction between NEMO and NAP1 or SINTBAD has been described. Given that SINTBAD and NAP1 also contain N-terminal coiled-coil regions it is an attractive hypothesis that C6 interacts with these molecules using the same domain, perhaps preventing them from interacting with a common binding partner, for example the non-canonical IKKs. However it is entirely possible that C6 binds to the three adaptors using different domains and potentially different mechanisms to inhibit IRF3 activation.

There are still many unanswered questions with regards to the signalling pathways that converge on the non-canonical IKKs and subsequently activate IRF3, some of which may be answered by understanding the mechanism by which viral proteins like C6 exert their immunomodulatory functions. Currently crystal structures for TANK, NAP1 and SINTBAD are not available, only a small peptide of TANK in complex with TRAF3 (Li et al, 2002). Producing soluble C6 and the adaptor proteins in *E. coli* has proved difficult, however co-expressing them may prove fruitful. It is currently not known if the interaction between C6 and these adaptors is direct and producing bacterially expressed proteins would help answer this question. In addition both TBK1 (Chien et al, 2006) and IKKε (Boehm et al, 2007) are oncogenic kinases and have been linked to cancer. It is currently unclear whether TANK, SINTBAD or NAP1 are involved in this process but if they are, inhibiting their activity by over-expressing C6 may provide some therapeutic benefit.

Despite the lack of binding between LUC-tagged C6 and the non-canonical IKK adaptor proteins, an interaction was observed with Ub (Figure 5.10). UBR1, a Ub ligase was identified as a potential C6 binding partner by mass spectrometry (Figure 6.5) and therefore it could be hypothesised that C6 is itself ubiquitinated, and potentially by UBR1. Prelimary data however suggests that the interaction between Ub and C6 is non-covalent and therefore it is unlikely that C6 is post-translationally modified in this way (C. Maluquer de Motes, unpublished results). A second hypothesis is that the interaction between C6 and TANK is not direct but is via Ub moieties on TANK. In support of this hypothesis TANK was found to be ubiquitinated between residues 71 and 110, which coincides with the region of TANK necessary for its interaction with C6 (Gatot et al, 2007). Ubiqutination of NAP1 and SINTBAD has not been described, although both proteins are able to interact with Ub (Thurston et al, 2009).

8.4 A non-biased approach for identifying C6 binding partners

The construction of a recombinant virus expressing TAP-tagged C6 has proved a very useful tool for identifying novel binding partners of this viral protein – both cellular partners and viral. In this study novel interaction partners were identified from the human HCT116 cell line and at only one time point p.i.. It would be interesting to continue this work further using

different cell lines from different species and with harvesting of the cells at various time points p.i. to ascertain whether the pattern of co-immunoprecipitated proteins differed.

Multiple novel binding partners for C6 were identified by mass spectrometry with very different cellular functions. Two of these; SMARCC1 (Figure 6.7) and UBR1 (Figure 6.8) were confirmed as interaction partners by conventional IP assay. It seems therefore that C6 is likely to have multiple functions during viral infection. Whilst this is very common for small RNA viruses with a highly limited coding capacity it is interesting that VACV, a large DNA virus with considerably larger coding capacity should express proteins with multiple binding partners and functions. Another example of a VACV protein with multiple functions is Bcl-2 family member N1, which is both anti-apoptotic (Cooray et al, 2007) and abrogates NF-κB signalling (DiPerna et al, 2004). It is possible that new functions for already characterised VACV proteins will be discovered in the future.

The Ub N-end rule of protein degradation, which UBR1, UBR2 and Hsp70 contribute to, is involved in the degradation of a number of viral proteins and potentially contributes to the host defence against viral infection. As preliminary data demonstrated C6 to interact with Ub, but it was not covalently linked to this moiety, an alternative hypothesis is that C6 binds to UBR1 and/or other members of the N-end rule pathway and hijacks them to degrade cellular proteins to the benefit of the virus, for example those important for an antiviral innate immune response. Few cellular targets of the N-end rule pathway have been identified, for example RGS4 and RGS5, which are negative regulators of specific G proteins whose functions include cardiac growth and angiogenesis (Lee et al, 2005), but these proteins have not currently been linked to the immune response. Although there are numerous examples of viral proteins that interfere with the host Ub system, mimicking its functions to degrade proteins to the advantage of the virus (recently reviewed in (Isaacson & Ploegh, 2009; Viswanathan et al, 2010)), such as the orthopoxvirus ankyrin-F-box-like and BTB-kelch-like protein families that interact with the cellular Cullin-1- and Cullin-3-containing Ub-protein ligases, respectively (Shchelkunov, 2010), none have been described that target UBR1 and the N-end rule of protein degradation. Thus VACV may have evolved a novel mechanism to modulate the Ub system through C6.

SMARCC1 is a core component of the SWI/SNF complex that remodels chromatin and controls the expression of numerous genes (Wang et al, 1996). This complex is important during development and a number of components have also been linked to cancer (Klochendler-Yeivin et al, 2002). The SWI/SNF complex also plays a crucial role in the immune response. It is involved in IFNβ induction, the expression of IFNα target genes, CD4 T cell repression and T cell activation (Chi, 2004). C6 is able to inhibit both IFNβ induction and ISRE induction downstream of IFNα, and its binding to SMARCC1 may mechanistically explain these functions. Inhibition of IFNβ induction by C6 has been attributed in this study to its ability to inhibit the IRF3 innate immune signalling pathway. As C6 was not able to inhibit IFNβ induction downstream of IRF3 over-expression, it is presumed that this viral protein does not exert its effects in the nucleus. Indeed, in the presence of C6 IRF3 translocation to the nucleus in response to SeV infection was inhibited (Unterholzner et al, 2011). It is possible however that over-expressing IRF3, or a constitutively active form of the protein (Unterholzner et al, 2011) circumvents the need for the SWI/SNF complex at the IFNβ promoter, or the reporter plasmid does not require this complex for expression of the luciferase gene. These dependencies may also be cell-type specific. Again, it therefore remains possible that C6 inhibits IFNβ induction by multiple methods.

In addition the SWI/SNF complex has also been linked to the AP-1 transcription factor. Increased expression of the SWI/SNF complex resulted in enhanced AP-1 activity, production of AP-1-dependent cytokines such as IFNγ, IL-4 and IL-17 and proliferation of peripheral T cells (Jeong et al, 2009). These finding were in T cells, which are not readily infected with VACV (Zhao et al, 2009), however whether the SWI/SNF complex affects AP-1 activity and subsequent pro-inflammatory and antiviral cytokine production in other cells remains to be tested.

Given the important roles of the SWI/SNF complex in the immune system this is potentially a good candidate for exploitation by viruses. Indeed, the HIV integrase was shown to directly bind SWI/SNF component BAF47 (Kalpana et al, 1994). Currently it is not clear what advantage this provides the virus but it has been suggested that HIV-1 may exploit the SWI/SNF complex during the process of viral integration into the host genome. SMARCC1 is a core component of the SWI/SNF complex, functioning as a scaffold protein that controls the stability of the complex by directly interacting with the other major components. An

alteration in the expression or activity of SMARCC1 causes changes in the overall level of the SWI/SNF complex and its activity (Sohn et al, 2007), making this protein a good target for modulation by a virus.

Ro ribonucleoprotein (RNP) complexes are small cytoplasmic particles that were initially identified as major targets of autoantibodies in patients with systemic lupus erythematosus and Sjögren's syndrome (Youinou et al, 1994). The human Ro RNP is composed of one molecule of a small non-coding Y RNA and two proteins; Ro60 (TROVE2) and La. TROVE2, to which C6 may bind to, has been described to be necessary for nuclear export and stabilization of Y RNAs (Deutscher et al, 1988). The La protein on the other hand was found to stabilise newly synthesized RNA polymerase III transcripts and to protect them from exonuclease attack (Wolin & Cedervall, 2002). In addition La is involved in cap-independent translation of cellular and viral mRNAs, including RNAs from adenovirus and Epstein-Barr virus (Wolin & Cedervall, 2002). It is possible therefore that through the binding of C6 to TROVE2, VACV may exploit the cellular Ro RNP complex for the transcription and/or translation, or stability of viral RNAs.

Finally, VACV protein I1, encoded by the *I1L* gene, was identified as a potential binding partner for C6. I1 has DNA-binding activity, is packaged in the virion core and is essential for the assembly of mature viruses (Klemperer et al, 1997). Small amounts of C6 protein were detected in the virion core (Chung et al, 2006) and it is possible that C6 is packaged by its interaction with I1. The significance of this interaction is not understood, but the presence of C6 within the virion might be of an advantage to the virus akin to the VH1 phosphatase in which cellular signalling pathways can be silenced before early virus gene expression.

A yeast two-hybrid screen of VACV-host protein-protein interactions identified keratin 4 (KRT4), programmed cell death 6 interacting protein (PDCD6IP) and troponin I (TNNI2) as potential C6 interaction partners (Zhang et al, 2009). Neither PDCD6IP nor TNNI2 were identified by mass spectrometry in this study. Multiple hits however were obtained for various forms of keratin, but this is likely to be keratin contamination routinely observed in mass spectrometry analysis due to the high sensitivity of the technique.

8.5 The contribution of C6 to VACV virulence

The construction of vΔC6 in this study, and MVA-BΔC6 (Garcia-Arriaza et al, 2011) demonstrated that C6 is a non-essential VACV protein. Further, in cell culture both WR and MVA lacking C6 were found to replicate to equivalent titres as their wild type equivalents. *In vivo* however, recombinant WR viruses lacking C6 expression (vΔC6 and vC6FS) were found to be attenuated in both the i.n. (Figure 7.4) and i.d. (Figure 7.12) models of infection, suggesting an important role for this protein during the infection of an animal. With almost 200 genes it is intriguing that the deletion of a single ORF can have drastic effects to virulence in an animal model of infection. The deletion of several genes involved in innate immune modulation results in viral attenuation in one, or more models of murine infection, presumably because in their absence an improved immune response to the pathogen is mounted, thus enhancing viral clearance. In the case of C6 viral titres in the lung following i.n. infection were indistinguishable between recombinant viruses at the time points tested (Figure 7.5C). These data were obtained from a single experiment and require further analysis, including viral titres in the ear following i.d. infection. The deletion of immune modulators however does not always lead to viral attenuation *in vivo*, for example the deletion of B15 leads to an exacerbated response due to higher levels of IL-1β that actually enhance pathology in mice in the i.n. model (Alcami & Smith, 1992). Further, the deletion of B13 leads to a larger lesion size in the i.d. model of murine infection (Tscharke et al, 2002). These experiments demonstrate the complexities of the immune response and the fine balance between a beneficial immune response and immune pathology.

What is not clear from this study is whether it is the innate immunomodulatory role of C6 that leads to viral attenuation in its absence, or in fact any other function that C6 plays during viral infection. Indeed C6 was found to interact with a number of cellular proteins and any or all of these interactions may contribute to the attenuation of vΔC6 and vC6FS *in vivo*. Testing which of these interactions contributes, or is most important during *in vivo* infection is challenging, but may be aided by infecting mice null for the identified C6 interaction partners, or with mutants of C6 that are able to interact with certain cellular proteins and not others. The structure of C6 in complex with its cellular binding partners would be very advantageous. These kinds of experiments have been completed recently with mutants of N1

that lack either anti-apoptotic ability, or anti-NF-κB signalling ability and demonstrated that the anti-signalling ability of N1 is more important *in vivo* (Maluquer de Motes et al, 2011).

In the i.n. model of infection more infiltrating neutrophils (Figure 7.11A) and macrophages (Figure 7.11C) were found in the spleens of mice infected with vΔC6 compared to the wild-type and revertant viruses at day 2 p.i.. By day 4 p.i. no differences were observed, suggesting that the effects of C6 are exerted very quickly, consistent with the rapid onset of the innate immune response. Differences in macrophage and neutrophil populations might also exist in the lung and BAL of vΔC6-infected animals at early time points p.i. and this remains to be tested. Increased numbers of these innate immune cell populations may contribute to the attenuated phenotype of the knockout virus, because these cells play a crucial role in the defence against VACV infection and macrophages in particular are important for activating the adaptive immune response. Macrophages and neutrophils are attracted to the site of infection by pro-inflammatory cytokines and chemokines, such as CCL2, CCL5 and CXCL10 for macrophages and members of the CXC group of chemokines for neutrophils (reviewed in (Laing & Secombes, 2004)). The expression of many of these genes is IRF3-dependent, and for CCL5 and CXCL10, their expression or production was reduced in the presence of C6 *in vitro* in this study (Figure 4.7). Further, human macrophages infected with MVA-BΔC6 showed enhanced transcription of CCL2 (Garcia-Arriaza et al, 2011). *In vivo* C6 may therefore act to suppress the production of these proteins, resulting in reduced recruitment of innate immune cells such as macrophages and neutrophils.

VACVs (strain WR) lacking C6 expression were also attenuated in the i.d. model of murine infection (Figure 7.12), although currently the mechanism of this attenuation has not been investigated. Given that C6 may be modulating macrophage and neutrophil recruitment in the i.n. model of infection, these cell populations may also be altered in the ear of i.d.-infected animals and this requires testing experimentally. Differences in the local expression and production of pro-inflammatory cytokines and chemokines, and the expression of type I IFN-inducible genes in the VACV lesion could also be tested.

In this study a virus lacking C6 expression was shown to provide enhanced protection against a lethal challenge dose of VACV WR, indicating these viruses to be better vaccines, with

enhanced immunogenicity compared to vaccination with wild-type WR (Figure 7.13). These data indicate that C6 may act to dampen parts of the immune response that contribute to immune memory. Enhanced immunogenicity has also been observed following the deletion of a number of other VACV proteins with immunomodulatory functions including A41 (Clark et al, 2006), an A41 and B16 double deletion (Garcia-Arriaza et al, 2010), A35 (Rehm & Roper, 2011), C21 (Girgis et al, 2011), B15 (Staib et al, 2005) and N1 (H. Ren et al, unpublished results). Removal of immunomodulatory genes, however does not always lead to enhanced immunogenicity in a challenge experiment, as observed for C16 (Fahy et al, 2008).

Currently, the mechanism of this enhanced immunogenicity is not known, but given that a poorer neutralising Ab response was observed following vaccination with a virus lacking C6 expression (Figure 7.14A), the enhanced immunogenicity may reflect an enhancement in T cell-mediated immunological memory. Supporting this hypothesis, Garcia-Arriaza et al found significantly enhanced HIV-1-specific CD4+ and CD8+ T cell memory responses when mice were vaccinated with MVA-BΔC6 compared to MVA-B (Garcia-Arriaza et al, 2011). The authors of this study did not measure T cell memory responses to VACV antigens however. Given that C6 expressed from MVA is also able to inhibit IFNβ induction (Figure 4.3) and thus dampen the immune response this is a good candidate gene for rational deletion from the MVA genome to potentially enhance immunogenicity of this vaccine vector. This hypothesis has been tested by Garcia-Arriaza et al and although enhanced HIV-1 memory responses were measured with MVA-BΔC6, this virus remains to be tested in an HIV challenge study to confirm enhanced protection over wild-type MVA-B (Garcia-Arriaza et al, 2011).

Thus far no differences have been observed in the number of T memory cells present in mice vaccinated with the various C6 recombinant viruses (Figure 7.15), or their ability to produce IFNγ (Figure 7.17) in response to VACV peptides, or to kill VACV-infected target cells (Figure 7.16). These experiments were specific for the activity of CD8+ T cells and therefore experiments examining the function of other T cell subsets, such as CD4+ T cells, T_{H17} cells, Treg cells or gamma-delta T cells should be considered. Other markers of immune memory could also be tested, for example Garcia-Arriaza et al used CD44 in conjunction with CD62L to examine memory populations by flow cytometry (Garcia-Arriaza et al, 2011). In addition to long-term protection offered by Ab and memory T cells, Thy1+ NK 'innate memory' cells from VACV-primed mice were shown to confer protection against challenge in the absence

of adaptive lymphocytes and thus are a further subset of immune cells to analyse (Gillard et al, 2011).

The SWI/SNF complex, to which C6 binds the SMARCC1 component, plays an important role in CD4/CD8-lineage bifurcation, repressing CD4+ T cell development and favouring CD8+ development (Chi, 2004). In addition it has been questioned whether the SWI/SNF complex plays a role in T_{H1}/T_{H2} cell polarization (Chi, 2004). T_{H1} cells aid the killing capacity of macrophages and CTLs whereas T_{H2} play an important role in the production of Ab. By inhibiting the SWI/SNF complex C6 may skew the immune response, potentially explaining why in the absence of this viral protein a lower Ab neutralisation function was measured.

8.6 Summary

In conclusion this study presents the *in vitro* and *in vivo* characterisation of VACV WR ORF *022* expressing protein C6. This protein is a predicted member of the VACV Bcl-2 protein family and like other members of this family C6 possesses immunomodulatory properties. C6 is a broad spectrum inhibitor of IRF3 activation, as well as an inhibitor of ISRE activation downstream of IFNα. Three adaptor proteins of the non-canonical IKK complex; TANK, SINTBAD and NAP1 were identified as C6 binding partners and may explain the ability of C6 to inhibit IRF3 activation. Furthermore UBR1, UBR2, Hsp70, SMARCC1, TROVE2 and VACV protein I1 were identified as C6 interaction partners by mass spectrometry. Why VACV may want to target these cellular proteins is currently unclear, however these data suggest that C6 has multiple functions during the course of a viral infection. *In vivo* C6 is a virulence factor because viruses lacking C6 expression were attenuated in both the i.n. and i.d. models of murine infection. In addition, a virus lacking C6 showed enhanced immunogenicity in a VACV challenge model, identifying this gene as a good target for removal to improve VACV as a vaccine vector. The mechanism of this enhanced immunogenicity is currently unclear, but presents exciting future work and highlights the important role of the innate immune response in shaping the outcome of the adaptive and subsequent memory immune response.

Bibliography

Ablasser A, Bauernfeind F, Hartmann G, Latz E, Fitzgerald KA, Hornung V (2009) RIG-I-dependent sensing of poly(dA:dT) through the induction of an RNA polymerase III-transcribed RNA intermediate. *Nat Immunol* **10**(10)**:** 1065-1072

Adli M, Baldwin AS (2006) IKK-i/IKKepsilon controls constitutive, cancer cell-associated NF-kappaB activity via regulation of Ser-536 p65/RelA phosphorylation. *J Biol Chem* **281**(37)**:** 26976-26984

Agalioti T, Lomvardas S, Parekh B, Yie J, Maniatis T, Thanos D (2000) Ordered recruitment of chromatin modifying and general transcription factors to the IFN-beta promoter. *Cell* **103**(4)**:** 667-678

Aguiar RS, Peterlin BM (2008) APOBEC3 proteins and reverse transcription. *Virus Res* **134**(1-2)**:** 74-85

Alcami A, Smith GL (1992) A soluble receptor for interleukin-1 beta encoded by vaccinia virus: a novel mechanism of virus modulation of the host response to infection. *Cell* **71**(1)**:** 153-167

Alcami A, Smith GL (1996) A mechanism for the inhibition of fever by a virus. *Proc Natl Acad Sci U S A* **93**(20)**:** 11029-11034

Alcami A, Symons JA, Collins PD, Williams TJ, Smith GL (1998) Blockade of chemokine activity by a soluble chemokine binding protein from vaccinia virus. *J Immunol* **160**(2)**:** 624-633

Alexopoulou L, Holt AC, Medzhitov R, Flavell RA (2001) Recognition of double-stranded RNA and activation of NF-kappaB by Toll-like receptor 3. *Nature* **413**(6857)**:** 732-738

Andersen J, VanScoy S, Cheng TF, Gomez D, Reich NC (2008) IRF-3-dependent and augmented target genes during viral infection. *Genes Immun* **9**(2)**:** 168-175

Andrejeva J, Childs KS, Young DF, Carlos TS, Stock N, Goodbourn S, Randall RE (2004) The V proteins of paramyxoviruses bind the IFN-inducible RNA helicase, mda-5, and inhibit its activation of the IFN-beta promoter. *Proc Natl Acad Sci U S A* **101**(49)**:** 17264-17269

Aoyagi M, Zhai D, Jin C, Aleshin AE, Stec B, Reed JC, Liddington RC (2007) Vaccinia virus N1L protein resembles a B cell lymphoma-2 (Bcl-2) family protein. *Protein Sci* **16**(1)**:** 118-124

Arase H, Saito T, Phillips JH, Lanier LL (2001) Cutting edge: the mouse NK cell-associated antigen recognized by DX5 monoclonal antibody is CD49b (alpha 2 integrin, very late antigen-2). *J Immunol* **167**(3)**:** 1141-1144

Arimoto K, Takahashi H, Hishiki T, Konishi H, Fujita T, Shimotohno K (2007) Negative regulation of the RIG-I signaling by the ubiquitin ligase RNF125. *Proc Natl Acad Sci U S A* **104**(18)**:** 7500-7505

Assarsson E, Greenbaum JA, Sundstrom M, Schaffer L, Hammond JA, Pasquetto V, Oseroff C, Hendrickson RC, Lefkowitz EJ, Tscharke DC, Sidney J, Grey HM, Head SR, Peters B, Sette A (2008) Kinetic analysis of a complete poxvirus transcriptome reveals an immediate-early class of genes. *Proc Natl Acad Sci U S A* **105**(6)**:** 2140-2145

Austyn JM, Gordon S (1981) F4/80, a monoclonal antibody directed specifically against the mouse macrophage. *Eur J Immunol* **11**(10)**:** 805-815

Baaten BJ, Li CR, Deiro MF, Lin MM, Linton PJ, Bradley LM (2010) CD44 regulates survival and memory development in Th1 cells. *Immunity* **32**(1)**:** 104-115

Bahar MW, Kenyon JC, Putz MM, Abrescia NG, Pease JE, Wise EL, Stuart DI, Smith GL, Grimes JM (2008) Structure and function of A41, a vaccinia virus chemokine binding protein. *PLoS Pathog* **4**(1)**:** e5

Balachandran S, Roberts PC, Brown LE, Truong H, Pattnaik AK, Archer DR, Barber GN (2000) Essential role for the dsRNA-dependent protein kinase PKR in innate immunity to viral infection. *Immunity* **13**(1)**:** 129-141

Baldick CJ, Jr., Moss B (1993) Characterization and temporal regulation of mRNAs encoded by vaccinia virus intermediate-stage genes. *J Virol* **67**(6)**:** 3515-3527

Ball LA (1995) Fidelity of homologous recombination in vaccinia virus DNA. *Virology* **209**(2)**:** 688-691

Baltimore D (1971) Expression of animal virus genomes. *Bacteriol Rev* **35**(3)**:** 235-241

Barlan AU, Griffin TM, McGuire KA, Wiethoff CM (2011) Adenovirus membrane penetration activates the NLRP3 inflammasome. *J Virol* **85**(1)**:** 146-155

Baroudy BM, Venkatesan S, Moss B (1982) Incompletely base-paired flip-flop terminal loops link the two DNA strands of the vaccinia virus genome into one uninterrupted polynucleotide chain. *Cell* **28**(2)**:** 315-324

Bartlett N, Symons JA, Tscharke DC, Smith GL (2002) The vaccinia virus N1L protein is an intracellular homodimer that promotes virulence. *J Gen Virol* **83**(Pt 8)**:** 1965-1976

Baxby D (1981) Jenner's smallpox vaccine. In *The Riddle of the Origin of Vaccinia Virus*. London: Heinemann

Beg AA, Finco TS, Nantermet PV, Baldwin AS, Jr. (1993) Tumor necrosis factor and interleukin-1 lead to phosphorylation and loss of I kappa B alpha: a mechanism for NF-kappa B activation. *Mol Cell Biol* **13**(6)**:** 3301-3310

Beg AA, Sha WC, Bronson RT, Ghosh S, Baltimore D (1995) Embryonic lethality and liver degeneration in mice lacking the RelA component of NF-kappa B. *Nature* **376**(6536)**:** 167-170

Bell JK, Botos I, Hall PR, Askins J, Shiloach J, Segal DM, Davies DR (2005) The molecular structure of the Toll-like receptor 3 ligand-binding domain. *Proc Natl Acad Sci U S A* **102**(31)**:** 10976-10980

Benfield CT, Mansur DS, McCoy LE, Ferguson BJ, Bahar MW, Oldring AP, Grimes JM, Stuart DI, Graham SC, Smith GL (2011) Mapping the IkappaB kinase beta (IKKbeta)-binding interface of the B14 protein, a vaccinia virus inhibitor of IKKbeta-mediated activation of nuclear factor kappaB. *J Biol Chem* **286**(23)**:** 20727-20735

Benko S, Magalhaes JG, Philpott DJ, Girardin SE (2010) NLRC5 limits the activation of inflammatory pathways. *J Immunol* **185**(3)**:** 1681-1691

Birbach A, Gold P, Binder BR, Hofer E, de Martin R, Schmid JA (2002) Signaling molecules of the NF-kappa B pathway shuttle constitutively between cytoplasm and nucleus. *J Biol Chem* **277**(13)**:** 10842-10851

Bishop KN, Holmes RK, Sheehy AM, Davidson NO, Cho SJ, Malim MH (2004) Cytidine deamination of retroviral DNA by diverse APOBEC proteins. *Curr Biol* **14**(15)**:** 1392-1396

Blanchard TJ, Alcami A, Andrea P, Smith GL (1998) Modified vaccinia virus Ankara undergoes limited replication in human cells and lacks several immunomodulatory proteins: implications for use as a human vaccine. *J Gen Virol* **79 (Pt 5):** 1159-1167

Boehm JS, Zhao JJ, Yao J, Kim SY, Firestein R, Dunn IF, Sjostrom SK, Garraway LA, Weremowicz S, Richardson AL, Greulich H, Stewart CJ, Mulvey LA, Shen RR, Ambrogio L, Hirozane-Kishikawa T, Hill DE, Vidal M, Meyerson M, Grenier JK, Hinkle G, Root DE, Roberts TM, Lander ES, Polyak K, Hahn WC (2007) Integrative genomic approaches identify IKBKE as a breast cancer oncogene. *Cell* **129**(6)**:** 1065-1079

Bonif M, Meuwis MA, Close P, Benoit V, Heyninck K, Chapelle JP, Bours V, Merville MP, Piette J, Beyaert R, Chariot A (2006) TNFalpha- and IKKbeta-mediated TANK/I-TRAF phosphorylation: implications for interaction with NEMO/IKKgamma and NF-kappaB activation. *Biochem J* **394**(Pt 3)**:** 593-603

Bonnard M, Mirtsos C, Suzuki S, Graham K, Huang J, Ng M, Itie A, Wakeham A, Shahinian A, Henzel WJ, Elia AJ, Shillinglaw W, Mak TW, Cao Z, Yeh WC (2000) Deficiency of T2K leads to apoptotic liver degeneration and impaired NF-kappaB-dependent gene transcription. *EMBO J* **19**(18)**:** 4976-4985

Boulter EA, Appleyard G (1973) Differences between extracellular and intracellular forms of poxvirus and their implications. *Prog Med Virol* **16:** 86-108

Bowie A, Kiss-Toth E, Symons JA, Smith GL, Dower SK, O'Neill LA (2000) A46R and A52R from vaccinia virus are antagonists of host IL-1 and toll-like receptor signaling. *Proc Natl Acad Sci U S A* **97**(18)**:** 10162-10167

Bowie AG, Unterholzner L (2008) Viral evasion and subversion of pattern-recognition receptor signalling. *Nature reviews* **8**(12)**:** 911-922

Boyden ED, Dietrich WF (2006) Nalp1b controls mouse macrophage susceptibility to anthrax lethal toxin. *Nat Genet* **38**(2)**:** 240-244

Boyle DB, Coupar BE (1988) A dominant selectable marker for the construction of recombinant poxviruses. *Gene* **65**(1)**:** 123-128

Brandt TA, Jacobs BL (2001) Both carboxy- and amino-terminal domains of the vaccinia virus interferon resistance gene, E3L, are required for pathogenesis in a mouse model. *J Virol* **75**(2)**:** 850-856

Breitbach CJ, Burke J, Jonker D, Stephenson J, Haas AR, Chow LQ, Nieva J, Hwang TH, Moon A, Patt R, Pelusio A, Le Boeuf F, Burns J, Evgin L, De Silva N, Cvancic S, Robertson T, Je JE, Lee YS, Parato K, Diallo JS, Fenster A, Daneshmand M, Bell JC, Kirn DH (2011) Intravenous delivery of a multi-mechanistic cancer-targeted oncolytic poxvirus in humans. *Nature* **477**(7362)**:** 99-102

Brinkmann V, Reichard U, Goosmann C, Fauler B, Uhlemann Y, Weiss DS, Weinrauch Y, Zychlinsky A (2004) Neutrophil extracellular traps kill bacteria. *Science* **303**(5663)**:** 1532-1535

Brooks DG, Trifilo MJ, Edelmann KH, Teyton L, McGavern DB, Oldstone MB (2006) Interleukin-10 determines viral clearance or persistence in vivo. *Nat Med* **12**(11)**:** 1301-1309

Brooks MA, Ali AN, Turner PC, Moyer RW (1995) A rabbitpox virus serpin gene controls host range by inhibiting apoptosis in restrictive cells. *J Virol* **69**(12)**:** 7688-7698

Broyles SS (2003) Vaccinia virus transcription. *J Gen Virol* **84**(Pt 9)**:** 2293-2303

Brum LM, Lopez MC, Varela JC, Baker HV, Moyer RW (2003) Microarray analysis of A549 cells infected with rabbitpox virus (RPV): a comparison of wild-type RPV and RPV deleted for the host range gene, SPI-1. *Virology* **315**(2)**:** 322-334

Brutkiewicz RR, Klaus SJ, Welsh RM (1992) Window of vulnerability of vaccinia virus-infected cells to natural killer (NK) cell-mediated cytolysis correlates with enhanced NK cell triggering and is concomitant with a decrease in H-2 class I antigen expression. *Nat Immun* **11**(4)**:** 203-214

Bukowski JF, Woda BA, Habu S, Okumura K, Welsh RM (1983) Natural killer cell depletion enhances virus synthesis and virus-induced hepatitis in vivo. *J Immunol* **131**(3)**:** 1531-1538

Burckstummer T, Baumann C, Bluml S, Dixit E, Durnberger G, Jahn H, Planyavsky M, Bilban M, Colinge J, Bennett KL, Superti-Furga G (2009) An orthogonal proteomic-genomic screen identifies AIM2 as a cytoplasmic DNA sensor for the inflammasome. *Nat Immunol* **10**(3)**:** 266-272

Carswell EA, Old LJ, Kassel RL, Green S, Fiore N, Williamson B (1975) An endotoxin-induced serum factor that causes necrosis of tumors. *Proc Natl Acad Sci U S A* **72**(9)**:** 3666-3670

Carter GC, Law M, Hollinshead M, Smith GL (2005) Entry of the vaccinia virus intracellular mature virion and its interactions with glycosaminoglycans. *J Gen Virol* **86**(Pt 5)**:** 1279-1290

Carter GC, Rodger G, Murphy BJ, Law M, Krauss O, Hollinshead M, Smith GL (2003) Vaccinia virus cores are transported on microtubules. *J Gen Virol* **84**(Pt 9)**:** 2443-2458

Chang HW, Watson JC, Jacobs BL (1992) The E3L gene of vaccinia virus encodes an inhibitor of the interferon-induced, double-stranded RNA-dependent protein kinase. *Proc Natl Acad Sci U S A* **89**(11)**:** 4825-4829

Chariot A, Leonardi A, Muller J, Bonif M, Brown K, Siebenlist U (2002) Association of the adaptor TANK with the I kappa B kinase (IKK) regulator NEMO connects IKK complexes with IKK epsilon and TBK1 kinases. *J Biol Chem* **277**(40)**:** 37029-37036

Chau TL, Gioia R, Gatot JS, Patrascu F, Carpentier I, Chapelle JP, O'Neill L, Beyaert R, Piette J, Chariot A (2008) Are the IKKs and IKK-related kinases TBK1 and IKK-epsilon similarly activated? *Trends Biochem Sci* **33**(4)**:** 171-180

Chen RA, Jacobs N, Smith GL (2006a) Vaccinia virus strain Western Reserve protein B14 is an intracellular virulence factor. *J Gen Virol* **87**(Pt 6)**:** 1451-1458

Chen RA, Ryzhakov G, Cooray S, Randow F, Smith GL (2008) Inhibition of IkappaB kinase by vaccinia virus virulence factor B14. *PLoS Pathog* **4**(2)**:** e22

Chen Z, Earl P, Americo J, Damon I, Smith SK, Zhou YH, Yu F, Sebrell A, Emerson S, Cohen G, Eisenberg RJ, Svitel J, Schuck P, Satterfield W, Moss B, Purcell R (2006b) Chimpanzee/human mAbs to vaccinia virus B5 protein neutralize vaccinia and smallpox viruses and protect mice against vaccinia virus. *Proc Natl Acad Sci U S A* **103**(6)**:** 1882-1887

Cheng G, Baltimore D (1996) TANK, a co-inducer with TRAF2 of TNF- and CD 40L-mediated NF-kappaB activation. *Genes Dev* **10**(8)**:** 963-973

Chi T (2004) A BAF-centred view of the immune system. *Nature reviews* **4**(12)**:** 965-977

Chien Y, Kim S, Bumeister R, Loo YM, Kwon SW, Johnson CL, Balakireva MG, Romeo Y, Kopelovich L, Gale M, Jr., Yeaman C, Camonis JH, Zhao Y, White MA (2006) RalB GTPase-mediated activation of the IkappaB family kinase TBK1 couples innate immune signaling to tumor cell survival. *Cell* **127**(1)**:** 157-170

Chin AI, Shu J, Shan Shi C, Yao Z, Kehrl JH, Cheng G (1999) TANK potentiates tumor necrosis factor receptor-associated factor-mediated c-Jun N-terminal kinase/stress-activated protein kinase activation through the germinal center kinase pathway. *Mol Cell Biol* **19**(10)**:** 6665-6672

Chiu YH, Macmillan JB, Chen ZJ (2009) RNA polymerase III detects cytosolic DNA and induces type I interferons through the RIG-I pathway. *Cell* **138**(3)**:** 576-591

Choe J, Kelker MS, Wilson IA (2005) Crystal structure of human toll-like receptor 3 (TLR3) ectodomain. *Science* **309**(5734)**:** 581-585

Chung CS, Chen CH, Ho MY, Huang CY, Liao CL, Chang W (2006) Vaccinia virus proteome: identification of proteins in vaccinia virus intracellular mature virion particles. *J Virol* **80**(5)**:** 2127-2140

Chung CS, Hsiao JC, Chang YS, Chang W (1998) A27L protein mediates vaccinia virus interaction with cell surface heparan sulfate. *J Virol* **72**(2)**:** 1577-1585

Clark K, Peggie M, Plater L, Sorcek RJ, Young ER, Madwed JB, Hough J, McIver EG, Cohen P (2011) Novel cross-talk within the IKK family controls innate immunity. *Biochem J* **434**(1)**:** 93-104

Clark RH, Kenyon JC, Bartlett NW, Tscharke DC, Smith GL (2006) Deletion of gene A41L enhances vaccinia virus immunogenicity and vaccine efficacy. *J Gen Virol* **87**(Pt 1)**:** 29-38

Claudio E, Brown K, Park S, Wang H, Siebenlist U (2002) BAFF-induced NEMO-independent processing of NF-kappa B2 in maturing B cells. *Nat Immunol* **3**(10)**:** 958-965

Colamonici OR, Domanski P, Sweitzer SM, Larner A, Buller RM (1995) Vaccinia virus B18R gene encodes a type I interferon-binding protein that blocks interferon alpha transmembrane signaling. *J Biol Chem* **270**(27)**:** 15974-15978

Comeau MR, Johnson R, DuBose RF, Petersen M, Gearing P, VandenBos T, Park L, Farrah T, Buller RM, Cohen JI, Strockbine LD, Rauch C, Spriggs MK (1998) A poxvirus-encoded semaphorin induces cytokine production from monocytes and binds to a novel cellular semaphorin receptor, VESPR. *Immunity* **8**(4)**:** 473-482

Coope HJ, Atkinson PG, Huhse B, Belich M, Janzen J, Holman MJ, Klaus GG, Johnston LH, Ley SC (2002) CD40 regulates the processing of NF-kappaB2 p100 to p52. *EMBO J* **21**(20)**:** 5375-5385

Cooray S, Bahar MW, Abrescia NG, McVey CE, Bartlett NW, Chen RA, Stuart DI, Grimes JM, Smith GL (2007) Functional and structural studies of the vaccinia virus virulence factor N1 reveal a Bcl-2-like anti-apoptotic protein. *J Gen Virol* **88**(Pt 6)**:** 1656-1666

Cui J, Zhu L, Xia X, Wang HY, Legras X, Hong J, Ji J, Shen P, Zheng S, Chen ZJ, Wang RF (2010) NLRC5 negatively regulates the NF-kappaB and type I interferon signaling pathways. *Cell* **141**(3)**:** 483-496

Czerny CP, Eis-Hubinger AM, Mayr A, Schneweis KE, Pfeiff B (1991) Animal poxviruses transmitted from cat to man: current event with lethal end. *Zentralbl Veterinarmed B* **38**(6)**:** 421-431

Dai P, Cao H, Merghoub T, Avogadri F, Wang W, Parikh T, Fang CM, Pitha PM, Fitzgerald KA, Rahman MM, McFadden G, Hu X, Houghton AN, Shuman S, Deng L (2011) Myxoma virus induces type I IFN production in murine plasmacytoid dendritic cells via a TLR9/MyD88, IRF5/IRF7, and IFNAR-dependent pathway. *J Virol*

Danoff TM, Lalley PA, Chang YS, Heeger PS, Neilson EG (1994) Cloning, genomic organization, and chromosomal localization of the Scya5 gene encoding the murine chemokine RANTES. *J Immunol* **152**(3)**:** 1182-1189

Davies MV, Elroy-Stein O, Jagus R, Moss B, Kaufman RJ (1992) The vaccinia virus K3L gene product potentiates translation by inhibiting double-stranded-RNA-activated protein kinase and phosphorylation of the alpha subunit of eukaryotic initiation factor 2. *J Virol* **66**(4)**:** 1943-1950

de Groot RJ, Rumenapf T, Kuhn RJ, Strauss EG, Strauss JH (1991) Sindbis virus RNA polymerase is degraded by the N-end rule pathway. *Proc Natl Acad Sci U S A* **88**(20)**:** 8967-8971

Dejardin E, Droin NM, Delhase M, Haas E, Cao Y, Makris C, Li ZW, Karin M, Ware CF, Green DR (2002) The lymphotoxin-beta receptor induces different patterns of gene expression via two NF-kappaB pathways. *Immunity* **17**(4)**:** 525-535

Delaloye J, Roger T, Steiner-Tardivel QG, Le Roy D, Knaup Reymond M, Akira S, Petrilli V, Gomez CE, Perdiguero B, Tschopp J, Pantaleo G, Esteban M, Calandra T (2009) Innate immune sensing of modified vaccinia virus Ankara (MVA) is mediated by TLR2-TLR6, MDA-5 and the NALP3 inflammasome. *PLoS Pathog* **5**(6)**:** e1000480

Deng L, Wang C, Spencer E, Yang L, Braun A, You J, Slaughter C, Pickart C, Chen ZJ (2000) Activation of the IkappaB kinase complex by TRAF6 requires a dimeric ubiquitin-conjugating enzyme complex and a unique polyubiquitin chain. *Cell* **103**(2)**:** 351-361

Deutscher SL, Harley JB, Keene JD (1988) Molecular analysis of the 60-kDa human Ro ribonucleoprotein. *Proc Natl Acad Sci U S A* **85**(24)**:** 9479-9483

DiDonato JA, Hayakawa M, Rothwarf DM, Zandi E, Karin M (1997) A cytokine-responsive IkappaB kinase that activates the transcription factor NF-kappaB. *Nature* **388**(6642)**:** 548-554

Diebold SS, Kaisho T, Hemmi H, Akira S, Reis e Sousa C (2004) Innate antiviral responses by means of TLR7-mediated recognition of single-stranded RNA. *Science* **303**(5663)**:** 1529-1531

DiPerna G, Stack J, Bowie AG, Boyd A, Kotwal G, Zhang Z, Arvikar S, Latz E, Fitzgerald KA, Marshall WL (2004) Poxvirus protein N1L targets the I-kappaB kinase complex, inhibits signaling to NF-kappaB by the tumor necrosis factor superfamily of receptors, and inhibits NF-kappaB and IRF3 signaling by toll-like receptors. *J Biol Chem* **279**(35)**:** 36570-36578

Dixit E, Boulant S, Zhang Y, Lee AS, Odendall C, Shum B, Hacohen N, Chen ZJ, Whelan SP, Fransen M, Nibert ML, Superti-Furga G, Kagan JC (2010) Peroxisomes are signaling platforms for antiviral innate immunity. *Cell* **141**(4)**:** 668-681

Dobbelstein M, Shenk T (1996) Protection against apoptosis by the vaccinia virus SPI-2 (B13R) gene product. *J Virol* **70**(9)**:** 6479-6485

Doceul V, Hollinshead M, van der Linden L, Smith GL (2010) Repulsion of superinfecting virions: a mechanism for rapid virus spread. *Science* **327**(5967)**:** 873-876

Dorfleutner A, Talbott SJ, Bryan NB, Funya KN, Rellick SL, Reed JC, Shi X, Rojanasakul Y, Flynn DC, Stehlik C (2007) A Shope Fibroma virus PYRIN-only protein modulates the host immune response. *Virus Genes* **35**(3)**:** 685-694

Douglas AE, Corbett KD, Berger JM, McFadden G, Handel TM (2007) Structure of M11L: A myxoma virus structural homolog of the apoptosis inhibitor, Bcl-2. *Protein Sci* **16**(4)**:** 695-703

Elco CP, Guenther JM, Williams BR, Sen GC (2005) Analysis of genes induced by Sendai virus infection of mutant cell lines reveals essential roles of interferon regulatory factor 3, NF-kappaB, and interferon but not toll-like receptor 3. *J Virol* **79**(7)**:** 3920-3929

Essbauer S, Pfeffer M, Meyer H (2010) Zoonotic poxviruses. *Vet Microbiol* **140**(3-4)**:** 229-236

Eswar N, Webb B, Marti-Renom MA, Madhusudhan MS, Eramian D, Shen MY, Pieper U, Sali A (2006) Comparative protein structure modeling using Modeller. *Curr Protoc Bioinformatics* **Chapter 5:** Unit 5 6

Everett H, Barry M, Lee SF, Sun X, Graham K, Stone J, Bleackley RC, McFadden G (2000) M11L: a novel mitochondria-localized protein of myxoma virus that blocks apoptosis of infected leukocytes. *J Exp Med* **191**(9)**:** 1487-1498

Fahy AS, Clark RH, Glyde EF, Smith GL (2008) Vaccinia virus protein C16 acts intracellularly to modulate the host response and promote virulence. *J Gen Virol* **89**(Pt 10)**:** 2377-2387

Falkner FG, Moss B (1988) Escherichia coli gpt gene provides dominant selection for vaccinia virus open reading frame expression vectors. *J Virol* **62**(6)**:** 1849-1854

Faustin B, Lartigue L, Bruey JM, Luciano F, Sergienko E, Bailly-Maitre B, Volkmann N, Hanein D, Rouiller I, Reed JC (2007) Reconstituted NALP1 inflammasome reveals two-step mechanism of caspase-1 activation. *Mol Cell* **25**(5)**:** 713-724

Fenner F, Anderson DA, Arita I, Jezek Z, Ladnyi ID (1988) Smallpox and its Eradication. *Geneva: World Health Organisation*

Fensterl V, Sen GC (2009) Interferons and viral infections. *Biofactors* **35**(1)**:** 14-20

Fernandes-Alnemri T, Yu JW, Datta P, Wu J, Alnemri ES (2009) AIM2 activates the inflammasome and cell death in response to cytoplasmic DNA. *Nature* **458**(7237)**:** 509-513

Fernandes-Alnemri T, Yu JW, Juliana C, Solorzano L, Kang S, Wu J, Datta P, McCormick M, Huang L, McDermott E, Eisenlohr L, Landel CP, Alnemri ES (2010) The AIM2 inflammasome is critical for innate immunity to Francisella tularensis. *Nat Immunol* **11**(5)**:** 385-393

Ferrer PE, Potthoff S, Kirschnek S, Gasteiger G, Kastenmuller W, Ludwig H, Paschen SA, Villunger A, Sutter G, Drexler I, Hacker G (2011) Induction of Noxa-Mediate Apoptosis by Modified Vaccinia Virus Ankara Depends on Viral Recognition by Cytosolic Helicases,

Leading to IRF-3/IFN-β-Dependent Indcution of Pro-Apoptotic Noxa *PLoS Pathog* **7**(6)**:** e1002083

Finn RD, Tate J, Mistry J, Coggill PC, Sammut SJ, Hotz HR, Ceric G, Forslund K, Eddy SR, Sonnhammer EL, Bateman A (2008) The Pfam protein families database. *Nucleic Acids Res* **36**(Database issue)**:** D281-288

Finnie NJ, Gottlieb TM, Blunt T, Jeggo PA, Jackson SP (1995) DNA-dependent protein kinase activity is absent in xrs-6 cells: implications for site-specific recombination and DNA double-strand break repair. *Proc Natl Acad Sci U S A* **92**(1)**:** 320-324

Fitzgerald KA, McWhirter SM, Faia KL, Rowe DC, Latz E, Golenbock DT, Coyle AJ, Liao SM, Maniatis T (2003) IKKepsilon and TBK1 are essential components of the IRF3 signaling pathway. *Nat Immunol* **4**(5)**:** 491-496

Fleming TJ, Fleming ML, Malek TR (1993) Selective expression of Ly-6G on myeloid lineage cells in mouse bone marrow. RB6-8C5 mAb to granulocyte-differentiation antigen (Gr-1) detects members of the Ly-6 family. *J Immunol* **151**(5)**:** 2399-2408

Franca R, Belfiore A, Spadari S, Maga G (2007) Human DEAD-box ATPase DDX3 shows a relaxed nucleoside substrate specificity. *Proteins* **67**(4)**:** 1128-1137

Frischknecht F, Moreau V, Rottger S, Gonfloni S, Reckmann I, Superti-Furga G, Way M (1999) Actin-based motility of vaccinia virus mimics receptor tyrosine kinase signalling. *Nature* **401**(6756)**:** 926-929

Fujii Y, Shimizu T, Kusumoto M, Kyogoku Y, Taniguchi T, Hakoshima T (1999) Crystal structure of an IRF-DNA complex reveals novel DNA recognition and cooperative binding to a tandem repeat of core sequences. *EMBO J* **18**(18)**:** 5028-5041

Fujita F, Taniguchi Y, Kato T, Narita Y, Furuya A, Ogawa T, Sakurai H, Joh T, Itoh M, Delhase M, Karin M, Nakanishi M (2003) Identification of NAP1, a regulatory subunit of IkappaB kinase-related kinases that potentiates NF-kappaB signaling. *Mol Cell Biol* **23**(21)**:** 7780-7793

Funami K, Sasai M, Ohba Y, Oshiumi H, Seya T, Matsumoto M (2007) Spatiotemporal mobilization of Toll/IL-1 receptor domain-containing adaptor molecule-1 in response to dsRNA. *J Immunol* **179**(10)**:** 6867-6872

Gack MU, Shin YC, Joo CH, Urano T, Liang C, Sun L, Takeuchi O, Akira S, Chen Z, Inoue S, Jung JU (2007) TRIM25 RING-finger E3 ubiquitin ligase is essential for RIG-I-mediated antiviral activity. *Nature* **446**(7138)**:** 916-920

Garcia-Arriaza J, Najera JL, Gomez CE, Sorzano CO, Esteban M (2010) Immunogenic profiling in mice of a HIV/AIDS vaccine candidate (MVA-B) expressing four HIV-1 antigens and potentiation by specific gene deletions. *PLoS One* **5**(8)**:** e12395

Garcia-Arriaza J, Najera JL, Gomez CE, Tewabe N, Sorzano CO, Calandra T, Roger T, Esteban M (2011) A Candidate HIV/AIDS Vaccine (MVA-B) Lacking Vaccinia Virus Gene *C6L* Enhances Memory HIV-1-Specific T-Cell Responses. *PLoS One* **6**(8)**:** e24244

Gatot JS, Gioia R, Chau TL, Patrascu F, Warnier M, Close P, Chapelle JP, Muraille E, Brown K, Siebenlist U, Piette J, Dejardin E, Chariot A (2007) Lipopolysaccharide-mediated interferon regulatory factor activation involves TBK1-IKKepsilon-dependent Lys(63)-linked polyubiquitination and phosphorylation of TANK/I-TRAF. *J Biol Chem* **282**(43)**:** 31131-31146

Gedey R, Jin XL, Hinthong O, Shisler JL (2006) Poxviral regulation of the host NF-kappaB response: the vaccinia virus M2L protein inhibits induction of NF-kappaB activation via an ERK2 pathway in virus-infected human embryonic kidney cells. *J Virol* **80**(17)**:** 8676-8685

Gilfoy FD, Mason PW (2007) West Nile virus-induced interferon production is mediated by the double-stranded RNA-dependent protein kinase PKR. *J Virol* **81**(20)**:** 11148-11158

Gillard GO, Bivas-Benita M, Hovav AH, Grandpre LE, Panas MW, Seaman MS, Haynes BF, Letvin NL (2011) Thy1 Nk Cells from Vaccinia Virus-Primed Mice Confer Protection against Vaccinia Virus Challenge in the Absence of Adaptive Lymphocytes. *PLoS Pathog* **7**(8)**:** e1002141

Girgis NM, Dehaven BC, Xiao Y, Alexander E, Viner KM, Isaacs SN (2011) The Vaccinia virus complement control protein modulates adaptive immune responses during infection. *J Virol* **85**(6)**:** 2547-2556

Gitlin L, Barchet W, Gilfillan S, Cella M, Beutler B, Flavell RA, Diamond MS, Colonna M (2006) Essential role of mda-5 in type I IFN responses to polyriboinosinic:polyribocytidylic acid and encephalomyocarditis picornavirus. *Proc Natl Acad Sci U S A* **103**(22)**:** 8459-8464

Gloeckner CJ, Boldt K, Schumacher A, Roepman R, Ueffing M (2007) A novel tandem affinity purification strategy for the efficient isolation and characterisation of native protein complexes. *Proteomics* **7**(23)**:** 4228-4234

Gomez CE, Najera JL, Krupa M, Esteban M (2008) The poxvirus vectors MVA and NYVAC as gene delivery systems for vaccination against infectious diseases and cancer. *Curr Gene Ther* **8**(2)**:** 97-120

Gonzalez JM, Esteban M (2010) A poxvirus Bcl-2-like gene family involved in regulation of host immune response: sequence similarity and evolutionary history. *Virol J* **7:** 59

Gottlieb TM, Jackson SP (1993) The DNA-dependent protein kinase: requirement for DNA ends and association with Ku antigen. *Cell* **72**(1)**:** 131-142

Graham SC, Bahar MW, Cooray S, Chen RA, Whalen DM, Abrescia NG, Alderton D, Owens RJ, Stuart DI, Smith GL, Grimes JM (2008) Vaccinia virus proteins A52 and B14 Share a Bcl-2-like fold but have evolved to inhibit NF-kappaB rather than apoptosis. *PLoS Pathog* **4**(8)**:** e1000128

Grandvaux N, Servant MJ, tenOever B, Sen GC, Balachandran S, Barber GN, Lin R, Hiscott J (2002) Transcriptional profiling of interferon regulatory factor 3 target genes: direct involvement in the regulation of interferon-stimulated genes. *J Virol* **76**(11)**:** 5532-5539

Gratz MS, Suezer Y, Kremer M, Volz A, Majzoub M, Hanschmann KM, Kalinke U, Schwantes A, Sutter G (2011) N1L is an ectromelia virus virulence factor and essential for in vivo spread upon respiratory infection. *J Virol* **85**(7)**:** 3557-3569

Gubser C, Bergamaschi D, Hollinshead M, Lu X, van Kuppeveld FJ, Smith GL (2007) A new inhibitor of apoptosis from vaccinia virus and eukaryotes. *PLoS Pathog* **3**(2)**:** e17

Gubser C, Hue S, Kellam P, Smith GL (2004) Poxvirus genomes: a phylogenetic analysis. *J Gen Virol* **85**(Pt 1)**:** 105-117

Guerra S, Caceres A, Knobeloch KP, Horak I, Esteban M (2008) Vaccinia virus E3 protein prevents the antiviral action of ISG15. *PLoS Pathog* **4**(7)**:** e1000096

Guo B, Cheng G (2007) Modulation of the interferon antiviral response by the TBK1/IKKi adaptor protein TANK. *J Biol Chem* **282**(16)**:** 11817-11826

Haga IR, Bowie AG (2005) Evasion of innate immunity by vaccinia virus. *Parasitology* **130 Suppl:** S11-25

Halle A, Hornung V, Petzold GC, Stewart CR, Monks BG, Reinheckel T, Fitzgerald KA, Latz E, Moore KJ, Golenbock DT (2008) The NALP3 inflammasome is involved in the innate immune response to amyloid-beta. *Nat Immunol* **9**(8)**:** 857-865

Haller O, Kochs G (2011) Human MxA protein: an interferon-induced dynamin-like GTPase with broad antiviral activity. *J Interferon Cytokine Res* **31**(1)**:** 79-87

Hanson D, Diven DG (2003) Molluscum contagiosum. *Dermatol Online J* **9**(2)**:** 2

Harris J, Oliere S, Sharma S, Sun Q, Lin R, Hiscott J, Grandvaux N (2006) Nuclear accumulation of cRel following C-terminal phosphorylation by TBK1/IKK epsilon. *J Immunol* **177**(4)**:** 2527-2535

Harte MT, Haga IR, Maloney G, Gray P, Reading PC, Bartlett NW, Smith GL, Bowie A, O'Neill LA (2003) The poxvirus protein A52R targets Toll-like receptor signaling complexes to suppress host defense. *J Exp Med* **197**(3)**:** 343-351

Hauer J, Puschner S, Ramakrishnan P, Simon U, Bongers M, Federle C, Engelmann H (2005) TNF receptor (TNFR)-associated factor (TRAF) 3 serves as an inhibitor of TRAF2/5-mediated activation of the noncanonical NF-kappaB pathway by TRAF-binding TNFRs. *Proc Natl Acad Sci U S A* **102**(8)**:** 2874-2879

Hemmi H, Takeuchi O, Sato S, Yamamoto M, Kaisho T, Sanjo H, Kawai T, Hoshino K, Takeda K, Akira S (2004) The roles of two IkappaB kinase-related kinases in lipopolysaccharide and double stranded RNA signaling and viral infection. *J Exp Med* **199**(12)**:** 1641-1650

Hiller G, Weber K (1985) Golgi-derived membranes that contain an acylated viral polypeptide are used for vaccinia virus envelopment. *J Virol* **55**(3)**:** 651-659

Hinthong O, Jin XL, Shisler JL (2008) Characterization of wild-type and mutant vaccinia virus M2L proteins' abilities to localize to the endoplasmic reticulum and to inhibit NF-kappaB activation during infection. *Virology* **373**(2)**:** 248-262

Hise AG, Tomalka J, Ganesan S, Patel K, Hall BA, Brown GD, Fitzgerald KA (2009) An essential role for the NLRP3 inflammasome in host defense against the human fungal pathogen Candida albicans. *Cell Host Microbe* **5**(5)**:** 487-497

Hoebe K, Beutler B (2004) LPS, dsRNA and the interferon bridge to adaptive immune responses: Trif, Tram, and other TIR adaptor proteins. *J Endotoxin Res* **10**(2)**:** 130-136

Holtmann H, Enninga J, Kalble S, Thiefes A, Dorrie A, Broemer M, Winzen R, Wilhelm A, Ninomiya-Tsuji J, Matsumoto K, Resch K, Kracht M (2001) The MAPK kinase kinase TAK1 plays a central role in coupling the interleukin-1 receptor to both transcriptional and RNA-targeted mechanisms of gene regulation. *J Biol Chem* **276**(5)**:** 3508-3516

Honda K, Yanai H, Negishi H, Asagiri M, Sato M, Mizutani T, Shimada N, Ohba Y, Takaoka A, Yoshida N, Taniguchi T (2005) IRF-7 is the master regulator of type-I interferon-dependent immune responses. *Nature* **434**(7034)**:** 772-777

Horng T, Barton GM, Medzhitov R (2001) TIRAP: an adapter molecule in the Toll signaling pathway. *Nat Immunol* **2**(9)**:** 835-841

Hornung V, Ablasser A, Charrel-Dennis M, Bauernfeind F, Horvath G, Caffrey DR, Latz E, Fitzgerald KA (2009) AIM2 recognizes cytosolic dsDNA and forms a caspase-1-activating inflammasome with ASC. *Nature* **458**(7237)**:** 514-518

Hornung V, Bauernfeind F, Halle A, Samstad EO, Kono H, Rock KL, Fitzgerald KA, Latz E (2008) Silica crystals and aluminum salts activate the NALP3 inflammasome through phagosomal destabilization. *Nat Immunol* **9**(8)**:** 847-856

Hornung V, Ellegast J, Kim S, Brzozka K, Jung A, Kato H, Poeck H, Akira S, Conzelmann KK, Schlee M, Endres S, Hartmann G (2006) 5'-Triphosphate RNA is the ligand for RIG-I. *Science* **314**(5801)**:** 994-997

Hsiao JC, Chung CS, Chang W (1999) Vaccinia virus envelope D8L protein binds to cell surface chondroitin sulfate and mediates the adsorption of intracellular mature virions to cells. *J Virol* **73**(10)**:** 8750-8761

Huang S, Hendriks W, Althage A, Hemmi S, Bluethmann H, Kamijo R, Vilcek J, Zinkernagel RM, Aguet M (1993) Immune response in mice that lack the interferon-gamma receptor. *Science* **259**(5102)**:** 1742-1745

Ichihashi Y (1996) Extracellular enveloped vaccinia virus escapes neutralization. *Virology* **217**(2)**:** 478-485

Ikeda F, Hecker CM, Rozenknop A, Nordmeier RD, Rogov V, Hofmann K, Akira S, Dotsch V, Dikic I (2007) Involvement of the ubiquitin-like domain of TBK1/IKK-i kinases in regulation of IFN-inducible genes. *EMBO J* **26**(14)**:** 3451-3462

Isaacs A, Lindenmann J (1957) Virus interference. I. The interferon. *Proc R Soc Lond B Biol Sci* **147**(927)**:** 258-267

Isaacs SN, Kotwal GJ, Moss B (1992) Vaccinia virus complement-control protein prevents antibody-dependent complement-enhanced neutralization of infectivity and contributes to virulence. *Proc Natl Acad Sci U S A* **89**(2)**:** 628-632

Isaacson MK, Ploegh HL (2009) Ubiquitination, ubiquitin-like modifiers, and deubiquitination in viral infection. *Cell Host Microbe* **5**(6)**:** 559-570

Ishii KJ, Coban C, Kato H, Takahashi K, Torii Y, Takeshita F, Ludwig H, Sutter G, Suzuki K, Hemmi H, Sato S, Yamamoto M, Uematsu S, Kawai T, Takeuchi O, Akira S (2006) A Toll-like receptor-independent antiviral response induced by double-stranded B-form DNA. *Nat Immunol* **7**(1)**:** 40-48

Ishii KJ, Kawagoe T, Koyama S, Matsui K, Kumar H, Kawai T, Uematsu S, Takeuchi O, Takeshita F, Coban C, Akira S (2008) TANK-binding kinase-1 delineates innate and adaptive immune responses to DNA vaccines. *Nature* **451**(7179)**:** 725-729

Ishikawa H, Barber GN (2008) STING is an endoplasmic reticulum adaptor that facilitates innate immune signalling. *Nature* **455**(7213)**:** 674-678

Ishikawa H, Ma Z, Barber GN (2009) STING regulates intracellular DNA-mediated, type I interferon-dependent innate immunity. *Nature* **461**(7265)**:** 788-792

Izaguirre A, Barnes BJ, Amrute S, Yeow WS, Megjugorac N, Dai J, Feng D, Chung E, Pitha PM, Fitzgerald-Bocarsly P (2003) Comparative analysis of IRF and IFN-alpha expression in human plasmacytoid and monocyte-derived dendritic cells. *J Leukoc Biol* **74**(6)**:** 1125-1138

Jacobs N, Bartlett NW, Clark RH, Smith GL (2008) Vaccinia virus lacking the Bcl-2-like protein N1 induces a stronger natural killer cell response to infection. *J Gen Virol* **89**(Pt 11)**:** 2877-2881

Janeway CA, Jr. (1989) Approaching the asymptote? Evolution and revolution in immunology. *Cold Spring Harb Symp Quant Biol* **54 Pt 1:** 1-13

Jeong SM, Lee C, Lee SK, Kim J, Seong RH (2009) The SWI/SNF chromatin-remodeling complex modulates peripheral T cell activation and proliferation by controlling AP-1 expression. *J Biol Chem* **285**(4)**:** 2340-2350

Jin MS, Kim SE, Heo JY, Lee ME, Kim HM, Paik SG, Lee H, Lee JO (2007) Crystal structure of the TLR1-TLR2 heterodimer induced by binding of a tri-acylated lipopeptide. *Cell* **130**(6)**:** 1071-1082

Johnston JB, Barrett JW, Nazarian SH, Goodwin M, Ricciuto D, Wang G, McFadden G (2005) A poxvirus-encoded pyrin domain protein interacts with ASC-1 to inhibit host inflammatory and apoptotic responses to infection. *Immunity* **23**(6)**:** 587-598

Jounai N, Takeshita F, Kobiyama K, Sawano A, Miyawaki A, Xin KQ, Ishii KJ, Kawai T, Akira S, Suzuki K, Okuda K (2007) The Atg5 Atg12 conjugate associates with innate antiviral immune responses. *Proc Natl Acad Sci U S A* **104**(35)**:** 14050-14055

Kaiser WJ, Offermann MK (2005) Apoptosis induced by the toll-like receptor adaptor TRIF is dependent on its receptor interacting protein homotypic interaction motif. *J Immunol* **174**(8)**:** 4942-4952

Kalpana GV, Marmon S, Wang W, Crabtree GR, Goff SP (1994) Binding and stimulation of HIV-1 integrase by a human homolog of yeast transcription factor SNF5. *Science* **266**(5193)**:** 2002-2006

Kalverda AP, Thompson GS, Vogel A, Schroder M, Bowie AG, Khan AR, Homans SW (2008) Poxvirus K7 Protein Adopts a Bcl-2 Fold: Biochemical Mapping of Its Interactions with Human DEAD Box RNA Helicase DDX3. *J Mol Biol*

Kanayama A, Seth RB, Sun L, Ea CK, Hong M, Shaito A, Chiu YH, Deng L, Chen ZJ (2004) TAB2 and TAB3 activate the NF-kappaB pathway through binding to polyubiquitin chains. *Mol Cell* **15**(4)**:** 535-548

Kang DC, Gopalkrishnan RV, Lin L, Randolph A, Valerie K, Pestka S, Fisher PB (2004) Expression analysis and genomic characterization of human melanoma differentiation associated gene-5, mda-5: a novel type I interferon-responsive apoptosis-inducing gene. *Oncogene* **23**(9)**:** 1789-1800

Kang DC, Gopalkrishnan RV, Wu Q, Jankowsky E, Pyle AM, Fisher PB (2002) mda-5: An interferon-inducible putative RNA helicase with double-stranded RNA-dependent ATPase activity and melanoma growth-suppressive properties. *Proc Natl Acad Sci U S A* **99**(2)**:** 637-642

Kanneganti TD (2010) Central roles of NLRs and inflammasomes in viral infection. *Nature reviews* **10**(10)**:** 688-698

Karupiah G, Buller RM, Van Rooijen N, Duarte CJ, Chen J (1996) Different roles for CD4+ and CD8+ T lymphocytes and macrophage subsets in the control of a generalized virus infection. *J Virol* **70**(12)**:** 8301-8309

Kates JR, McAuslan BR (1967) Poxvirus DNA-dependent RNA polymerase. *Proc Natl Acad Sci U S A* **58**(1)**:** 134-141

Kato H, Sato S, Yoneyama M, Yamamoto M, Uematsu S, Matsui K, Tsujimura T, Takeda K, Fujita T, Takeuchi O, Akira S (2005) Cell type-specific involvement of RIG-I in antiviral response. *Immunity* **23**(1)**:** 19-28

Kato H, Takeuchi O, Mikamo-Satoh E, Hirai R, Kawai T, Matsushita K, Hiiragi A, Dermody TS, Fujita T, Akira S (2008) Length-dependent recognition of double-stranded ribonucleic acids by retinoic acid-inducible gene-I and melanoma differentiation-associated gene 5. *J Exp Med* **205**(7)**:** 1601-1610

Kawai T, Sato S, Ishii KJ, Coban C, Hemmi H, Yamamoto M, Terai K, Matsuda M, Inoue J, Uematsu S, Takeuchi O, Akira S (2004) Interferon-alpha induction through Toll-like receptors involves a direct interaction of IRF7 with MyD88 and TRAF6. *Nat Immunol* **5**(10)**:** 1061-1068

Keating SE, Maloney GM, Moran EM, Bowie AG (2007) IRAK-2 participates in multiple toll-like receptor signaling pathways to NFkappaB via activation of TRAF6 ubiquitination. *J Biol Chem* **282**(46)**:** 33435-33443

Keck JG, Baldick CJ, Jr., Moss B (1990) Role of DNA replication in vaccinia virus gene expression: a naked template is required for transcription of three late trans-activator genes. *Cell* **61**(5)**:** 801-809

Kettle S, Alcami A, Khanna A, Ehret R, Jassoy C, Smith GL (1997) Vaccinia virus serpin B13R (SPI-2) inhibits interleukin-1beta-converting enzyme and protects virus-infected cells from TNF- and Fas-mediated apoptosis, but does not prevent IL-1beta-induced fever. *J Gen Virol* **78 (Pt 3):** 677-685

Kibler KV, Shors T, Perkins KB, Zeman CC, Banaszak MP, Biesterfeldt J, Langland JO, Jacobs BL (1997) Double-stranded RNA is a trigger for apoptosis in vaccinia virus-infected cells. *J Virol* **71**(3)**:** 1992-2003

Kim HM, Park BS, Kim JI, Kim SE, Lee J, Oh SC, Enkhbayar P, Matsushima N, Lee H, Yoo OJ, Lee JO (2007) Crystal structure of the TLR4-MD-2 complex with bound endotoxin antagonist Eritoran. *Cell* **130**(5)**:** 906-917

Kim YM, Brinkmann MM, Paquet ME, Ploegh HL (2008) UNC93B1 delivers nucleotide-sensing toll-like receptors to endolysosomes. *Nature* **452**(7184)**:** 234-238

Kischkel FC, Hellbardt S, Behrmann I, Germer M, Pawlita M, Krammer PH, Peter ME (1995) Cytotoxicity-dependent APO-1 (Fas/CD95)-associated proteins form a death-inducing signaling complex (DISC) with the receptor. *EMBO J* **14**(22)**:** 5579-5588

Kishore N, Huynh QK, Mathialagan S, Hall T, Rouw S, Creely D, Lange G, Caroll J, Reitz B, Donnelly A, Boddupalli H, Combs RG, Kretzmer K, Tripp CS (2002) IKK-i and TBK-1 are enzymatically distinct from the homologous enzyme IKK-2: comparative analysis of recombinant human IKK-i, TBK-1, and IKK-2. *J Biol Chem* **277**(16)**:** 13840-13847

Klemperer N, Ward J, Evans E, Traktman P (1997) The vaccinia virus I1 protein is essential for the assembly of mature virions. *J Virol* **71**(12)**:** 9285-9294

Klochendler-Yeivin A, Muchardt C, Yaniv M (2002) SWI/SNF chromatin remodeling and cancer. *Curr Opin Genet Dev* **12**(1)**:** 73-79

Koop A, Lepenies I, Braum O, Davarnia P, Scherer G, Fickenscher H, Kabelitz D, Adam-Klages S (2011) Novel splice variants of human IKKepsilon negatively regulate IKKepsilon-induced IRF3 and NF-kB activation. *Eur J Immunol* **41**(1)**:** 224-234

Kotwal GJ, Hugin AW, Moss B (1989) Mapping and insertional mutagenesis of a vaccinia virus gene encoding a 13,800-Da secreted protein. *Virology* **171**(2)**:** 579-587

Kotwal GJ, Isaacs SN, McKenzie R, Frank MM, Moss B (1990) Inhibition of the complement cascade by the major secretory protein of vaccinia virus. *Science* **250**(4982)**:** 827-830

Kravchenko VV, Mathison JC, Schwamborn K, Mercurio F, Ulevitch RJ (2003) IKKi/IKKepsilon plays a key role in integrating signals induced by pro-inflammatory stimuli. *J Biol Chem* **278**(29)**:** 26612-26619

Kroemer G, Galluzzi L, Brenner C (2007) Mitochondrial membrane permeabilization in cell death. *Physiol Rev* **87**(1)**:** 99-163

Kudo N, Matsumori N, Taoka H, Fujiwara D, Schreiner EP, Wolff B, Yoshida M, Horinouchi S (1999) Leptomycin B inactivates CRM1/exportin 1 by covalent modification at a cysteine residue in the central conserved region. *Proc Natl Acad Sci U S A* **96**(16)**:** 9112-9117

Kuenzel S, Till A, Winkler M, Hasler R, Lipinski S, Jung S, Grotzinger J, Fickenscher H, Schreiber S, Rosenstiel P (2010) The nucleotide-binding oligomerization domain-like receptor NLRC5 is involved in IFN-dependent antiviral immune responses. *J Immunol* **184**(4)**:** 1990-2000

Kumar H, Kawai T, Akira S (2011) Pathogen recognition by the innate immune system. *Int Rev Immunol* **30**(1)**:** 16-34

Kumar H, Kawai T, Kato H, Sato S, Takahashi K, Coban C, Yamamoto M, Uematsu S, Ishii KJ, Takeuchi O, Akira S (2006) Essential role of IPS-1 in innate immune responses against RNA viruses. *J Exp Med* **203**(7)**:** 1795-1803

Kumar H, Pandey S, Zou J, Kumagai Y, Takahashi K, Akira S, Kawai T (2010) NLRC5 deficiency does not influence cytokine induction by virus and bacteria infections. *J Immunol* **186**(2)**:** 994-1000

Kvansakul M, Yang H, Fairlie WD, Czabotar PE, Fischer SF, Perugini MA, Huang DC, Colman PM (2008) Vaccinia virus anti-apoptotic F1L is a novel Bcl-2-like domain-swapped dimer that binds a highly selective subset of BH3-containing death ligands. *Cell Death Differ* **15**(10)**:** 1564-1571

Kyriakis JM, Avruch J (2001) Mammalian mitogen-activated protein kinase signal transduction pathways activated by stress and inflammation. *Physiol Rev* **81**(2)**:** 807-869

Laing KJ, Secombes CJ (2004) Chemokines. *Dev Comp Immunol* **28**(5)**:** 443-460

Lalani AS, McFadden G (1997) Secreted poxvirus chemokine binding proteins. *J Leukoc Biol* **62**(5)**:** 570-576

Law M, Carter GC, Roberts KL, Hollinshead M, Smith GL (2006) Ligand-induced and nonfusogenic dissolution of a viral membrane. *Proc Natl Acad Sci U S A* **103**(15)**:** 5989-5994

Le Goffic R, Balloy V, Lagranderie M, Alexopoulou L, Escriou N, Flavell R, Chignard M, Si-Tahar M (2006) Detrimental contribution of the Toll-like receptor (TLR)3 to influenza A virus-induced acute pneumonia. *PLoS Pathog* **2**(6)**:** e53

Leddy JP, Simons RL, Douglas RG (1977) Effect of selective complement deficiency on the rate of neutralization of enveloped viruses by human sera. *J Immunol* **118**(1)**:** 28-34

Lee MJ, Tasaki T, Moroi K, An JY, Kimura S, Davydov IV, Kwon YT (2005) RGS4 and RGS5 are in vivo substrates of the N-end rule pathway. *Proc Natl Acad Sci U S A* **102**(42)**:** 15030-15035

Lefkowitz EJ, Wang C, Upton C (2006) Poxviruses: past, present and future. *Virus Res* **117**(1)**:** 105-118

Lemaitre B, Nicolas E, Michaut L, Reichhart JM, Hoffmann JA (1996) The dorsoventral regulatory gene cassette spatzle/Toll/cactus controls the potent antifungal response in Drosophila adults. *Cell* **86**(6)**:** 973-983

Li C, Ni CZ, Havert ML, Cabezas E, He J, Kaiser D, Reed JC, Satterthwait AC, Cheng G, Ely KR (2002) Downstream regulator TANK binds to the CD40 recognition site on TRAF3. *Structure* **10**(3)**:** 403-411

Li K, Chen Z, Kato N, Gale M, Jr., Lemon SM (2005) Distinct poly(I-C) and virus-activated signaling pathways leading to interferon-beta production in hepatocytes. *J Biol Chem* **280**(17)**:** 16739-16747

Li Q, Van Antwerp D, Mercurio F, Lee KF, Verma IM (1999a) Severe liver degeneration in mice lacking the IkappaB kinase 2 gene. *Science* **284**(5412)**:** 321-325

Li ZW, Chu W, Hu Y, Delhase M, Deerinck T, Ellisman M, Johnson R, Karin M (1999b) The IKKbeta subunit of IkappaB kinase (IKK) is essential for nuclear factor kappaB activation and prevention of apoptosis. *J Exp Med* **189**(11)**:** 1839-1845

Lin CL, Chung CS, Heine HG, Chang W (2000) Vaccinia virus envelope H3L protein binds to cell surface heparan sulfate and is important for intracellular mature virion morphogenesis and virus infection in vitro and in vivo. *J Virol* **74**(7)**:** 3353-3365

Lin R, Heylbroeck C, Genin P, Pitha PM, Hiscott J (1999a) Essential role of interferon regulatory factor 3 in direct activation of RANTES chemokine transcription. *Mol Cell Biol* **19**(2)**:** 959-966

Lin R, Mamane Y, Hiscott J (1999b) Structural and functional analysis of interferon regulatory factor 3: localization of the transactivation and autoinhibitory domains. *Mol Cell Biol* **19**(4)**:** 2465-2474

Lin SC, Lo YC, Wu H (2010) Helical assembly in the MyD88-IRAK4-IRAK2 complex in TLR/IL-1R signalling. *Nature* **465**(7300)**:** 885-890

Liu K, Lemon B, Traktman P (1995) The dual-specificity phosphatase encoded by vaccinia virus, VH1, is essential for viral transcription in vivo and in vitro. *J Virol* **69**(12)**:** 7823-7834

Lovell SC, Davis IW, Arendall III WB, de Bakker PIW, Word JM, Prisant MG, Richardson JS, Richardson DC (2002) Structure validation by Calpha geometry: phi,psi and Cbeta deviation. *Proteins: Structure, Function & Genetics* **50:** 437-450

Lu G, Reinert JT, Pitha-Rowe I, Okumura A, Kellum M, Knobeloch KP, Hassel B, Pitha PM (2006) ISG15 enhances the innate antiviral response by inhibition of IRF-3 degradation. *Cell Mol Biol (Noisy-le-grand)* **52**(1)**:** 29-41

Lysakova-Devine T, Keogh B, Harrington B, Nagpal K, Halle A, Golenbock DT, Monie T, Bowie AG (2010) Viral inhibitory peptide of TLR4, a peptide derived from vaccinia protein A46, specifically inhibits TLR4 by directly targeting MyD88 adaptor-like and TRIF-related adaptor molecule. *J Immunol* **185**(7)**:** 4261-4271

Macdonald A, Downie AW (1950) Serological study of the soluble antigens of variola, vaccinia, cowpox and ectromelia viruses. *Br J Exp Pathol* **31**(6)**:** 784-788

Mahy BW (2003) An overview on the use of a viral pathogen as a bioterrorism agent: why smallpox? *Antiviral Res* **57**(1-2)**:** 1-5

Malathi K, Dong B, Gale M, Jr., Silverman RH (2007) Small self-RNA generated by RNase L amplifies antiviral innate immunity. *Nature* **448**(7155)**:** 816-819

Maloney G, Schroder M, Bowie AG (2005) Vaccinia virus protein A52R activates p38 mitogen-activated protein kinase and potentiates lipopolysaccharide-induced interleukin-10. *J Biol Chem* **280**(35)**:** 30838-30844

Maluquer de Motes C, Cooray S, Ren H, Almeida GMF, McGourty K, Bahar MW, Stuart DI, Grimes JM, Graham SC, Smith GL (2011) Inhibition of Apoptosis and NF-κB Activation by Vaccinia Protein N1 Occur via Distinct Binding Surfaces and Make Different Contributions to Virulence. *PLoS Pathog* **7**(12)**:** e1002430

Mancuso G, Gambuzza M, Midiri A, Biondo C, Papasergi S, Akira S, Teti G, Beninati C (2009) Bacterial recognition by TLR7 in the lysosomes of conventional dendritic cells. *Nat Immunol* **10**(6)**:** 587-594

Mann BA, Huang JH, Li P, Chang HC, Slee RB, O'Sullivan A, Anita M, Yeh N, Klemsz MJ, Brutkiewicz RR, Blum JS, Kaplan MH (2008) Vaccinia virus blocks Stat1-dependent and Stat1-independent gene expression induced by type I and type II interferons. *J Interferon Cytokine Res* **28**(6)**:** 367-380

Marq JB, Hausmann S, Luban J, Kolakofsky D, Garcin D (2009) The double-stranded RNA binding domain of the vaccinia virus E3L protein inhibits both RNA- and DNA-induced activation of interferon beta. *J Biol Chem* **284**(38)**:** 25471-25478

Martinez FO, Sica A, Mantovani A, Locati M (2008) Macrophage activation and polarization. *Front Biosci* **13:** 453-461

Martinon F, Burns K, Tschopp J (2002) The inflammasome: a molecular platform triggering activation of inflammatory caspases and processing of proIL-beta. *Mol Cell* **10**(2)**:** 417-426

Mattioli I, Geng H, Sebald A, Hodel M, Bucher C, Kracht M, Schmitz ML (2006) Inducible phosphorylation of NF-kappa B p65 at serine 468 by T cell costimulation is mediated by IKK epsilon. *J Biol Chem* **281**(10)**:** 6175-6183

McCoy LE, Fahy AS, Chen RA, Smith GL (2010) Mutations in modified virus Ankara protein 183 render it a non-functional counterpart of B14, an inhibitor of nuclear factor kappaB activation. *J Gen Virol* **91**(Pt 9)**:** 2216-2220

McCraith S, Holtzman T, Moss B, Fields S (2000) Genome-wide analysis of vaccinia virus protein-protein interactions. *Proc Natl Acad Sci U S A* **97**(9)**:** 4879-4884

McDonald C, Inohara N, Nunez G (2005) Peptidoglycan signaling in innate immunity and inflammatory disease. *J Biol Chem* **280**(21)**:** 20177-20180

McGeachy MJ, Cua DJ (2008) Th17 cell differentiation: the long and winding road. *Immunity* **28**(4)**:** 445-453

McWhirter SM, Fitzgerald KA, Rosains J, Rowe DC, Golenbock DT, Maniatis T (2004) IFN-regulatory factor 3-dependent gene expression is defective in Tbk1-deficient mouse embryonic fibroblasts. *Proc Natl Acad Sci U S A* **101**(1)**:** 233-238

Meager A, Visvalingam K, Dilger P, Bryan D, Wadhwa M (2005) Biological activity of interleukins-28 and -29: comparison with type I interferons. *Cytokine* **31**(2)**:** 109-118

Medzhitov R (2009) Approaching the asymptote: 20 years later. *Immunity* **30**(6)**:** 766-775

Medzhitov R, Preston-Hurlburt P, Kopp E, Stadlen A, Chen C, Ghosh S, Janeway CA, Jr. (1998) MyD88 is an adaptor protein in the hToll/IL-1 receptor family signaling pathways. *Mol Cell* **2**(2)**:** 253-258

Meier A, Alter G, Frahm N, Sidhu H, Li B, Bagchi A, Teigen N, Streeck H, Stellbrink HJ, Hellman J, van Lunzen J, Altfeld M (2007) MyD88-dependent immune activation mediated by human immunodeficiency virus type 1-encoded Toll-like receptor ligands. *J Virol* **81**(15)**:** 8180-8191

Meissner TB, Li A, Biswas A, Lee KH, Liu YJ, Bayir E, Iliopoulos D, van den Elsen PJ, Kobayashi KS (2010) NLR family member NLRC5 is a transcriptional regulator of MHC class I genes. *Proc Natl Acad Sci U S A* **107**(31)**:** 13794-13799

Mercer J, Helenius A (2008) Vaccinia virus uses macropinocytosis and apoptotic mimicry to enter host cells. *Science* **320**(5875)**:** 531-535

Merika M, Thanos D (2001) Enhanceosomes. *Curr Opin Genet Dev* **11**(2)**:** 205-208

Meyer H, Sutter G, Mayr A (1991) Mapping of deletions in the genome of the highly attenuated vaccinia virus MVA and their influence on virulence. *J Gen Virol* **72 (Pt 5):** 1031-1038

Meylan E, Burns K, Hofmann K, Blancheteau V, Martinon F, Kelliher M, Tschopp J (2004) RIP1 is an essential mediator of Toll-like receptor 3-induced NF-kappa B activation. *Nat Immunol* **5**(5)**:** 503-507

Meylan E, Curran J, Hofmann K, Moradpour D, Binder M, Bartenschlager R, Tschopp J (2005) Cardif is an adaptor protein in the RIG-I antiviral pathway and is targeted by hepatitis C virus. *Nature* **437**(7062)**:** 1167-1172

Moore CB, Bergstralh DT, Duncan JA, Lei Y, Morrison TE, Zimmermann AG, Accavitti-Loper MA, Madden VJ, Sun L, Ye Z, Lich JD, Heise MT, Chen Z, Ting JP (2008) NLRX1 is a regulator of mitochondrial antiviral immunity. *Nature* **451**(7178)**:** 573-577

Morgan GW, Hollinshead M, Ferguson BJ, Murphy BJ, Carpentier DC, Smith GL (2010) Vaccinia protein F12 has structural similarity to kinesin light chain and contains a motor binding motif required for virion export. *PLoS Pathog* **6**(2)**:** e1000785

Mori M, Yoneyama M, Ito T, Takahashi K, Inagaki F, Fujita T (2004) Identification of Ser-386 of interferon regulatory factor 3 as critical target for inducible phosphorylation that determines activation. *J Biol Chem* **279**(11)**:** 9698-9702

Moss B (1994) Vaccinia virus transcription. In *Transcription Mechanisms and Regulation*, Conaway RCC, J.W. (ed), pp 185-205. New York: Raven Press

Moss B (2007) *Poxviruses*: Lippincott, Williams & Wilkins.

Moss B, Carroll MW, Wyatt LS, Bennink JR, Hirsch VM, Goldstein S, Elkins WR, Fuerst TR, Lifson JD, Piatak M, Restifo NP, Overwijk W, Chamberlain R, Rosenberg SA, Sutter G (1996) Host range restricted, non-replicating vaccinia virus vectors as vaccine candidates. *Adv Exp Med Biol* **397:** 7-13

Moss B, Rosenblum EN (1973) Letter: Protein cleavage and poxvirus morphogenesis: tryptic peptide analysis of core precursors accumulated by blocking assembly with rifampicin. *J Mol Biol* **81**(2)**:** 267-269

Moyer RW, Graves RL (1981) The mechanism of cytoplasmic orthopoxvirus DNA replication. *Cell* **27**(2 Pt 1)**:** 391-401

Mukaida N, Mahe Y, Matsushima K (1990) Cooperative interaction of nuclear factor-kappa B- and cis-regulatory enhancer binding protein-like factor binding elements in activating the interleukin-8 gene by pro-inflammatory cytokines. *J Biol Chem* **265**(34)**:** 21128-21133

Mulder LC, Muesing MA (2000) Degradation of HIV-1 integrase by the N-end rule pathway. *J Biol Chem* **275**(38)**:** 29749-29753

Murphy K, Travers, P, Walport, M, Janeway, C (2008) *Janeway's immunobiology*: Garland Science.

Muruve DA, Petrilli V, Zaiss AK, White LR, Clark SA, Ross PJ, Parks RJ, Tschopp J (2008) The inflammasome recognizes cytosolic microbial and host DNA and triggers an innate immune response. *Nature* **452**(7183)**:** 103-107

Myskiw C, Arsenio J, van Bruggen R, Deschambault Y, Cao J (2009) Vaccinia virus E3 suppresses expression of diverse cytokines through inhibition of the PKR, NF-kappaB, and IRF3 pathways. *J Virol* **83**(13)**:** 6757-6768

Najarro P, Traktman P, Lewis JA (2001) Vaccinia virus blocks gamma interferon signal transduction: viral VH1 phosphatase reverses Stat1 activation. *J Virol* **75**(7)**:** 3185-3196

Neerincx A, Lautz K, Menning M, Kremmer E, Zigrino P, Hosel M, Buning H, Schwarzenbacher R, Kufer TA (2010) A role for the human nucleotide-binding domain, leucine-rich repeat-containing family member NLRC5 in antiviral responses. *J Biol Chem* **285**(34)**:** 26223-26232

Ng A, Tscharke DC, Reading PC, Smith GL (2001) The vaccinia virus A41L protein is a soluble 30 kDa glycoprotein that affects virus virulence. *J Gen Virol* **82**(Pt 9)**:** 2095-2105

Niles EG, Seto J (1988) Vaccinia virus gene D8 encodes a virion transmembrane protein. *J Virol* **62**(10)**:** 3772-3778

Nillegoda NB, Theodoraki MA, Mandal AK, Mayo KJ, Ren HY, Sultana R, Wu K, Johnson J, Cyr DM, Caplan AJ (2010) Ubr1 and Ubr2 function in a quality control pathway for degradation of unfolded cytosolic proteins. *Mol Biol Cell* **21**(13)**:** 2102-2116

Nomura F, Kawai T, Nakanishi K, Akira S (2000) NF-kappaB activation through IKK-i-dependent I-TRAF/TANK phosphorylation. *Genes Cells* **5**(3)**:** 191-202

Novick D, Kim SH, Fantuzzi G, Reznikov LL, Dinarello CA, Rubinstein M (1999) Interleukin-18 binding protein: a novel modulator of the Th1 cytokine response. *Immunity* **10**(1)**:** 127-136

Oda S, Schroder M, Khan AR (2009) Structural basis for targeting of human RNA helicase DDX3 by poxvirus protein K7. *Structure* **17**(11)**:** 1528-1537

Oganesyan G, Saha SK, Guo B, He JQ, Shahangian A, Zarnegar B, Perry A, Cheng G (2006) Critical role of TRAF3 in the Toll-like receptor-dependent and -independent antiviral response. *Nature* **439**(7073)**:** 208-211

Ohmori Y, Hamilton TA (1993) Cooperative interaction between interferon (IFN) stimulus response element and kappa B sequence motifs controls IFN gamma- and lipopolysaccharide-stimulated transcription from the murine IP-10 promoter. *J Biol Chem* **268**(9)**:** 6677-6688

Oseroff C, Kos F, Bui HH, Peters B, Pasquetto V, Glenn J, Palmore T, Sidney J, Tscharke DC, Bennink JR, Southwood S, Grey HM, Yewdell JW, Sette A (2005) HLA class I-restricted responses to vaccinia recognize a broad array of proteins mainly involved in virulence and viral gene regulation. *Proc Natl Acad Sci U S A* **102**(39)**:** 13980-13985

Oshiumi H, Matsumoto M, Funami K, Akazawa T, Seya T (2003a) TICAM-1, an adaptor molecule that participates in Toll-like receptor 3-mediated interferon-beta induction. *Nat Immunol* **4**(2)**:** 161-167

Oshiumi H, Matsumoto M, Hatakeyama S, Seya T (2009) Riplet/RNF135, a RING finger protein, ubiquitinates RIG-I to promote interferon-beta induction during the early phase of viral infection. *J Biol Chem* **284**(2)**:** 807-817

Oshiumi H, Sakai K, Matsumoto M, Seya T (2010) DEAD/H BOX 3 (DDX3) helicase binds the RIG-I adaptor IPS-1 to up-regulate IFN-beta-inducing potential. *Eur J Immunol* **40**(4)**:** 940-948

Oshiumi H, Sasai M, Shida K, Fujita T, Matsumoto M, Seya T (2003b) TIR-containing adapter molecule (TICAM)-2, a bridging adapter recruiting to toll-like receptor 4 TICAM-1 that induces interferon-beta. *J Biol Chem* **278**(50)**:** 49751-49762

Park JH, Kim YG, McDonald C, Kanneganti TD, Hasegawa M, Body-Malapel M, Inohara N, Nunez G (2007) RICK/RIP2 mediates innate immune responses induced through Nod1 and Nod2 but not TLRs. *J Immunol* **178**(4)**:** 2380-2386

Parker S, Nuara A, Buller RM, Schultz DA (2007) Human monkeypox: an emerging zoonotic disease. *Future Microbiol* **2**(1)**:** 17-34

Parkinson JE, Smith GL (1994) Vaccinia virus gene A36R encodes a M(r) 43-50 K protein on the surface of extracellular enveloped virus. *Virology* **204**(1)**:** 376-390

Payne LG (1980) Significance of extracellular enveloped virus in the in vitro and in vivo dissemination of vaccinia. *J Gen Virol* **50**(1)**:** 89-100

Paz S, Sun Q, Nakhaei P, Romieu-Mourez R, Goubau D, Julkunen I, Lin R, Hiscott J (2006) Induction of IRF-3 and IRF-7 phosphorylation following activation of the RIG-I pathway. *Cell Mol Biol (Noisy-le-grand)* **52**(1)**:** 17-28

Perry AK, Chow EK, Goodnough JB, Yeh WC, Cheng G (2004) Differential requirement for TANK-binding kinase-1 in type I interferon responses to toll-like receptor activation and viral infection. *J Exp Med* **199**(12)**:** 1651-1658

Petros AM, Olejniczak ET, Fesik SW (2004) Structural biology of the Bcl-2 family of proteins. *Biochim Biophys Acta* **1644**(2-3)**:** 83-94

Pichlmair A, Schulz O, Tan CP, Naslund TI, Liljestrom P, Weber F, Reis e Sousa C (2006) RIG-I-mediated antiviral responses to single-stranded RNA bearing 5'-phosphates. *Science* **314**(5801)**:** 997-1001

Poltorak A, He X, Smirnova I, Liu MY, Van Huffel C, Du X, Birdwell D, Alejos E, Silva M, Galanos C, Freudenberg M, Ricciardi-Castagnoli P, Layton B, Beutler B (1998) Defective LPS signaling in C3H/HeJ and C57BL/10ScCr mice: mutations in Tlr4 gene. *Science* **282**(5396)**:** 2085-2088

Pomerantz JL, Baltimore D (1999) NF-kappaB activation by a signaling complex containing TRAF2, TANK and TBK1, a novel IKK-related kinase. *EMBO J* **18**(23)**:** 6694-6704

Poyet JL, Srinivasula SM, Tnani M, Razmara M, Fernandes-Alnemri T, Alnemri ES (2001) Identification of Ipaf, a human caspase-1-activating protein related to Apaf-1. *J Biol Chem* **276**(30)**:** 28309-28313

Prideaux CT, Kumar S, Boyle DB (1990) Comparative analysis of vaccinia virus promoter activity in fowlpox and vaccinia virus recombinants. *Virus Res* **16**(1)**:** 43-57

Putz MM, Midgley CM, Law M, Smith GL (2006) Quantification of antibody responses against multiple antigens of the two infectious forms of Vaccinia virus provides a benchmark for smallpox vaccination. *Nat Med* **12**(11)**:** 1310-1315

Quan LT, Caputo A, Bleackley RC, Pickup DJ, Salvesen GS (1995) Granzyme B is inhibited by the cowpox virus serpin cytokine response modifier A. *J Biol Chem* **270**(18)**:** 10377-10379

Ramirez MC, Sigal LJ (2002) Macrophages and dendritic cells use the cytosolic pathway to rapidly cross-present antigen from live, vaccinia-infected cells. *J Immunol* **169**(12)**:** 6733-6742

Ramsey-Ewing A, Moss B (1998) Apoptosis induced by a postbinding step of vaccinia virus entry into Chinese hamster ovary cells. *Virology* **242**(1)**:** 138-149

Rathinam VA, Jiang Z, Waggoner SN, Sharma S, Cole LE, Waggoner L, Vanaja SK, Monks BG, Ganesan S, Latz E, Hornung V, Vogel SN, Szomolanyi-Tsuda E, Fitzgerald KA (2010) The AIM2 inflammasome is essential for host defense against cytosolic bacteria and DNA viruses. *Nat Immunol* **11**(5)**:** 395-402

Ray CA, Black RA, Kronheim SR, Greenstreet TA, Sleath PR, Salvesen GS, Pickup DJ (1992) Viral inhibition of inflammation: cowpox virus encodes an inhibitor of the interleukin-1 beta converting enzyme. *Cell* **69**(4)**:** 597-604

Reading PC, Symons JA, Smith GL (2003) A soluble chemokine-binding protein from vaccinia virus reduces virus virulence and the inflammatory response to infection. *J Immunol* **170**(3)**:** 1435-1442

Rehm KE, Roper RL (2011) Deletion of the A35 gene from Modified Vaccinia Virus Ankara increases immunogenicity and isotype switching. *Vaccine* **29**(17)**:** 3276-3283

Reynolds MG, Cono J, Curns A, Holman RC, Likos A, Regnery R, Treadwell T, Damon I (2004) Human monkeypox. *Lancet Infect Dis* **4**(10)**:** 604-605; discussion 605

Ricklin D, Hajishengallis G, Yang K, Lambris JD (2010) Complement: a key system for immune surveillance and homeostasis. *Nat Immunol* **11**(9)**:** 785-797

Rigaut G, Shevchenko A, Rutz B, Wilm M, Mann M, Seraphin B (1999) A generic protein purification method for protein complex characterization and proteome exploration. *Nat Biotechnol* **17**(10)**:** 1030-1032

Roberts KL, Smith GL (2008) Vaccinia virus morphogenesis and dissemination. *Trends Microbiol*

Roberts TL, Idris A, Dunn JA, Kelly GM, Burnton CM, Hodgson S, Hardy LL, Garceau V, Sweet MJ, Ross IL, Hume DA, Stacey KJ (2009) HIN-200 proteins regulate caspase activation in response to foreign cytoplasmic DNA. *Science* **323**(5917)**:** 1057-1060

Rocak S, Linder P (2004) DEAD-box proteins: the driving forces behind RNA metabolism. *Nat Rev Mol Cell Biol* **5**(3)**:** 232-241

Rodriguez JR, Rodriguez D, Esteban M (1991) Interferon treatment inhibits early events in vaccinia virus gene expression in infected mice. *Virology* **185**(2)**:** 929-933

Rothe M, Xiong J, Shu HB, Williamson K, Goddard A, Goeddel DV (1996) I-TRAF is a novel TRAF-interacting protein that regulates TRAF-mediated signal transduction. *Proc Natl Acad Sci U S A* **93**(16)**:** 8241-8246

Rothenfusser S, Goutagny N, DiPerna G, Gong M, Monks BG, Schoenemeyer A, Yamamoto M, Akira S, Fitzgerald KA (2005) The RNA helicase Lgp2 inhibits TLR-independent sensing of viral replication by retinoic acid-inducible gene-I. *J Immunol* **175**(8)**:** 5260-5268

Rothwarf DM, Zandi E, Natoli G, Karin M (1998) IKK-gamma is an essential regulatory subunit of the IkappaB kinase complex. *Nature* **395**(6699)**:** 297-300

Rudensky AY (2011) Regulatory T cells and Foxp3. *Immunol Rev* **241**(1)**:** 260-268

Rudolph D, Yeh WC, Wakeham A, Rudolph B, Nallainathan D, Potter J, Elia AJ, Mak TW (2000) Severe liver degeneration and lack of NF-kappaB activation in NEMO/IKKgamma-deficient mice. *Genes Dev* **14**(7)**:** 854-862

Ryzhakov G, Randow F (2007) SINTBAD, a novel component of innate antiviral immunity, shares a TBK1-binding domain with NAP1 and TANK. *EMBO J* **26**(13)**:** 3180-3190

Saha SK, Pietras EM, He JQ, Kang JR, Liu SY, Oganesyan G, Shahangian A, Zarnegar B, Shiba TL, Wang Y, Cheng G (2006) Regulation of antiviral responses by a direct and specific interaction between TRAF3 and Cardif. *EMBO J* **25**(14)**:** 3257-3263

Sahu A, Isaacs SN, Soulika AM, Lambris JD (1998) Interaction of vaccinia virus complement control protein with human complement proteins: factor I-mediated degradation of C3b to iC3b1 inactivates the alternative complement pathway. *J Immunol* **160**(11)**:** 5596-5604

Saitoh T, Yamamoto M, Miyagishi M, Taira K, Nakanishi M, Fujita T, Akira S, Yamamoto N, Yamaoka S (2005) A20 is a negative regulator of IFN regulatory factor 3 signaling. *J Immunol* **174**(3)**:** 1507-1512

Salzman NP (1960) The rate of formation of vaccinia deoxyribonucleic acid and vaccinia virus. *Virology* **10:** 150-152

Sarkar SN, Peters KL, Elco CP, Sakamoto S, Pal S, Sen GC (2004) Novel roles of TLR3 tyrosine phosphorylation and PI3 kinase in double-stranded RNA signaling. *Nat Struct Mol Biol* **11**(11)**:** 1060-1067

Sasai M, Oshiumi H, Matsumoto M, Inoue N, Fujita F, Nakanishi M, Seya T (2005) Cutting Edge: NF-kappaB-activating kinase-associated protein 1 participates in TLR3/Toll-IL-1 homology domain-containing adapter molecule-1-mediated IFN regulatory factor 3 activation. *J Immunol* **174**(1)**:** 27-30

Sasai M, Shingai M, Funami K, Yoneyama M, Fujita T, Matsumoto M, Seya T (2006) NAK-associated protein 1 participates in both the TLR3 and the cytoplasmic pathways in type I IFN induction. *J Immunol* **177**(12)**:** 8676-8683

Satoh T, Kato H, Kumagai Y, Yoneyama M, Sato S, Matsushita K, Tsujimura T, Fujita T, Akira S, Takeuchi O (2010) LGP2 is a positive regulator of RIG-I- and MDA5-mediated antiviral responses. *Proc Natl Acad Sci U S A* **107**(4)**:** 1512-1517

Scherer DC, Brockman JA, Chen Z, Maniatis T, Ballard DW (1995) Signal-induced degradation of I kappa B alpha requires site-specific ubiquitination. *Proc Natl Acad Sci U S A* **92**(24)**:** 11259-11263

Schlee M, Roth A, Hornung V, Hagmann CA, Wimmenauer V, Barchet W, Coch C, Janke M, Mihailovic A, Wardle G, Juranek S, Kato H, Kawai T, Poeck H, Fitzgerald KA, Takeuchi O, Akira S, Tuschl T, Latz E, Ludwig J, Hartmann G (2009) Recognition of 5' triphosphate by RIG-I helicase requires short blunt double-stranded RNA as contained in panhandle of negative-strand virus. *Immunity* **31**(1)**:** 25-34

Schmidt A, Schwerd T, Hamm W, Hellmuth JC, Cui S, Wenzel M, Hoffmann FS, Michallet MC, Besch R, Hopfner KP, Endres S, Rothenfusser S (2009) 5'-triphosphate RNA requires base-paired structures to activate antiviral signaling via RIG-I. *Proc Natl Acad Sci U S A* **106**(29)**:** 12067-12072

Schmidt FI, Bleck CK, Helenius A, Mercer J (2011) Vaccinia extracellular virions enter cells by macropinocytosis and acid-activated membrane rupture. *EMBO J*

Schroder K, Hertzog PJ, Ravasi T, Hume DA (2004) Interferon-gamma: an overview of signals, mechanisms and functions. *J Leukoc Biol* **75**(2)**:** 163-189

Schroder M, Baran M, Bowie AG (2008) Viral targeting of DEAD box protein 3 reveals its role in TBK1/IKKepsilon-mediated IRF activation. *Embo J* **27**(15)**:** 2147-2157

Schultz U, Kaspers B, Staeheli P (2004) The interferon system of non-mammalian vertebrates. *Dev Comp Immunol* **28**(5)**:** 499-508

Schwandner R, Dziarski R, Wesche H, Rothe M, Kirschning CJ (1999) Peptidoglycan- and lipoteichoic acid-induced cell activation is mediated by toll-like receptor 2. *J Biol Chem* **274**(25)**:** 17406-17409

Segal AW (2005) How neutrophils kill microbes. *Annu Rev Immunol* **23:** 197-223

Senkevich TG, Ojeda S, Townsley A, Nelson GE, Moss B (2005) Poxvirus multiprotein entry-fusion complex. *Proc Natl Acad Sci U S A* **102**(51)**:** 18572-18577

Servant MJ, Grandvaux N, tenOever BR, Duguay D, Lin R, Hiscott J (2003) Identification of the minimal phosphoacceptor site required for in vivo activation of interferon regulatory factor 3 in response to virus and double-stranded RNA. *J Biol Chem* **278**(11)**:** 9441-9447

Seth RB, Sun L, Ea CK, Chen ZJ (2005) Identification and characterization of MAVS, a mitochondrial antiviral signaling protein that activates NF-kappaB and IRF 3. *Cell* **122**(5)**:** 669-682

Sharma S, tenOever BR, Grandvaux N, Zhou GP, Lin R, Hiscott J (2003) Triggering the interferon antiviral response through an IKK-related pathway. *Science* **300**(5622)**:** 1148-1151

Shaw MH, Reimer T, Sanchez-Valdepenas C, Warner N, Kim YG, Fresno M, Nunez G (2009) T cell-intrinsic role of Nod2 in promoting type 1 immunity to Toxoplasma gondii. *Nat Immunol* **10**(12)**:** 1267-1274

Shchelkunov SN (2010) Interaction of orthopoxviruses with the cellular ubiquitin-ligase system. *Virus Genes* **41**(3)**:** 309-318

Shen HB, Chou KC (2010) Virus-mPLoc: a fusion classifier for viral protein subcellular location prediction by incorporating multiple sites. *J Biomol Struct Dyn* **28**(2)**:** 175-186

Shimada T, Kawai T, Takeda K, Matsumoto M, Inoue J, Tatsumi Y, Kanamaru A, Akira S (1999) IKK-i, a novel lipopolysaccharide-inducible kinase that is related to IkappaB kinases. *Int Immunol* **11**(8)**:** 1357-1362

Shimazu R, Akashi S, Ogata H, Nagai Y, Fukudome K, Miyake K, Kimoto M (1999) MD-2, a molecule that confers lipopolysaccharide responsiveness on Toll-like receptor 4. *J Exp Med* **189**(11)**:** 1777-1782

Shisler JL, Jin XL (2004) The vaccinia virus K1L gene product inhibits host NF-kappaB activation by preventing IkappaBalpha degradation. *J Virol* **78**(7)**:** 3553-3560

Shortman K, Naik SH (2007) Steady-state and inflammatory dendritic-cell development. *Nature reviews* **7**(1)**:** 19-30

Silva AM, Whitmore M, Xu Z, Jiang Z, Li X, Williams BR (2004) Protein kinase R (PKR) interacts with and activates mitogen-activated protein kinase kinase 6 (MKK6) in response to double-stranded RNA stimulation. *J Biol Chem* **279**(36)**:** 37670-37676

Silverman RH (2007) Viral encounters with 2',5'-oligoadenylate synthetase and RNase L during the interferon antiviral response. *J Virol* **81**(23)**:** 12720-12729

Siu KL, Kok KH, Ng MH, Poon VK, Yuen KY, Zheng BJ, Jin DY (2009) Severe acute respiratory syndrome coronavirus M protein inhibits type I interferon production by impeding the formation of TRAF3.TANK.TBK1/IKKepsilon complex. *J Biol Chem* **284**(24)**:** 16202-16209

Smith CA, Davis T, Wignall JM, Din WS, Farrah T, Upton C, McFadden G, Goodwin RG (1991a) T2 open reading frame from the Shope fibroma virus encodes a soluble form of the TNF receptor. *Biochem Biophys Res Commun* **176**(1)**:** 335-342

Smith CA, Smith TD, Smolak PJ, Friend D, Hagen H, Gerhart M, Park L, Pickup DJ, Torrance D, Mohler K, Schooley K, Goodwin RG (1997a) Poxvirus genomes encode a secreted, soluble protein that preferentially inhibits beta chemokine activity yet lacks sequence homology to known chemokine receptors. *Virology* **236**(2)**:** 316-327

Smith GL, Chan YS (1991) Two vaccinia virus proteins structurally related to the interleukin-1 receptor and the immunoglobulin superfamily. *J Gen Virol* **72 (Pt 3):** 511-518

Smith GL, Chan YS, Howard ST (1991b) Nucleotide sequence of 42 kbp of vaccinia virus strain WR from near the right inverted terminal repeat. *J Gen Virol* **72 (Pt 6):** 1349-1376

Smith GL, Moss B (1983) Infectious poxvirus vectors have capacity for at least 25 000 base pairs of foreign DNA. *Gene* **25**(1)**:** 21-28

Smith GL, Symons JA, Khanna A, Vanderplasschen A, Alcami A (1997b) Vaccinia virus immune evasion. *Immunol Rev* **159:** 137-154

Smith GL, Vanderplasschen A, Law M (2002) The formation and function of extracellular enveloped vaccinia virus. *J Gen Virol* **83**(Pt 12)**:** 2915-2931

Smith VP, Bryant NA, Alcami A (2000) Ectromelia, vaccinia and cowpox viruses encode secreted interleukin-18-binding proteins. *J Gen Virol* **81**(Pt 5)**:** 1223-1230

Sohn DH, Lee KY, Lee C, Oh J, Chung H, Jeon SH, Seong RH (2007) SRG3 interacts directly with the major components of the SWI/SNF chromatin remodeling complex and protects them from proteasomal degradation. *J Biol Chem* **282**(14)**:** 10614-10624

Soulat D, Burckstummer T, Westermayer S, Goncalves A, Bauch A, Stefanovic A, Hantschel O, Bennett KL, Decker T, Superti-Furga G (2008) The DEAD-box helicase DDX3X is a critical component of the TANK-binding kinase 1-dependent innate immune response. *EMBO J* **27**(15)**:** 2135-2146

Spriggs MK, Hruby DE, Maliszewski CR, Pickup DJ, Sims JE, Buller RM, VanSlyke J (1992) Vaccinia and cowpox viruses encode a novel secreted interleukin-1-binding protein. *Cell* **71**(1)**:** 145-152

Springer T, Galfre G, Secher DS, Milstein C (1979) Mac-1: a macrophage differentiation antigen identified by monoclonal antibody. *Eur J Immunol* **9**(4)**:** 301-306

Stack J, Haga IR, Schroder M, Bartlett NW, Maloney G, Reading PC, Fitzgerald KA, Smith GL, Bowie AG (2005) Vaccinia virus protein A46R targets multiple Toll-like-interleukin-1 receptor adaptors and contributes to virulence. *J Exp Med* **201**(6)**:** 1007-1018

Staib C, Kisling S, Erfle V, Sutter G (2005) Inactivation of the viral interleukin 1beta receptor improves CD8+ T-cell memory responses elicited upon immunization with modified vaccinia virus Ankara. *J Gen Virol* **86**(Pt 7)**:** 1997-2006

Stamenkovic I, Seed B (1988) CD19, the earliest differentiation antigen of the B cell lineage, bears three extracellular immunoglobulin-like domains and an Epstein-Barr virus-related cytoplasmic tail. *J Exp Med* **168**(3)**:** 1205-1210

Stetson DB, Medzhitov R (2006) Recognition of cytosolic DNA activates an IRF3-dependent innate immune response. *Immunity* **24**(1)**:** 93-103

Stewart TL, Wasilenko ST, Barry M (2005) Vaccinia virus F1L protein is a tail-anchored protein that functions at the mitochondria to inhibit apoptosis. *J Virol* **79**(2)**:** 1084-1098

Symons JA, Alcami A, Smith GL (1995) Vaccinia virus encodes a soluble type I interferon receptor of novel structure and broad species specificity. *Cell* **81**(4)**:** 551-560

Symons JA, Tscharke DC, Price N, Smith GL (2002) A study of the vaccinia virus interferon-gamma receptor and its contribution to virus virulence. *J Gen Virol* **83**(Pt 8)**:** 1953-1964

Takahashi K, Kawai T, Kumar H, Sato S, Yonehara S, Akira S (2006) Roles of caspase-8 and caspase-10 in innate immune responses to double-stranded RNA. *J Immunol* **176**(8)**:** 4520-4524

Takaoka A, Wang Z, Choi MK, Yanai H, Negishi H, Ban T, Lu Y, Miyagishi M, Kodama T, Honda K, Ohba Y, Taniguchi T (2007) DAI (DLM-1/ZBP1) is a cytosolic DNA sensor and an activator of innate immune response. *Nature* **448**(7152)**:** 501-505

Takaoka A, Yanai H (2006) Interferon signalling network in innate defence. *Cell Microbiol* **8**(6)**:** 907-922

Takaoka A, Yanai H, Kondo S, Duncan G, Negishi H, Mizutani T, Kano S, Honda K, Ohba Y, Mak TW, Taniguchi T (2005) Integral role of IRF-5 in the gene induction programme activated by Toll-like receptors. *Nature* **434**(7030)**:** 243-249

Takeuchi O, Akira S (2008) MDA5/RIG-I and virus recognition. *Curr Opin Immunol* **20**(1)**:** 17-22

Taniguchi T, Ogasawara K, Takaoka A, Tanaka N (2001) IRF family of transcription factors as regulators of host defense. *Annu Rev Immunol* **19:** 623-655

Tatematsu M, Ishii A, Oshiumi H, Horiuchi M, Inagaki F, Seya T, Matsumoto M (2010) A molecular mechanism for Toll-IL-1 receptor domain-containing adaptor molecule-1-mediated IRF-3 activation. *J Biol Chem* **285**(26)**:** 20128-20136

Tattersall P, Ward DC (1976) Rolling hairpin model for replication of parvovirus and linear chromosomal DNA. *Nature* **263**(5573)**:** 106-109

Taylor JM, Barry M (2006) Near death experiences: poxvirus regulation of apoptotic death. *Virology* **344**(1)**:** 139-150

Tenoever BR, Ng SL, Chua MA, McWhirter SM, Garcia-Sastre A, Maniatis T (2007) Multiple functions of the IKK-related kinase IKKepsilon in interferon-mediated antiviral immunity. *Science* **315**(5816)**:** 1274-1278

Testi R, Phillips JH, Lanier LL (1988) Constitutive expression of a phosphorylated activation antigen (Leu 23) by CD3bright human thymocytes. *J Immunol* **141**(8)**:** 2557-2563

Thanos D, Maniatis T (1995) Virus induction of human IFN beta gene expression requires the assembly of an enhanceosome. *Cell* **83**(7)**:** 1091-1100

Thurston TL, Ryzhakov G, Bloor S, von Muhlinen N, Randow F (2009) The TBK1 adaptor and autophagy receptor NDP52 restricts the proliferation of ubiquitin-coated bacteria. *Nat Immunol* **10**(11)**:** 1215-1221

Tojima Y, Fujimoto A, Delhase M, Chen Y, Hatakeyama S, Nakayama K, Kaneko Y, Nimura Y, Motoyama N, Ikeda K, Karin M, Nakanishi M (2000) NAK is an IkappaB kinase-activating kinase. *Nature* **404**(6779)**:** 778-782

Tooze J, Hollinshead M, Reis B, Radsak K, Kern H (1993) Progeny vaccinia and human cytomegalovirus particles utilize early endosomal cisternae for their envelopes. *Eur J Cell Biol* **60**(1)**:** 163-178

Townsley AC, Weisberg AS, Wagenaar TR, Moss B (2006) Vaccinia virus entry into cells via a low-pH-dependent endosomal pathway. *J Virol* **80**(18)**:** 8899-8908

Trauth BC, Klas C, Peters AM, Matzku S, Moller P, Falk W, Debatin KM, Krammer PH (1989) Monoclonal antibody-mediated tumor regression by induction of apoptosis. *Science* **245**(4915)**:** 301-305

Tscharke DC, Karupiah G, Zhou J, Palmore T, Irvine KR, Haeryfar SM, Williams S, Sidney J, Sette A, Bennink JR, Yewdell JW (2005) Identification of poxvirus CD8+ T cell determinants to enable rational design and characterization of smallpox vaccines. *J Exp Med* **201**(1)**:** 95-104

Tscharke DC, Reading PC, Smith GL (2002) Dermal infection with vaccinia virus reveals roles for virus proteins not seen using other inoculation routes. *J Gen Virol* **83**(Pt 8)**:** 1977-1986

Tscharke DC, Smith GL (1999) A model for vaccinia virus pathogenesis and immunity based on intradermal injection of mouse ear pinnae. *J Gen Virol* **80 (Pt 10):** 2751-2755

Tscharke DC, Woo WP, Sakala IG, Sidney J, Sette A, Moss DJ, Bennink JR, Karupiah G, Yewdell JW (2006) Poxvirus CD8+ T-cell determinants and cross-reactivity in BALB/c mice. *J Virol* **80**(13)**:** 6318-6323

Underhill DM, Ozinsky A, Smith KD, Aderem A (1999) Toll-like receptor-2 mediates mycobacteria-induced proinflammatory signaling in macrophages. *Proc Natl Acad Sci U S A* **96**(25)**:** 14459-14463

Unterholzner L, Keating SE, Baran M, Horan KA, Jensen SB, Sharma S, Sirois CM, Jin T, Latz E, Xiao TS, Fitzgerald KA, Paludan SR, Bowie AG (2010) IFI16 is an innate immune sensor for intracellular DNA. *Nat Immunol* **11**(11)**:** 997-1004

Unterholzner L, Sumner RP, Baran M, Ren H, Mansur DS, Bourke NM, Randow F, Smith GL, Bowie AG (2011) Vaccinia Virus Protein C6 Is a Virulence Factor that Binds TBK-1 Adaptor Proteins and Inhibits Activation of IRF3 and IRF7. *PLoS Pathog* **7**(9)**:** e1002247

Upton C, Mossman K, McFadden G (1992) Encoding of a homolog of the IFN-gamma receptor by myxoma virus. *Science* **258**(5086)**:** 1369-1372

Upton C, Slack S, Hunter AL, Ehlers A, Roper RL (2003) Poxvirus orthologous clusters: toward defining the minimum essential poxvirus genome. *J Virol* **77**(13)**:** 7590-7600

Valentine R, Smith GL (2010) Inhibition of the RNA polymerase III-mediated dsDNA-sensing pathway of innate immunity by vaccinia virus protein E3. *J Gen Virol* **91**(Pt 9)**:** 2221-2229

Vallabhapurapu S, Karin M (2009) Regulation and function of NF-kappaB transcription factors in the immune system. *Annu Rev Immunol* **27:** 693-733

van den Broek MF, Muller U, Huang S, Aguet M, Zinkernagel RM (1995) Antiviral defense in mice lacking both alpha/beta and gamma interferon receptors. *J Virol* **69**(8)**:** 4792-4796

Vanderplasschen A, Mathew E, Hollinshead M, Sim RB, Smith GL (1998) Extracellular enveloped vaccinia virus is resistant to complement because of incorporation of host complement control proteins into its envelope. *Proc Natl Acad Sci U S A* **95**(13)**:** 7544-7549

Verstrepen L, Bekaert T, Chau TL, Tavernier J, Chariot A, Beyaert R (2008) TLR-4, IL-1R and TNF-R signaling to NF-kappaB: variations on a common theme. *Cell Mol Life Sci* **65**(19)**:** 2964-2978

Visvanathan KV, Goodbourn S (1989) Double-stranded RNA activates binding of NF-kappa B to an inducible element in the human beta-interferon promoter. *EMBO J* **8**(4)**:** 1129-1138

Viswanathan K, Fruh K, DeFilippis V (2010) Viral hijacking of the host ubiquitin system to evade interferon responses. *Curr Opin Microbiol* **13**(4)**:** 517-523

Vivier E, Tomasello E, Baratin M, Walzer T, Ugolini S (2008) Functions of natural killer cells. *Nat Immunol* **9**(5)**:** 503-510

Vos JC, Mercer AA, Fleming SB, Robinson AJ (1992) In vitro recognition of an orf virus early promoter in a vaccinia virus extract. *Arch Virol* **123**(1-2)**:** 223-228

Walzer T, Galibert L, De Smedt T (2005) Poxvirus semaphorin A39R inhibits phagocytosis by dendritic cells and neutrophils. *Eur J Immunol* **35**(2)**:** 391-398

Wang W, Xue Y, Zhou S, Kuo A, Cairns BR, Crabtree GR (1996) Diversity and specialization of mammalian SWI/SNF complexes. *Genes Dev* **10**(17)**:** 2117-2130

Wang Z, Choi MK, Ban T, Yanai H, Negishi H, Lu Y, Tamura T, Takaoka A, Nishikura K, Taniguchi T (2008) Regulation of innate immune responses by DAI (DLM-1/ZBP1) and other DNA-sensing molecules. *Proc Natl Acad Sci U S A* **105**(14)**:** 5477-5482

Ward BM, Moss B (2001) Vaccinia virus intracellular movement is associated with microtubules and independent of actin tails. *J Virol* **75**(23)**:** 11651-11663

Weber F, Wagner V, Rasmussen SB, Hartmann R, Paludan SR (2006) Double-stranded RNA is produced by positive-strand RNA viruses and DNA viruses but not in detectable amounts by negative-strand RNA viruses. *J Virol* **80**(10)**:** 5059-5064

Wertz IE, O'Rourke KM, Zhou H, Eby M, Aravind L, Seshagiri S, Wu P, Wiesmann C, Baker R, Boone DL, Ma A, Koonin EV, Dixit VM (2004) De-ubiquitination and ubiquitin ligase domains of A20 downregulate NF-kappaB signalling. *Nature* **430**(7000)**:** 694-699

Wietek C, Cleaver CS, Ludbrook V, Wilde J, White J, Bell DJ, Lee M, Dickson M, Ray KP, O'Neill LA (2006) IkappaB kinase epsilon interacts with p52 and promotes transactivation via p65. *J Biol Chem* **281**(46)**:** 34973-34981

Wiley SR, Schooley K, Smolak PJ, Din WS, Huang CP, Nicholl JK, Sutherland GR, Smith TD, Rauch C, Smith CA, et al. (1995) Identification and characterization of a new member of the TNF family that induces apoptosis. *Immunity* **3**(6)**:** 673-682

Williamson JD, Reith RW, Jeffrey LJ, Arrand JR, Mackett M (1990) Biological characterization of recombinant vaccinia viruses in mice infected by the respiratory route. *J Gen Virol* **71 (Pt 11):** 2761-2767

Wolin SL, Cedervall T (2002) The La protein. *Annu Rev Biochem* **71:** 375-403

Woronicz JD, Gao X, Cao Z, Rothe M, Goeddel DV (1997) IkappaB kinase-beta: NF-kappaB activation and complex formation with IkappaB kinase-alpha and NIK. *Science* **278**(5339)**:** 866-869

Worschech A, Haddad D, Stroncek DF, Wang E, Marincola FM, Szalay AA (2009) The immunologic aspects of poxvirus oncolytic therapy. *Cancer Immunol Immunother* **58**(9)**:** 1355-1362

Xiao G, Fong A, Sun SC (2004) Induction of p100 processing by NF-kappaB-inducing kinase involves docking IkappaB kinase alpha (IKKalpha) to p100 and IKKalpha-mediated phosphorylation. *J Biol Chem* **279**(29)**:** 30099-30105

Xu G, Lo YC, Li Q, Napolitano G, Wu X, Jiang X, Dreano M, Karin M, Wu H (2011) Crystal structure of inhibitor of kappaB kinase beta. *Nature* **472**(7343)**:** 325-330

Xu LG, Wang YY, Han KJ, Li LY, Zhai Z, Shu HB (2005) VISA is an adapter protein required for virus-triggered IFN-beta signaling. *Mol Cell* **19**(6)**:** 727-740

Yang P, An H, Liu X, Wen M, Zheng Y, Rui Y, Cao X (2010) The cytosolic nucleic acid sensor LRRFIP1 mediates the production of type I interferon via a beta-catenin-dependent pathway. *Nat Immunol* **11**(6)**:** 487-494

Yasumoto K, Okamoto S, Mukaida N, Murakami S, Mai M, Matsushima K (1992) Tumor necrosis factor alpha and interferon gamma synergistically induce interleukin 8 production in

a human gastric cancer cell line through acting concurrently on AP-1 and NF-kB-like binding sites of the interleukin 8 gene. *J Biol Chem* **267**(31)**:** 22506-22511

Yeretssian G, Correa RG, Doiron K, Fitzgerald P, Dillon CP, Green DR, Reed JC, Saleh M (2011) Non-apoptotic role of BID in inflammation and innate immunity. *Nature* **474**(7349)**:** 96-99

Yonehara S, Ishii A, Yonehara M (1989) A cell-killing monoclonal antibody (anti-Fas) to a cell surface antigen co-downregulated with the receptor of tumor necrosis factor. *J Exp Med* **169**(5)**:** 1747-1756

Yoneyama M, Kikuchi M, Natsukawa T, Shinobu N, Imaizumi T, Miyagishi M, Taira K, Akira S, Fujita T (2004) The RNA helicase RIG-I has an essential function in double-stranded RNA-induced innate antiviral responses. *Nat Immunol* **5**(7)**:** 730-737

Yoshida R, Takaesu G, Yoshida H, Okamoto F, Yoshioka T, Choi Y, Akira S, Kawai T, Yoshimura A, Kobayashi T (2008) TRAF6 and MEKK1 play a pivotal role in the RIG-I-like helicase antiviral pathway. *J Biol Chem* **283**(52)**:** 36211-36220

Youinou P, Adler Y, Muller S, Lamour A, Baron D, Humbel RL (1994) Anti-Ro(SSA) and anti-La(SSB) antibodies in autoimmune rheumatic diseases. *Clin Rev Allergy* **12**(3)**:** 253-274

Youle RJ, Strasser A (2008) The BCL-2 protein family: opposing activities that mediate cell death. *Nat Rev Mol Cell Biol* **9**(1)**:** 47-59

Zandi E, Rothwarf DM, Delhase M, Hayakawa M, Karin M (1997) The IkappaB kinase complex (IKK) contains two kinase subunits, IKKalpha and IKKbeta, necessary for IkappaB phosphorylation and NF-kappaB activation. *Cell* **91**(2)**:** 243-252

Zeng W, Sun L, Jiang X, Chen X, Hou F, Adhikari A, Xu M, Chen ZJ (2010) Reconstitution of the RIG-I pathway reveals a signaling role of unanchored polyubiquitin chains in innate immunity. *Cell* **141**(2)**:** 315-330

Zhai D, Yu E, Jin C, Welsh K, Shiau CW, Chen L, Salvesen GS, Liddington R, Reed JC (2010) Vaccinia virus protein F1L is a caspase-9 inhibitor. *J Biol Chem* **285**(8)**:** 5569-5580

Zhang L, Villa NY, Rahman MM, Smallwood S, Shattuck D, Neff C, Dufford M, Lanchbury JS, Labaer J, McFadden G (2009) Analysis of vaccinia virus-host protein-protein interactions: validations of yeast two-hybrid screenings. *J Proteome Res* **8**(9)**:** 4311-4318

Zhang WH, Wilcock D, Smith GL (2000) Vaccinia virus F12L protein is required for actin tail formation, normal plaque size, and virulence. *J Virol* **74**(24)**:** 11654-11662

Zhang X, Brann TW, Zhou M, Yang J, Oguariri RM, Lidie KB, Imamichi H, Huang DW, Lempicki RA, Baseler MW, Veenstra TD, Young HA, Lane HC, Imamichi T (2011) Cutting edge: Ku70 is a novel cytosolic DNA sensor that induces type III rather than type I IFN. *J Immunol* **186**(8)**:** 4541-4545

Zhao C, Denison C, Huibregtse JM, Gygi S, Krug RM (2005) Human ISG15 conjugation targets both IFN-induced and constitutively expressed proteins functioning in diverse cellular pathways. *Proc Natl Acad Sci U S A* **102**(29)**:** 10200-10205

Zhao T, Yang L, Sun Q, Arguello M, Ballard DW, Hiscott J, Lin R (2007) The NEMO adaptor bridges the nuclear factor-kappaB and interferon regulatory factor signaling pathways. *Nat Immunol* **8**(6)**:** 592-600

Zhao Y, De Trez C, Flynn R, Ware CF, Croft M, Salek-Ardakani S (2009) The adaptor molecule MyD88 directly promotes CD8 T cell responses to vaccinia virus. *J Immunol* **182**(10)**:** 6278-6286

Zhong B, Yang Y, Li S, Wang YY, Li Y, Diao F, Lei C, He X, Zhang L, Tien P, Shu HB (2008) The adaptor protein MITA links virus-sensing receptors to IRF3 transcription factor activation. *Immunity* **29**(4)**:** 538-550

Zhou Q, Snipas S, Orth K, Muzio M, Dixit VM, Salvesen GS (1997) Target protease specificity of the viral serpin CrmA. Analysis of five caspases. *J Biol Chem* **272**(12)**:** 7797-7800

Zou H, Li Y, Liu X, Wang X (1999) An APAF-1.cytochrome c multimeric complex is a functional apoptosome that activates procaspase-9. *J Biol Chem* **274**(17)**:** 11549-11556